

The Synthesis of Bicyclic Guanidino Amino Acids

Steven Hill

*Submitted in fulfilment of the requirement for the degree
of Doctor of Philosophy.*

*School of Chemistry
Cardiff University*



Declaration

This work has not been submitted in substance for any other degree or award at this or any other university or place of learning, nor is being submitted concurrently in candidature for any degree or other award.

Signed (candidate) Date

STATEMENT 1

This thesis is being submitted in partial fulfillment of the requirements for the degree of(insert MCh, MD, MPhil, PhD etc, as appropriate)

Signed (candidate) Date

STATEMENT 2

This thesis is the result of my own independent work/investigation, except where otherwise stated.

Other sources are acknowledged by explicit references. The views expressed are my own.

Signed (candidate) Date

STATEMENT 3

I hereby give consent for my thesis, if accepted, to be available for photocopying and for inter-library loan, and for the title and summary to be made available to outside organisations.

Signed (candidate) Date

STATEMENT 4: PREVIOUSLY APPROVED BAR ON ACCESS

I hereby give consent for my thesis, if accepted, to be available for photocopying and for inter-library loans **after expiry of a bar on access previously approved by the Academic Standards & Quality Committee.**

Signed (candidate) Date

Abstract

Small molecules, such as oligopeptides can interact with nucleic acid targets and subsequently stimulate or suppress biological functions. The purpose of this thesis was to produce nucleic acid targeting oligopeptides which contain non-natural amino acids as part of their sequence.

Certain amino acids display selectivity for certain nucleobases. Arginine has a high propensity for being present at the binding interface of both protein-DNA and protein-RNA complexes. This thesis was aimed at the synthesis of two arginine analogues in which the guanidino side chain was locked in a bicyclic framework. It was expected that this would result in highly directional H-bonding capabilities of the side chains of the two analogues, which was predicted to give superior selectivity when discriminating between targets.

This thesis discusses the synthetic routes undertaken in an attempt to produce these two analogues. The synthesis of the two analogues proceeded by quite different routes. The first entailed manipulation of a chiral starting material to ultimately produce the bicyclic guanidine. However, incorporation of the amino acid moiety proved difficult and thus is incomplete. However, there is scope for further work to build on the endeavours mentioned in this work. The attempted synthesis of the second analogue focused on the formation of a substituted triamine prior to cyclisation to give the bicyclic guanidine. This method also produced many problems and so the synthesis still requires further work.

The thesis also details the design and synthesis of a peptide library with the majority of peptides possessing at least one arginine residue within their sequence. This produced a range of peptides in small quantities (nanomolar) which was screened against an enzyme-linked immunosorbent assay (ELISA). The results of the assay highlighted library members who displayed a binding affinity towards the oligonucleotide targets and from this their sequences were determined. Future work can be performed using these results so that binding association constants can be determined. Once the arginine analogues have been successfully synthesised these can be incorporated into these peptide sequences in place of the arginine residues.

Acknowledgements

I would like to thank Dr James Redman for supervision, guidance and advice during the course of this PhD. I would also like to thank the technical and administrative staff at the School of chemistry for their invaluable contribution, in particular Dr Rob Jenkins, Robin Hicks and Dave Walker for an efficient NMR and mass spectrometry service.

I am grateful to the EPSRC and Cardiff University for the funding and facilities which allowed me to perform my research. I would also like to thank my colleagues (past and present) during the last four years. I would also like to thank Prof. Rudolf Allemann for advice and the use of equipment and facilities.

Finally I wish to thank my friends and family who have helped me over the entire course of my education. Their contributions have been fundamental to my success and are fully appreciated.

List of Abbreviations

18-C-6	18-crown-6
4-DMAP	4-dimethylaminopyridine
Abs.	absolute
Ac	acetyl
AH-2-P	(S)-2-amino-3-((S)-2,3,4,6,7,8-hexahydro-1H-pyrimido[1,2-a]pyrimidin-2-yl) propanoic acid
AH-3-P	(S)-2-amino-3-((S)-2,3,4,6,7,8-hexahydro-1H-pyrimido[1,2-a]pyrimidin-3-yl) propanoic acid
Ala (A)	alanine
AM-RAM	Rink-amide (aminomethyl)polystyrene
aq.	aqueous
Ar	aryl
Arg (R)	arginine
Asn (N)	asparagine
Asp (D)	aspartic acid
atm.	atmosphere
BINOL	1,1'-bi-2-naphthol
Bn	benzyl
Boc	<i>tert</i> -Butyloxycarbonyl
CAM	ceric ammonium molybdate
CAN	ceric ammonium nitrate
Cbz	carboxybenzyl
CI	chemical ionisation
COSY	correlation spectroscopy

Cy	cyclohexyl
Cys (C)	cysteine
DABCO	1,4-diazabicyclo[2.2.2]octane
DBU	1,8-diazabicyclo[5.4.0]undec-7-ene
DCC	dicyclohexylcarbodiimide
DCM	dichloromethane
de	diastereomeric excess
DEAD	diethylazodicarboxylate
DIBALH	diisobutylaluminium hydride
DIC	diisopropylcarbodiimide
DIEA	diisopropylethyl amine
DMC	2-chloro-1,3-dimethylimidazolium chloride
DME	dimethoxyethane
DMF	dimethylformamide
DMP	Dess-Martin periodinane
DMPU	1,3-Dimethyl-3,4,5,6-tetrahydro-2(1 <i>H</i>)-pyrimidinone
DMS	dimethylsulfide
DMSO	dimethylsulfoxide
DMT	dimethoxytrityl
DNA	2'-Deoxyribonucleic acid
DNP	2,4-Dinitrophenylhydrazine
dsDNA	double stranded 2'-Deoxyribonucleic acid
EDC	1-ethyl-3-(3-dimethylaminopropyl)carbodiimide
ee	enantiomeric excess

EI	electron impact
ELISA	enzyme-linked immunosorbent assay
ESI	electrospray ionisation
Et	ethyl
FT-IR	fourier transform-infrared spectroscopy
Gln (Q)	glutamine
Glu (E)	glutamic acid
Gly (G)	glycine
HATU	<i>O</i> -(7-Azabenzotriazole-1-yl)- <i>N,N,N',N'</i> -tetramethyluronium hexafluorophosphate
HBTU	<i>O</i> -Benzotriazole- <i>N,N,N',N'</i> -tetramethyl-uronium-hexafluorophosphate
HFIP	hexafluoroisopropanol
His (H)	histidine
HMPA	hexamethylphosphoramide
HOAt	1-Hydroxy-7-aza-benzotriazole
HOBt	1-Hydroxybenzotriazole
HPLC	High performance liquid chromatography
HRMS	High resolution mass spectrometry
HRP	Horseradish peroxidase
HSQC	Heteronuclear single quantum coherence
HTH	Helix-turn-helix
Ile (I)	Isoleucine
Im	imidazole
<i>i</i> -Pr	isopropyl

LDA	lithium diisopropylamide
Leu (L)	leucine
LiHMDS	lithium bis(trimethylsilyl)amide
Lys (K)	lysine
MALDI	Matrix Assisted Laser Desorption/Ionisation
Me	methyl
mesyl (Ms)	methanesulfonyl
Met (M)	methionine
mMol (mM)	milimolar
MMT	methoxytrityl
Mol (M)	molar
MOM	methoxymethyl
mRNA	messenger Ribonucleic acid
MS	mass spectrometry
NaHMDS	sodium bis(trimethylsilyl)amide
NBD	Nucleic acids database
<i>n</i> -Bu	<i>n</i> -Butyl
NMM	<i>N</i> -methylmorpholine
NMP	<i>N</i> -methylpyrrolidinone
NMR	nuclear magnetic resonance
<i>n</i> -Pr	<i>n</i> -propyl
NSI	nanospray ionisation
Triflate (OTf)	trifluoromethanesulfonate
Pbf	2,2,4,6,7-pentamethyl-2,3-dihydro-1-benzofurna-5-sulfonyl

PDB	Protein Data Bank
PEG	polyethylene glycol
PG	protecting group
Ph	phenyl
Phe (F)	phenylalanine
PhH	benzene
PhMe	toluene
<i>p</i> NPP	<i>para</i> -nitrophenylphosphate
PSI	pounds per square inch
<i>p</i> -TsOH	<i>para</i> -toluenesulfonic acid
Py	pyridine
PyBOP	benzotriazol-1-yl-oxytripyrrolidinophosphonium hexafluorophosphate
RNA	Ribonucleic acid
rRNA	ribosomal Ribonucleic acid
Ser (S)	serine
SPPS	solid phase peptide synthesis
ssDNA	single stranded 2'-Deoxyribonucleic acid
SSE	secondary structural element
TATU	<i>O</i> -(7-Azabenzotriazole-1-yl)- <i>N,N,N',N'</i> -tetramethyluronium tetrafluoroborate
TBAF	tetra- <i>n</i> -butylammonium fluoride
TBD	triazabicyclodecene
TBDPS	<i>tert</i> -Butyldiphenylsilyl
TBO	triazabicyclo[3.3.0]oct-4-ene

TBS	<i>t</i> -butydimethylsilyl
TBTU	<i>O</i> -(Benzotriazol-1-yl)- <i>N,N,N',N'</i> -tetramethyluronium tetrafluoroborate
<i>t</i> -Bu	<i>tert</i> -Butyl
TCA	Trichloroacetate
TEA	triethylamine
TES	triethylsilane
TFA	trifluoroacetic acid
THF	tetrahydrofuran
Thr (T)	threonine
TIPS	triisopropylsilane
TMB	3,3',5,5'-tetramethylbenzidine
TMS	trimethylsilyl
Tosyl (Ts)	<i>para</i> -toluenesulfonyl
tRNA	transfer Ribonucleic acid
Trp (W)	tryptophan
Tyr (Y)	tyrosine
UV	ultra violet
vRNA	viral Ribonucleic acid
WC	Watson-Crick
Znf	Zinc-finger
μmol (μM)	micomole(s)

Contents

Declarations	i
Abstract	iii
Acknowledgments	iv
List of abbreviations	v
1.0 Introduction	1
1.1 Motivation	1
1.2 Background	1
1.2.1 Nucleic acid interactions	1
1.2.1.1 Protein-DNA interactions	2
1.2.1.2 Protein-RNA interactions	5
1.2.2 Guanidines and their derivatives	8
1.2.2.1 Bicyclic guanidines	10
1.2.2.2 Structure, properties and uses of bicyclic guanidines	10
1.2.2.3 Synthesis of bicyclic guanidines	11
1.2.2.3.1 Non-functionalised guanidines	11
1.2.2.3.2 Functionalised bicyclic guanidines	14
1.2.2.3.3 Chiral bicyclic guanidines	19
1.2.3 Amino acid synthesis	26
1.2.3.1 Strecker synthesis	27
1.2.3.1.1 Racemic synthesis	27
1.2.3.1.2 Asymmetric synthesis	28
1.2.3.1.3 Chiral auxiliaries	29

1.2.3.1.4	Organocatalysis	31
1.2.3.1.5	Metal-ligand catalysts	37
1.2.3.2	Corey-Link amino acid synthesis	40
1.2.3.3	Chiral glycine equivalent	44
1.2.3.3.1	Electrophilic glycinates	45
1.2.3.3.2	Nucleophilic glycinates	49
1.2.3.4	Petasis reaction	53
1.2.3.4.1	Asymmetric Petasis synthesis	55
1.2.3.4.2	Catalysis	56
1.3	Objectives	58
2.0	Results and discussions. Synthesis of AH-2-P	60
2.1	Introduction	60
2.2	Homologation	62
2.2.1	Via Ac- <i>N</i> -animo nitrile	62
2.2.1.1	Acetylation	63
2.2.1.2	Reduction	63
2.2.1.3	Activation of alcohol	64
2.2.2	Arndt Eistert reaction	66
2.3	Synthesis of bicyclic guanidines	67
2.3.1	Reduction	68
2.3.2	Boc-deprotection	69
2.3.3	Silyl Protection	70
2.3.4	Isothiocyanate formation	74
2.3.5	Protection of Diamine	76

2.3.5.1	Tosyl-N-mono-protection	77
2.3.5.2	Pbf-N-mono-protection	77
2.3.6	Thiourea formation	78
2.3.7	Bicyclic guanidine formation via cyclization	81
2.4	Synthesis of AH-2-P via chiral glycine enolate	83
2.4.1	TBS Cleavage	84
2.4.1.1	TBAF de-protection	84
2.4.2	Conversion to iodide	85
2.4.3	Reaction with Williams' template	86
2.5	Synthesis of AH-2-P via Strecker reaction	88
2.5.1	TBS removal	89
2.5.1.1	TBAF removal	89
2.5.1.2	CsF removal	89
2.5.1.3	TBS cleavage using Iodine	90
2.5.2	Oxidation	90
3.0	Results and discussions. Synthesis of AH-3-P	94
3.1	Introduction	94
3.2	Hydroxymethyl-triamine (236) synthesis via pyrazolidinedione	95
3.2.1	Hydrazinyl propylamine	95
3.2.2	Coupling to the triester	96
3.3	Hydroxymethyl triamine (236) synthesis via acrylic acid derivative	98
3.3.1	Protection of acrylic acid	100
3.4	Synthesis of triamine via hydroxyl activation	102

3.4.1	Baylis Hillman	103
3.4.2	Activation of hydroxyl group	103
3.4.3	Coupling to diamine	104
3.5	Triamine synthesis through amide bond formation	104
3.5.1	Aza-Michael addition	105
3.5.2	Benzyl protection	108
3.5.3	t-Butyl cleavage	108
3.5.4	Coupling reactions	109
3.5.4.1	Peptide coupling	109
3.5.4.2	Aminolysis of ester	111
3.6	Hydroxyl protection	112
3.6.1	Hydroxyl protection of dibenzylamino propanoic acid 258	113
3.6.2	Hydroxyl protection of esters 257 and 260	113
4.0	Peptide synthesis and binding studies	117
4.1	Introduction	117
4.1.1	Enzyme linked immunosorbent assay (ELISA)	118
4.1.2	Solid phase peptide synthesis (SPPS)	119
4.1.2.1	Solid supports	120
4.1.2.2	Methodology	122
4.1.2.2.1	Fmoc methodology	123
4.1.2.2.2	Boc methodology	124
4.1.2.3	Coupling reagents	125
4.1.2.3.1	Carbodiimides	125
4.1.2.3.2	Uronium/guanidinium reagents	127

4.1.2.3.3	Phosponium coupling reagents	128
4.2	Results and discussions	128
4.2.1	Assessment of applicability of assay	128
4.2.1.1	Synthesis of controls	129
4.2.1.2	Quantitation of peptides	130
4.2.1.3	ELISA of controls	131
4.2.2	Peptide library	133
4.2.2.1	Peptide library design	133
4.2.2.2	Library synthesis	134
4.2.2.3	Oxidation of peptides – formation of disulfide bond	135
4.2.2.4	ELISA of peptide library	137
5.0	Conclusions and future work	139
6.0	Experimental section	141
7.0	References	183
8.0	Appendix	189

1. Introduction

1.1 Motivation

The synthesis of optically pure non-natural amino acids has seen much success in synthetic chemistry. A wide variety of non-natural amino acids have been produced, including homologues of parent amino acids (such as β or γ amino acids)¹⁻³ as well as structural or stereo isomers of naturally occurring amino acids.⁴⁻⁶ Several techniques currently exist for synthesising non-natural amino acids, these techniques have been used to synthesise a plethora of amino acids containing a wide range of functionality in their side chains.⁷⁻¹²

The use of combinatorial chemistry affords the simple and relatively quick synthesis of a wide range of compounds that possess similar structures but can vary in their steric and electronic properties from one compound to another. Using combinatorial chemistry to introduce the non-natural amino acids into peptides/small molecules is an important tool in medicinal and biochemistry. These compounds, containing the un-natural amino acids, can be used in combination with various biological assays to deliver high throughput binding studies for ligand specificity towards a protein or nucleic acid.¹³⁻¹⁶

In the following sections the background to this thesis is discussed. I initially mention the interactions of proteins with their nucleic acid targets, with a particular focus on the interactions of the side chain of arginine in these complexes (section 1.2.1). Section 1.2.2 describes the properties, uses and synthesis of guanidines, with an emphasis on its constrained derivatives. The different techniques currently employed to produce amino acids is assessed in section 1.2.3. Finally I describe the objectives of this thesis in section 1.3.

1.2 Background

1.2.1 Nucleic acid interactions

Since the first single-crystal X-ray structure of a nucleic acid was elucidated in the 1980's,¹⁷ much research has taken place within the area of identifying and understanding complexes

involving the interaction of nucleic acids with proteins or small molecules. Nowadays, a plethora of the tertiary structures of these complexes is available from databases such as the nucleic acids database (NDB) and the RCSB protein data bank (PDB). The data from these complexes can be analysed using sophisticated computing algorithms and, from this, one can gain a variety of information, which can help to understand how the molecules interact with one another.¹⁸

Molecular recognition between proteins and nucleic acids is imperative to many biological processes, from transcription of a particular gene to packaging and organising DNA. These proteins interact with their nucleic acid target in several ways. The most common interaction involves electrostatic contacts between the positively charged side chains of the amino acids in the protein and the negatively charged phosphate backbone of the nucleic acid.¹⁹ The other interactions include hydrogen bonding (H-bonding) from the amino acid side chains and the exposed edges of the base pairs, as well as hydrophobic stacking, both of which, have been noted to be important for the recognition of a protein for its nucleic acid target.²⁰ Due to the inherent differences between protein-DNA and protein-RNA complexes both will be addressed separately.

1.2.1.1 Protein-DNA interactions

Seeman *et al.*²¹ hypothesised that certain amino acids could discriminate between various bases in a Watson-Crick double helix, and thus a code for molecular recognition could exist. It had been proposed by Seeman *et al.*²¹ and later by Hélène and co-workers²² that the guanidinium moiety of arginine, which displays only H-bond donors, could preferentially form dual H-bonds with the exposed edges of guanine (at O₆ and N₇) in the major groove (at the Hoogsteen edge) in Watson-Crick DNA (figure 1.1). This was corroborated by Pabo, who also speculated that most site specific contacts were made between α -helical regions of the protein and DNA's major groove.²⁰

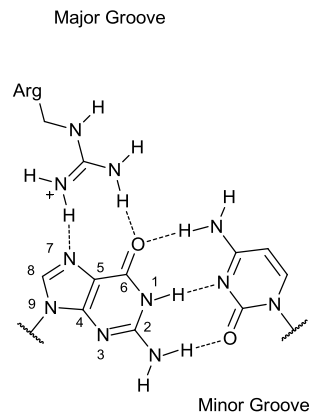


Figure 1.1 – Seeman's²¹ hypothesised dual H-bonding between arginine's side chain (guanidinium moiety) and the Hoogsteen edge of the guanine in a G:C base pair.

Matthews (1988) claimed that the complexity of different DNA-protein complexes meant that there was no simple code for recognition.²³ However, this did little to deter research in this field. The study of NMR and X-ray crystal structures of DNA-transcription factor complexes has shown that distinct structural motifs, such as the helix-turn-helix (HTH) and the zinc finger (Znf), are important for specific recognition.²⁰ These structural motifs have been categorised into several families.²⁴ The crystal structure of a Znf-DNA complex demonstrated the site specific interactions between arginine and guanine, which were present at the binding interface of each of the three fingers.²⁵

Suzuki performed a survey of the crystal structures of 20 DNA-transcription factor complexes. He reported that some amino acid residues recognise two chemical groups on the same DNA base and that these 'bidentate' H-bonds would result in stronger interactions when compared to single H-bonding. He also noted that Arg is usually found to be interacting with guanine rather than any other base, frequently through dual H-bonding.²⁶ Gutfreund and co-workers were in agreement with Suzuki and also noted that specific contacts between arginine and guanine were prevalent across the different families of transcription factors and that they were the major interactions that determine specific recognition.¹⁹

Luscombe *et al.*²⁷ emphasized that arginine side chains can adopt several geometries in order to donate a pair of H-bonds. The most common conformation shown is described as an ‘end-on approach’, in which guanine interacts with the two distal nitrogen atoms N η^1 and N η^2 , as originally predicted by Seeman *et al.* (Figure 1.2A). The side chain can also orientate itself to interact in a ‘side-on approach’, where the N ϵ and N η^2 are used for H-bond donation (figure 1.2B). However, this form of interaction is uncommon, probably due to the ease of access in the case of the former compared with the latter, which has to extend its side chain across the bottom of the major groove. Other examples of the bidentate H-bonding observed, involved a single N atom donating two H-bonds, in the same manner as a lysine residue can form bidentate interactions (figure 1.2C and D).

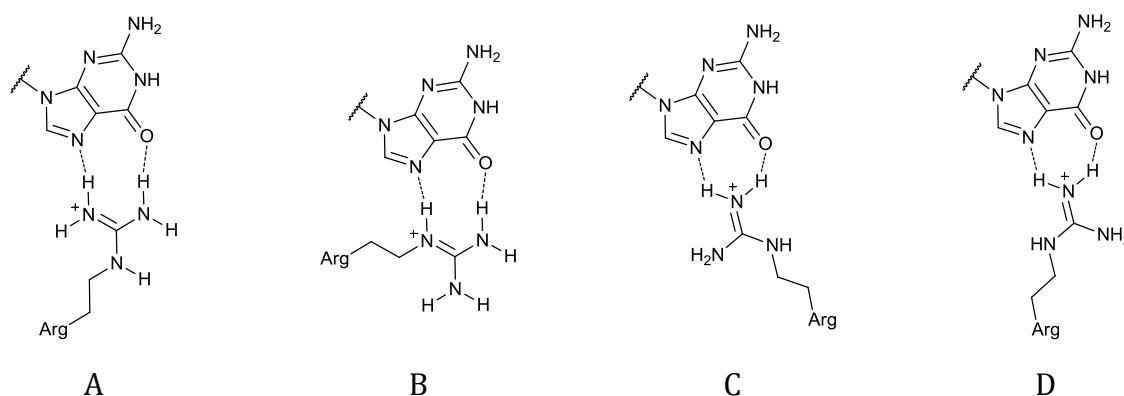


Figure 1.2 – Interactions between the guanidinium moiety of arginine and the Hoogsteen edge of guanine observed by Luscombe and co-workers.²⁷

Jones *et al.* performed a computational analysis of the 26 non-homologous protein-DNA complexes, consisting of at least 10 base pairs, which were available from the Protein Data Bank (PDB) and Nucleic Acid Database (NDB) at that time. This showed that regardless of the binding motifs used, the protein binding proceeded predominantly in the major grooves of the complexes. In fact the minor groove featured in very few complexes as it is too compact to accommodate common binding motifs.²⁸ Further studies have highlighted the importance of the positively charged side chain of arginine, which interacts through H-bonding or electrostatic interactions with the negatively charged phosphate backbone of

the DNA.^{19, 29, 30} These interactions are thought to be important for the stabilisation of the protein-DNA complex.^{27, 31}

Upon binding its DNA target, a protein can induce a conformational change in the DNAs secondary structure. The degree of deformation can vary from a slight kink³² to the large bends observed in the structure of the nucleosomes.³³ Other conformational changes have seen A/B hybrid DNA formed between a Zif265-DNA complex.³⁴ A consequence of the change in tertiary structure allows recognition of another motif of the protein or another protein/small molecule to take place at these previously inaccessible sites of the DNA. This is demonstrated in the structure of the nucleosome core, in which, the deformation of the DNA results in a narrow minor groove. Arginine residues in the protein side chains of the complex have been observed to regularly interact within this narrow minor groove.³⁵ This interaction has been frequently observed in distorted protein-DNA complexes that contain a narrowing of the minor groove.³⁶

Overall there are many factors governing the molecular recognition of a protein-DNA complex, such as the shape of the DNA backbone and the contacts involved. However, it is observed that arginine, which has the ability to form base-specific contact with guanine, as well as make contacts with the DNA phosphate backbone, is a prominent player in the recognition of a protein for its target DNA.^{19, 20, 24-27, 29} The importance of the aforementioned interaction between arginine and guanine is further highlighted in the bacteriophage transcription regulator p4. The binding of this protein to its nucleic acid target relies exclusively on the recognition of a specific arginine-guanine interaction.³⁷

1.2.1.2 Protein-RNA interactions

Proteins that interact with RNA control many cellular functions, including transcription, splicing and translation. Therefore, a greater understanding of the modes of molecular recognition of a protein for its RNA target has long been desired.

Protein-RNA complexes are much more structurally diverse than that of protein-DNA complexes. Like DNA, RNA is made up of Watson-Crick base pairing of four nucleobases. However, unlike its DNA counterpart, RNA forms A-form helices instead of the classic B-

form helices generally encountered with DNA. This is due to hindrance from the 2' OH of ribose. Classic A-form helices contain a deeper less accessible major groove than B-form helices and thus base-specific interactions between arginine and guanines Hoogsteen edge are inhibited. RNA also contains a much higher frequency of unpaired and 'mismatched' or non-Watson-crick (non-WC) base pairs, such as G·G and A·A as well as the G·U wobble pairs frequently encountered. The presence of these non-WC base pairs gives rise to loops, bulges and hairpins within the RNAs tertiary structure. Several base-specific interactions between proteins and their RNA target have been reported to take place at these sites. RNA also frequently forms base triples, whereby, a third nucleotide interacts with a Watson-Crick base pair. This can be initiated on binding to a protein, as described in the TAR RNA complex.³⁸ The presence of these bends, bulges, loops, hairpins and unpaired regions of RNA gives rise to its complex tertiary structures, which can vary considerably from one functional classification to another.

Prior to the beginning of the century, very little statistical information was available due to the lack of x-ray crystal and NMR structural data, which has made understanding the molecular recognition difficult. However, the turn of the century has seen a vast increase in published structures of protein-RNA complexes. Jones and co-workers conducted a statistical analysis of 32 protein-RNA structures from the PDB. They reported that arginine has a high propensity for being present in the binding site of protein-RNA complexes, with the preferred method of interaction taking place through H-bonding with the phosphates.³⁹ This has been corroborated by many.⁴⁰⁻⁴³ Although it has been suggested that many of these arginine residues at the interface are in close enough proximity to have strong electrostatic interaction with the phosphate oxygen atoms without being of the appropriate geometry to form H-bonds.¹⁸

With the increase in structural data becoming available there has been an increase in the number of analyses of different datasets. However, there is some disparity between these studies. Some have suggested that arginine primarily interacts with the phosphates and therefore shows no H-bonding specificity towards the bases.^{39, 41, 42} Others have suggested that the arginine interacts in a bidentate manner with O₆ and N₇ at the Hoogsteen edge of guanine, in the same way as observed in protein-DNA complexes, although much less

frequently.^{18, 40, 43, 44} This has also been noted from NMR experiments involving the TAR RNA complex, the base-specific interaction of arginine with the Hoogsteen edge of guanine results in the formation of a base triple.³⁸ Burke suggests that this interaction is also imperative for aminoacyl-tRNA synthetases to catalyse the attachment of a specific amino acid to its cognate tRNA in *Escherichia coli*.⁴⁵

Unpaired cytosine has also been observed in bidentate interactions with arginine, with the interaction taking place at the Watson-Crick base edge, with N₃ and O₂ accepting H-bonds from the N^{η1} and N^{η2} of the guanidino moiety of arginine (figure 1.3A).^{18, 40, 43, 44, 46} H-bonding interactions between arginine and Uracil have also been reported to be frequently present at the binding interface.^{18, 40, 43} Kim has described occurrences of a bidentate H-bonding interaction between O₂ of Uracil and N^ε and N^η of arginine's guanidino moiety (figure 1.3B).⁴⁶

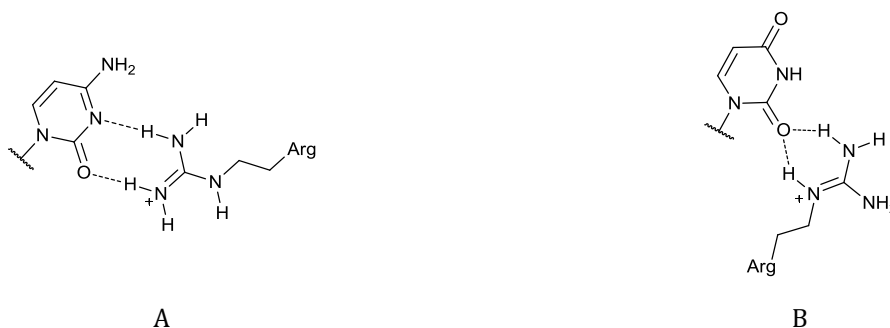


Figure 1.3 - Bidentate H-bonding interactions observed in protein-RNA complexes. A. H-bonding between N^{η1} and N^{η2} of arginine and O₂ and N₃ of cytosine.^{18, 40, 43, 44, 46} B. H-bonding of N^ε and N^η for arg with O₂ of Uracil.⁴⁶

The disparities reported between surveys could be attributed to the increasing number of complexes analysed and the inclusion of different proportions of proteins binding to different functional classes of RNA.⁴² Differences in the parameters set in the computing algorithms could also explain these differences of opinion. The conflicting results demonstrate the difficulty in identifying a specific code for the recognition of a protein for its RNA target. Jones intimated that proteins could interact by different modes with the different functional classes of RNA.³⁹ Proteins complexed with messenger RNA (mRNA),

transfer RNA (tRNA) and viral RNA (vRNA) display a greater number of contacts with the bases when compared with ribosomal RNA (rRNA), which is likely due to more frequent helical structure in rRNA.⁴² Arginine has however, been reported to have the highest tendency to be at the binding interface across several RNA functional classes when compared to any other amino acid.⁴¹

Another consideration is that of the secondary structure of the protein. Kim noticed that amino acids in β -sheets interacted more frequently than those in α -helices and turns. Furthermore, the β -sheet residues have a high tendency to recognize unpaired bases.⁴⁶ Hua Li *et al.* performed a computational analysis of 251 protein-RNA complexes and intentionally omitted rRNA complexes from their data set. They looked at the secondary structural elements (SSEs) of both the proteins and the RNAs. Their study shows non-WC base pairs and unpaired nucleotides have high propensities to be present in the binding site. The protein SSEs show that π -helices, 3_{10} -helices and bends are favoured while α -helices and β -turns are disfavoured.⁴⁷

Overall, the research in this field has demonstrated that although molecular recognition between a protein and its RNA target is difficult to predict, common themes are observed. It seems to be unanimous that arginine has a preference to be present at the binding interface and although disparity exists between the particular interactions observed, much research suggests base-specific interactions take place involving arginine and the exposed edges of various base pairs. The observation that single stranded sequences and non-Watson-Crick base pairs have a high propensity for being present at the binding site would allow interactions with the arginine residues via the various modes that have been observed (as mentioned above).

1.2.2 Guanidines and their derivatives

Due to the Y shaped CN_3 moiety, guanidine's double bond is delocalised over the three nitrogen atoms and the sp^2 hybridized carbon atom. This results in a high basicity, in which protonation takes place at the sp^2 hybridized N atom. The pK_{aH} of the guanidine is 13.6, therefore it exists as the cationic species (or guanidinium) when in aqueous solutions at

physiological pH and so is able to form electrostatic interactions with negatively charged species, as demonstrated between arginine's side chain and the phosphates in RNA and DNA (*vide supra*).

Substitution at the N-atoms of guanine results in different chemical properties due to steric and electronic contributions. The direction of H-bonding is influenced by the substituents on the guanidine, Figure 1.4 shows the different conformations (described as *E,E*, *E,Z* and *Z,Z*) a tetra-substituted guanidine can adopt and ultimately shows the different directions in which H-bonding can take place.⁴⁸

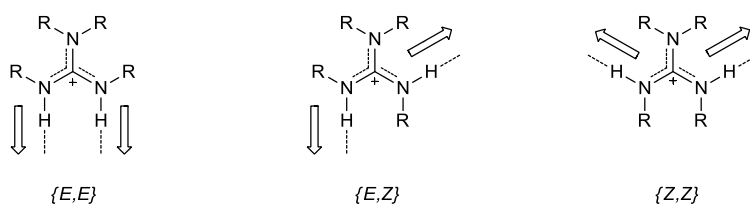


Figure 1.4 – Possible conformations of tetra-substituted guanidines, showing H-bond directionality.⁴⁸

Many natural products contain the guanidinium moiety within their structures. The presence of arginine in proteins has already been discussed, but an array of natural products have been isolated that contain various derivatives of guanidinium functionality as part of their structure. A few examples are shown in figure 1.5. Netropsin (figure 1.5a) is a naturally occurring oligopeptide, which contains the acyclic guanidinium moiety and was discovered in the 1950s.⁴⁹ It has since been used as an antibiotic which binds in the minor groove of DNA. The capreomycins⁵⁰ (figure 1.5b) are derivatives of the natural compound capreomycin, discovered by Herr in 1960. These cyclic peptides, which contain a monocyclic guanidine are used as a treatment for tuberculosis. Ptilomycin A (figure 1.5c) is an antitumor, antiviral and antifungal compound which contains a tricyclic guanidinium moiety in its structure and was isolated from the Caribbean sponge *Ptilocaulis spiculijer*.⁵¹

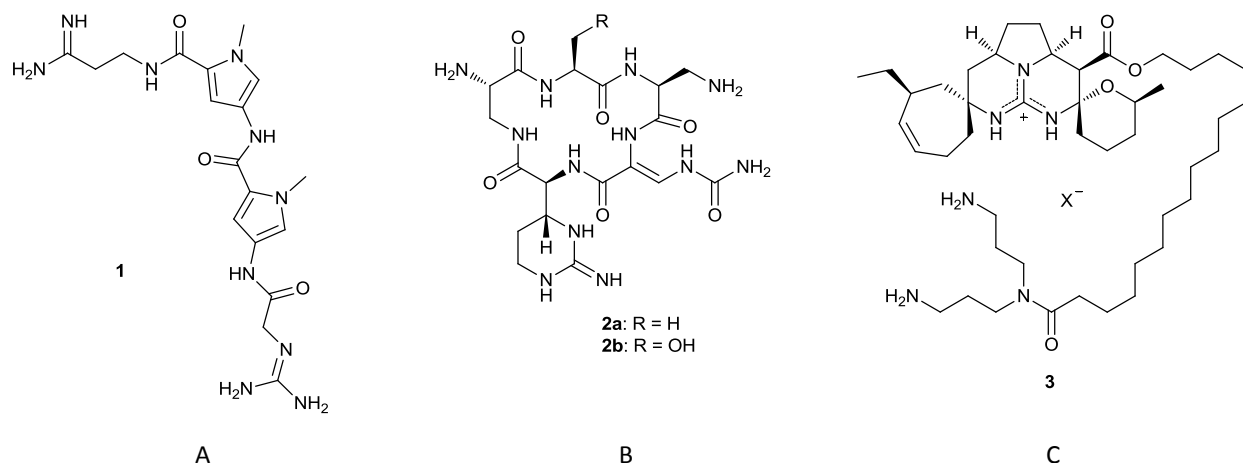


Figure 1.5 – Structures of naturally occurring compounds containing guanidinium moieties. A. Netropsin; B. Capreomycin; C. Ptilomycin A.

1.2.2.1 Bicyclic guanidines

Constraining the guanidine in a bicyclic framework locks the position of H-bonding in the $[E,E]$ conformation (figure 1.6). Furthermore, this limits the H-bonding to take place at a single face, in the same manner as observed in **3**. This is unlike its monocyclic derivatives, which can H-bond from two possible faces, as demonstrated by capreomycins **2a** and **2b** (figure 1.5). Much work has taken place in synthesising these bicyclic guanidines (*vide infra*). From herein, the structure of these bicyclic guanidines will be described as $[n,m]$ relating to the number of carbon atoms present in each ring of the bicycle. Figure 1.6 shows both the $[5,5]$ and $[6,6]$ bicyclic guanidines.

1.2.2.2 Structure, properties and uses of bicyclic guanidines

The constraints imposed by the ridged bicyclic framework dictate the projection of the H-bond donation by the guanidinium (as shown in figure 1.6). When protonated the $[6,6]$ bicyclic guanidine retains the ability to form bidentate H-bonds, in the same way as previously seen with the arginine side chain. This takes place because both H-bond donor atoms, in the guanidinium species, are of the correct geometry to form bidentate H-bonds with suitable H-bond acceptors, such as nitronates,⁵² carboxylates⁵³ and phosphates.⁵³ This is in contrast to the $[5,5]$ bicyclic guanidine, whose angle of H-bonding is forced outwards,

due to the ring strain. On the other hand, the tetra-substituted guanidinium species undergoes the opposite effect, where the R groups force the angle of H-bonding inwards.⁵⁴

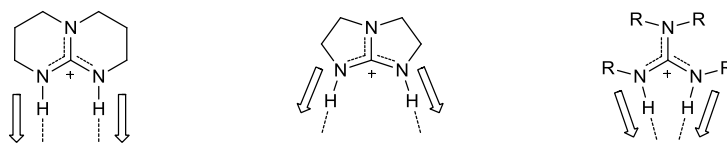


Figure 1.6 – Slight variations in H-bonding angles between the [6,6], [5,5] and tetra-substituted guanidinium species.

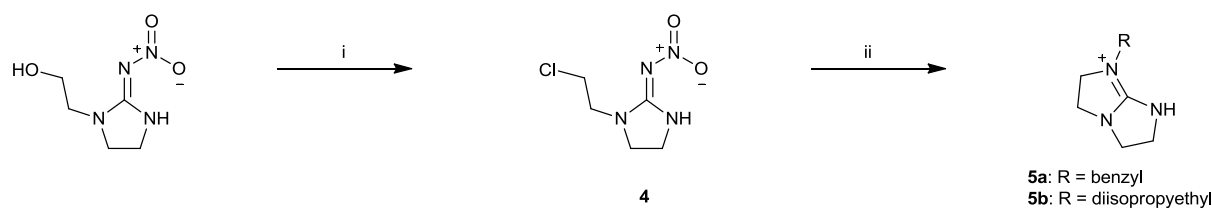
Due to its excellent ability to form dual H-bonds with a variety of substrates, the [6,6] bicyclic guanidine (triazabicyclodecene, or TBD) has gained a lot of use as a catalyst for a wide range of reactions, including: Michael additions,^{55, 56} aldol condensations,⁵⁷ aminolysis of esters⁵⁸ and Wittig reactions.⁵⁹ The homologous [5,5] bicyclic guanidine (1,4,6-triazabicyclo[3.3.0]oct-4-ene, or TBO) is much less commonly used as a catalyst. This could be due to its lower basicity compared to TBD⁶⁰ as well as the previously mentioned wider 'bidentate' H-bonding angle.

1.2.2.3 Synthesis of bicyclic guanidines

Due to the diversity of their uses the synthesis of bicyclic guanidines has received frequent attention over the past 60 years. There are two strategies which have been employed in order to produce the bicyclic guanidinium moiety. In the infancy of the work in this field the strategy centred on the cyclization of a mono-cyclic guanidine.⁶¹⁻⁶⁶ While in later work, the synthetic route has focused on the insertion of the central carbon atom to a long chained triamine.⁶⁷⁻⁷³

1.2.2.3.1 Non-functionalised guanidines

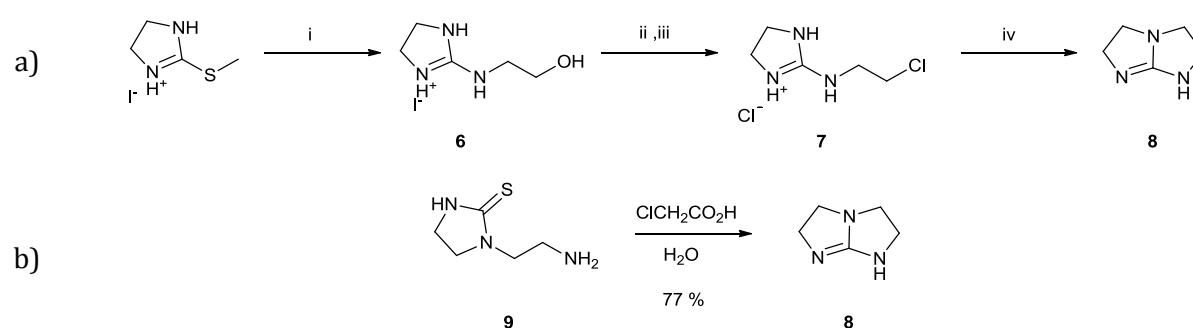
The pioneer in the synthesis of bicyclic guanidines was McKay and co-workers in the mid 1950's. They described the synthesis of *N*-benzyl and *N,N*-diisopropylethylenediamine bicyclic guanidines from 1-(β -chloroethyl)-2-nitriminoimidazolidine (**4**), which, when heated with the corresponding amine (benzyl or *N,N*-diisopropylethylenediamine) in anhydrous media produced its bicyclic guanidine derivative **5a** or **5b** (scheme 1.1).⁶¹



i. SOCl_2 , anhydrous PhH, 58 °C, 8.5h (**48 %**); ii. either BnNH_2 , PhMe, reflux, 9.5 h (**57 %**) or $((\text{CH}_3)_2\text{CH})_2\text{N}(\text{CH}_2)_2\text{NH}_2$, PhMe, reflux, 22 h (**45 %**)

Scheme 1.1 – First synthetic pathway to bicyclic guanidines.⁶¹

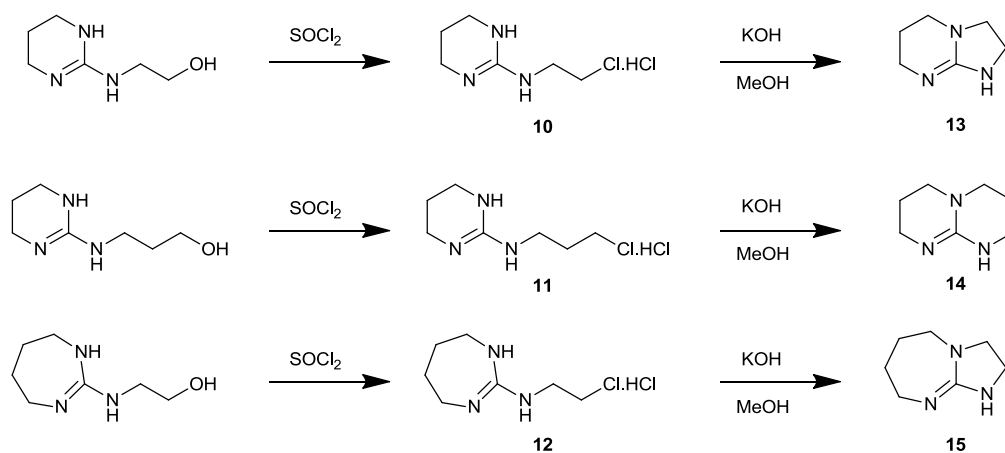
McKay also documented the synthesis of the free base.⁶² The synthesis (scheme 1.2a) began with formation of a substituted cyclic guanidinium moiety through the reaction of 2-methylmercapto-2-imidazolinium iodide and 2-aminoethanol, which liberated methane thiol to give **6**. This was converted to the corresponding chloride (**7**) on treatment with thionyl chloride. Refluxing in an ethanolic solution of potassium hydroxide yielded TBO (**8**) in respectable overall yield (62 %). Another method for production of TBO involved refluxing **9** in water containing either: silver nitrate, silver oxide, mercuric oxide or chloroacetic acid (Scheme 1.2b). Highest yield were obtained in the chloroacetic acid case (77.3 %).⁶³



i. $\text{H}_2\text{N}(\text{EtOH})$, CHCl_3 , reflux, 4 h (**95 %**); ii. Amberlyte® ion-exchange resin. HCl (**100 %**); iii. SOCl_2 , CHCl_3 , 5.5 h (**100 %**); iv. KOH, EtOH, reflux, 5 h (**66 %**).

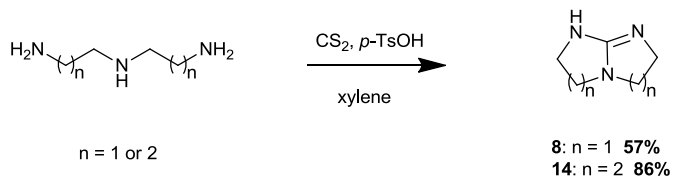
Scheme 1.2 – a) McKay's synthesis of TBO.⁶² b) TBO synthesis via conversion of a thiourea.⁶³

Further work documented the synthesis of three other bicyclic guanidines.⁶⁴ With the synthesis taking place in a similar manner, the 2-(ω -hydroxyalkylamino)- Δ^2 -1,3-diazacycloalkanes underwent chlorination by thionyl chloride. The cyclization was then achieved by refluxing with two molar equivalents of KOH in methanol (scheme 1.3). The [6, 7] derivative has been synthesised using a similar protocol.⁶⁵ An analogous approach has seen the synthesis of [5, 5], [5, 6], [6, 6] and [5, 7] *N*-benzhydryl bicyclic guanidine derivatives via cyanoimino-1,3-diazacycloalkanes.⁷⁴



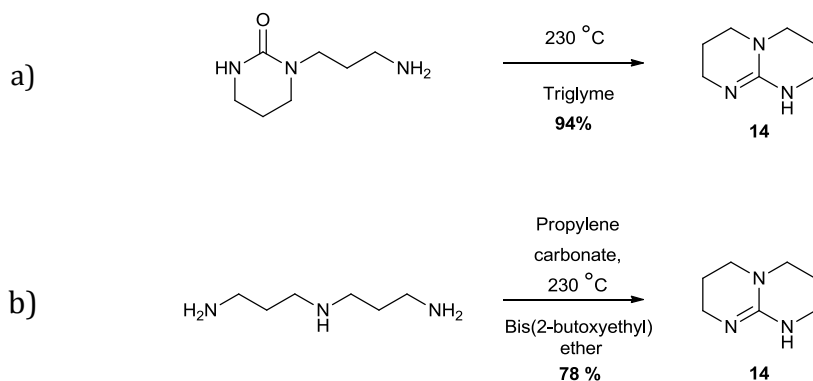
Scheme 1.3 –Synthesis of [6,5], [6,6] and [7,5] bicyclic guanidines via dehalogenation.⁶⁴

Endeavours to improve the synthesis of these bicyclic guanidines have seen the synthesis proceed in a single step from commercially available starting materials. The [5,5] and [6,6] bicyclic guanidines were produced in good to high yields from the cyclization of bis-(3-aminoalkyl)amines using carbon disulfide and *p*-toluenesulfonic acid (Scheme 1.4).⁶⁷ Cotton *et al.* used the same technique to produce the 6,5 derivative.⁶⁸



Scheme 1.4 – Formation of bicyclic guanidine.⁶⁷

Another approach to synthesize these bicyclic guanidines attempts to avoid the use of the hazardous reagent carbon disulfide (CS₂).⁶⁹ The synthesis (Scheme 1.5) however, required high reaction temperatures (200-250 °C), used polyethylene glycol as the solvent and had long reaction times, typically 2-3 days. Highest yields were observed when starting from a cyclic urea (94 %, scheme 1.5a). However the cyclic urea has also been formed *in situ* from 3,3'-diaminodipropylamine and propylene carbonate, followed by heating to 230 °C for 2-3 days (78.2 %, scheme 1.5b). Organometallic chemistry has been used to synthesise both the TBD and TBO bicyclic guanidines in good to high yields via the titanium catalysed addition of triamines to carbodiimides.⁷⁰



Scheme 1.5 – Synthesis of TBD.⁶⁹ a) Cyclization of monocyclic urea, b) synthesis proceeded through the *in situ* formation of a cyclic urea

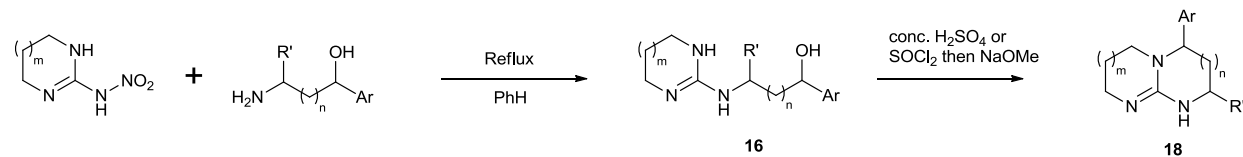
1.2.2.3.2 Functionalised bicyclic guanidines

In a patent by Van Gelder *et al.* the synthesis of a variety of aryl substituted bicyclic guanidines was described.⁷¹ The repertoire of these compounds included both bicyclic imidazoline and pyrimidine guanidines containing a range of aryl functionality, with examples of phenyl, alkylphenyl, halophenyl and dihalophenyl guanidines being reported.

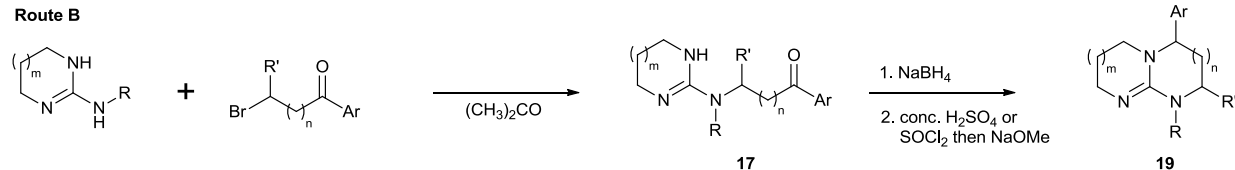
These compounds were synthesised by formation of the aryl substituted monocyclic alcohols **16** (scheme 1.6, Route A). Formation of the bicycle then proceeded via condensation or de-halogenation depending on reagents used. Similarly the *N*-benzyl species were synthesised through alkylation of the *N*-benzyl monocyclic guanidine (scheme

1.6, Route B). Following reduction of the ketone, the cyclization of the second ring took place in the same manner as stated for the unprotected species.

Route A



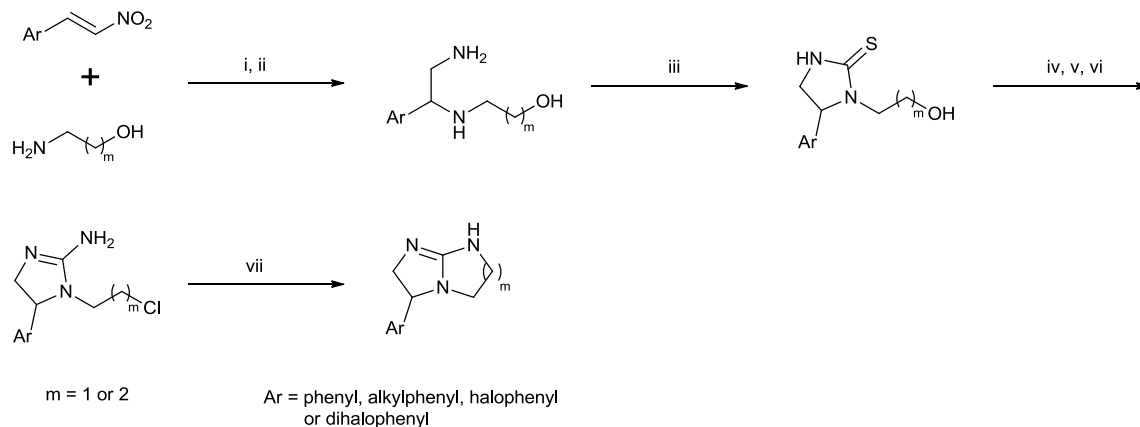
Route B



m = 0 or 1 R = H or Bn
n = 0 or 1 R' = H or Me

Ar = phenyl, alkylphenyl, halophenyl
or dihalophenyl

Scheme 1.6 –Van Gelder’s synthesis of aryl substituted bicyclic guanidines.⁷¹



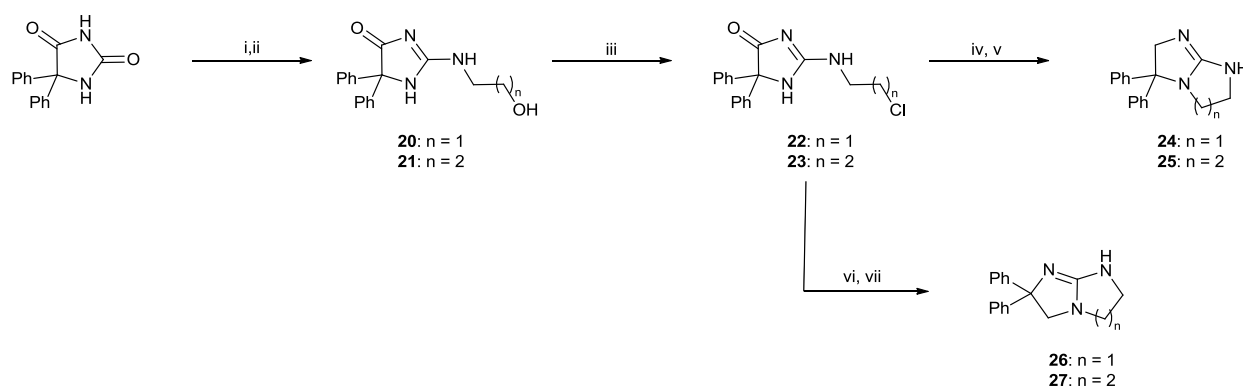
i. MeOH/Et₂O, 5 °C; ii. Raney® Ni, CO₂, MeOH, 50 PSI, 2 h; iii. 10 N NaOH, CS₂, EtOH/H₂O, reflux, 1 h; iv. MeI, MeOH, 40 °C, 4 h; v. NH₃, MeOH, reflux, 2 h; vi. SOCl₂, CHCl₃, reflux, 0.5 h; vii. NaOMe, MeOH, 1.5 h.

Scheme 1.7 – First synthesis of bicyclic guanidine via thiourea.⁷¹

This work also documented the first synthesis of a bicyclic guanidine which proceeded through a cyclic thiourea intermediate (scheme 1.7), which was formed by treatment of a

diamine with carbon disulphide (CS₂). Following methylation, the methylated thiourea was converted to the guanidine and cyclization was performed in the same manner as mentioned above.

Kosabayama *et al.* described a method for synthesis of 2,2- and 3,3-diphenyl substituted [5,5] bicyclic guanidines (**24** and **26** respectively). The synthesis (scheme 1.8) follows a similar trend to those previously mentioned. Formation of monocyclic guanidino alcohol **20** was proceeded by conversion to the chloride **22**. Intramolecular nucleophilic substitution was followed by Red-Al reduction, which yielded the 2,2-diphenyl derivatives (**24**). However, when performed at elevated temperatures (200 °C) the 3,3-diphenyl derivatives (**26**) are exclusively produced. The synthesis was also used to prepare the [5,6] derivatives **25** and **27**.⁷²

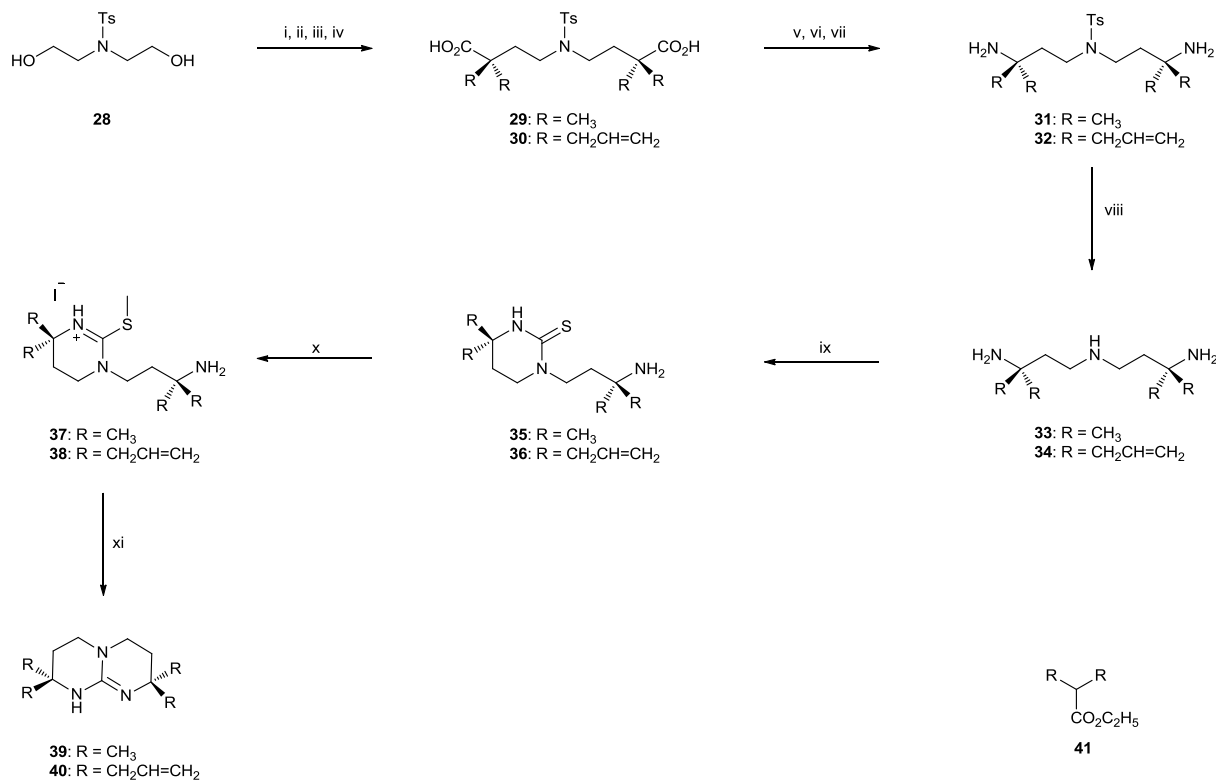


i. (C₂H₅)₃OBf₄, CH₂Cl₂, Δ (**88** %); ii. H₂NCH₂(CH₂)_nOH, EtOH, Δ (n=1 **85** %, n=2 **88** %); iii. SOCl₂, Δ (n=1 **97** %, n=2 **94** %); iv. NaH, DMF (n=1 **87** %, n=2 **88** %); v. NaAlH₂(OCH₂CH₂OCH₃)₂, THF, Δ (n=1 **57** %, n=2 **62** %); vi. NaH, DMF, Δ (n=1 **88** %, n=2 **90** %); vii. NaAlH₂(OCH₂CH₂OCH₃)₂, THF (n=1 **29** %, n=2 **81** %).

Scheme 1.8 – Synthesis of 2,2 and 3,3-diphenyl bicyclic guanidines.⁷²

The first documented synthesis of alkyl and allyl substituted bicyclic guanidines was published in 1980 by Schmidtchen.⁷³ The synthesis (scheme 1.9) began with conversion of **28** to its corresponding di-iodide, which was subsequently alkylated with **41**. The resulting tetra-substituted di-ester then underwent acid hydrolysis to give di-acid **29**. Conversion to the carboxylic azide was followed by a Curtius rearrangement and hydrolysis, which gave the tetra-substituted diamine **31**. Dissolving metal reduction removed tosyl protection to

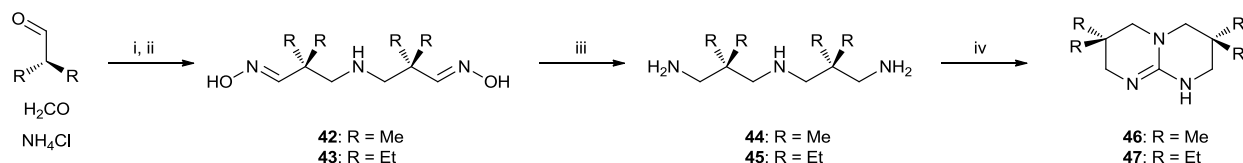
give triamine **33**. Treatment with thiophosgene, followed by methylation produced the thiouronium species **37**. Finally treatment of **37** with sodium methoxide in methanol yielded the $\alpha,\alpha,\alpha',\alpha'$ -[6,6]-bicyclic guanidines **39**.



i. MsCl, TEA, CH₂Cl₂ (**90** %); ii. NaI, (CH₃)₂CO (**70** %); iii. LDA, **41**, THF, 0 °C; iv. KOH, H₂O, Δ (**29** = **75** %, **30** = **73** % 2 steps); v. Oxalyl chloride, DMF, PhH; vi. NaN₃, H₂O, (CH₃)₂CO, Δ, CCl₄; vii. 6M HCl, H₂O, THF (**31** = **71** %, **32** = **72** % 3 steps); viii. Li, NH₃(l), THF (**33** = **75** %, **34** = **81** %); ix. CSeCl₂, TEA, CH₂Cl₂ (**35** = **80** %, **36** = **81** %); x. MeI, CH₃NO₂; xi. NaOCH₃, CH₃OH or KO*t*-Bu, *t*-BuOH (**39** = **79** %, **40** = **70** % 2 steps).

Scheme 1.9 – Production of tetramethyl and tetrapropenyl $\alpha,\alpha,\alpha',\alpha'$ -[6,6]-bicyclic guanidines.⁷³

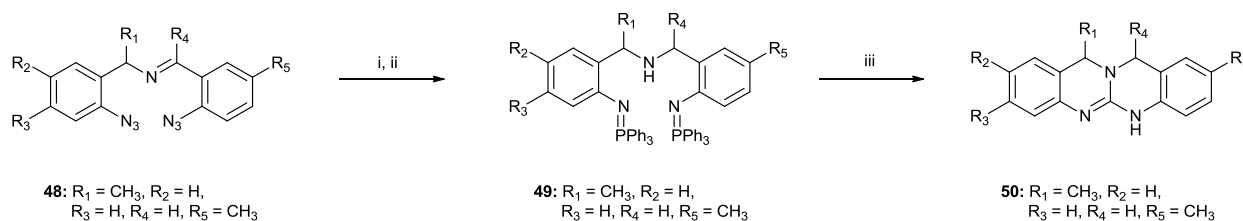
Cotton *et al.* developed a synthesis to methyl and ethyl $\beta,\beta,\beta',\beta'$ -[6,6]-bicyclic guanidine derivatives **46** and **47**.⁷⁵ The synthesis (scheme 1.10) used a Mannich-style reaction to synthesise the tetra-methyl and ethyl triamines **44** and **45**, respectively. This was followed by Raney[®] nickel hydrogenolysis and was subsequently cyclized by the same method used by A'Court.⁶⁷



i. Reflux; ii. $\text{NH}_2\text{OH}\cdot\text{HCl}$, NaOH ; iii. H_2 , Raney[®] Ni, 100 °C, 100 atm; iv. CS_2 , *p*-TsOH, *p*-xylene, reflux

Scheme 1.10 – Synthesis of methyl and ethyl $\beta,\beta,\beta',\beta'$ -[6,6]-bicyclic guanidines.⁷⁵

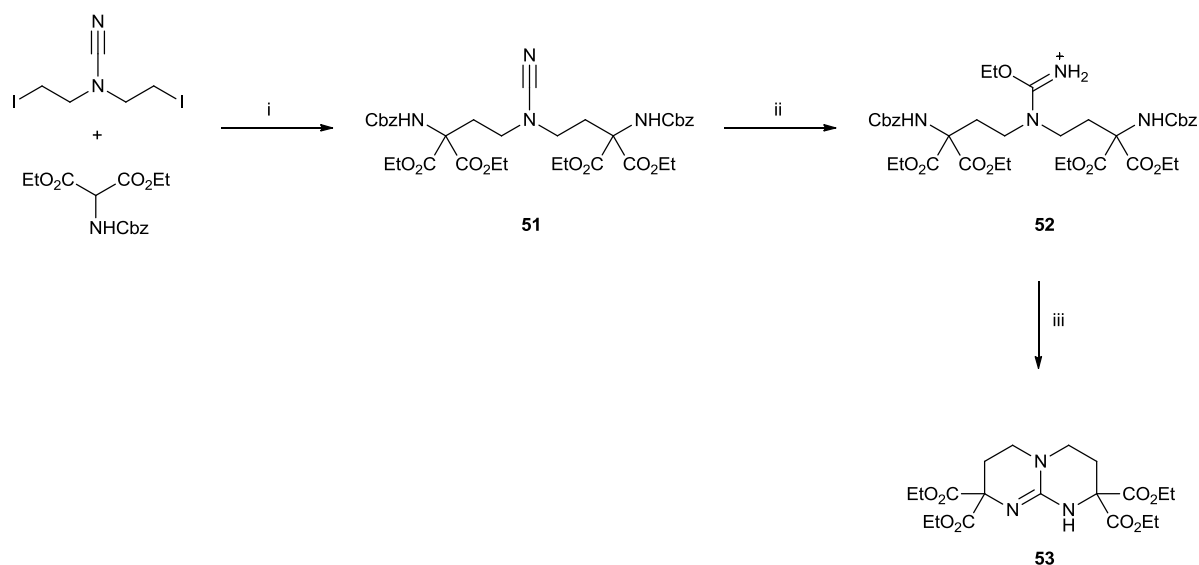
Molina⁷⁶ used a procedure involving the reaction of bis(iminophosphoranes) with aryl isocyanates or isothiocyanates to produce a range of tetracyclic compounds which contain bicyclic guanidino functionality (an example is shown in scheme 1.11). The reaction has been performed using a broad range of substrates, producing [5,5], [5,7], [6,6] and [6,8] derivatives with varying functionality at the R positions (see scheme 1.10) as well as a wide variety of aromatics.^{77, 78}



i. PPh_3 , $\text{CH}_2\text{Cl}_2/\text{Et}_2\text{O}$; ii. NaBH_4 , $\text{CH}_2\text{Cl}_2/\text{MeOH}$, 0 °C; iii. ArNCO (2eq.), PhH (**68 %** 3 steps).

Scheme 1.11 – An example of Molina's approach to the synthesis of tetracyclic guanidino compounds.⁷⁶

Jadhav *et al.* synthesised bicyclic guanidino tetraester **53** by constructing the *N,N*-bis(aminoalkyl)cyanamide **51**.⁷⁹ They used a Pinner reaction to give the iminium species **52**, which was followed by hydrogenolysis, the cyclization proceeded by heating in TEA to furnish bicyclic guanidine **53** in 74 % yield.

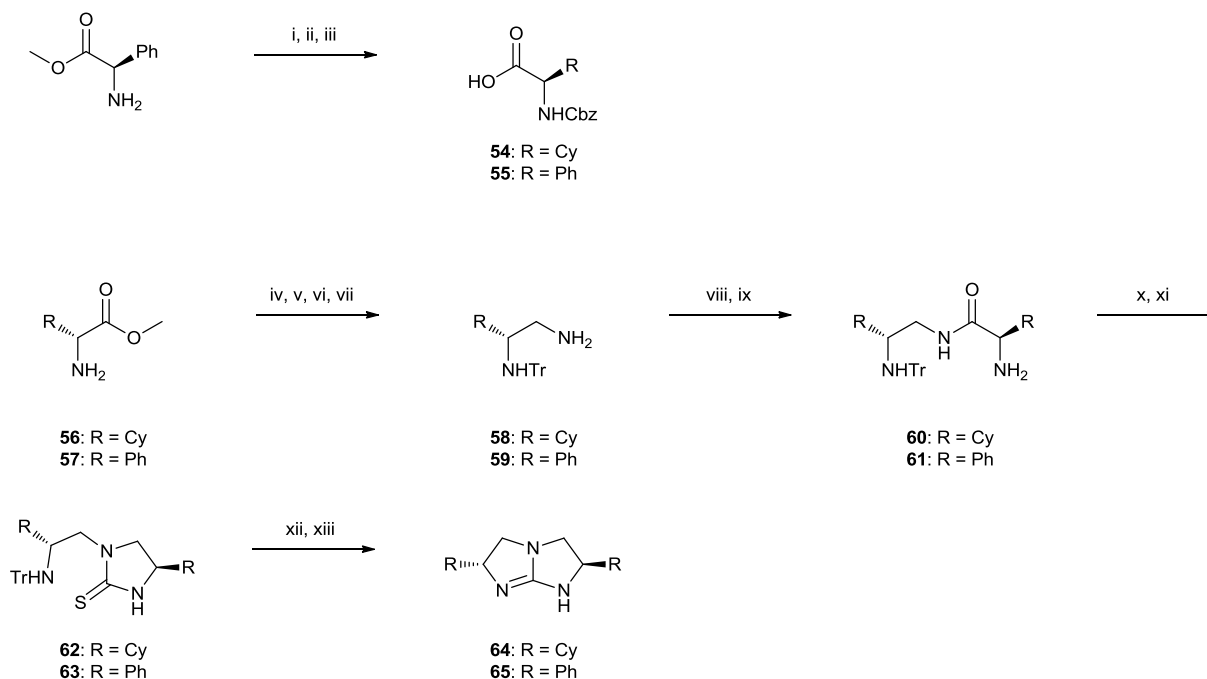


i. NaH, DMF, 3 days (72 %); ii. HCl, EtOH, 45 °C; iii. (a) Pd/C, H₂, (b) TEA, 50 °C, 2 hours (74 % 4 steps).

Scheme 1.12. – Synthesis of bicyclic guanidino tetraethyl ester **53**.⁷⁹

1.2.2.3.3 Chiral bicyclic guanidines

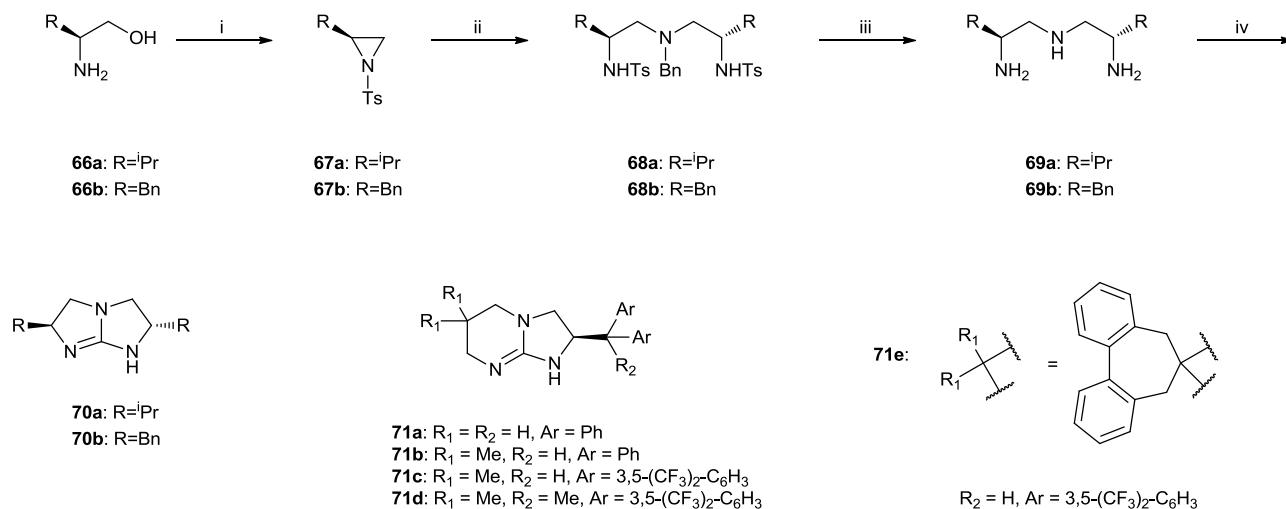
The synthesis of a C₂ symmetric chiral bicyclic guanidine (R = Cy) was first described in 1989 by Corey and Ohtani.⁸⁰ Their route (scheme 1.13) proceeded through the coupling of the mono-protected diamine **58** with the *N*-protected amino acid **54**, both of which had been previously synthesised from D- α -phenylglycine methyl ester, which gave the substituted triamine **60**. Following hydrogenolysis and reduction, thiourea **62** was formed by reaction with thiophosgene. Methylation at the sulfur atom preceded cyclisation, which furnished **64**. This synthetic route has been expanded to produce the α,α' -diphenyl derivative **65** (R = Ph).⁸¹



i. H₂, PtO₂-H₂O, AcOH, 23 °C; ii. Cbz-Cl, Py, CH₂Cl₂, 0 °C, 1 h; iii. NaOH, H₂O/MeOH, 23 °C; iv. NH₃, MeOH, 0 °C, 3 h, 23 °C, 16 h (**84 %**); v. H₂, PtO₂-H₂O, AcOH, 23 °C, 40 h (**87 %**); vi. TrCl, TEA, CH₂Cl₂, 23 °C (**94 %** for R = Cy, **97 %** for R = Ph); vii. LiAlH₄, Et₂O, reflux, (**97 %** for **58**, **95 %** for **59**); viii. **54** or **55**, DCC, HOBT, THF, (**85 %** for R = Cy, **77 %** for R = Ph); ix. H₂, 10 % Pd/C, 1:1 THF/MeOH, 23 °C (**100 %** for **60**). x. Red-Al, PhH, reflux, (**100 %** for R = Cy, **76 %** for R = Ph). xi. For **62** CSCl₂, TEA, CH₂Cl₂ (**69 %**); for **63** CSCl₂, Na₂CO₃, 1:1 CH₂Cl₂/H₂O (**95 %**); for **64**, xii. MeI, MeOH, 60 °C (**100 %**); xii. DMF, 100 °C, (**60 %**); for **64**, xii. MeI, MeOH, 60 °C; xiii. DMF 100 °C (**55 %** for **65**, 2 steps).

Scheme 1.13 – C₂ symmetric chiral bicyclic guanidines **64**⁸⁰ and **65**.⁸¹

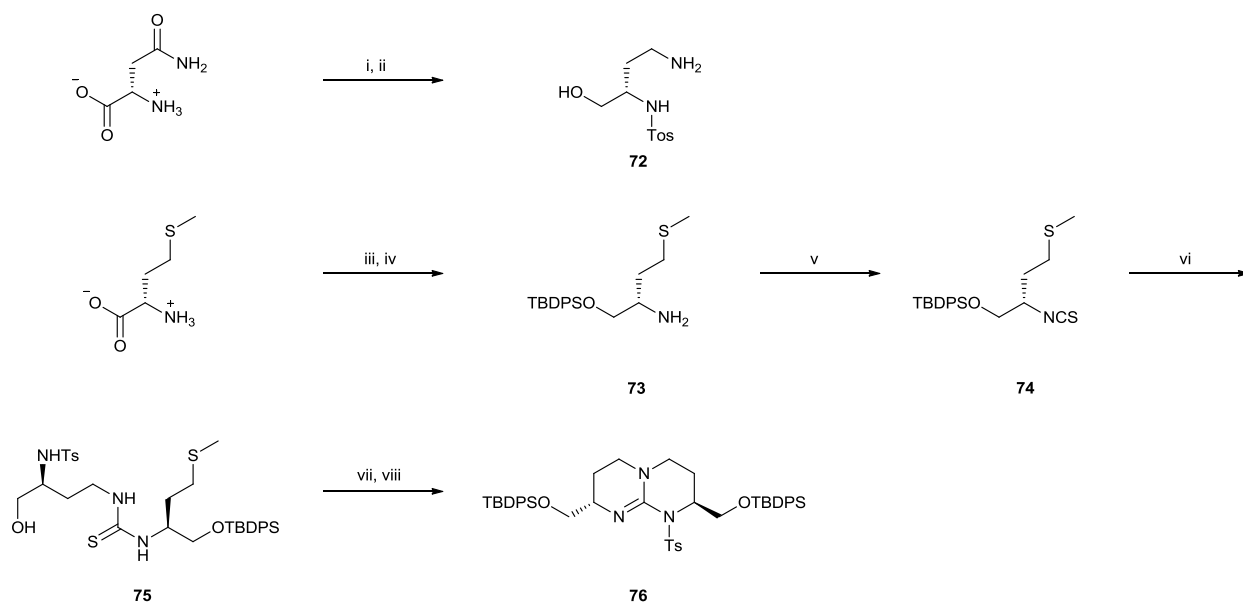
Further endeavours have seen the synthesis of α,α' -disubstituted derivatives take place in only five steps via an aziridine ring opening reaction with benzylamine to furnish the di-substituted triamines **68a-b**. These were then de-protected and converted to their corresponding bicyclic guanidines **70a-b** using dimethyl carbonotrithioate (scheme 1.14).⁸² Misaki *et al.* used a similar approach to produce a broad range of chiral bicyclic guanidinium catalysts (**71a-e**) for aldol reactions.⁸³



i. TsCl, Et₃N, MeCN, (**92 %** for **67a**, **94 %** for **67b**); ii. 0.5 equiv BnNH₂, MeOH, 60 °C, 3 days, (**92 %** for **68a**, **75 %** for **68b**); iii. (a) Na, NH₃(l), 78 °C, THF; (b) H₂, Pd/C, MeOH; iv. (MeS)₂CS then MeI/AcOH, MeNO₂, reflux, (**89 %** for **70a** from **68a**, **61 %** for **70b**, from **68b**).

Scheme 1.14 – α - α -disubstituted bicyclic guanidines via aziridine ring opening.^{82, 83}

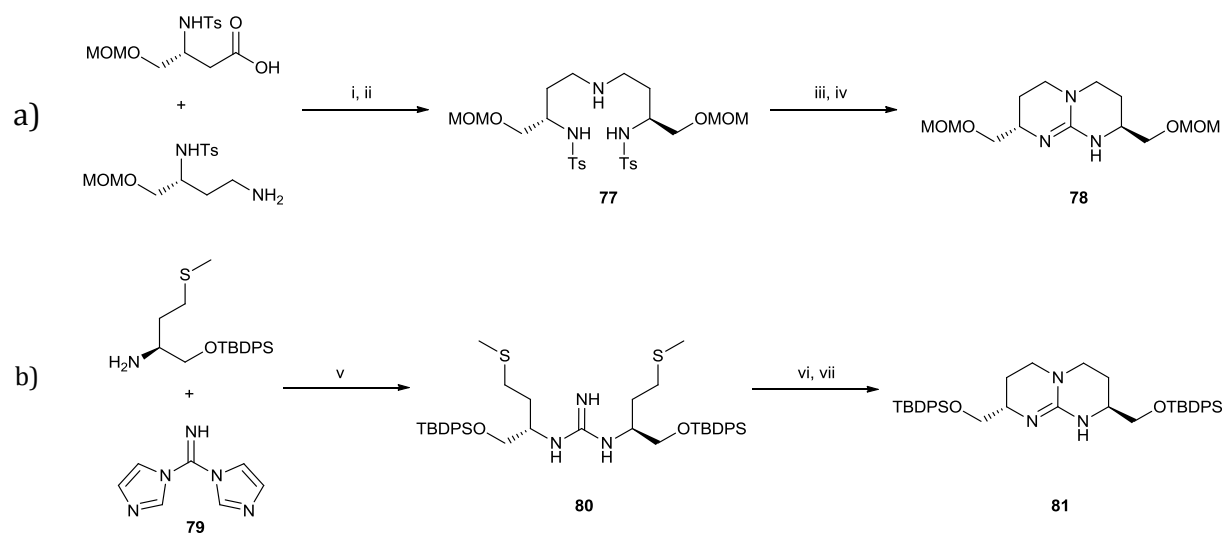
The asymmetric synthesis of chiral bicyclic guanidines has seen the natural chiral pool exploited. Schmidtchen *et al.* synthesized bicyclic guanidinium salts as anchor modules for abiotic anion receptor functions.^{84, 85} Their synthetic pathway (scheme 1.15) started with α -amino acids L-methionine and L-asparagine. L-methionine was reduced, silyl protected and converted to its corresponding isothiocyanate (**74**). This was then coupled to Tosyl-protected diamino alcohol **72**, which had been prepared from L-asparagine. Cyclization of the resulting thiourea **75** was achieved through methylation at the sulfur atoms to give **76**. Münster *et al.* synthesised the homologue by an analogous route from β -homomethionine and 5-hydroxymethyl-2-pyrrolidinone.⁸⁶



i. Ts-Cl, $(\text{CH}_3)_2\text{CO}$ (**80** %); ii. LiBH_4 , TMS-Cl, THF (**86** %); iii. $\text{BH}_3\cdot\text{DMS}$, THF (**85** %); iv. TBDPS-Cl, imidazole, CH_3CN (yield not given); v. CSCl_2 , Na_2CO_3 , $\text{CH}_2\text{Cl}_2/\text{H}_2\text{O}$ (1:1) (**87** %); vi. **72**, CH_3CN (**85** %); vii. TBDPS-Cl, imidazole, CH_2Cl_2 (**91** %); viii. a) TEA, MeOTf, b) TEA (**87** %).

Scheme 1.15 –Chiral bicyclic guanidine synthesis from L- α -methionine and L- α -asparagine.^{84, 85}

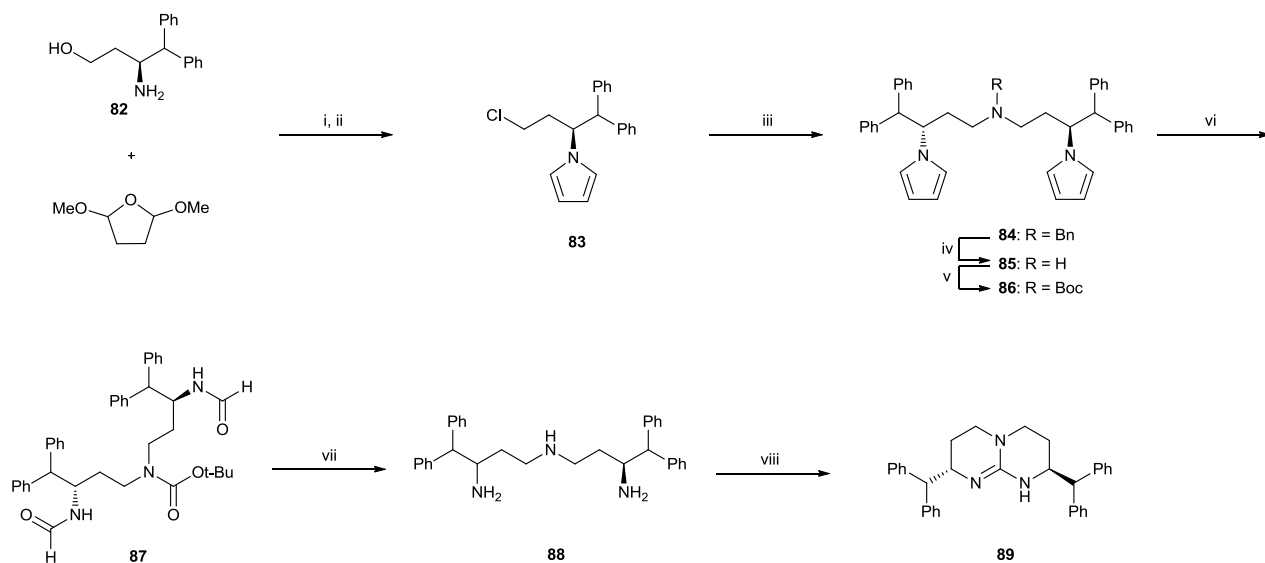
These chiral bicyclic guanidines containing bis(hydroxymethyl) functionality have also been synthesised from the coupling of an acid and amine derived from optically pure α -asparagine, followed by reduction to give triamine **77**. The introduction of the guanidinium C-atom was achieved in 40 % yield using tetramethyl orthocarbonate, which gave the di-protected bicyclic guanidine **78** (scheme 1.16a).⁸⁷ Another method for production of these di-substituted bicyclic guanidino compounds involved guanidinylation of L- α -methionine using di(1H-imidazol-1-yl)methanimine **79** (scheme 1.16b).⁸⁸ The cyclization of **80** takes place in a similar manner to that of others, via methylation followed by stirring in an excess of base to furnish **81**.



i. CDI, CH₂Cl₂, 24 h (**70 %**); ii. LAH, THF, reflux, 24 h (**60 %**); iii. Na, NH₃(l), THF (**70 %**); iv. C(OCH₃)₄, DMSO, 120 °C, 40 h (**40 %**); v. cat. CF₃CO₂H, 105 °C, 4 h (**77 %**); vi. MeI (**98 %**); vii. DBU, CH₂Cl₂, 4 h (**45 %**).

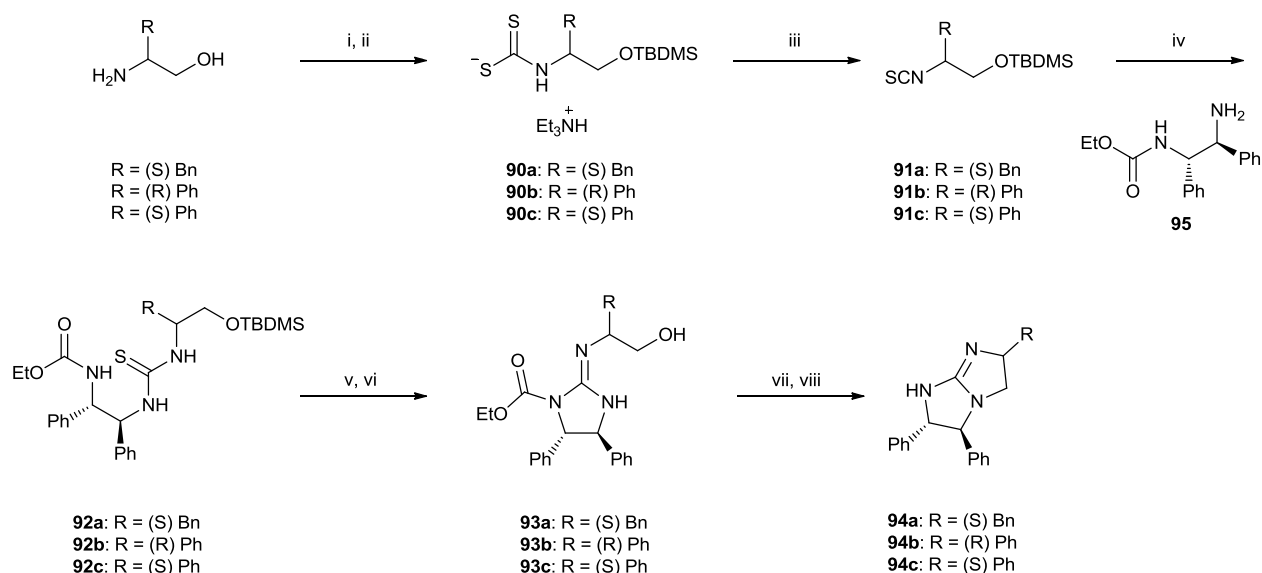
Scheme 1.16 – Synthesis of α,α' -di-protected-methoxy-bicyclic guanidines **78**⁸⁷ and **81**.⁸⁸

Di-benzhydryl bicyclic guanidines have been synthesised via the bis-alkylation of benzylamine.⁵² The synthesis began with 3-amino-4,4-diphenylbutan-1-ol (**82**), which has been enantiospecifically synthesised from L-homoserine lactone hydrochloride.⁸⁹ This was pyrrole-protected and converted to chloride **83**. Bis-alkylation of benzylamine with **83** was followed by removal of the protecting groups, thus furnishing the tetraphenyl triamine **88**. The cyclization proceeded in a similar manner to that of others, in this instance dimethyl carbonotrithioate was used to introduce the central carbon of the guanidine moiety and cyclization was achieved through methylation of the resulting thiourea to give **89**.⁵²



Scheme 1.17 – Benzhydryl-bicyclic guanidine **89** via bis-alkylation of benzylamine.⁵²

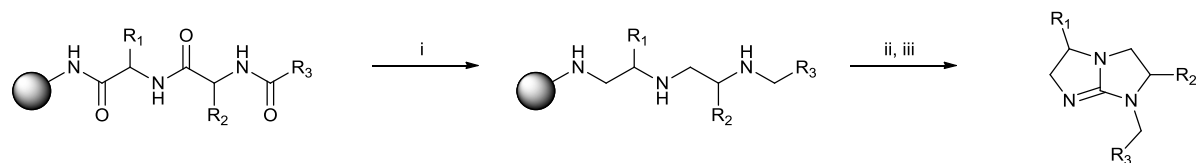
Isobe has utilized the versatile reagent 2-chloro-1,3-dimethylimidazolium chloride (DMC) to synthesize diphenylbenzyl and triphenyl substituted bicyclic guanidines.⁹⁰ This approach (scheme 1.18) proceeded in a similar manner to that of previous syntheses. The synthetic route began with optically pure amino alcohols which were silyl protected. The central carbon was inserted via carbon disulfide producing dithiols **90a-c**, which were converted to isothiocyanates **91a-c** using DMC, coupling to protected diamine **95** gave thioureas **92a-c**. DMC was then used to form monocyclic guanidines **93a-c** by displacement of sulfur. Deprotection then preceded the second cyclization again utilizing DMC to give the protected substituted bicyclic guanidines **94a-c**. This method has also been used to produce tetra-substituted C₂-symmetric [5,5] bicyclic guanidines.⁹¹



i. TBDMS-Cl, TEA, DMAP, CH₂Cl₂ (**100 %**); ii. CS₂, TEA, CH₂Cl₂; iii. DMC, TEA, CH₂Cl₂ (**96 %** 2 steps); iv. **95**, CH₂Cl₂, reflux (**98 %**); v. DMC, TEA, MeCN, reflux (**88 %**); vi. TBAF, THF (**96 %**); vii. DMC, TEA, MeCN, reflux (**57 %**); viii. NaOMe, MeOH (**89 %**)

Scheme 1.18 – The synthesis of tri-aryl substituted [5,5] bicyclic guanidines.⁹⁰

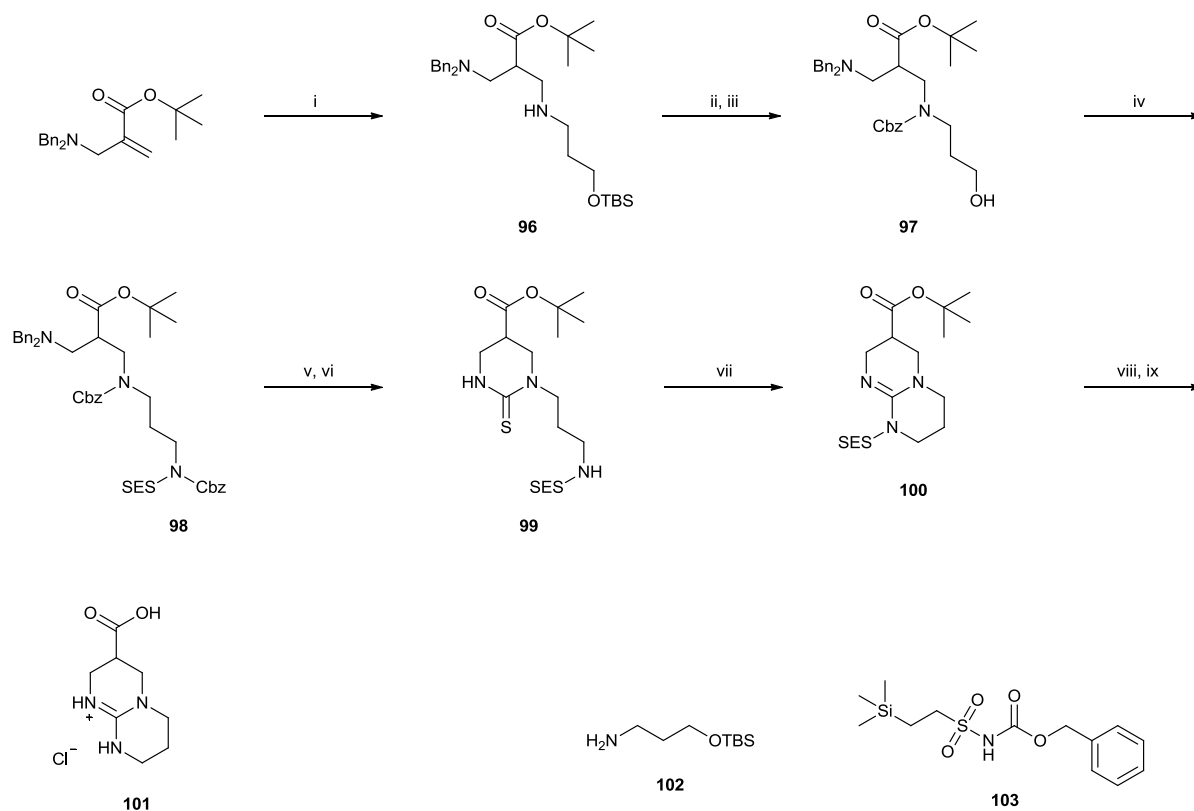
Nefzi *et al.* utilized combinatorial chemistry to synthesise a series of functionalised bicyclic guanidines using solid phase chemistry.^{92, 93} Tripeptides containing a variety of functionality were converted to their corresponding triamines by reduction. A library of tri-alkyl-substituted bicyclic guanidines was produced following cyclization using thiocarbonyldiimidazole and cleaved from the resin.⁹⁴ Further work has seen the production of libraries of bicyclic guanidines tri-substituted with a variety of amino acid side chains.⁹⁵



i. BH₃.THF, THF; ii. CS(Im)₂; iii. HF

Scheme 1.19 – Solid-phase synthesis of tri-substituted [5,5] bicyclic guanidines.^{92, 93}

Grillot and Hart synthesised a bicyclic guanidine functionalised at the C₃ position (scheme 1.20).⁹⁶ Their synthesis focused on formation of substituted triamine **98**. Following deprotection and thiourea formation, the bicyclic guanidine (**100**) was formed by sulfur alkylation and intramolecular nucleophilic substitution.



i. **102**, *n*-BuLi, THF, -78 °C (**66** %); ii. PhCH₂OCOCl, TEA, THF, 0 °C (**84** %); iii. TBAF, THF, rt (**97** %); iv. PPh₃, DEAD, **103**, THF, rt (**94** %); v. Pd(OH)₂, H₂, EtOH; vi. (Im)₂C=S, CH₂Cl₂, Δ (**51** % **2** steps); vii. CH₃I, MeOH, Δ (**81** %); viii. HCl, CH₂Cl₂ (**93** %); ix. TBAF, DMF, HCl, H₂O (**100** %).

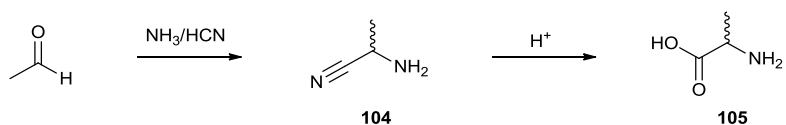
Scheme 1.20 – Grillot and Hart's synthesis of C₃ substituted bicyclic guanidine **101**.⁹⁶

1.2.3 Amino acid synthesis

The synthesis of non-natural amino acids is of high importance in the field of molecular biology. These amino acids can be incorporated into peptides which bind to specific targets and either stimulate or inhibit a certain response. There are several methods for synthesising or inserting amino acid functionality into organic compounds.

1.2.3.1 Strecker synthesis

Much research has taken place involving the synthesis and introduction of the amino acid moiety into a variety of compounds both simple and more complex. This work dates back to the 19th century, when Adolph Strecker devised a condensation reaction that synthesized racemic alanine from acetaldehyde.⁹⁷ The reaction (scheme 1.21) proceeded through the formation of α -amino nitrile **104**, which then underwent acid hydrolysis to furnish α -alanine (**105**).



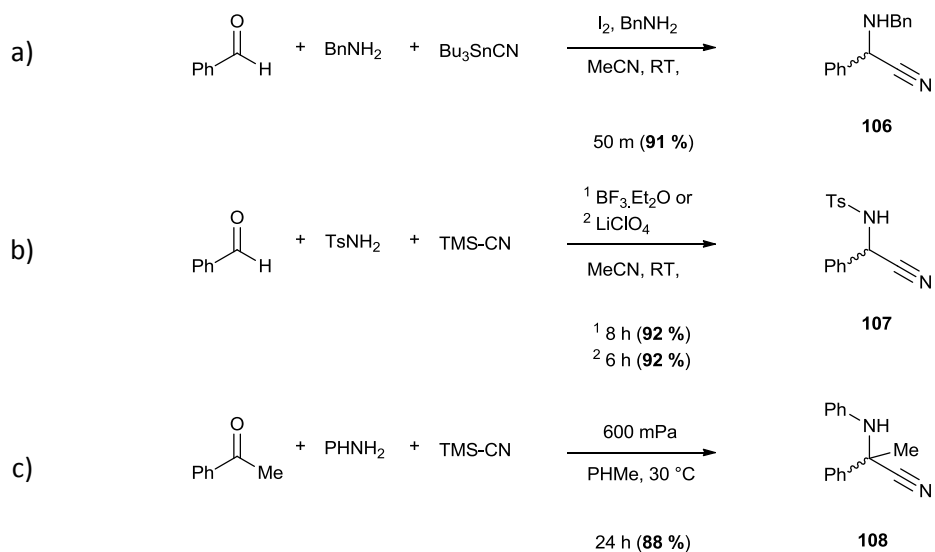
Scheme 1.21 – The Strecker synthesis, discovered by Adolf Strecker in 1850.⁹⁷

1.2.3.1.1 Racemic synthesis

Since the early days of the Strecker synthesis, the chemistry of this method has been expanded. Different starting materials have been explored, with a wide range of aldehydes and ketones being employed.

As well as naturally occurring amino acids the Strecker reaction has been employed to synthesize a variety of racemic non-natural amino acids. Since the early days of the Strecker synthesis, much work has been performed to expand its usefulness. The synthesis discovered by Adolph Strecker was quite sluggish, typical reaction times were 3-5 days and only moderate yields were achieved. Since then the reaction times and yields have been dramatically improved. Iodine catalysed reactions using aryl or alkyl amines as the amino source and using tributyltin cyanide have seen yields of the racemic product above 80 % with a reaction time less than 65 minutes.⁹⁸ Moreover, conversion to the tosylaldimine followed by introduction of TMS-CN, catalysed by either BF₃.Et₂O or LiClO₄ has seen formation of the corresponding tosyl-amino nitriles proceed with yields greater than 90 %.⁹⁹

Strecker reaction using ketones is very slow and produces very poor yields or none at all. However, performing the reaction at high pressures has seen the Strecker synthesis of a range of ketones, aniline and TMS-CN take place in the absence of catalyst, while proceeding in high yields (up to 99 %) at 600 mPa.^{100, 101}



Scheme 1.22 – Endeavours to improve the yield of the Strecker synthesis. a) Iodine catalysed.⁹⁸ b) Lewis acid catalysed.⁹⁹ c) High pressure Strecker synthesis.^{100, 101}

Attempts to simplify and speed up the work up and purification while producing the α -aminonitriles in high yields have seen the Strecker reaction proceed in the presence of solid supported catalysts. These can be recovered simply by filtration at the end of the reaction.^{102, 103}

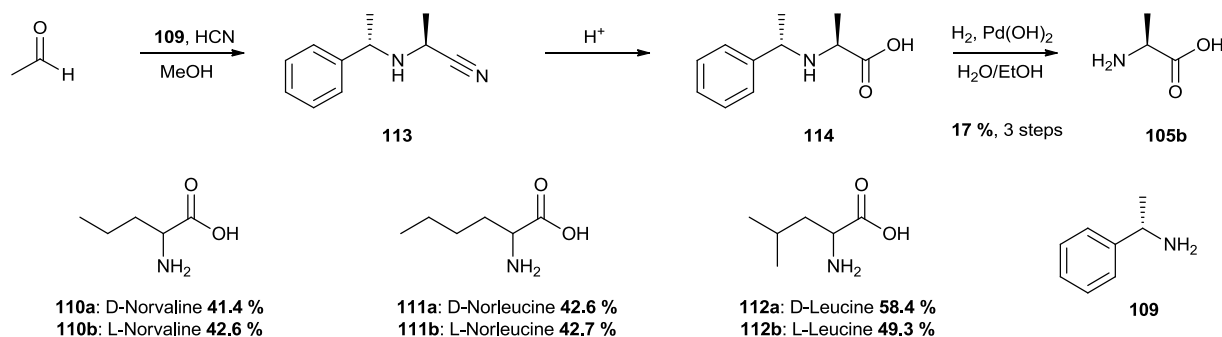
1.2.3.1.2 Asymmetric synthesis

The disadvantage with the racemic Strecker reaction is the necessity to optically resolve the enantiomers. For this reason the implementation of asymmetric methods for the Strecker synthesis has been studied; such attempts have included utilizing chiral auxiliaries, thus increasing the stereospecificity of the reaction, although often resulting in a reduction in yield. More recently, the continuing development of this method has focused

on the use of inorganic as well as organic catalysts to produce the enantiopure products in high yields and high enantiomeric excess.

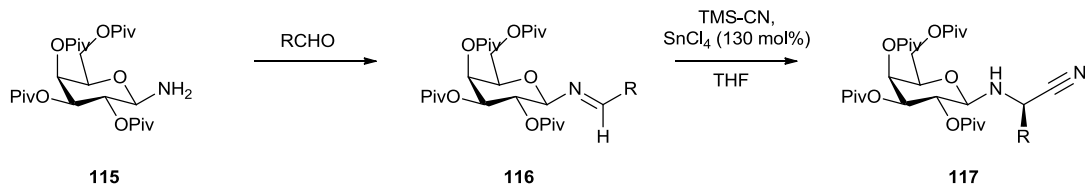
1.2.3.1.3 Chiral auxiliaries

The first documented asymmetric synthesis of an α -amino acid utilizing a chiral auxiliary saw Harada make use of D- α -methylbenzylamine as the amino source in the Strecker reaction.⁶ This resulted in the formation of the Schiff base which preceded cyanide addition. Subsequent hydrolysis followed by hydrogenation to remove the *N*-alkyl residue afforded the optically active L-alanine (**105b**) in low yield (17 %). Furthermore, α -methylbenzylamine has been employed to synthesise optically pure norvaline (**110a-b**), leucine (**112a-b**) and norleucine (**111a-b**) in both L and D stereoisomers.¹⁰⁴ However, the high optical purity obtained when using this chiral auxiliary was likely to be due to re-crystallisations during the products isolation.^{105, 106}



Scheme 1.23 – Harada's asymmetric Strecker reaction using α -methylbenzylamine as chiral auxiliary.⁶

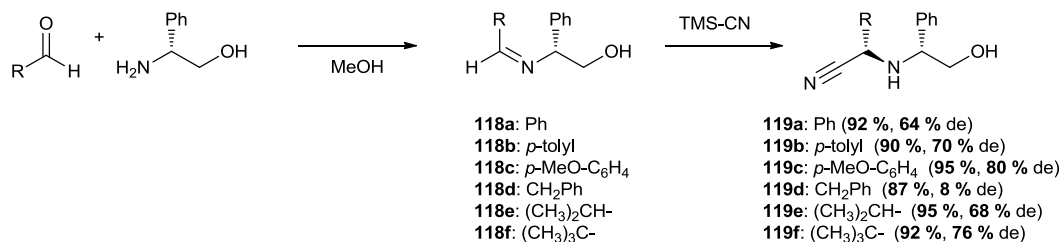
Kunz synthesized optically pure α -amino nitriles (table 1.1) in high yields using the galactosylamine auxiliary (**115**) and stoichiometric amounts of Lewis acid.¹⁰⁷ The reaction again took place through formation of a Schiff base intermediate (**116**) which partially directed the nucleophilic attack from TMS-CN. Highest yields and enantioselectivity was seen when using THF as the solvent, the α -amino nitriles were obtained in high yields (74-91 %) and up to 86 % enantiomeric excess (ee). The direction of asymmetric induction of cyanide has been reversed by changing the solvent to chloroform while using zinc chloride as the Lewis acid.¹⁰⁸



R	Temp (°C)	Reaction Time (h)	Diastereoselectivity (R:S)	Yield (%)
<i>p</i> -tolyl	-78 – -30	8	12:1	87
<i>o</i> -NO ₂ C ₆ H ₄	-30	8	Only (R)	91
<i>p</i> -F-C ₆ H ₄	-78 – -30	8	10:1	84
<i>p</i> -Cl-C ₆ H ₄	-60 – -10	6	11:1	84
Me ₂ CH-	-78 – -10	5	8:1	74
Me ₃ C-	-78 – -10	3	13:1	86

Table 1.1 – Asymmetric Strecker synthesis, catalysed by galactosylamine **107** and SnCl₄.¹⁰⁷

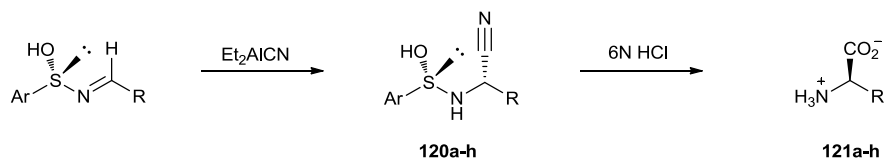
α -Phenylglycinol has been employed as a chiral auxiliary for the asymmetric Strecker reaction of aliphatic and aromatic substrates. In most cases, high yields (90-95 %) and good diastereoselectivities (64-80 %) of the *syn* product were obtained when used in combination with TMS-CN (scheme 1.24).^{109, 110}



Scheme 1.24 – α -phenylglycinol auxiliary three component asymmetric Strecker reaction.^{109, 110}

Chiral sulfinimines have been employed as chiral auxiliaries and have received some success in increasing the stereospecificity of the Strecker synthesis with a range of substrates.¹¹¹⁻¹¹⁵ Davis documented the use of sulfinimines in combination with diethylaluminium cyanide (table 1.2). This produced good yields (62-78 %) and modest diastereomeric excess (38-66 %) of the α -aminonitriles **120a-f**. These were converted to the corresponding α -amino acids (**121a-f**) in high yields and excellent ee following

purification (>95 %). Addition of a stoichiometric amount of isopropanol has seen the production of α -amino nitriles with improved yields and higher de (**120g** and **h**).¹¹² An advantage of using these sulfinimines is their mild removal, a typical sulfinimine cleavage is possible by refluxing in 3M HCl.¹¹⁴



Compound	R =	Ar =	Solvent/Temp (°C)	Yield of 120 (%) ^a	de (%) ^b	% Yield of 121 (ee) ^d
a	Ph	tolyl	Et ₂ O/ -78 – -15	72	40	71 (>95)
b	<i>n</i> -Pr	tolyl	Et ₂ O/ -78 – -15	67	38	79 (>95)
c	<i>i</i> -Bu	tolyl	Et ₂ O/ -78 – -15	62	42	67 (>95)
d	Ph	2-methoxy-1-naphthyl	Et ₂ O-THF/ -78 – -10	78	60	81 (>95)
e	<i>i</i> -Pr	2-methoxy-1-naphthyl	THF/ -78 – -40	75	66	73 (>95)
f	<i>i</i> -Bu	2-methoxy-1-naphthyl	THF/ -78 – -40	72	66	71 (>95)
g	Ph	tolyl	THF- <i>i</i> -PrOH ^e / -78 – rt	64 (33) ^f	80	-
h	<i>t</i> -Bu	tolyl	THF- <i>i</i> -PrOH ^e / -78 – rt	80	91	-

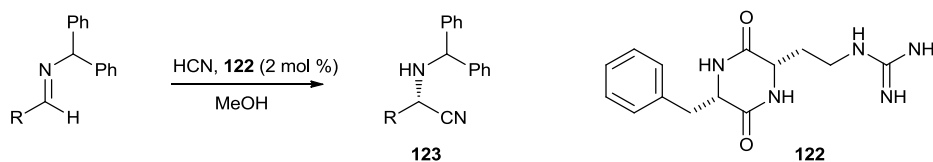
^a isolated yield of diastereomeric mixtures. ^b determined by ¹H NMR spectroscopy, ^c Isolated yield of **121** from the major diastereoisomer. ^d ee was determined by comparisons of their optical rotations with authentic samples. ^e 1 equivalent of *i*-PrOH was used in the reaction. ^f number in parenthesis is the % of starting material recovered.

Table 1.2 – The asymmetric Strecker reaction of sulfinimines and diethylaluminium cyanide.¹¹¹⁻¹¹⁵

1.2.3.1.4 Organocatalysis

Lipton *et al.* used a cyclic dipeptide composed of L-phenylalanine and the lower homologue of L-arginine as a catalyst for the enantioselective Strecker synthesis.⁷ The dipeptide **122**

catalysed the cyanide addition to benzhydryl protected aryl imines in good to high yields and in high to excellent ee (table 1.3).

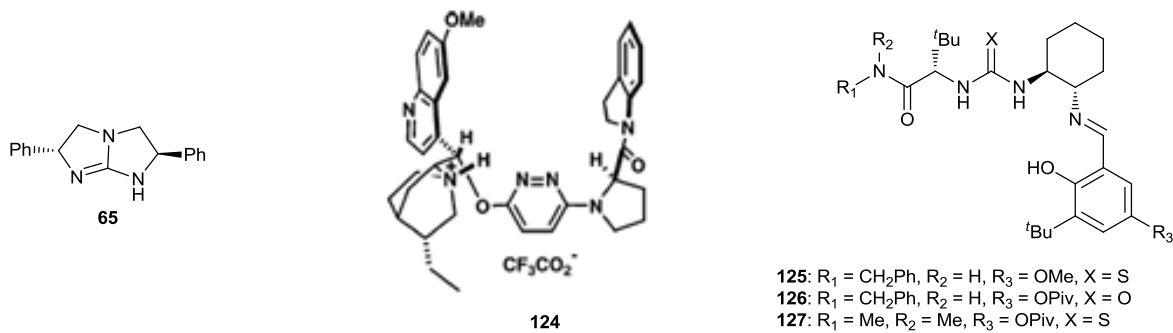


R	Temp (°C)	Yield (%) ^a	ee (%) ^b
Ph	-25	97	>99
4-Cl-C ₆ H ₄	-25	97	83
4-Cl-C ₆ H ₄	-75	94	>99
4-OMe-C ₆ H ₄	-25	96	64
4-OMe-C ₆ H ₄	-75	90	96
3-Cl-C ₆ H ₄	-75	80	>99
3-OMe-C ₆ H ₄	-75	82	80
3-NO ₂	-75	71	<10
3-Pyridyl	-75	86	<10
2-furyl	-75	94	32
<i>i</i> -Pr	-75	81	<10
<i>t</i> -Bu	-75	80	17

^a Based on ¹H NMR of the crude product. ^b Determined by chiral HPLC.

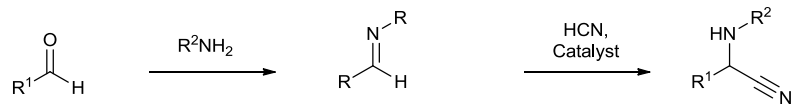
Table 1.3 – The organocatalysed Strecker reaction using Lipton’s cyclic dipeptide.⁷

Corey and Grogan achieved high yields and enantioselectivities (up to 86 % ee) of *N*-benzhydryl amino nitriles from their corresponding *N*-benzhydryl arylimines using their chiral di-phenyl substituted [5,5] bicyclic guanidine catalyst **65** (*vide supra*) at -40 °C.⁸¹ Huang and Corey used a chiral ammonium salt (**124**) to catalyse a series of aromatic *N*-allyl imines to their corresponding amino nitriles which were isolated as their *N*-trifluoroacetyl derivatives in good enantiomeric excess (79->99 %) and high yields (86-98 %).¹¹⁶



Tsogoeva and co-workers synthesised a range of thiourea derived catalysts and assessed their catalytic efficiency towards the asymmetric addition of HCN to aromatic imines. The enantioselectivity however, was very low (4-14 % ee).¹¹⁷ Modifying the catalysts did improve the enantioselectivity (up to 68 % ee). However, the new range of catalysts proved to be entirely substrate dependant, with a significant reduction in enantiomeric excess from the one substrate to the another.¹¹⁸

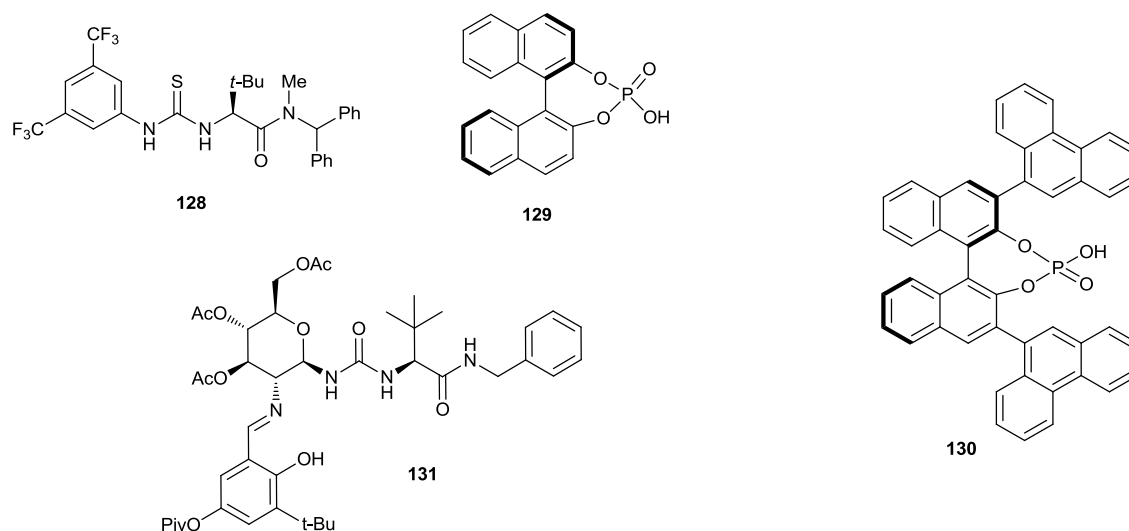
Sigman *et al.* exploited combinatorial chemistry to develop thiourea base catalyst (**125**) which was employed to convert several *N*-allyl protected aldimine substrates, both aromatic and aliphatic, to their corresponding α -amino acids in good to high yields (65-92 %) and enantiospecificities (70-91 % ee) using HCN at -70 °C (table 1.4, entries 1-6).¹¹⁹ The use of a urea derivative with aryl pivaloyl functionality (catalyst **126**) resulted in increased yields (up to 99 %) and asymmetric induction (up to 96 % ee) for a diverse repertoire of *N*-protected aldimine substrates under the same conditions (entries 7-20).⁸ This catalyst has also been used for the addition of cyanide to ketimines.¹²⁰ It was later discovered that replacement of the secondary amine and urea moieties of **126** with a tertiary amine and thiourea respectively to give **127**, resulted in further increase in enantioselectivity (up to >99 %) of the catalyst (entries 21-24).¹²¹



Entry	R ₁	R ₂	Catalyst	Yield (%)	ee (%)
1	Ph	allyl	125	78	91
2	<i>p</i> -OCH ₃ -C ₆ H ₄	allyl	125	92	70
3	<i>p</i> -Br-C ₆ H ₄	allyl	125	65	86
4	2-naphthyl	allyl	125	88	88
5	<i>t</i> -butyl	allyl	125	70	85
6	cyclohexyl	allyl	125	77	83
7	C ₆ H ₅	allyl	126	74	95
8	<i>t</i> -Butyl	allyl	126	75	95
9	<i>p</i> -OCH ₃ -C ₆ H ₄	allyl	126	98	95
10	<i>m</i> -OCH ₃ -C ₆ H ₄	allyl	126	99	93
11	<i>o</i> -OCH ₃ -C ₆ H ₄	allyl	126	93	77
12	<i>p</i> -CH ₃ -C ₆ H ₄	allyl	126	99	95
13	<i>p</i> -(CH ₃) ₃ CC ₆ H ₅	allyl	126	89	97
14	<i>t</i> -Butyl	benzyl	126	88	96
15	Cyclohexyl	benzyl	126	85	87
16	1-Cyclohexenyl	benzyl	126	90	91
17	(CH ₃) ₃ CCH ₂	benzyl	126	85	90
18	CH ₃ (CH ₂) ₄	benzyl	126	69	78
19	Cyclopropyl	benzyl	126	89	91
20	cyclooctyl	allyl	126	65	90
21	<i>i</i> -Pr	benzyl	127	-	97
22	<i>n</i> -Pent	benzyl	127	-	96
23	<i>t</i> -Bu	benzyl	127	-	99.3
24	Ph	benzyl	127	-	99.3

Table 1.4 – Organocatalysed Strecker reaction, comparison of catalysts **125**, **126** and **127**.¹⁰¹⁻¹⁰⁴

While organocatalyst **127**, developed by Jacobsen, gave high yields and enantiospecificity with a plethora of substrates, its synthesis was laborious, requiring 8 steps for its construction. Moreover, its catalytic efficiency is only applicable to HCN as a cyanide source, with only a 25 % ee achieved when using TMS-CN and aldimines.¹²² The use of a similar catalyst (**128**), which was synthesised in only three steps, has seen the Strecker reaction proceed using TMS-CN and produced yields and levels of asymmetric induction comparable with **127**.¹²³

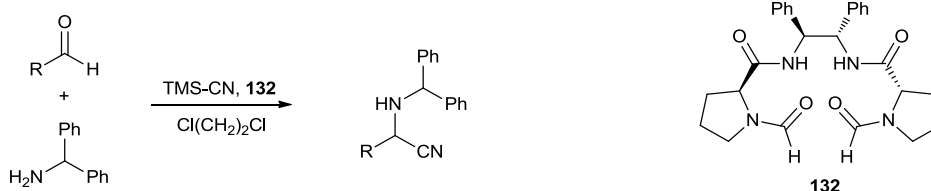


Zhang *et al.* used Brønsted acid **129** to catalyse the Strecker reaction. This binaphthyl phosphoric acid catalyst encouraged the conversion of a range of aryl ketones to racemic α -amino nitriles in high yields using TMS-CN as the cyanide source.¹²⁴ Similarly, aryl substituted binaphthyl phosphoric acid catalyst **130** has been used to transform *N*-benzyl protected aryl aldimines to their α -amino nitrile derivatives at -40 °C. Good to excellent yields (53-97 %) along with high enantioselectivities (85-99 % ee) were obtained for a range of aryl substrates, including heteroaromatic, substituted naphthyl and substituted phenyl derivatives.¹²⁵

Becker *et al.* developed a catalyst constructed from glucosamine (**131**) which was used for the asymmetric Strecker synthesis. Conversion of aromatic aldehydes to their

corresponding amino nitriles was achieved in high yields and enantiomeric excess up to 84 %.¹²⁶

Chiral bisformamides have also been shown to be effective towards the asymmetric Strecker synthesis. This synthesis, like many others, proceeds through the *in situ* formation of a Schiff base (*N*-benzhydryl) prior to addition of cyanide. Again a range of substrates were assessed, the best results in terms of stereospecificity were obtained from the aryl substituted substrates (75-86 % ee).⁹

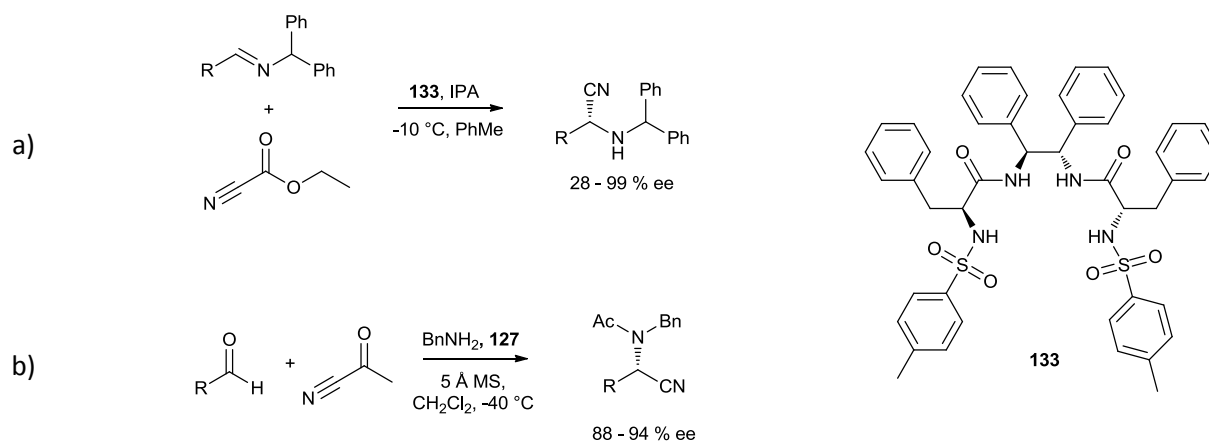


Entry	R	Time (h)	Yield ^a	ee ^b
1	phenyl	10	99	81 (R) ^c
2	4-methylphenyl	10	98	84 (>99) ^d
3	2-methylphenyl	10	99	80 (R) ^c
4	3-methylphenyl	10	97	76
5	4-methoxyphenyl	10	96	85
6	3-methoxyphenyl	14	97	76
7	4-chlorophenyl	50	98	83
8	3-chlorophenyl	60	74	73
9	2-chlorophenyl	50	81	75 (R) ^c
10	4-bromophenyl	60	85	86 (>99) ^d
11	4-phenylphenyl	14	94	86
12	2-naphthyl	50	75	81 (R) ^c
13	<i>tert</i> -butyl	14	92	73
14	2-furyl	14	94	43

^a Isolated yield. ^b Determined by chiral HPLC. ^c The absolute configuration was established as *R* by comparison of literature. ^d After single recrystallization.

Table 1.5 – Chiral bisformamide **132** catalysed Strecker reaction.⁹

Attempts to avoid the use of highly toxic HCN or TMS-CN have seen the formation of amino nitriles in high yields and high ee for a range of alkyl and aryl *N*-benzhydryl protected imines by utilizing the chiral amide based organocatalyst **133** and using ethylcyanoformate as the cyanide source (scheme 1.25a).¹²⁷ Furthermore, List and co-workers produced a variety of di-protected α -amino nitriles with high levels of asymmetric induction (88-94 % ee) using a three-step, one-pot reaction containing acetylcyanide as the cyanide source, Jacobsen's catalyst (**127**) and the corresponding aldehydes (scheme 1.25b).¹²⁸

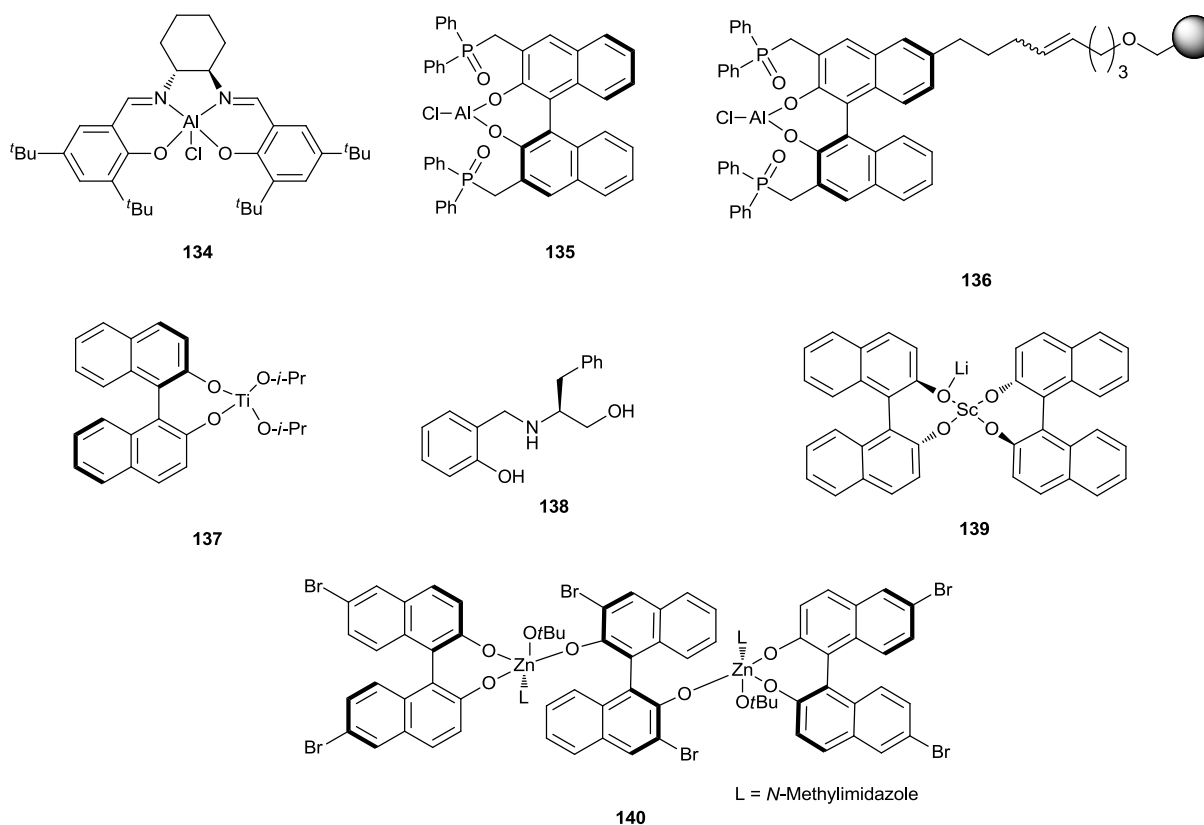


Scheme 1.25 – Strecker reactions using unusual cyanide sources. a) Asymmetric Strecker reaction of aldimines with ethylcyanoformate catalysed by **133**.¹²⁷ b) Three component asymmetric Strecker reaction using benzylamine, acetylcyanide and Jacobsen's catalyst **127**.¹²⁸

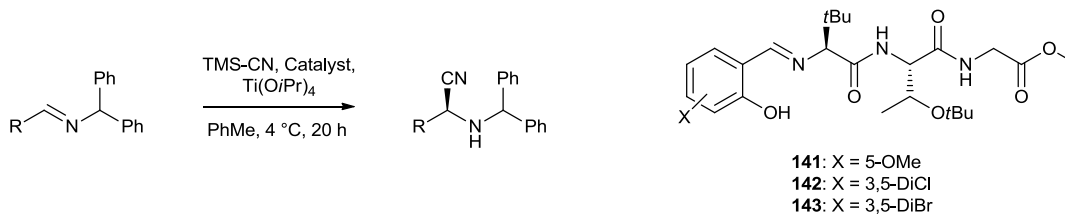
1.2.3.1.5 Metal-ligand catalysts

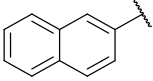
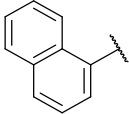
Jacobsen *et al.* developed a chiral (salen)Al(III) complex (**134**) that was successful in catalysing the addition of cyanide to *N*-allyl protected aryl imines. The reaction proceeded to give the corresponding α -amino nitriles in high yields (91-95 %) and good to excellent enantiospecificity (79-95 % ee). However, yields and ee for aliphatic substrates were poor (up to 77 % and 57 % ee).¹²⁹ The use of the aluminium-binaphthol catalyst **135**, which contains both Lewis acid and Lewis base functionality, has been utilized in combination with the additive $\text{Bu}_3\text{P}(\text{O})$ to vastly increase the yields (97-100 %) and ee (83-98 %) of aliphatic substrates.¹³⁰ Furthermore, the binaphthol di-functional catalyst has been bound

to a solid support (**136**) which allows its simple retrieval, while still producing high yields (96-100 %) and ee of 83-87 % for aryl and α - β -unsaturated imines.¹³¹



Many complexes comprising transition metals bearing ligands have been used while attempting to increase the enantioselectivities of the Strecker reaction. Many have focused on titanium complexes.¹³²⁻¹³⁴ An enantiomeric excess of 30 % was seen when using BINOL-Ti-O^{*i*}Pr₂ complex **137**.¹³² However, enantiopurity has been increased when the *N*-salicyl- β -aminoalcohol **138** was used as a ligand for Ti(O^{*i*}Pr)₄ complexes (up to 80 % ee).¹³³ This has been increased further when employing ligands **141-143**. These ligands, which consist of two amino acids and an aryl Schiff base, form complexes with titanium and convert a range of aromatic achiral imines to their optically pure α -amino nitriles (<99 % ee, after purification) in excellent yields (80-97 %).¹³⁴



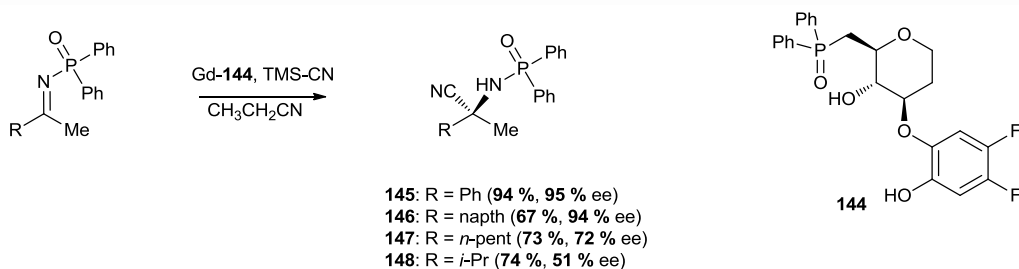
entry	R =	catalyst	conv (%), ee (%) ^a	yield (%), ee (%) ^a
1	Ph	141	99 (97)	82 (>99) ^b
2	<i>o</i> -Cl-C ₆ H ₄	142	96 (93)	85 (>99) ^b
3	<i>o</i> -Br-C ₆ H ₄	142	99 (94)	93 (>99) ^b
4	<i>p</i> -MeO-C ₆ H ₄	142	100 (94)	99 (94) ^c
5	Naphthyl 	141	100 (93)	80 (>99) ^b
6	Naphthyl 	141	93 (90)	87 (>99) ^b
7	<i>t</i> -Butyl	143	100 (85)	97 (85) ^c

^a Enantioselectivities determined by HPLC in comparison with authentic racemic materials. ^b Purified by recrystallization. ^c Purified by silica gel chromatography.

Table 1.6 – Asymmetric Strecker reaction catalysed by Ti-complexes **141**, **142** and **143**.¹³⁴

Other complexes of binaphthols (or BINOLs) and transition metals have been used to improve stereoselectivity in the asymmetric Strecker synthesis. The zirconium complex **140** has been used to catalyse the conversion of *N*-protected alkyl or aryl aldimines, to their corresponding enantioenriched α -aminonitriles in good yields (76-100 %) and high enantiopurities (84-94 %) using HCN or Bu₃SnCN as the cyanide source.¹³⁵ Similarly, the Sc[(*R*)-BINOL]₂Li complex **139** has seen the addition of cyanide to ketimines proceed in high yield (80->95 %) and 86 – 88 % ee when using TMS-CN as the cyanide source. Yields and optical purity are slightly lower when HCN is used.¹³⁶ Lanthanide complexes have also

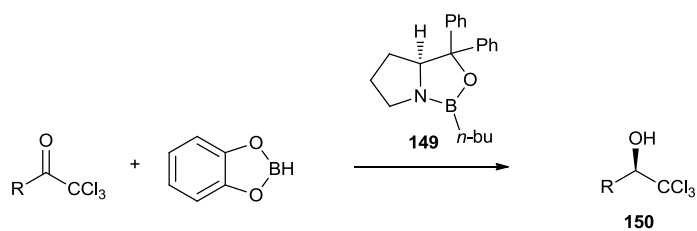
been used to achieve good to excellent ee (up to 98 %) of P(O)Ph₂ protected ketoimines using gadolinium(III) tris(isopropoxide) (Gd(O*i*Pr)₃) and ligand **144** (scheme 1.26).¹³⁷



Scheme 1.26 – Synthesis of enantioenriched *N*-diphenylphosphinoyl α -amino nitriles catalysed by a Gd-**144** complex.¹³⁷

1.2.3.2 Corey-Link amino acid synthesis

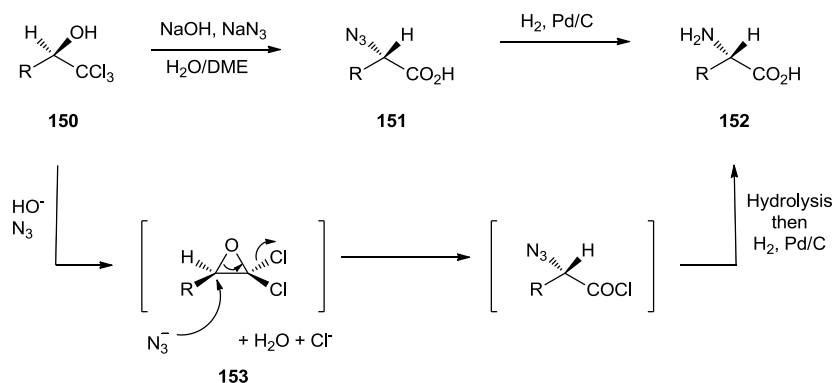
Corey, Link and co-workers¹⁰ devised a two-step method to produce optically pure α -amino acids. The first step involves asymmetric reduction of trihalomethyl ketones to their corresponding secondary alcohols using catecholborane and a chiral oxazaborolidine catalyst **149** (table 1.7). The second step (scheme 1.27) began with nucleophilic attack by an azide, which produced clean inversion of stereochemistry via a ‘gem-dichlorooxirane’ intermediate (**153**) to give the acid chloride which was quickly hydrolysed to the azido acid **151**. This was then converted to its corresponding amino acid (**152**) by palladium catalysed hydrogenolysis.



R	solvent	temp (°C)	duration (h)	ee (%) ^a
<i>n</i> -C ₅ H ₁₁	PhMe	-60 ^b	12	95
C ₆ H ₅ (CH ₂) ₂	PhMe	-78	12	95
4-C ₆ H ₅ C ₆ H ₄ CH ₂	CH ₂ Cl ₂	-44	10	96
2-naphthylmethyl	CH ₂ Cl ₂	-23	1.7	93
<i>c</i> -C ₆ H ₁₁	CH ₂ Cl ₂	-20 ^b	48	92
<i>t</i> -C ₄ H ₉	PhMe	-20 ^b	56	98
<i>t</i> -C ₄ H ₉	PhMe	23	12	95

^a Alcohol ee % determined by chiral HPLC. ^b These reactions were initiated at -78 °C and brought to the indicated temperature after 1 h.

Table 1.7 – Enantioselective reduction of trichloromethyl ketones.¹⁰



Scheme 1.27 – Conversion of trichloromethyl carbinol to azido acid **151** and amino acid **152**.¹⁰

R	% yield of 151	% yield of 152	$[\alpha]^{24}_D$ of 152 (solv) ^a
<i>n</i> -C ₅ H ₁₁	89	94	+23.6° (6 N HCl)
C ₆ H ₅ (CH ₂) ₂	91	92	+48.8° (1 N HCl)
4-C ₆ H ₅ C ₆ H ₄ CH ₂	82	98	+12.4° (MeOH)
2-naphthylmethyl	84	88	-29.6° (AcOH)
<i>c</i> -C ₆ H ₁₁	89	92	+30.2° (5 N HCl)
<i>t</i> -C ₄ H ₉	80	94	-10.8° (H ₂ O)

^a all optical rotations agreed with the literature for optically pure compounds

Table 1.8 – Conversion of trichloromethyl carbinols (**150**) to their corresponding (S)-azido acids (**151**) and (S) amino acids (**152**).

The asymmetric reduction is rate limited by the formation of a catecholborane-oxaxaborolidine-trihaloketone complex **153** (figure 1.7a),^{138, 139} the formation of this intermediate takes place through the lone pair on the oxygen atom of the trihalomethyl ketone. On forming the complex, only the lone pair that is *anti* can form this interaction, with the *syn* conformation being inhibited by the bulky trihalomethyl group (as demonstrated in figure 1.7b).

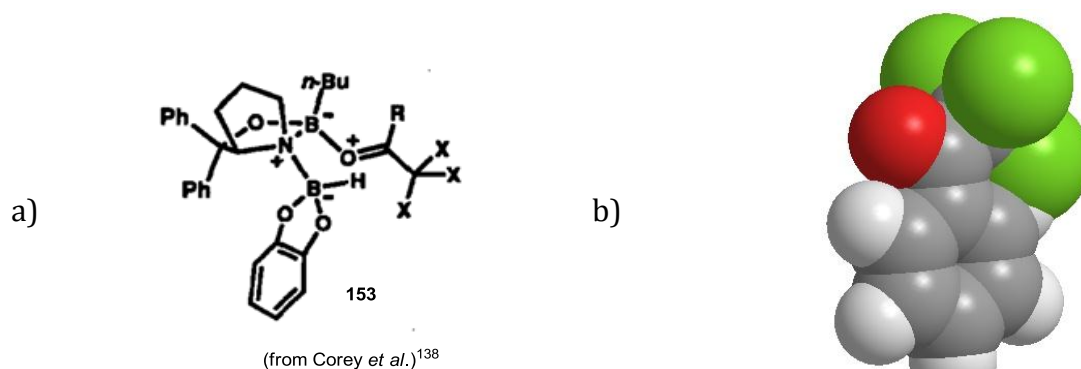
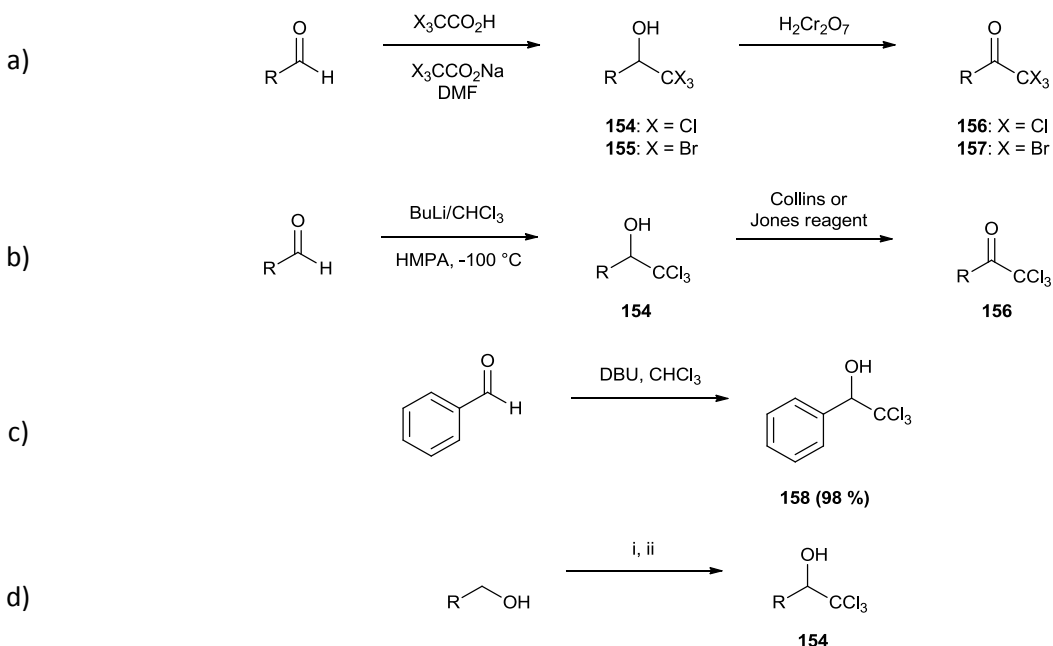


Figure 1.7 – a) Catecholborane-oxaxaborolidine-trihaloketone complex **153**. b) 3D space filling model of trichloroacetone, illustrating the steric hindrance by the trichloro group on the *syn* lone-pair.^{138, 139}

Introducing trichloromethyl ketone functionality into a compound is imperative for the Corey-Link amino acid synthesis. Several methods to introduce this functionality have been

documented. Corey *et al.* demonstrated a procedure, which involved de-carboxylation of sodium trichloroacetate (NaTCA), which took place in DMF at room temperature (scheme 1.28a). This produced the highly reactive trichloromethyl anion, which rapidly added to the aldehyde thus furnishing trichloromethyl carbinol **154**. This was then oxidised with chromium (IV) to its corresponding trichloromethyl ketone (**156**).¹⁴⁰

A similar method has seen generation of the trichloromethyl anion using *n*-butyllithium to deprotonate chloroform; again this rapidly attacked the aldehyde to produce **154** which was oxidised to **156** using Collins reagent or Jones reagent (scheme 1.28b).¹⁴¹ Mereu *et al.* used DBU to deprotonate chloroform in the presence of benzaldehyde, under solvent free conditions thus furnishing **158** in 98 % yield (scheme 1.28c).¹⁴² In a similar vein, Snowden and co-workers described a one pot reaction to the synthesis of trichloromethyl carbinols from their corresponding alcohols. Following oxidation using Des-Martin periodinane (DMP) in CHCl₃, TBD was added and ultimately furnished the corresponding trichloromethyl carbinols in high yields (scheme 1.28d).¹⁴³

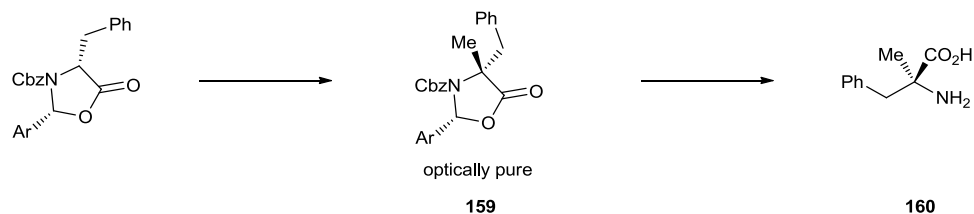


i. DMP, CHCl₃, rt, 4-8 h; ii. TBD, 0 °C → rt,

Scheme 1.28 – Synthesis of trihalomethyl carbinols and ketones.¹²⁵⁻¹²⁸

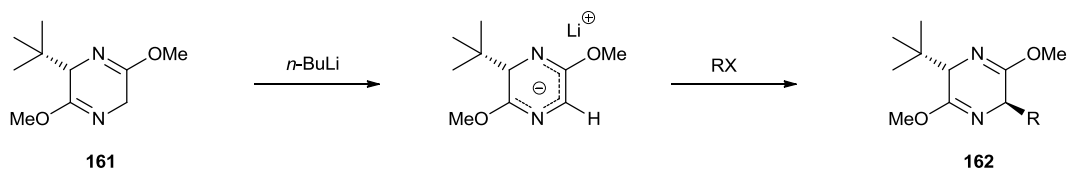
1.2.3.3 Chiral glycine equivalent.

The use of chiral glycine equivalents has seen increasing use as a way to introduce the amino acid moiety to a compound through the formation of a C-C bond. Early work in this field involved the asymmetric alkylation of amino acid derived enolates, which ultimately produced optically pure α -disubstituted amino acids (scheme 1.29).^{144, 145} Schollkopf published a bis-lactim ether of 2,5-diketopiperazine (**161**) which was alkylated by alkyl or aryl halides to give mono-substituted amino acids following hydrolysis (table 1.9).¹⁴⁶ Expanding on this early work, Williams *et al.* developed diastereomeric lactones **164-167**¹⁴⁷ which have been asymmetrically coupled to a range of substrates in high optical purity with reportedly good to high yields. These compounds have then been transformed into their corresponding α -amino acids by hydrogenolysis,¹⁴⁸ dissolving metal reduction¹⁴⁹ or periodate oxidation.¹⁵⁰



i. K(HMDS), THF, $-78\text{ }^{\circ}\text{C} \rightarrow \text{rt}$, MeI, (**80 %**); ii. 1 N NaOH, MeOH, rt; iii. H_2 , Pd/C, MeOH, 40 psi, 2 h.

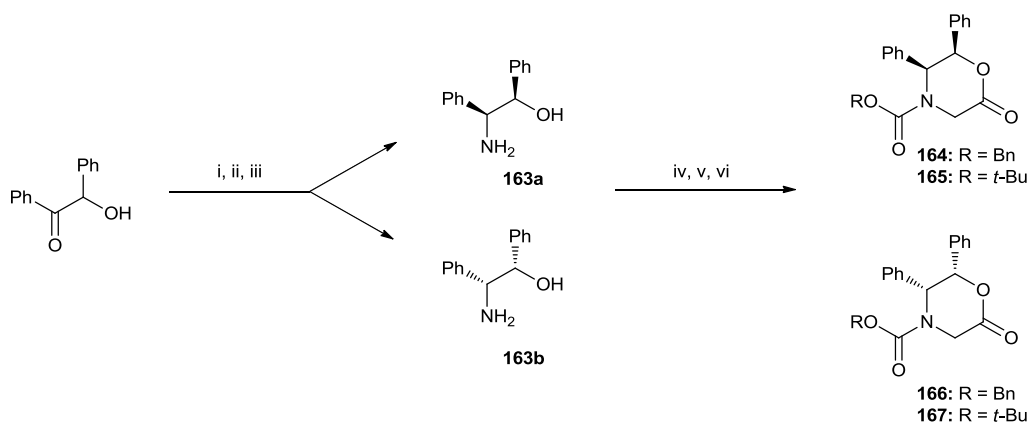
Scheme 1.29 – Early work towards the formation of di-substituted α -amino acids.^{144, 145}



162	a	b	c	d	e
R	CH ₃	CH ₂ CH=CH ₂	CH ₂ C≡CH	C ₇ H ₁₅	CH ₂ CO ₂ tBu
de	80	>95	>95	>95	>95

Table 1.9 – Schollkopf's stereoselective bis-lactim ether alkylation.¹⁴⁶

The glycine templates **164-167** were synthesised from commercially available benzoin, which was condensed to its corresponding oxime. This was hydrogenated and optically resolved using L-glutamic acid to give **163**. *N*-alkylation with ethylbromoacetate preceded further *N*-acylation with either Cbz or Boc protecting groups and finally cyclization was catalysed by *p*-toluenesulfonic acid in refluxing benzene (scheme 1.30).^{11, 148}



i. NH₂OH.HCl; ii. H₂/Pd C; iii. L-Glu; iv. BrCH₂CO₂Et, TEA, THF; v. ROCOCl, NaHCO₃, CH₂Cl₂; vi. *p*-TsOH, PhH, reflux.

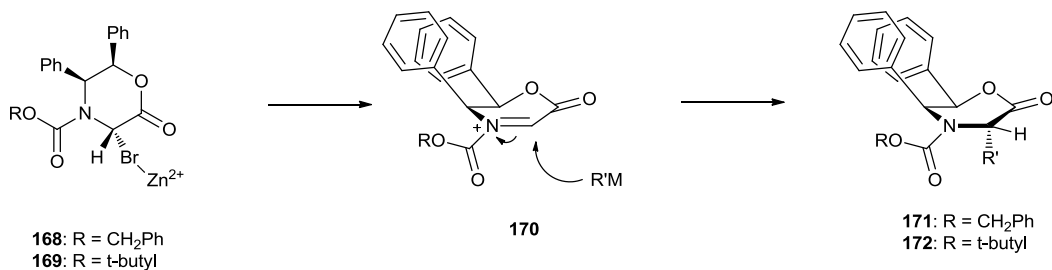
Scheme 1.30 – Synthesis of Williams' glycine template.^{11, 148}

Much work has been performed using these 'chiral glycine equivalents' developed by Williams and co-workers (referred to herein as 'Williams' template') since their development. Williams *et al.* have demonstrated two possible routes to the formation of optically pure α -monosubstituted amino acids from their template. The route to the C-C bond formation has taken place through formation of a cationic species^{11, 147, 148, 150-153} or through formation of an enolate anionic species.

1.2.3.3.1 Electrophilic glycinates

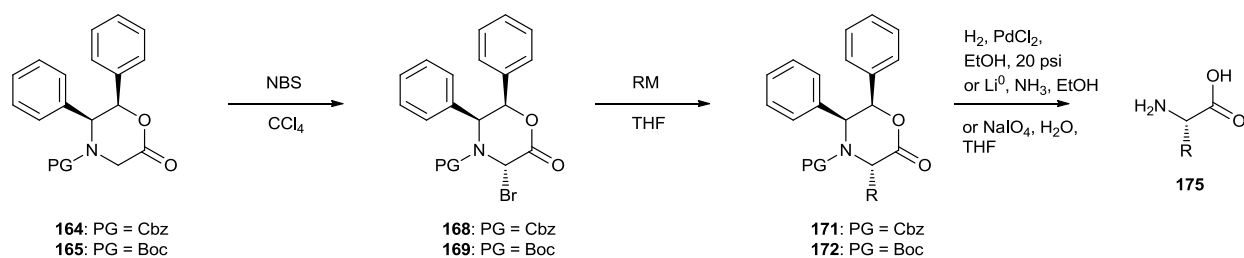
The early work utilizing Williams' template focussed on its conversion to bromoglycinate derivatives **168** and **169**. *N*-bromosuccinimide was used to produce the optically pure bromide in the *anti*-configuration in excellent yield. The alkylation of the bromide takes place through formation of a reactive iminium species, which is catalysed by a Lewis acid, typically zinc chloride. It is hypothesized that the Lewis acid coordinates the bromide,

breaking the Br-C bond and thus produces the iminium species (**170**).^{11, 148, 154} This then undergoes nucleophilic attack by the carbon nucleophile from the least sterically encumbered face, which consequently affords the *anti*-diastereoisomer (scheme 1.31).



Scheme 1.31 – Alkylation of Williams' template via reactive iminium species

A variety of carbon nucleophiles have been coupled to the amino acid precursor in high optical purity with a net retention of stereochemistry. Allyltrimethylsilyl derivatives have had a lot of success when coupling, both in terms of yield of the *anti*-stereoisomer and optical purity (table 1.10, entries 2-5, 13 and 14).^{11, 148} However, the use of silyl enol ethers has been observed to produce the *syn* isomer as the major product (entry 1).^{148, 152} It has been postulated that the reaction is proceeding through a S_N2 mechanism, in which, the nucleophile is attacking the electrophile at a faster rate than that of iminium ion formation, thus resulting in formation of the *syn* isomer. Increasing the polarity of the reaction solvent, thereby stabilising the formation of the iminium species and using a more halophilic Lewis acid (typically AgOTf) has had a dramatic effect on the stereoselectivity (table 1.11).¹¹

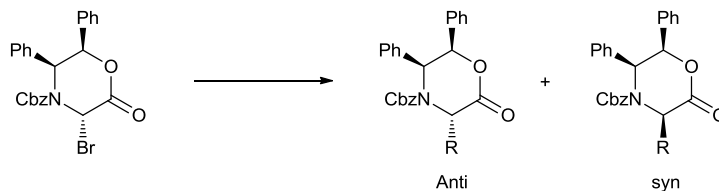


	Nucleophile	Reaction Conditions	171/172 ^a % yield	Deprotection method ^b	Amino Acid (175), % yield	ee (%)
1		ZnCl ₂ /THF, 25 °C	74	A	D-β-ethyl aspartate, 85 ^c	>96
2		ZnCl ₂ /THF, 25 °C	66	A	Norvaline, 93	>98
3		ZnCl ₂ /THF, 25 °C	66	B	Allylglycine, 90	>91
4		ZnCl ₂ /THF, 25 °C	82	A	Cyclopentylglycine, 91	>96
5		ZnCl ₂ /THF, 25 °C	82	B	Cyclopentenylglycine, 94	>96
6		ZnCl ₂ , MeCN, 25 °C	72	A	Homophenylalanine, 91	>96
7	H ₃ CZnCl	THF -78 °C	46	A	Alanine, 100	>96
8	Bu ₂ Cu(CN)Li	THF/Et ₂ O, -78 °C	48	A	Norleucine, 52	>99
9	Me ₂ CuCNLi ₂	THF, -78 °C	28	A	-	-
10	Bu ₂ CuCNLi ₂	THF, -78 °C	48	A	Norleucine, 100	99.5
11	(C ₆ H ₄) ₂ CuLi	Et ₂ O/THF, -78 °C	56	C	Phenyglycine, 52	82
12	(naphth) ₂ CuLi	Et ₂ O/THF, -78 °C	55	C	Naphthylglycine, 29	94
13		ZnCl ₂ /THF, 25 °C	63	B	Allylglycine, 70 ^d	>96
14		ZnCl ₂ /THF, 25 °C	59	B	Cyclopentenylglycine, 70 ^d	>95

^a Entries 1-10 are **171**, entries 11-14 are **172**. ^b Deprotection method A = H₂, PdCl₂(cat), EtOH, 20 psi, B = Li⁰/NH₃/EtOH, C = NaIO₄/H₂O/THF. ^c The absolute configuration of the amino acid in each case was (S) with the exception of entry 1, which is the (R) enantiomer. ^d Isolated products were Boc protected.

Table 1.10 - Amino acid synthesis using bromoglycinates **168** and **169**.

Trialkyl tin acetylides have been used to synthesise *E*-vinyl glycine derivatives in fair yields and optical purities of up to 68 % ee. However, this was attributed to racemization during the dissolving metal reduction, which was used for the removal of the chiral auxiliary.¹⁵⁵ This was corroborated by obviating the dissolving metal reduction and instead using hydrogenolysis to remove the chiral auxiliary which furnished the hydrogenated amino acid derivatives in 94-98 % ee.¹⁵³



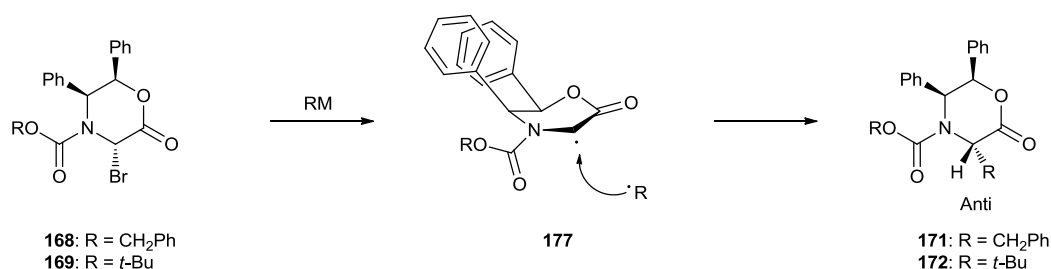
Entry	Reagent	Solvent	Lewis Acid	R =	anti:syn ^a
1		CH ₂ Cl ₂	ZnCl ₂		1:45
2		THF	ZnCl ₂		1:14
3		THF	AgOTf		1:2
4		CH ₂ Cl ₂	ZnCl ₂		1:11.2
5		THF	ZnCl ₂		1:1.6
6		MeCN	ZnCl ₂		2.9:1
7		THF	AgOTf		5.9:1
8		CH ₂ Cl ₂	ZnCl ₂		1:3.4
9		CHCl ₃	ZnCl ₂		1.4:1
10		THF	ZnCl ₂		7:1
11		MeCN	ZnCl ₂		14.5:1
12		THF	AgOTf		24.5:1

^a Ratios were determined by ¹H NMR of the crude mixture, in DMSO-*d*₆ at 393 K.

Table 1.11 – Effect of conditions on the ratio of diastereoisomers.¹¹

Other organometallic compounds have been used with **168**. The use of organocuprate compounds has seen the reaction proceed with high optical purity of the isolated amino acids (up to <99 % ee, table 1.10, entries 8-12), albeit with low yields. α -arylglycine derivatives have been synthesised from their corresponding cuprates. Again the *anti*-

stereoselectivity was achieved in high optical purity (82-94 % ee). However, conversion to the amino acid required periodate oxidation.¹⁵⁰ Organozinc substrates have also achieved high levels of stereoselectivity although yields were again low (table 1.10, entry 7).^{11, 148} Williams *et al.* have suggested that these electron-rich organometallic substrates undergo a free radical mechanism when coupling (as illustrated in scheme 1.32). They state that the low yields are a consequence of the reduction of **168/169** to **164/165**, which takes place via the same type of electron-transfer radical-reduction mechanism.^{11, 154}



Scheme 1.32 – Proposed free radical mechanism of coupling.¹¹

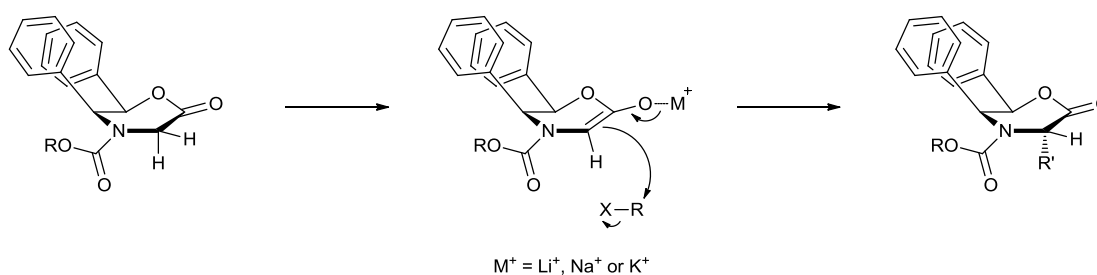
1.2.3.3.2 Nucleophilic glycinates

Although the electrophilic glycinates method (*vide supra*) has been used to synthesise a variety of α -amino acids, its use has become obsolete over the last 20 years. Instead, much attention has been focused on the asymmetric alkylation of chiral glycine enolates, which have been prepared through the treatment of their corresponding chiral glycine equivalents with strong base.

Williams *et al.* used either the lithium or sodium salt of bis(trimethylsilyl)amide to deprotonate their chiral glycine equivalents **164-165** and **166-167** at $-80\text{ }^{\circ}\text{C}$, which thus produced the enolates. Addition of an activated alkyl halide, such as benzyl bromide, allyl bromide or methyl iodide (table 1.12, entries 1-11), furnished the corresponding alkylated oxazinones in good yields and excellent enantiomeric excess.¹⁵⁶ For unactivated alkyl halides (entries 14-21) such as long chain alkyl halides (*n*-propyl or *n*-butyl iodides) changing the order of addition of the reagents proved to be important.¹⁴⁹ The addition of an additive (e.g. crown ethers)¹⁵⁷ or co-solvents such as HMPA,^{158, 159} DMPU¹⁶⁰ or DME^{161, 162}

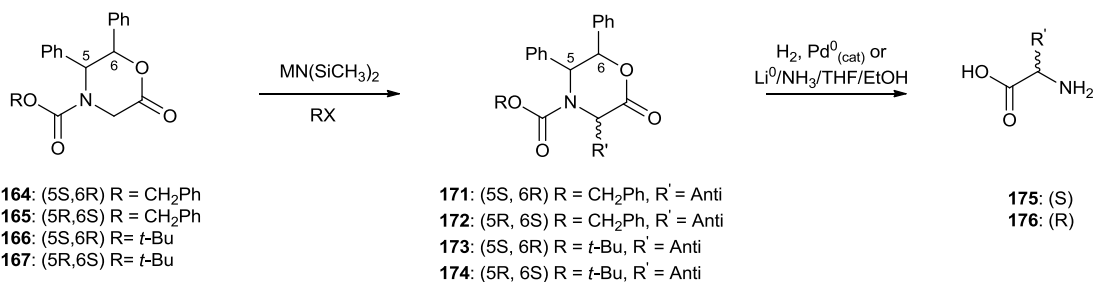
has also been shown to significantly increase yields by coordinating the metal cation, which results in a weakening of the bond to the oxygen atom and thus makes the enolate more reactive.

The reaction (scheme 1.33) takes place via a 'twisted boat' conformation with both phenyl groups sterically hindering the si-face. The metal cation coordinates the oxygen and a proton is extracted by the silyl amide base, thus producing the enolate. Nucleophilic attack by the enolate on the α -carbon of the halide takes place on the least sterically encumbered face (the re-face) resulting in high optical purity of the *anti*-products.



Scheme 1.33 – Enolate alkylation proceeding through a 'twisted boat' conformation.¹⁴⁹

Due to the high basicity of the metal silyl amide; anhydrous reaction conditions, aprotic solvents (typically THF) and inert atmospheres are imperative for these reactions. Formation of the mono-substituted α -amino acids has only been seen when using sodium or lithium bis(trimethylsilyl)amide. The potassium salt is too strong a base and so results in the di-substituted lactone or decomposition of the lactone. Furthermore, the use of other bases, such as: LDA, *n*-BuLi, *t*-BuLi and NaH have resulted in either no reaction or decomposition of the lactone.¹⁴⁹

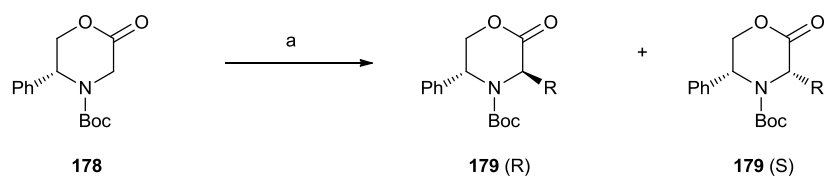


Entry	Oxazinone Substrate	Alkylation yield %	R'X	Method ^a	Base (equiv)	Amino Acid Yield % ee
1	166	20	CH ₂ =CHCH ₂ Br	A	LiN(Si(CH ₃) ₃) ₂ (1)	
2	166	71 (12) ^b	CH ₂ =CHCH ₂ Br	A	LiN(Si(CH ₃) ₃) ₂ (2)	
3	166	48 (21) ^c	CH ₂ =CHCH ₂ Br	A	NaN(Si(CH ₃) ₃) ₂ (1)	
4	166	86 (5) ^c	CH ₂ =CHCH ₂ I	B	LiN(Si(CH ₃) ₃) ₂ (1.2)	50-70 98
5	164	82	CH ₂ =CHCH ₂ I	B	LiN(Si(CH ₃) ₃) ₂ (1.2)	
6	166	91	CH ₃ I	A	NaN(Si(CH ₃) ₃) ₂ (1.1)	54 97
7	164	88	CH ₃ I	B	NaN(Si(CH ₃) ₃) ₂ (1.5)	
8	166	70 (9) ^c	PhCH ₂ Br	A	NaN(Si(CH ₃) ₃) ₂ (1)	76 98
9	167	77 (6) ^b	PhCH ₂ Br	B	NaN(Si(CH ₃) ₃) ₂ (1.2)	93 >99
10	166	68 (20) ^c	Me ₂ C=CHCH ₂ Br	A	NaN(Si(CH ₃) ₃) ₂ (1)	
11	166	84 (2) ^b	Me ₂ C=CHCH ₂ Br	B	NaN(Si(CH ₃) ₃) ₂ (1.1)	52 >99
12	166	64	BrCH ₂ CO ₂ Et	A	NaN(Si(CH ₃) ₃) ₂ (1.1)	
13	165	61 (20) ^c	BrCH ₂ CO ₂ Et	A	NaN(Si(CH ₃) ₃) ₂ (1)	71 96
14	166	0	<i>n</i> -C ₃ H ₇ I	A	NaN(Si(CH ₃) ₃) ₂ (1.2)	
15	166	77 (12) ^b	<i>n</i> -C ₃ H ₇ I	B	NaN(Si(CH ₃) ₃) ₂ (1.5)	
16	166	76 (3) ^c	<i>n</i> -C ₃ H ₇ I	B	NaN(Si(CH ₃) ₃) ₂ (1.5)	
17	167	47	ICH ₂ CH ₂ CH=CH ₂	B	LiN(Si(CH ₃) ₃) ₂ (1.8)	
18	165	72	I(CH ₂) ₃ Cl	B	LiN(Si(CH ₃) ₃) ₂ (1.5)	
19	165	86	I(CH ₂) ₃ I	B	LiN(Si(CH ₃) ₃) ₂ (1.5)	

^a Method A involves addition of the base to the oxazinone at -80 °C followed by addition of the electrophile; Method B involves addition of the base to a -80 °C mixture of the oxazinone containing electrophile. ^b Number in parenthesis denotes dialkylated product; ^c Number in parenthesis denotes recovered starting material; ^d mono alkylated product produced

Table 1.12 – Enolate alkylations of **164-167**.¹⁴⁹

The alkylation of Williams' template proceeding through enolate attack of an alkyl halide coincided with work by Dellaria and co-workers, who used the same technique for the diastereoselective alkylation of their chiral glycine equivalent **178**.^{161, 162} Like with the Williams template, **178** underwent alkylation in high yields and excellent de with activated alkyl halides (entries 1-4).¹⁶¹ However, reaction conditions needed to be altered to produce the amino acid precursors of un-activated alkyl halides (5-8).¹⁶¹ The amino acids were furnished in high yields from **179** by hydrolysis followed by hydrogenolysis at 1 atm in the presence of palladium (10 % Pd/C). The chiral glycine derivatives have also been synthesised with Cbz protection of the amino group. These underwent alkylation under analogous conditions.¹⁶²

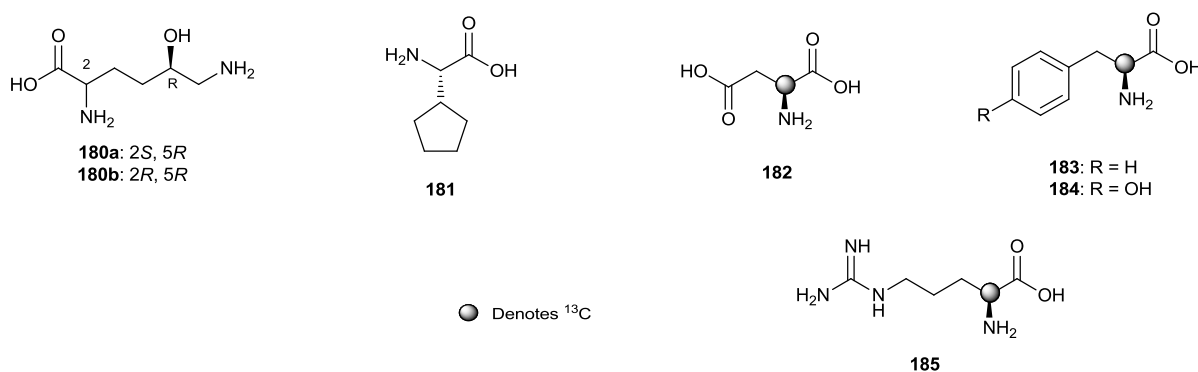


Entry	RX	Ratio ^b , 179(R):179(S)	Purified Yield (%)
1	BnBr	>200:1	78
2	MeI	>200:1	85
3	Methallyl iodide	>200:1	90
4	Allylbromide	>200:1	86
5	n-butyl iodide	-	0
6 ^c	n-butyl iodide	83:1	78
7	Benzyl 2- bromoacetate	3.5:1	59 ^f
8 ^d	Benzyl 2- bromoacetate	185:1 ^e	65 ^g

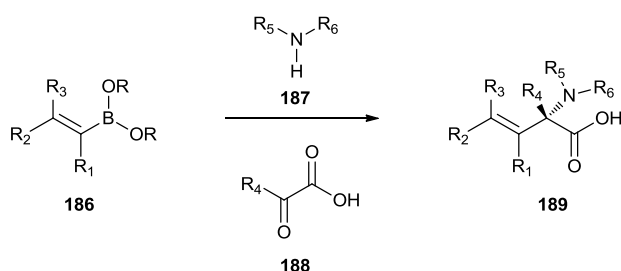
^a 0.98 equiv NaHMDS, 1:1 THF:DME (~0.2 M), RX, -78 °C. ^b ratios determined by analytical capillary gas chromatography. ^c 0.98 equiv NaHMDS, DME (~0.2 M), RX, -63 °C. ^d 0.98 equiv LiHMDS, THF, RX, -78 °C. ^e ratio determined by HPLC. ^f 17 % recovered **178**, ^g 18 % recovered **178**.

Table 1.13 – Enolate alkylations of Dellaria's chiral glycinate.¹⁴⁷

Since their development, both chiral glycinates by Williams and co-workers and Dellaria *et al.*, respectively have received much interest in the synthesis of a range of α -amino acids. Williams' template has been utilized to synthesise a range of optically pure non-natural amino acids including 5-hydroxyl-lysine (**180**)^{157, 163} and cyclopentylglycine (**181**).¹⁶⁰ ¹³C labelled α -amino acids L-asp (**182**), L-phe (**183**) and L-tyr (**184**), which were obtained optically pure and in high overall yields using Dellaria's chiral oxazinone (**178**).^{164, 165} Similarly Williams template has been used to in the synthesis of ¹³C labelled L-arg (**185**).¹⁶⁶ Casimir *et al.* have shown that replacing the phenyl substituent of **178** with methyl, benzyl or *sec*-butyl also gives excellent de for a range of activated electrophiles.¹⁶⁷



1.2.3.4 Petasis reaction



Scheme 1.33 – Petasis reaction

In the late 1990s Petasis and co-workers devised a new way to synthesise α -amino acids from a one pot, three component reaction containing a boronic acid or a boronate ester, an α -keto acid and an amino source (scheme 1.33).¹⁶⁸ This method has been used to

synthesise a range of α -amino acids including β - γ -unsaturated α -amino acids and α -arylglycines (table 1.14).¹⁶⁸⁻¹⁷⁰ The general procedure for the reaction involved stirring all components in a solvent, typically DCM or MeOH, at room temperature for 12-48 hours which produced the corresponding amino acids in high yields. Performing the reaction in hexafluoroisopropanol (HFIP) has seen a significant increase in reaction time, with a typical reaction completed in 4 hours.¹⁷¹

Entry	Boronic acid (186)	Conditions ^a	Amine (187)	Yield (%) ^b
1		A	BnNH ₂	87
2		B	BnNH ₂	94
3		A	Ph ₃ CNH ₂	54
4		A	HO(CH ₂) ₂ NH ₂	82
5		B	(<i>p</i> -MeOPh) ₂ CHNH ₂	92
6		A	<i>p</i> -MeO-aniline	94
7		C	Adam-NH ₂	96
8		B	Ph ₂ CHNH ₂	87
9		C	Ph ₂ CHNH ₂	80
10		D	Morpholine	78
11		E	Ph ₂ CHNH ₂	76

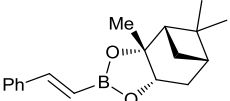
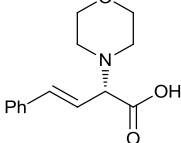
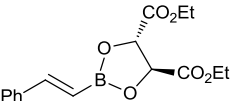
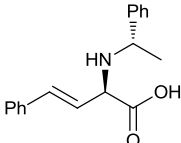
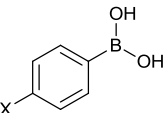
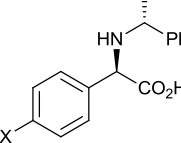
^a A: CHOCO₂H·H₂O (**186a**), EtOH, 25 °C; B: **186a**, PhMe, 25 °C; C: **186a**, CH₂Cl₂, 25 °C; D: **186a**, EtOH, 50 °C; E: MeCOCO₂H (**186b**), CH₂Cl₂, 25 °C. ^b Isolated yields after ion exchange chromatography (Dowex 50W-X8) or recrystallization from water/*t*-butyl alcohol.

Table 1.14 – Synthesis of amino acids by the Petasis reaction.¹⁶⁸⁻¹⁷⁰

1.2.3.4.1 Asymmetric Petasis synthesis

The use of chiral auxiliaries has seen much success in the asymmetric Petasis reaction. Koolmeister *et al.* used homochiral boronic esters as the chiral auxiliary and morpholine as the amino source. Despite decent yields of 59-81 % of the morpholine protected α -amino acids, the diastereoselectivity was poor (up to 15.4 % de, table 1.15, entry 1).¹² The optical purity has been improved when using chiral amines in addition to the chiral boronic acid esters (de up to 90 %). However, that came at the expense of the yields (1-60 %).¹⁷²

α -Methylbenzylamine has been used to produce both the D and L enantiomers of a variety of substrates in high yields. However, the enantioselectivity is substrate dependent, with a wide range of diastereomeric excess observed for the production of different amino acids (table 1.15 entries 2-3).^{168, 169, 172, 173} Employing optically pure amino acids or amino alcohols such as alanine, leucine, and phenylalanine as the chiral auxiliary have seen excellent yields and de up to <99 % for the *anti* diastereoisomer (entries 5-7). Conversely, phenylglycinol was an effective chiral auxiliary for the formation of the *syn* diastereoisomer in excellent yield and de (entry 4).^{168, 170}

Entry	Amino Source	Method ^a	Boronic acid/ester	Product	Yield % (% de)
1		A			78 % (15.4 %)
2		B			88 % (89 %)
3		B			X = OMe 82 % (35 %) X = CH(CH ₂) ₂ 77 % (28 %)

4		A			78 % (99 %) ^b
5		A			91 % (83 %)
6		A			88 % (66 %)
7		C			89 % (99 %)
8		C			85 % (94 %)
9		C			79 % (99 %)

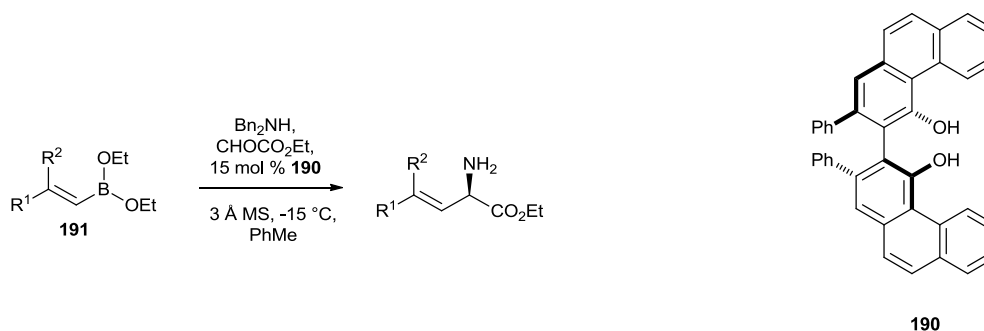
^a method A – CHOCO₂H.H₂O, CH₂Cl₂, 25 °C. B – CHOCO₂H.H₂O, PhMe, 25 °C. C – CHOCO₂H.H₂O, MeOH, 25 °C. ^b When (R)-phenylglycinol was used the opposite diastereoisomer was obtained in the same yield and de.

Table 1.15 – Synthesis of amino acids via the asymmetric Petasis reaction.

1.2.3.4.2 Catalysis

Catalytic attempts to improve the stereoselectivity of the Petasis reaction have been limited. Lou *et al.* used a chiral biphenanthryl catalyst (**190**) to produce a variety of α -amino acids from their corresponding styrenyl or alkenyl boronates in high yields and high

enantiomeric ratios (table 1.16).¹⁷⁴ The use of Lewis acids, in particular, indium(III) bromide (InBr₃) has seen success in catalysing the formation of enantioenriched α -amino acids (93-99 % de) from alkenyl, styrenyl, aromatic and heteroaromatic boronates in good yields using *N*-*t*-butanesulfinamide as the amino source.¹⁷⁵



Entry	R ¹	R ²	Yield (%) ^b	ee ^c
1	Ph	H	81	91
2	<i>p</i> -CH ₃ O-C ₆ H ₄	H	84	92
3	<i>p</i> -Br-C ₆ H ₄	H	82	90
4	<i>m</i> -F-C ₆ H ₄	H	80	90
5	<i>m</i> -CF ₃ -C ₆ H ₄	H	82	90
6	3-C ₄ H ₃ S	H	87	90
7 ^d	C ₆ H ₁₁	H	76	94
8 ^d	<i>n</i> -Bu	H	73	90
9 ^d	BnOCH ₂	H	74	91
10	Ph	CH ₃	78	90
11 ^d	<i>n</i> -Bu	CH ₃	71	86

^a Reactions were run with 0.25 mmol **190**, 0.25 mmol dibenzylamine, 0.25 mmol glyoxylate, 0.0375 mmol (*S*)-**190**, and 3 Å molecular sieves in toluene for 36 h under Ar, followed by flash chromatography on silica gel. ^b Isolated yield. ^c Determined by chiral HPLC analysis. ^d Reactions were run at 0 °C.

Table 1.16 – Asymmetric Petasis reaction catalysed by chiral bis(phenanthryl) catalyst **190**.¹⁷⁴

1.3 Objectives

The guanidinium side chain of arginine is a very important component in the recognition between a protein/peptide and its nucleic acid target. The guanidine functionality is linked to the amino acid moiety through a three carbon chain, which allows much torsional freedom, thus resulting in the ability to orientate the guanidino group to interact with a wide range of target molecules through bidentate H-bonding donation (figure 1.7).

Introduction of torsional constraints to the side chain would reduce the loss in conformational entropy on binding its target. Fixing the guanidine moiety in a rigid bicyclic framework would achieve this while also producing only a single face in which H-bonds can take place. This should result in a greater degree of specificity when discriminating between different targets.

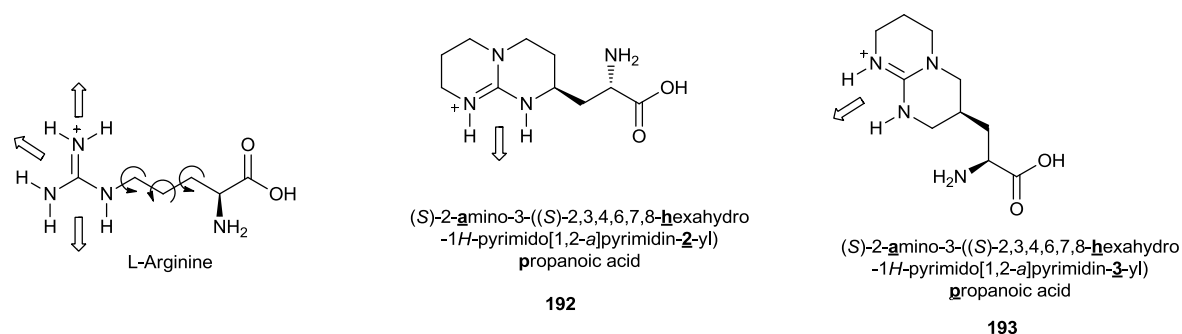


Figure 1.7 – Structure of arginine and the two bicyclic guanidino amino acids **192** and **193**. The white arrow denotes the faces of H-bond donation. The black arrow denotes torsional freedom.

As seen in the literature, the synthesis of bicyclic guanidines has received frequent attention over the past 65 years. However, a void exists in the incorporation of amino acid functionality within its structure. Integration of amino acid functionality would allow its application in solid phase peptide synthesis, which could be used to target specific sequences of nucleic acids.

The aim of this thesis is to synthesise the bicyclic guanidino amino acids AH-2-P (**192**) and AH-3-P (**193**) (figure 1.7). A second objective is to synthesise a library of polypeptides, each containing at least one arginine residue and test their binding specificity with several

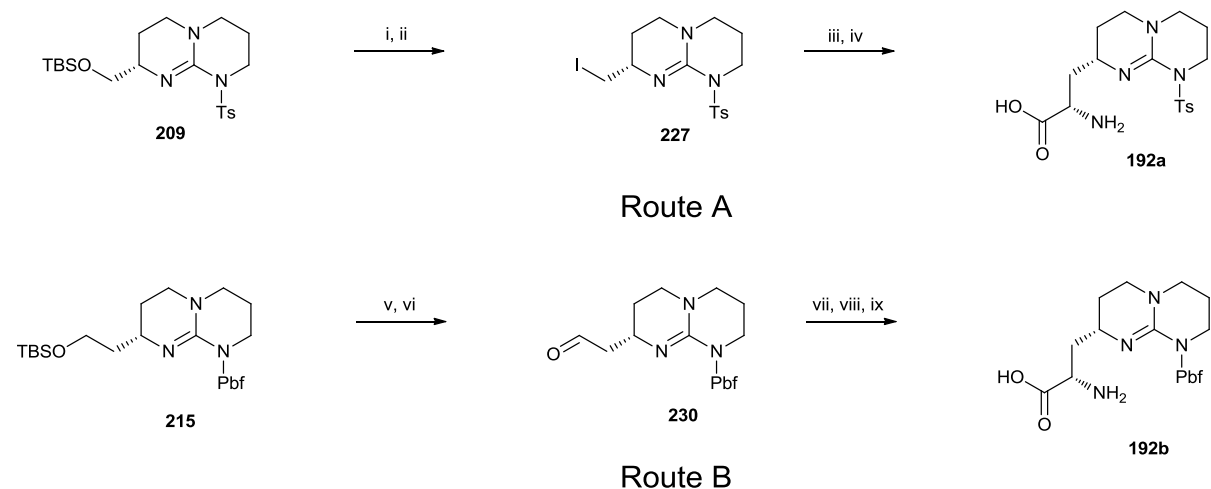
nucleic acid targets using an enzyme linked immunosorbent assay (ELISA). Finally these peptides can be re-synthesised containing the bicyclic guanidino amino acids in place of arginine and comparisons of their binding affinity can be assessed.

2. Results and discussions. Synthesis of AH-2-P

2.1 Introduction

The synthesis of *N*-protected AH-2-P (**192**) can be divided into two parts. Firstly, the synthesis of the *N*-protected bicyclic guanidino side chain and secondly, the introduction of amino acid functionality. It was predicted that the former could be synthesised by a modified route to di-substituted bicyclic guanidines described by Münster *et al.*⁸⁶ The latter can be introduced by a variety of methods such as the Strecker synthesis, Petasis reaction and via the introduction of chiral glycine equivalents.

Two possible routes to the synthesis of AH-2-P were explored. The first would install the amino acid's β -carbon towards the end of the synthesis by utilising the chiral glycine equivalent developed by Williams (route A). This begins with de-silylation of bicyclic guanidine **209** followed by conversion to the iodide. Introduction of the aforementioned chiral glycine equivalent would directly precede hydrogenolysis to afford bicyclic guanidino amino acid **192a**.



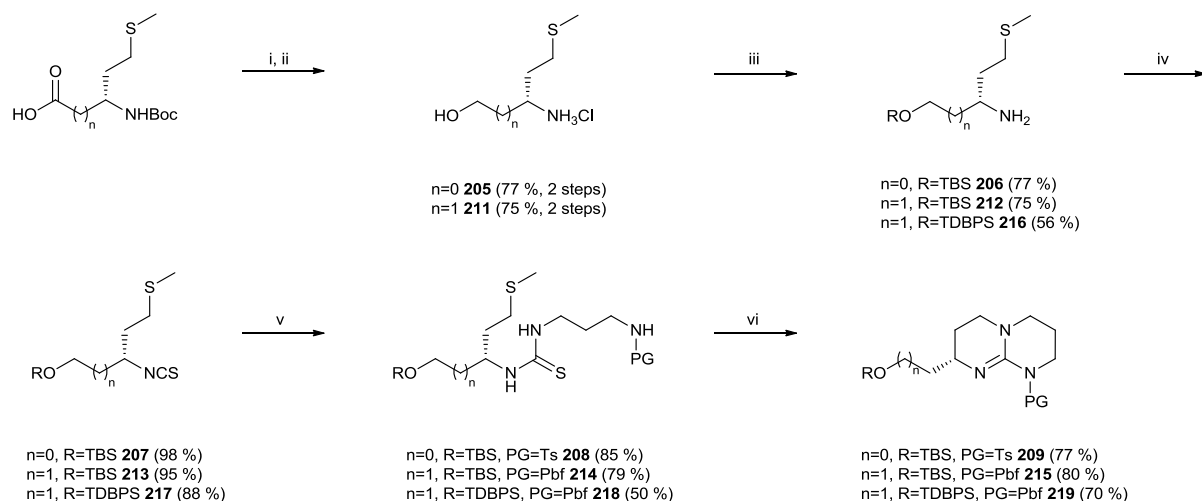
i. TBAF, THF, 25 °C; ii. I₂, PPh₃, imidazole, CH₂Cl₂, -20 – 25 °C; iii. Li or Na HMDS, **164**, THF, -78; iv. Pd(OH)₂, MeOH, 25 °C; v. I₂, MeOH, 65 °C; vi. C₂O₂Cl₂, DMSO, TEA, CH₂Cl₂, -78 – 25 °C; vii. Ph₂CHNH₂, KCN; viii. a) DIBALH, THF, b) HCl (0.1 M) ix. H₂, Pd(OH)₂, MeOH.

Scheme 2.1 – Proposed synthetic routes to AH-2-P (**192**).

The second proposed pathway (Route B) begins with the already homologated bicyclic guanidine **215**. Following de-silylation the alcohol is oxidised to aldehyde **230**. This then undergoes a Strecker

synthesis to produce the protected amino nitrile, which is converted to the amino acid by oxidation and hydrolysis. Finally benzhydryl removal yields AH-2-P (**192b**).

The proposed pathway to the silyl protected bicyclic guanidines **209**, **215** and **219** is an adapted approach based on the synthesis by Münster.⁸⁶ Full optimisation was necessary at each step in the synthesis outlined in scheme 2.2 and is discussed in detail later (section 2.3). The synthesis to bicyclic guanidines **209**, **215** and **219** began with reduction and de-protection of the α and β amino acids. This was proceeded by silyl protection, followed by formation of the isothiocyanate. Coupling to the relevant mono-protected diamine (Ts for **220** and Pbf for **222**) produced the thioureas **208**, **214** and **218**. Cyclization was achieved through methylation at the sulfur atoms followed by intramolecular nucleophilic substitution by the amino groups, thus producing bicyclic guanidines **209**, **215** and **219**.



i. (a) EtOC(O)Cl, NMM, THF, 1h, 0 °C, (b) NaBH₄, H₂O, 0 – 25 °C; ii. 2 M HCl, 25 °C; iii. TBS-OTf or TBDPS-Cl, imidazole, CH₂Cl₂, 0 – 25 °C; iv. CCl₄, NaHCO₃, CH₂Cl₂, 25 °C; v. **220** or **222**, NaHCO₃, MeCN, 25 – 75 °C; vi. (a) MeOTf, DIEA, CH₂Cl₂, 0 °C, (b) DIEA, 40 °C.

Scheme 2.2 – Synthetic pathway to bicyclic guanidines **209**, **215** and **219**.

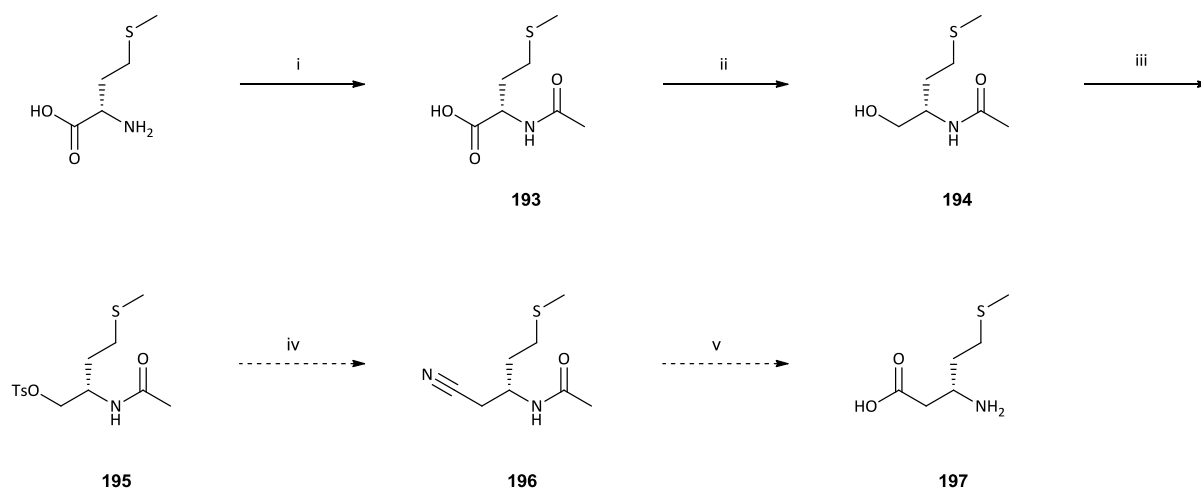
Using optically pure amino acids as the starting point for the synthesis is an ideal way to introduce the required stereocentre. However, despite enantiopure L- α -methionine being an inexpensive and commercially available compound, its β -homologue is highly expensive. In order for its use as an appropriate starting material, a route to its synthesis needed to be explored.

2.2 Homologation

The aforementioned expense of optically active β -homomethionine, led to the decision to synthesize it from its cheaper α -homologue. A common method for homologation of a carboxylic acid involves using the Arndt Eistert synthesis (Scheme 2.5). However, this method involves using the suspected carcinogenic and potentially explosive compound diazomethane. In an attempt to avoid generating this dangerous reagent other avenues were considered.

2.2.1 Via Ac-N-amino nitrile

It was proposed that β -homomethionine could be synthesised via formation of amino nitrile **196** (scheme 2.3), which could subsequently be converted to the amino acid (**197**). It would first be necessary to *N*-protect and reduce the amino acid. Conversion of the hydroxyl to a more appropriate leaving group would be followed by displacement with cyanide. Hydrolysis would then convert the nitrile to the acid while also removing acetyl protection.



i. Ac_2O , THF/ H_2O (9:1), sonication (**82 %**), ii. a) SOCl_2 , MeOH, 0°C , b) NaBH_4 , EtOH, 0°C (**88 %**, 2 steps); iii. Ts-Cl, 4-DMAP, TEA, CH_2Cl_2 (15 %); iv. KCN, 18-C-6, MeCN; v. 6 M NaOH.

Scheme 2.3 – Synthesis of β -homomethionine (**197**) via amino nitrile **196**.

2.2.1.1 Acetylation

Acetylation of α -methionine using anhydrous conditions proved to be challenging and only poor yields were obtained when a variety of conditions were employed. Varying the molar equivalents of both the base and the acetic anhydride failed to increase the reaction yield. Furthermore, the

introduction of 4-DMAP as a catalyst, only produced a slight increase in yield, raising it to a still poor 35 %.

Yields were significantly improved when employing a method described by Shindo *et al.*¹⁷⁶ in which, the base was omitted and the reaction was sonicated with acetic anhydride in aqueous THF. Monitoring the reaction using TLC showed that complete conversion to the acetylated methionine takes place in only 2 hours. Purification by recrystallization produced **193** in an 82 % yield.

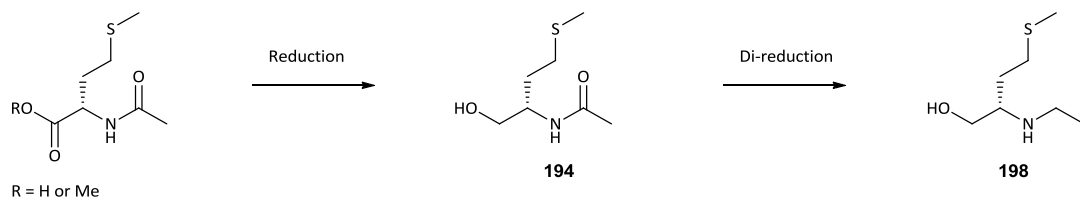
2.2.1.2 Reduction

It was important when reducing Ac-*N*-methionine (**193**) to its corresponding amino alcohol that the acetyl protecting group was not reduced, so consideration to the type of reducing agent was important. Reagents such as sodium or lithium borohydride are weak reducing agents and so would fail when attempting to reduce the acid. Conversely, lithium aluminium hydride (LiAlH₄) is a strong reducing agent, and so, would be capable of reduction to the alcohol. However, it was predicted that using such a reagent would also result in the reduction of the acetyl group.

Borane complexes, such as BH₃·THF and BH₃·DMS have seen success when reducing a variety of amino acids to their corresponding alcohols.^{177, 178} Attempts to reduce Ac-*N*-methionine (**193**) to the acetyl protected amino alcohol proved problematic when employing borane (BH₃) as the reducing agent (summarised in table 2.1). Despite varying the number of equivalents of reducing agent, performing the reaction at different temperatures and extending reaction times (up to 48 hours); isolation of **194** was unattainable in an adequate yield.

When a fourfold excess of BH₃ was used the ¹H NMR spectrum displayed a pair of doublet of doublets at 3.70 and 3.60 ppm, each integrating to 1H. This indicated that the acid had been reduced to the alcohol. However, the appearance of a quartet at 1.72 ppm and a triplet at 1.06 ppm, both with a coupling constant of 7 Hz, suggested that the acetyl had also been reduced to give the di-reduced compound **198**. Interestingly, the chemical shift of the quartet resonates at a higher frequency than is expected from a compound containing an *N*-Et moiety (~2.6 ppm).¹⁷⁹⁻¹⁸¹

Even when only two equivalents of BH₃ were used, the minimum required for reduction to the alcohol, the resulting ¹H NMR spectrum and TLC showed a mixture of compounds. Both the reduced and di-reduced compounds were present along with unreacted starting material. Cooling the reaction below 0 °C only reproduced the results already encountered. This clearly demonstrated that BH₃·THF was impractical for this reduction. Therefore, another approach was considered.



R =	Reducing agent	Number of equivalents	Temperature (°C)	Duration (hours)	Product (yield)
H	BH ₃ ·THF	2.5	25 ^a	12	193, 194, 198
H	BH ₃ ·THF	3	25 ^a	2.5	193, 194, 198
H	BH ₃ ·THF	2	25 ^a	5	193, 194, 198
H	BH ₃ ·THF	2	25 ^a	22 ^b	193, 194, 198
H	BH ₃ ·THF	4	25 ^a	2.5	198 (73 %)
Me	NaBH ₄	2	25 ^c	12	194 (65 %)
Me	NaBH ₄	2	25 ^c	24	194 (66 %)
Me	NaBH ₄	3	25 ^c	12	194 (88 %)
Me	LiBH ₄	2	25 ^d	24	194 (58 %)
Me	LiBH ₄	2	25 ^c	24	194 (60 %)

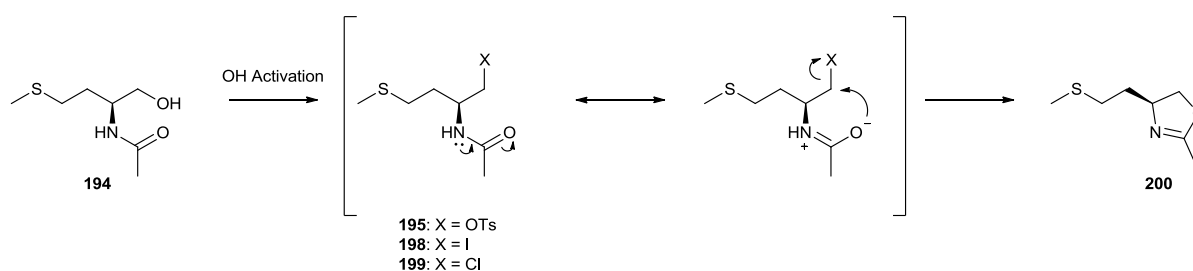
^a Reagents were introduced at 0 °C then reaction was warmed to 25 °C; ^b Reaction was heated to 80 °C for a further 2 hours; ^c 0 °C for 1 hour then warmed to 25 °C; ^d Stirred for 1 hour at –10 °C then warmed to 25 °C.

Table 2.3 – Conditions for reduction to Ac-N-methioninol (194)

Conversion of the acid to the methyl ester would allow the reduction to proceed using a mild reducing agent such as the previously mentioned sodium or lithium borohydride. The conversion to the methyl ester was achieved by stirring the acid in anhydrous methanol containing an excess of thionyl chloride (SOCl₂) overnight. Following an aqueous work up the methyl ester was used directly in the subsequent reduction. This was performed by introducing either NaBH₄ or LiBH₄ to a solution of the methyl ester in absolute ethanol at 0 °C. Increasing reaction times beyond 12 hours did little to improve yields. Optimum conditions were achieved when 3 equivalents of NaBH₄ were added to the methyl ester at 0 °C, followed by stirring overnight at 25 °C. Flash chromatography furnished **194** in an overall yield of 88 % over two steps.

2.2.1.3 Activation of Alcohol

Initial thoughts were to activate the oxygen atom of the alcohol by forming the tosylate. Nucleophilic substitution from cyanide would then liberate the tosylate and thus introduce the extra carbon atom into the compound. Tosylation was attempted using a variety of conditions, the most successful of which consisted of reacting **194** with tosyl chloride and TEA with a catalytic amount of 4-DMAP in DCM. However, only a 15 % yield of **195** was obtained from this reaction. It was possible that following the tosylation of the alcohol, the oxygen atom of the amide could perform an intramolecular nucleophilic attack on the carbon atom α to the tosylate, thus displacing the tosylate and forming the oxazoline **200** (Scheme 2.4).



Scheme 2.4 – Oxazoline formation

It was predicted that conversion to the less labile iodide (**198**) would reduce the possibility of intramolecular attack from the amide oxygen atom. The synthesis of the iodide proceeded via activation of the alcohol by triphenylphosphine followed by nucleophilic addition of iodide. It was difficult to determine whether the iodide had been successfully synthesised due to the presence of triphenylphosphine oxide. It was not possible to remove the triphenylphosphine oxide from the product using flash chromatography or recrystallisation.

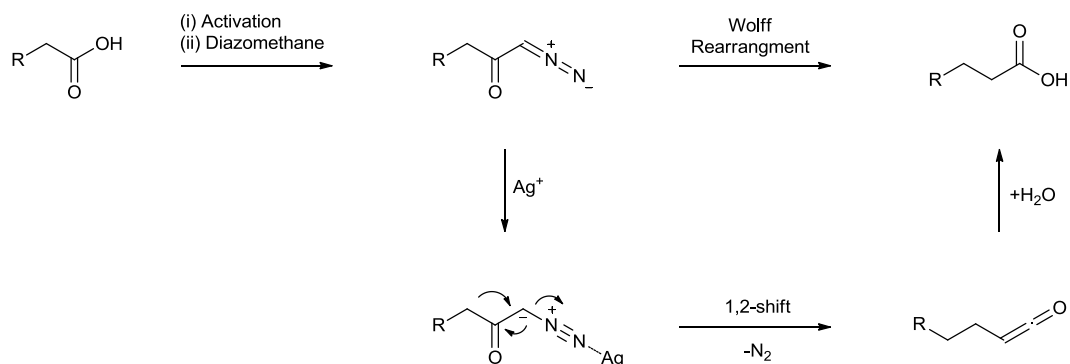
Formation of the even less labile chloride was expected to be less likely to undergo the intramolecular reaction. Furthermore, it could be produced in the absence of PPh_3 . The chloride **199** was synthesised by stirring **194** with an excess of thionyl chloride in DCM at 25 °C. ^1H NMR spectrum of the crude product indicated that two similar compounds had been synthesised in a ratio of 1.2:1. The spectrum was similar to that of tosylate **195**, but contained two sets of peaks for each resonance. Mass spectrometry confirmed the presence of two compounds with molecular weights consistent with that of chloride **199** and oxazoline **200**, thus suggesting that the intramolecular nucleophilic substitution, depicted in scheme 2.4 does indeed take place during the reaction. Isolation of the two compounds was attempted. However, neither compound could be

visualised by TLC (I₂, KMnO₄, CAM, ninhydrin) which made flash chromatography undesirable. Furthermore, recrystallisation of the two compounds ultimately failed.

2.2.2 Arndt Eistert reaction

The synthesis of β -homomethionine via the amino nitrile route (*vide supra*) was unsuitable due to the poor yield obtained from the activation of *N*-acetyl amino alcohol **194**. Therefore, it was deemed necessary to explore the previously mentioned and undesirable Arndt Eistert synthetic route to β -homomethionine.

The synthesis (scheme 2.5) proceeds through nucleophilic addition of diazomethane to an activated carboxyl, thus producing the diazoketone. This diazoketone then undergoes a Wolff rearrangement, during which a ketene intermediate is formed through the photochemical, thermal or silver catalysed liberation of N₂, followed by an intramolecular 1,2 carbon shift. The ketene subsequently undergoes hydrolysis to give the acid.

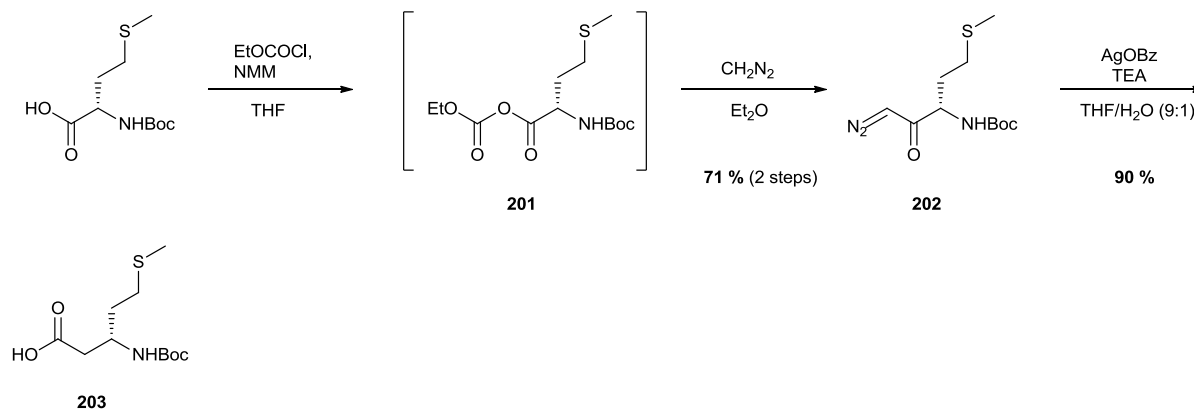


Scheme 2.5 – Silver catalysed Arndt Eistert synthesis

Classically, activation was achieved through the formation of an acid chloride, typically by reaction with thionyl chloride. In the case of amino acid homologation though, where acid chloride formation is not appropriate, activation through the formation of a mixed anhydride has seen much success.^{1, 182}

In the conversion of α -methionine to its β -homologue (scheme 2.6), it was necessary to use a *N*-protected amino acid to inhibit any nucleophilic attack from the amino group when forming the mixed anhydride. Mixed anhydride **201** was formed *in situ* from treatment of Boc-*N*- α -methionine with ethyl chloroformate. Addition of diazomethane to the reaction produced diazoketone **202** in 71 % yield following flash chromatography. This was successfully converted to Boc- β -

homomethionine (**203**) through a silver trifluoroacetate (Ag-TFA) catalysed Wolff rearrangement in 81 % yield, an overall yield of 57 % (3 steps). Substituting the costly Ag-TFA for the less expensive silver benzoate (AgOBz) resulted in a slight increase in yield (90 %) from the Wolff rearrangement, although recrystallization was necessary for purification. This gave an overall yield of 64 % (3 steps). The potentially explosive diazomethane can be substituted for its safer TMS derivative. However, diazoketone **202** was produced in significantly lower yield (51 %).



Scheme 2.6 – Arndt Eistert synthesis of Boc- β -homomethionine (**203**)

Isolating of **203** as its methyl ester was achieved using methanol as the medium for the Wolff rearrangement. However, this resulted in an average reaction yield (51 %) and required the more labour intensive flash chromatography for purification due to the formation of side products.

2.3 Synthesis of bicyclic guanidines

Scheme 2.2 illustrates the synthetic route to bicyclic guanidines **209**, **215** and **219**. Due to the lengthy process of producing β -homomethionine, its α -homologue was used for the optimisation of conditions for this synthesis. It was predicted that these optimised conditions could be directly transferred to that of the β -homologue without a significant reduction in yield.

2.3.1 Reduction

Optimum conditions for the reduction (step 1, scheme 2.2) are dependent on the nature of the starting material. The highest observed yield for the reduction of the free amino acid, methionine, was obtained when using the method described by Giannis and Sandhoff.¹⁸³ For this mild reduction a $\text{BH}_3 \cdot \text{THF}$ complex is formed *in situ* from lithium borohydride and TMS-Cl in anhydrous THF. TLC

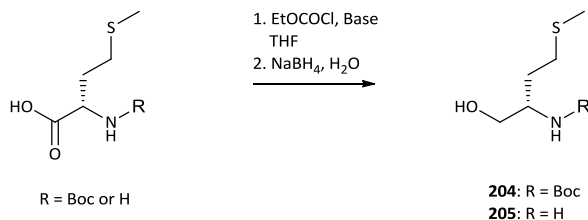
indicated the reaction had reached completion after 24 hours. Isolation of the product was difficult due to its solubility in water. Additionally, column chromatography was unsuitable as the amino alcohol was retained strongly by silica. Optimum conditions required extraction with 20 % KOH (w/v) and furnished L-methioninol in 63 % yield requiring no further purification according to the ^1H NMR spectrum. This method of reduction produced a higher yield than when $\text{BH}_3\cdot\text{THF}$ (1 M solution in THF) was added directly to a solution of the amino acid in THF (52 %).

Boc-protecting the amino moiety was thought to be advantageous as this could aid the handling of the product during work up and purification. Furthermore, Boc- α -methionine was commercially available and relatively inexpensive and Boc- N - β -homomethionine had previously been synthesised.

For the reduction of Boc-protected α -methionine, only a 53 % yield was obtained when employing the above conditions (TMS-Cl and LiBH_4). However, as expected, the recovery of the product was more reliable than for the free amino acid. The yield, when employing a 1 M solution of $\text{BH}_3\cdot\text{THF}$ as the reducing agent, was even lower (40 %).

Significantly higher yields were obtained when reduction directly followed activation of the acidic moiety (up to 77 %). Activation was achieved through formation of a mixed anhydride by reaction with ethyl chloroformate and an equimolar amount of base at 0 °C. During mixed anhydride formation, a white precipitate, which was the hydrochloride salt of the base, became apparent. Maximum yields of **204** were obtained when this precipitate was removed by filtration immediately before the reaction mixture was added to a cold solution of NaBH_4 in water (table 2.2, entries 7-12).

Altering the choice of base did little to improve efficiency, with an insignificant change in yield occurring regardless of the base employed (TEA, DIEA or NMM). Similarly, substituting NaBH_4 for LiBH_4 resulted in a negligible change in yield, as did extending the reaction times beyond 12 hours.



Entry	R =	Base for mixed anhydride	Reducing Agent ^a	Duration (hours)	Yield (%)
1	H	-	LiBH ₄ (2), TMS-Cl (4)	24	63
2	Boc	-	LiBH ₄ (2), TMS-Cl (4)	12	53
3	Boc	-	BH ₃ ·THF (2.3)	12	40
4	Boc	NMM	NaBH ₄ (2) ^b	48	65
5	Boc	NMM	NaBH ₄ (3) ^b	12	63
6	Boc	NMM	LiBH ₄ (3) ^b	12	60
7	Boc	TEA	NaBH ₄ (2) ^c	4	54
8	Boc	TEA	NaBH ₄ (2.1) ^c	18	63
9	Boc	DIEA	NaBH ₄ (2.1) ^c	4	70
10	Boc	DIEA	NaBH ₄ (2.1) ^c	12	60
11	Boc	DIEA	NaBH ₄ (2.1) ^c	24	65
12	Boc	NMM	NaBH ₄ (3) ^c	12	77

^a number of equivalents in parentheses; ^b reducing agent was added directly to the mixed anhydride, followed by the dropwise addition of MeOH; ^c following mixed anhydride formation, the reaction was filtered and filtrate was added to a cold solution of reducing agent in water.

Table 2.2 – Reduction of α -methionine and Boc- α -methionine.

The efficiency of the NaBH₄ reduction proceeding via formation of the mixed anhydride made it the obvious choice for reduction. The reaction produced Boc-*N*-amino alcohol **204** in 77 % yield following a simple aqueous work up procedure, with no further purification necessary. For the β -homologue (**210**), a comparable yield of 75 % was obtained. Additionally, 10 % of the starting material could also be recovered from the reaction using a simple aqueous work up.

2.3.2 Boc-deprotection

Successful removal of the Boc protecting group was achieved by stirring **204** in 20 % trifluoroacetic acid (TFA) in DCM for 2 hours at room temperature. This furnished the TFA salt of amino alcohol

205 in quantitative yield. Using as little as 5 % TFA in DCM also gave a quantitative yield, although, longer reaction times were necessary (ca. 6 hours).

The presence of the TFA salt of **205** consequently resulted in low yields when performing the subsequent step (silyl protection). This could be due to silylation of trifluoroacetate, as indicated by a rise in yield when an excess of the silylating agent was used. This will be discussed more in section 2.3.3. Conversion to the free amine was thought to alleviate this issue and was achieved by ion-exchange chromatography (Amberlite® IRA-400, HO⁻ form). This indeed, resulted in an increase in yield from 25 % to 45 % for silyl protection (again this will be reviewed in section 2.3.3). However, this approach entails elution with copious amounts of water and consequently requires lyophilisation.

It was expected that isolating amino alcohol **205** as the hydrochloride (HCl) salt, would ultimately improve the yield of the subsequent step as the chloride anion (Cl⁻) would not interfere with the silylating agent. Furthermore, it would eliminate the need to perform ion-exchange chromatography. Instead, removal of the solvent would be all that is necessary to produce the pure amino alcohol **205** as its HCl salt. Boc cleavage was achieved by stirring **204** in a 2 M solution of aqueous HCl for two hours at room temperature. Removal of solvent furnished **205** as its HCl salt, again in quantitative yield. The same reaction conditions were used to produce the β -homologue (**211**) in a quantitative yield from amino alcohol **210**.

2.3.3 Silyl Protection

It was suspected that silylation of the free amino form of α -methioninol (**205**) would be quite sluggish due to rapid silylation at the more nucleophilic amino moiety followed by the slow migration to the hydroxyl group. Ensuring α -methioninol (**205**) was protonated at all times would obviously alleviate this potential issue and should subsequently increase reaction times.

The p*K*_a of the protonated form of the amino alcohol was expected to be approximately 9-10, so employing a weak base, such as imidazole (p*K*_{aH} = 5.5), during the reaction would inhibit any nucleophilic reaction from the amino group and thus increase reaction time.

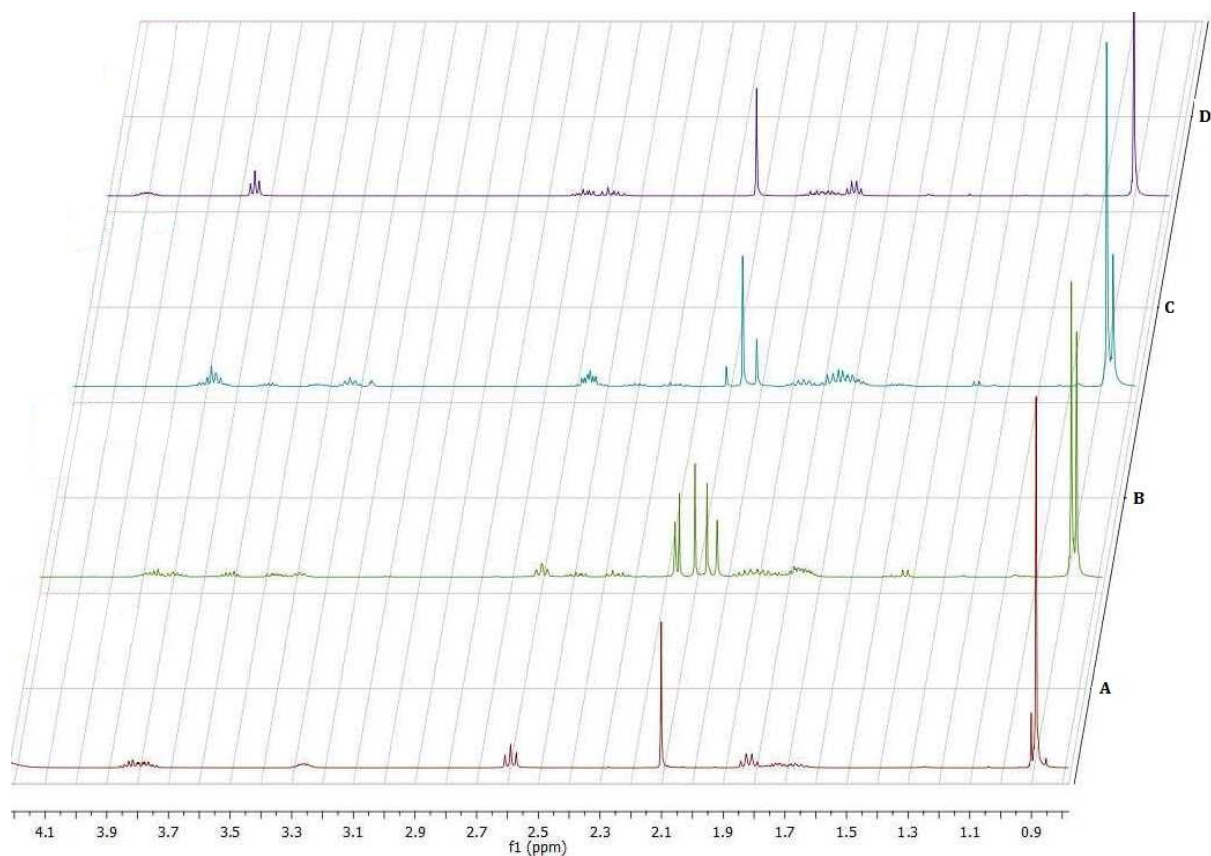


Scheme 2.7 – Silyl protection of **205** and **211**.

t-Butyldiphenylsilyl (TBDPS) protection of **211** was attempted by the addition of TBDPS-Cl to a solution containing **211** and imidazole in anhydrous DCM. Following an aqueous work up the reaction was purified by flash chromatography. This exposed a major stumbling block with the formation of the silyl ether. Although the ^1H NMR spectrum of the isolated product displayed many of the expected resonances, also apparent were a series of five singlet peaks around 2.0 ppm (figure 2.1B), when only one was expected. Also present was higher multiplicity with some of the expected multiplets.

The ^1H NMR spectrum of the crude TBDPS protection product (prior to flash chromatography) showed no sign of this impurity (figure 2.1A). Instead, it indicated just the presence of the silylated alcohol (**216**), imidazole and some assumed silanol by-products (indicated by shouldering of the *t*-butyl peak at 0.9 ppm).

Although evidently present, as observed in the ^1H NMR spectrum (figure 2.1B), the by-products could not be visualised by TLC. This suggested that the by-products were very similar in structure to **216** and so had a R_f value indistinguishable from it or, they were simply not visible using standard visualising techniques. It was also possible that when in contact with the TLC plate the by-products converted back to **216** or decomposed to something not visible by TLC staining. ESI+ mass spectrometry of the crude product only gave the molecular ion as expected for **216**. Reverse phase HPLC failed to resolve the peaks, instead giving just one large broad peak and GC-MS was unsuitable, displaying only peaks comprising low molecular weight peaks, possibly due to decomposition at elevated temperatures (up to 300 °C).



A. Crude spectrum of TBDPS protection; B. TBDPS protection following flash chromatography; C. Re-extraction of the TBDPS protected columned product; D. Pure TBDPS protected product (**216**) obtained using extensive work up.

Figure 2.1 – ^1H NMR spectra of TBDPS protection.

To determine what was causing the formation of these by-products, a series of tests were carried out. The stability of crude **216**, both in its dried form and dissolved in methanol as well as chloroform, was assessed. In all cases, after subjecting the crude material to the atmosphere for one week and then obtaining ^1H NMR spectrum, the acquired spectra were identical to that of the crude mixture. This demonstrated that the presence of these by-products was not due to reaction with the solvent, degradation, hydrolysis or air oxidation.

It was plausible that the by-products were formed by inter or intramolecular reactions catalysed by either acid or base. To evaluate this, a solution of columned **216** (containing the by-products) in CDCl_3 was stored over potassium carbonate. Obtaining ^1H NMR at varying times over the course of a week produced no observable change. Furthermore, when performing the same experiment using

crude **216** (this time containing no by-products), again no change was observed, thus giving evidence that formation of the side products are not acid or base catalysed.

Although unable to identify these by-products, their presence seems to be due to the instability of the TBDPS ether with silica gel. As a consequence of this, purification by flash chromatography was not viable and so a different purification technique needed to be devised. Re-performing the work up procedure on chromatographically purified **216** (containing by-products) resulted in removal of some but others were still evident (figure 2.1C).

Using the crude product from the TBDPS protection in the subsequent step produced several side products. Although, their removal was possible by flash chromatography, the resulting yield was poor (38 %). A literature search suggested Jadhav *et al.* had encountered similar problems and described an extensive work up procedure to remove side products formed during the reaction which avoided the use of flash chromatography.⁸⁸ This procedure involved numerous extractions with 1 M NaOH. The organic phase was then extracted several times with MeCN/H₂O/AcOH (40:60:2). Finally, following removal of MeCN, the aqueous phase was basified using Na₂CO₃ and extracted with Et₂O.

Utilisation of the work up procedure described by Jadhav *et al.* afforded **216** in 45 % yield from the corresponding free amino form of **211**. Despite the low yield, the product was obtained in high purity (indicated by ¹H NMR, figure 2.1D) which gave reason for optimism. Moreover, the yield was significantly higher than that obtained when performing the reaction with the trifluoroacetate salt of **211** (25 %). Increasing the number of equivalents of silylating agent resulted in a similar yield to that obtained from the free amino alcohol (43 %). It was assumed, as stated in the previous section, that silylation of trifluoroacetate was taking place. Changing the substrate from the trifluoroacetate to the hydrochloride salt of **211** was expected to overcome this potential issue. The use of the HCl salt of **211** increased the recovered yield of TBDPS protected amino alcohol **216** to 56 %. Endeavours to further increase the yield included altering the choice of base to TEA or DIEA and extending reaction times beyond 12 hours. However, this failed to improve yields, as did using DMF as the reaction medium.

The poor yields obtained were suspected to be due to the bulkiness of the silylating agent. The use of the less hindered *t*-butyldimethylsilyl (TBS) derivative was predicted to enhance the reaction yield. This proved to be correct and an isolated yield of 76 % of **206** was obtained from treatment of amino alcohol **205** with TBS-OTf in the presence of imidazole in anhydrous DCM. It was

necessary however to alter the extensive work up in order to avoid cleavage of the silyl protecting group. The TBS protection of the β -homologue was performed under the same condition and furnished **212** in a similar yield (74 %).

2.3.4 Isothiocyanate formation

The original procedure⁸⁶ used for the formation of the isothiocyanate involved addition of thiophosgene (CSCl_2) to a biphasic reaction (1:1 aq Na_2CO_3 :DCM) containing the silylated amino alcohol. Due to the toxic fumes formed during the reaction, the vessel was sealed and any gas was able to escape through a gas outlet tube, the exit of which was submerged in 2 M NaOH to quench these hazardous gases.

High yields were obtained when TBDPS-protected amino alcohol **216** was used (88 %), with the product requiring no further purification following aqueous extraction. However, cleavage of the silyl protecting group was apparent when the same reaction conditions were applied to the less robust TBS-protected amino alcohol **206**. This suggested that the high pH of the aqueous phase (pH~14) was responsible for silyl de-protection.

Changing the inorganic base to calcium carbonate (CaCO_3) still failed to yield the protected isothiocyanate, the pH of the solution was still high, ca. 14. Substituting for sodium bicarbonate (NaHCO_3) saw some success, although, the reaction product contained a mixture of protected and unprotected compounds. Separation was achieved through flash chromatography but the yield was low (24 %).

Replacing the inorganic base with an organic base and performing the reaction solely in DCM was also investigated, this produced the desired isothiocyanate **206** in a 67 % yield. However, using this procedure, flash chromatography was necessary for purification. These conditions, although successful, produced a less inspiring result than was obtained when using the TBDPS-protected amino alcohol (**216**) in the biphasic reaction mentioned earlier.

As previously stated, it was suspected that the cleavage of the TBS protecting group was taking place due to the high pH of the aqueous solution used in the biphasic reaction. A pH of approximately 14 was clearly too high and resulted in silyl cleavage, as was demonstrated when employing either CaCO_3 or Na_2CO_3 as the base. However, the presence of TBS-protected isothiocyanate **207**, when aqueous NaHCO_3 (pH~9) was employed gave reason to be optimistic and

suggested that it was the high concentration of hydroxide ions (HO^-) that resulted in the de-protection of the amino alcohol.

The reaction was repeated using NaHCO_3 , though, this time the aqueous phase was omitted. Thiophosgene was added to a mixture of silyl protected amino alcohol **206** and NaHCO_3 in DCM while stirring at room temperature. Again toxic fumes were allowed to escape the reaction and were quenched with 2 M NaOH . The heterogeneous reaction produced the TBS-*O*-isothiocyanate **207** in excellent yield (98 %) after aqueous work up and required no further purification. These conditions were successfully transferable to TBS-*O*- β -homomethioninol (**212**), which yielded the corresponding isothiocyanate **213** (95 %).

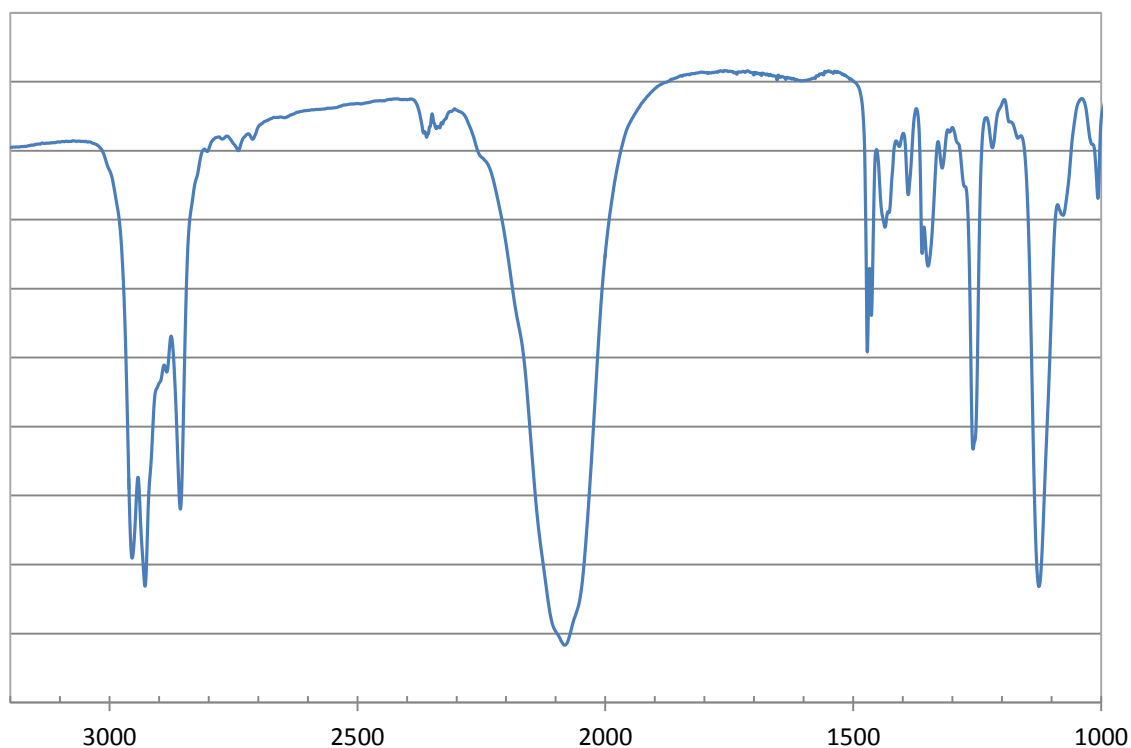


Figure 2.2 – IR spectrum of TBS-isothiocyanate **207**.

The FT-IR spectrum of the product displayed a characteristic stretch at 2085 cm^{-1} indicative of $\text{N}=\text{C}=\text{S}$ functionality (figure 2.2). Furthermore, the ^1H NMR spectrum displays all expected protons, and shows a 0.9 ppm increase in chemical shift for the proton bound to the chiral centre (figure 2.3).

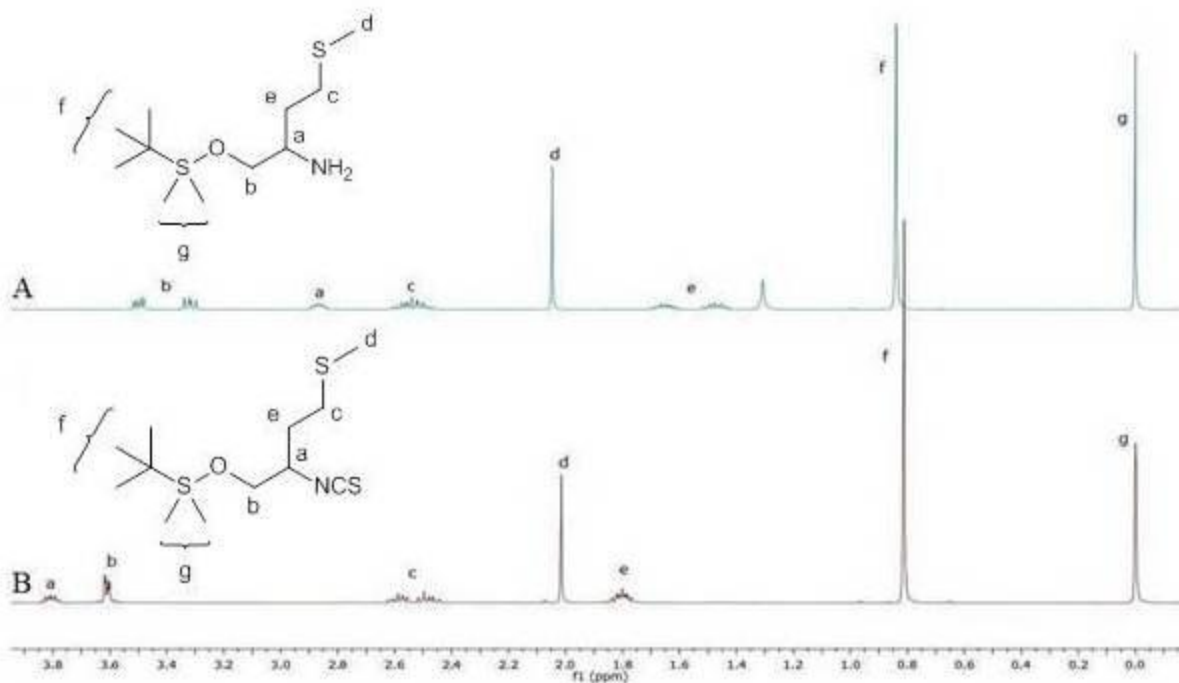


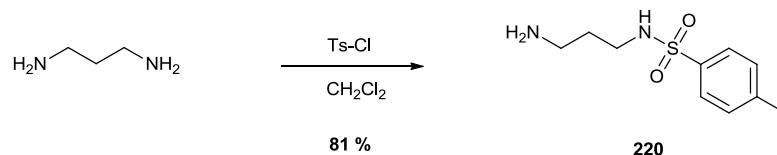
Figure 2.3 - A) ^1H NMR spectrum of TBS-O-Methioninol (**206**); B) ^1H NMR spectrum of isothiocyanate **207**.

2.3.5 Protection of Diamine

It was predicted that the 2,2,4,6,7-pentamethyl-2,3-dihydrobenzofuran-5-sulfonyl (Pbf) protecting group would be useful for the protection of 1,3-diaminopropane. It is similar in structure to the tosyl group and is robust against organic bases. Its removal does not require the use of hazardous HF; instead, cleavage can be achieved using concentrated TFA. Due to these reasons Pbf has gained a lot of popularity in peptide synthesis, where it has been used extensively to protect the side chain of arginine. Introduction of this to AH-2-P would allow its easy removal when performing peptide synthesis with the amino acid at a later stage. Although commercially available, Pbf-Cl is quite expensive and so the use of tosyl protected diamine **220** was thought to be a useful derivative for model reactions. Due to the similarities in structure it was predicted that the optimised reaction conditions would be transferable from the tosyl to the Pbf protected diamines.

2.3.5.1 Tosyl-*N*-mono-protection

Production of the mono-tosylated diamine **220** was achieved by refluxing tosyl chloride with an excess of 1,3-diaminopropane in DCM. The reaction was complete in two hours and the product was isolated by recrystallization from toluene in 81 % yield.



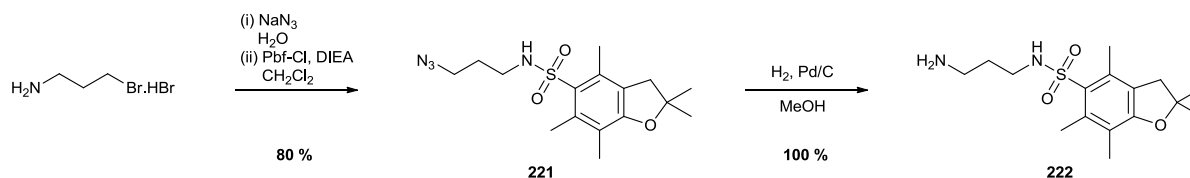
Scheme 2.8 – Synthesis of mono-protected Ts-diamine.

2.3.5.2 Pbf-*N*-mono-protection

The synthesis of Pbf protected diamine **222** proved to be more problematic than its tosylate counterpart. The reaction was performed under the same reaction conditions used for the *N*-tosylation. However, TLC suggested the reaction was not reaching completion. Addition of TEA encouraged complete consumption of Pbf-Cl.

Purification of **222** was challenging. Recrystallization, again from toluene, did produce the pure compound but in only 50 % yield. Flash chromatography was impractical because **222** was strongly retained by silica. Recrystallizations and precipitations from other solvents ultimately failed.

Because of the expense of Pbf-Cl, use of the above method to produce **222** was not viable. Development of an alternative method for the synthesis of **222** was desired (scheme 2.9). It was expected that following the synthesis of *N*-(3-azidopropyl)-2,2,4,6,7-pentamethyl-2,3-dihydrobenzofuran-5-sulfonamide (**221**), purification would be possible by flash chromatography. The remaining azide could then be converted to the diamine by hydrogenolysis.



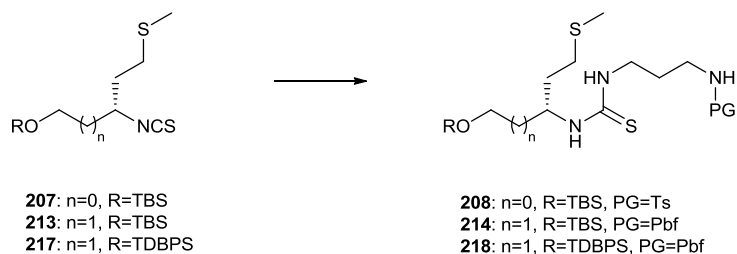
Scheme 2.9 – Synthesis of mono-protected Pbf-diamine **222**.

The formation of the azide was achieved by heating a solution of 1-bromopropylamine hydrobromide and sodium azide in water. Isolation of the product was unattainable due to its relatively low boiling point. It transpired that isolation of the azide at this point was unnecessary. Following an aqueous extraction, the organic phase containing an expected excess of 3-azidopropylamine was reacted with Pbf-Cl and DIEA at 50 °C. Isolation of **221** was achieved in 80 % yield after flash chromatography. Hydrogenolysis over Pd/C (10 %) at one atmosphere produced clean conversion to diamine **222** in quantitative yield.

2.3.6 Thiourea formation

Thiourea formation was achieved by stirring both the isothiocyanate **207** and Ts-*N*-diamine **220** in anhydrous THF at room temperature. However, only a 50 % yield of **208** was obtained after purification. Various attempts to improve the efficiency of this reaction were undertaken (table 2.3). Increasing the reaction temperature did little to improve yields, with the TLC showing that starting materials still remained even after 48 hours at reflux. Varying the solvent failed to improve yields, exchanging THF with acetonitrile gave similar results, while the use of absolute ethanol decreased yields further (38 %) this was likely due to reaction of ethanol with **207**.

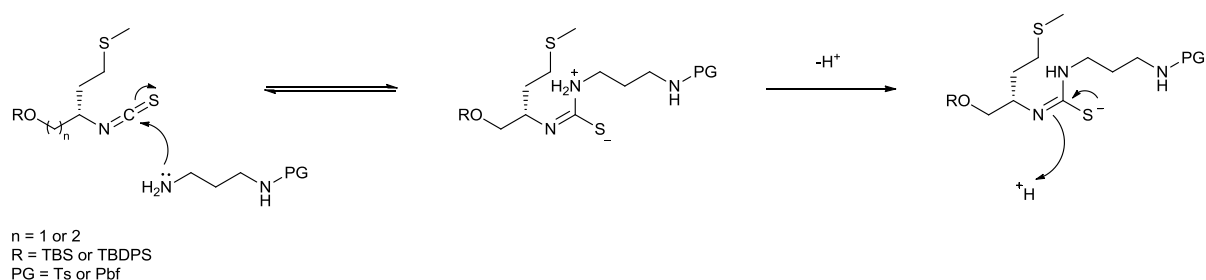
TLC during these reactions showed that the mediocre yields were indicative of incomplete consumption of starting materials. Consideration of the reaction mechanism gave insight into what could be taking place during the reaction. It was expected that the reaction proceeds through the formation of a thiuronium species (Scheme 2.10). It is plausible that following nucleophilic attack of the amino group on the isothiocyanate the reverse reaction is taking place at a faster rate than that of proton abstraction. Addition of a base to the reaction was predicted to remove the proton from the cationic nitrogen and so encourage the formation of the thiourea.



Substrate	Solvent	Temperature (°C)	Base/Catalyst ^a	Duration (hours)	Yield (%)
217	THF	70	-	24	43
207	THF	70	-	24	50
207	EtOH	20 – 80	-	24 ^b	38
207	MeCN	20 – 85	-	24 ^b	50
207	MeCN	20 – 85	-	72 ^c	55
207	THF	70	-	36	50
207	THF	20	Imidazole (2)	24	75
207	MeCN	20	DIEA (2)	24	60
207	MeCN	85	DIEA (0.2)	48	53
207	MeCN	20 – 85	DIEA (2)	24 ^b	78
207	MeCN	20 – 85	NaHCO ₃ (2)	20 ^b	85
213	MeCN	20 – 85	NaHCO ₃ (2)	20 ^b	79

^a number of equivalents in parentheses; ^b 8 h at 85 °C; ^c 48 h at 85 °C.

Table 2.3 – Conditions for thiourea formation



Scheme 2.10 – Mechanism of thiourea formation.

Imidazole was expected to be a good base for the reaction as it could also act as a catalyst through addition to the isothiocyanate. The addition of two equivalents of imidazole to a solution of **207** and **220** in anhydrous MeCN significantly increased the yield of thiourea **208** to 75 % following column chromatography. Furthermore, TLC indicated the complete consumption of starting materials, which had not been observed previously when the reaction was performed in the absence of base. TLC also displayed the presence of another compound, of similar R_f value (0.44) to that of the thiourea **208** (0.29), which had been previously encountered. This will be discussed in more detail later.

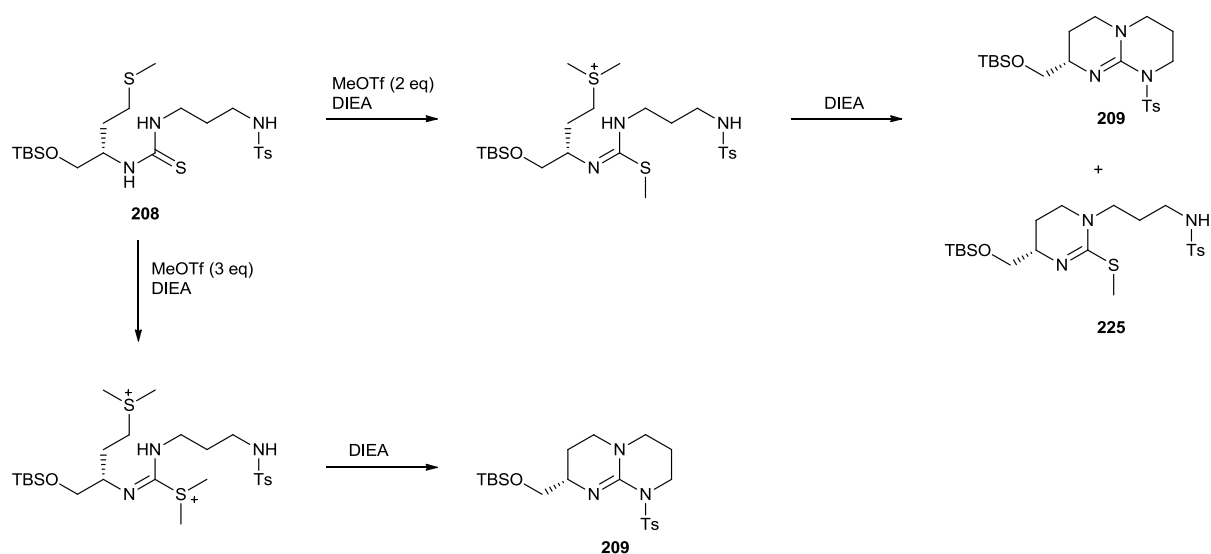
Experimenting with other bases further displayed their importance for the reaction. Employing two equivalents of DIEA also produced better yields than in the absence of base. The yield was slightly higher than previously seen with imidazole (78 %). Again the TLC indicated the completion of the reaction but unfortunately also showed the presence of the previously encountered side product. The use of only a catalytic amount of DIEA resulted in similar yields to those seen when the base was omitted (53 %); again this was due to incomplete consumption of starting materials.

Using the crude product in the subsequent step reduced the effectiveness of that reaction. It was unclear at this stage whether this was due to the side product itself, or if it was the presence of base which ultimately affected the cyclization effectiveness.

Although difficult, due to their similar affinity with silica gel, it was possible to separate the product from the side product by flash chromatography. However, a percentage of the product was always lost by co-elution of the two compounds which resulted in reduced yields.

Using an inorganic base, such as NaHCO_3 was thought to be advantageous, as this could be removed by filtration following completion of the reaction and so, the purification step could possibly be omitted. The reaction was performed under the same conditions as before, with NaHCO_3 replacing DIEA or imidazole. The crude product, following filtration, again resulted in a reduction in yield of the subsequent step, thus demonstrating the importance of purity for that reaction. The use of this heterogeneous system however, did produce **208** in the highest yield (85 %) following flash chromatography. These conditions could again be transferred to the β -homologue (**213**), with a 79 % yield of thiourea **214** produced, although the presence of a by-product of slightly higher R_f value was again evident.

Although it was possible that the Pbf protecting group could be removed during the formation of the thiourea, it was unlikely that removal of the *N*-tosyl group could take place under the conditions



Scheme 2.11 – Cyclization of thiourea to give bicyclic guanine **209**.

Münster intimated that only two equivalents of methylating agent were necessary for conversion to the bicyclic guanidine.⁸⁶ However, when employing only two equivalents of methyl triflate, as well as the expected bicyclic guanidine **209**; there was a significant amount of the monocyclic compound (**225**) present. It was predicted that increasing the number of equivalents would result in an increase in yield due to the expectancy that DMS would act as a better leaving group than the methanethiolate anion. Using three equivalents of methyl triflate resulted in a disappearance of the monocyclic compound (**225**) and thus resulted in an increase in yield of **209** (77 %). When the reaction was performed on the β -homologue, **215** was produced in a similar yield (80 %).

Full assignment of the ^1H NMR spectrum was challenging due to its complexity. It was necessary to perform 2D NMR studies to fully assign the spectrum. Figure 2.4a shows the ^1H NMR spectrum of **215**, which displays numerous multiplets which could not be assigned to their corresponding protons by 1D NMR alone. The COSY spectrum (figure 2.4b) helped to elucidate the resonances. This indicated that certain protons bound to the same carbon had significantly different chemical shifts. HSQC experiment confirmed that resonances at 3.18 and 3.04 ppm belong to protons a and b. The resonances at 1.82 and 1.43 ppm are those of protons c and d. Finally, protons f and g have resonances at 1.38 and 1.18 ppm.

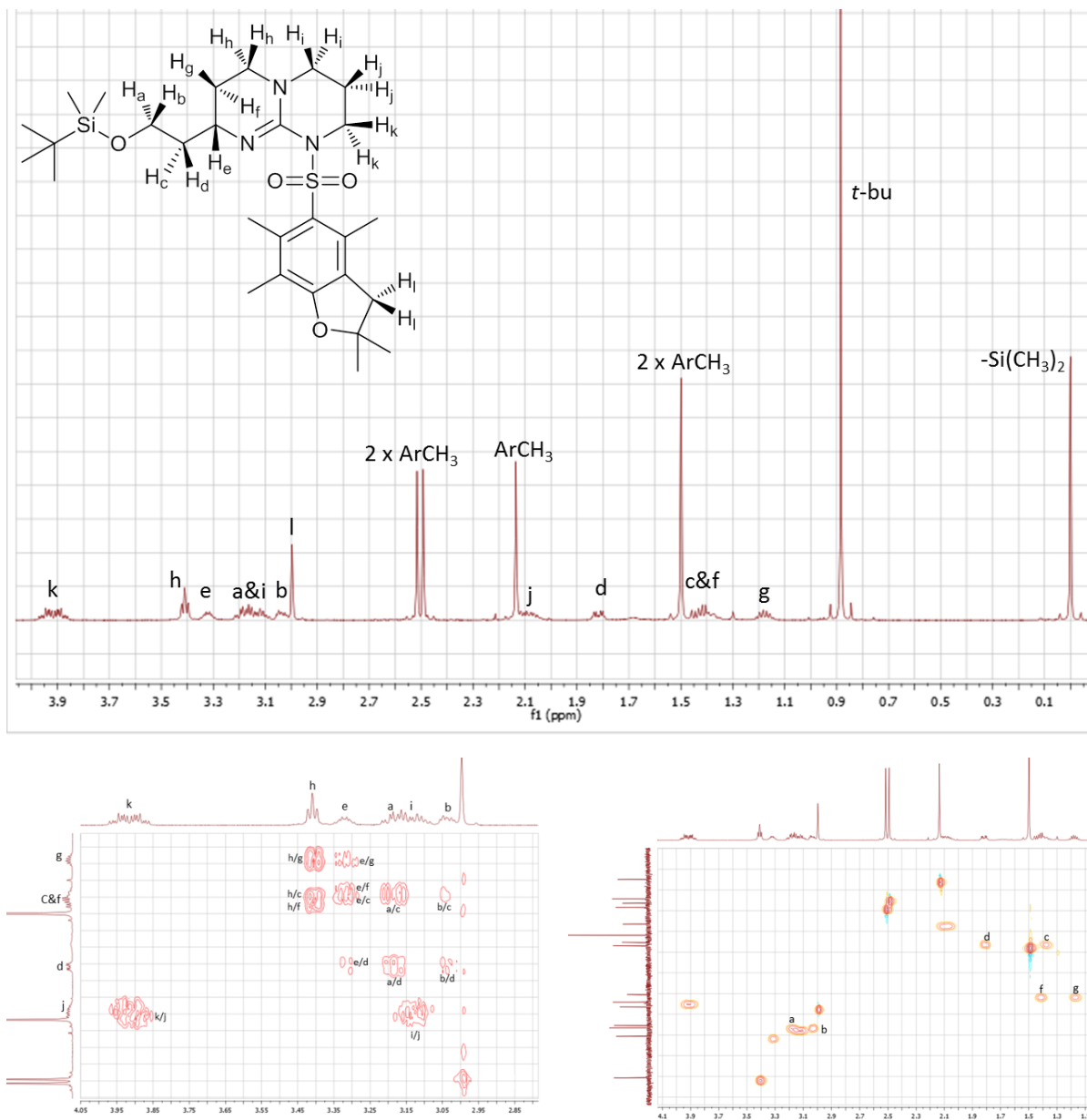
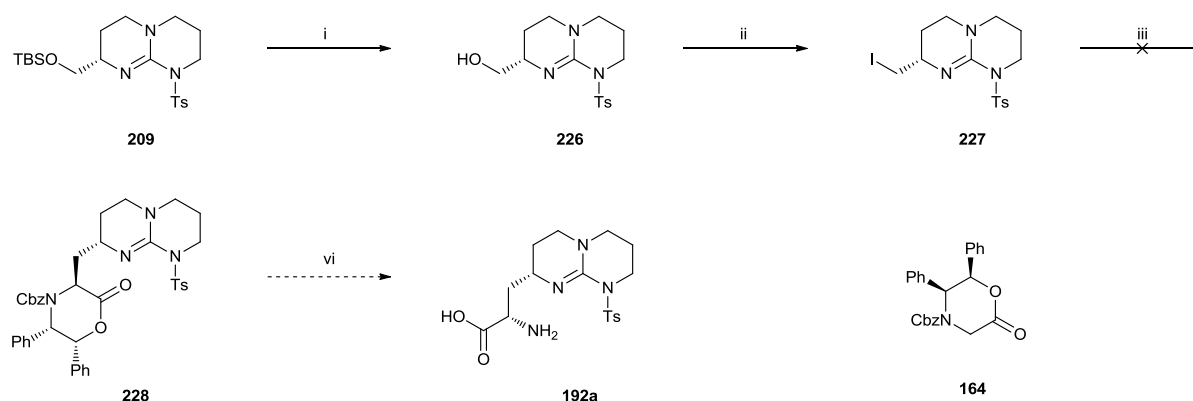


Figure 2.4 – a) ¹H NMR spectrum of bicyclic guanidine **215** with peak assignment. b) COSY NMR spectrum showing assignment of protons a, b, d, e, g, h, i, k. c) HSQC spectrum showing protons d&c, f&g and a&b are bound to the same carbons.

2.4 Synthesis of AH-2-P via chiral glycine enolate

Amino acid functionality can be introduced asymmetrically to a compound by utilizing chiral glycine enolates. The ‘Williams template’ is a commercially available chiral glycine equivalent, which, when in the presence of a strong base, is deprotonated producing the enolate. When

performed at $-78\text{ }^{\circ}\text{C}$ this enolate will react stereospecifically in an $\text{S}_{\text{N}}2$ type mechanism displacing the halide, thus giving the optically active product.



i. TBAF (1 M in THF), THF (**50 %**); ii. I_2 , PPh_3 , imidazole, CH_2Cl_2 , -20 - $25\text{ }^{\circ}\text{C}$ (**82 %**); iii. Li or Na HMDSA, **164**, THF $-78\text{ }^{\circ}\text{C}$; iv. H_2 , PdCl_2 , 20 PSI, EtOH.

Scheme 2.12 – Proposed synthesis of bicyclic guanidino amino acid **192a** via chiral glycine enolate.

The proposed synthesis of AH-2-P from **209** (scheme 2.12) begins with cleavage of the silyl ether followed by conversion of the bicyclic guanidino alcohol **226** to its corresponding iodide **227**. Displacement of the iodide by the aforementioned 'Williams template' was expected to give the precursor to the amino acid. Hydrogenolysis would then yield the bicyclic guanidino amino acid **192a**.

2.4.1 TBS cleavage

2.4.1.1 TBAF de-protection

Silyl group cleavage was possible using a 1 M solution of tetra-*n*-butylammonium fluoride (TBAF) in THF. TLC indicated that complete consumption of **209** had taken place within 4 hours. However, isolation of the pure compound proved difficult. The product was strongly retained by silica gel, and so flash chromatography was not a desirable purification technique. Furthermore, due to the presence of excess TBAF and the side products formed during the reaction, recrystallization and precipitation from a wide range of solvents proved unsuccessful.

The use of an aqueous work up procedure, in which, the crude product was partitioned between aqueous NaOH (1 M) and Et_2O , removed sufficient impurities that pure **226** could be obtained by recrystallisation from hexane-EtOAc in 50 % yield. It seems that a high percentage of the product is lost into the aqueous phase during the work up procedure.

Attempts to improve the reaction yield resulted in failure. It was predicted that the use of an acidic work up would encourage **226** into the aqueous phase while the side products were expected to be removed into the organics. Following neutralization and lyophilisation, the product was obtained along with an excess of ammonium chloride. The presence of NH_4Cl was expected to cause problems during the formation of the iodide so its removal would be necessary. Anion exchange chromatography (Amberlite® IRA-400, ^-OH form) was expected to convert the NH_4Cl to NH_4OH which could then be removed under reduced pressure, leaving the pure bicyclic guanidino alcohol. However, this failed to produce **226**, this could be due to decomposition on the ion-exchange resin, although, this was never proved as the compound could not be recovered from the column.

Kaburagi and Kishi developed a method for the removal of excess TBAF and materials derived from TBAF deprotection.¹⁸⁴ The protocol they employed involves stirring the crude reaction mixture with a sulfonic acid resin and CaCO_3 in MeOH. The sulfonic acid resin acts as a scavenger for the tetrabutylammonium cation and the CaCO_3 converts any HF to CaF_2 , CO_2 and H_2O . All of these can be removed by filtration or evaporation along with TBS-F thus yielding the pure alcohol. This protocol however failed to produce bicyclic guanidino alcohol **226**. It is likely that the guanidino moiety of **226** was protonated and was thus being retained by the sulfonic acid resin.

2.4.2 Conversion to iodide

Formation of the iodide was achieved in a similar manner to that of the Mitsunobu reaction. In this case though, triphenylphosphine (PPh_3) is activated by the formation of an iodotriphenylphosphonium intermediate, which is produced by addition of iodine to a solution of PPh_3 and imidazole in DCM. Nucleophilic attack from bicyclic guanidino alcohol **226** on the triphenylphosphonium intermediate displaces iodide, thus forming a bicyclic guanidine triphenylphosphonium intermediate. Further nucleophilic substitution, this time from iodide, liberated triphenylphosphine oxide and produced the bicyclic guanidino iodide **227** in 81 % yield following flash chromatography. A crystal structure of iodide **227** was obtained and confirmed that the product had been successfully synthesised and was isolated as its HI salt.

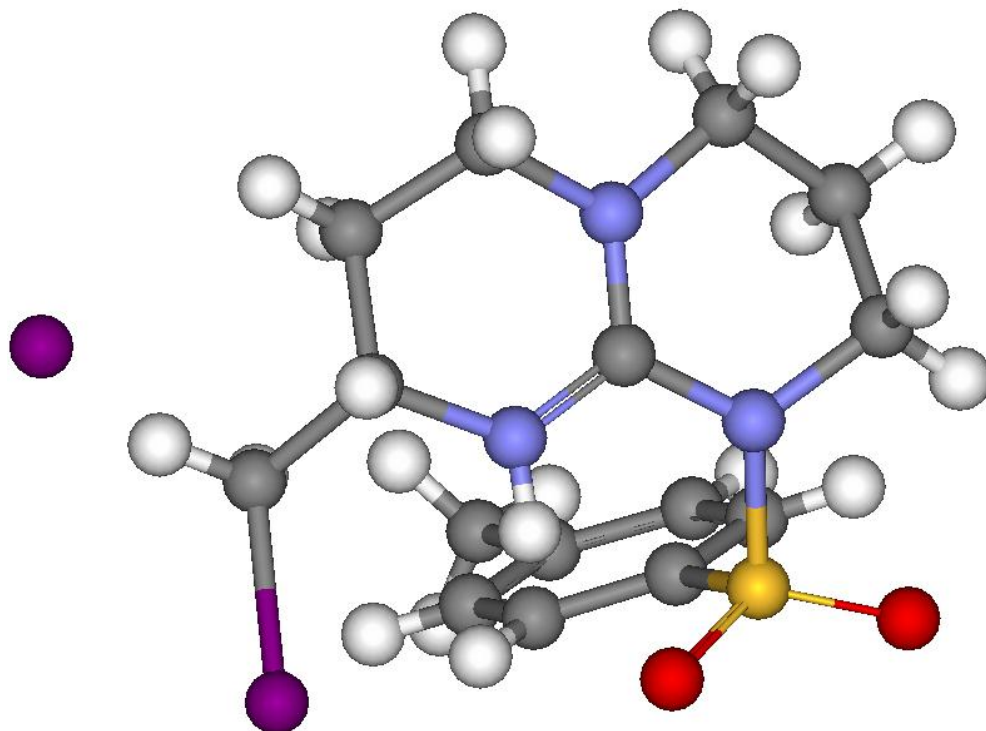
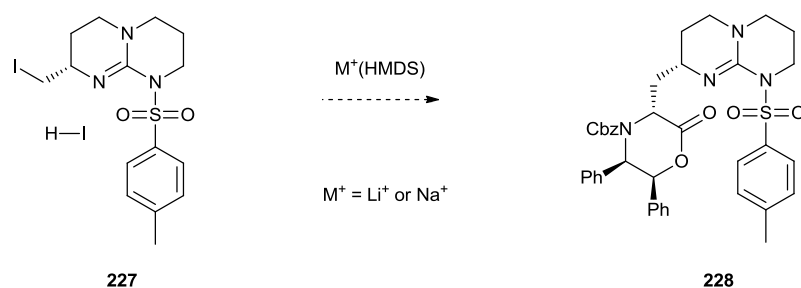


Figure 2.5 – Crystal structure of bicyclic guanidino iodide **227**, crystals were grown by vapour diffusion and the structure was elucidated by Dr Benson Kariuki (Cardiff University).

2.4.3 Reaction with Williams' template

The addition of Williams' template to the bicyclic guanidino iodide **227** was seen as an ideal way to asymmetrically introduce the amino acid. Initial efforts involved addition of lithium bis(trimethylsilyl)amide (LiHMDS) to a solution of **227** and the chiral glycine equivalent (**164**) in THF at -78 °C. No reaction was observed by the TLC after 4 hours at that temperature. Allowing longer reaction times and warmer temperatures failed to convert the iodide to the amino acid precursor. The use of co-solvents such as the carcinogenic solvent hexamethylphosphoramide (HMPA) has seen significant improvements in yields for unactivated alkyl halides.¹⁴⁹ However, when using this or the safer alternative DMPU¹⁸⁵ as a co-solvent, only starting materials were recovered. Changing the number of equivalents of base again failed to produce **228**.



Base ^a	No. equivalents ^b	Solvent	Conditions
LiHMDS	2	THF	-78 °C 2 h, 0 °C 4 h
LiHMDS	2	THF	-78 °C 2h, 25 °C 12 h
LiHMDS	2(1)	THF	-78 °C 1 h, 25 °C 12 h
LiHMDS	2 (1)	THF/DMPU (3:1)	-78 °C 1 h, 25 °C 1 h
LiHMDS	5	THF	-78 °C 2 h, 25 °C 12 h
LiHMDS	2.2 (1)	THF/DMPU (4:1)	-78 °C 1.5 h, 25 °C 12 h
LiHMDS	2.2 (5)	THF/HMPA (9:1)	-78 °C 1 h, 25 °C 12 h
NaHMDS	2 (2)	THF/HMPA (9:1)	-78 °C 0.5 h, 25 °C 12 h
NaHMDS	2.2 (1.2)	THF/DME (1:1)	-78 °C 1 h, 25 °C 12 h
NaHMDS	2.2 (1.2)	DME	-78 °C 1 h, 25 °C 12 h
NaHMDS	2.5	THF/DME (1:1)	-78 °C 2 h, 25 °C 12 h

^a In each case a 1 M solution of THF; ^b Number in parentheses was added after one hour at -78 °C.

Table 2.4 – Summary of reaction conditions employed for the attempted synthesis of **228**.

The use of dimethoxyethane (DME) has seen some success with similar chiral glycine equivalents.^{161, 162} Again though, no conversion was observed when using a variety of ratios with THF. The use of the sodium base was equally as ineffective as the lithium amide.

This observed lack of reactivity could be attributed to the steric bulk of bicyclic guanidino iodide **227**. Figure 2.5 shows the two lowest energy conformations of iodide **227** from the angle of nucleophilic attack from Williams' template. The conformer distribution calculations were performed at the AM1 semi-empirical level of theory. The first conformation (figure 2.6A) shows the carbon atom α to the iodide could be obscured by the sulfoxide of the tosylate. Figure 2.6B

shows that a proton on C₃ could possibly hinder the nucleophilic attack. Additionally, other conformations suffer similar problems.

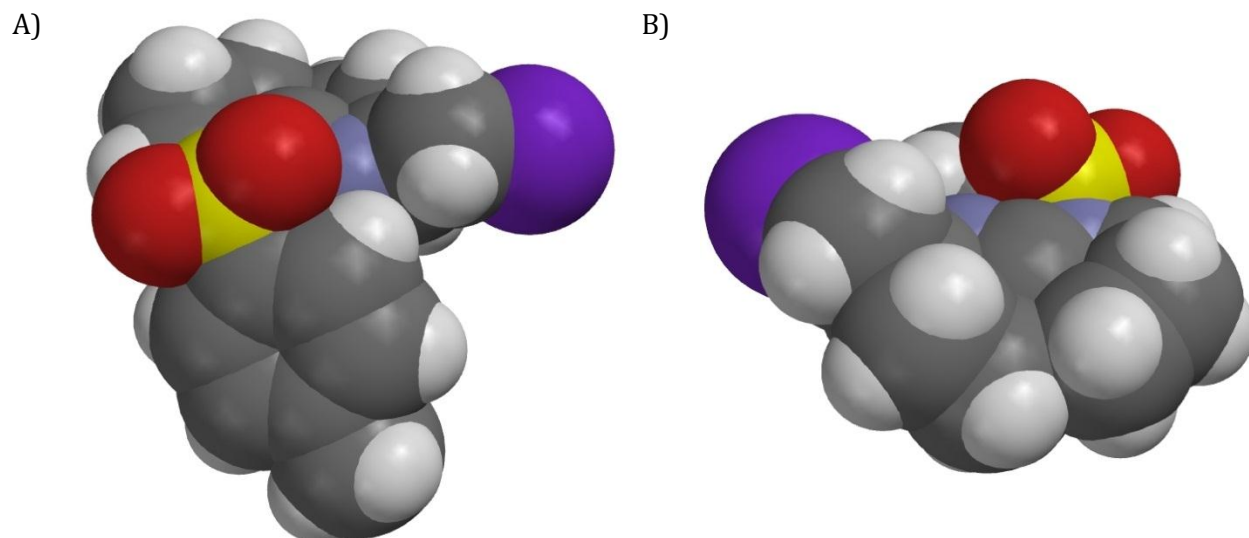
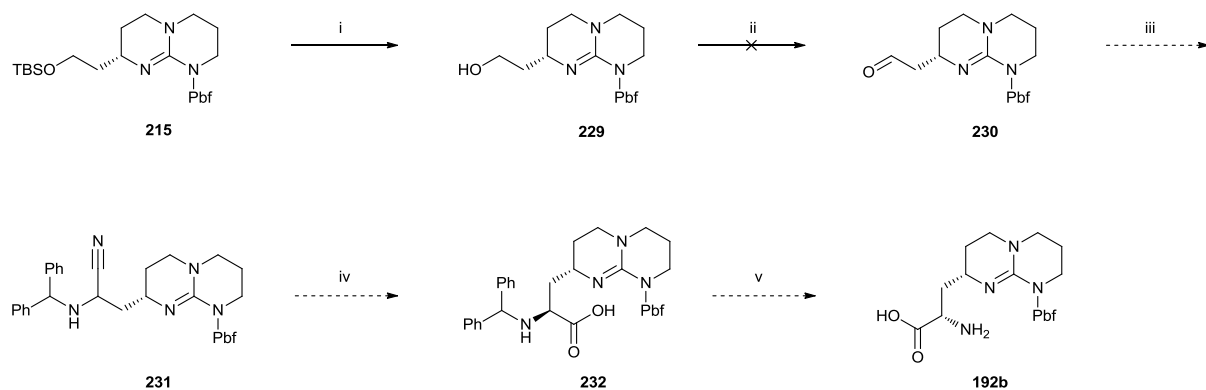


Figure 2.6 – Lowest energy conformations of iodobicyclic guanidine **227** determined by Dr Mark Elliot (Cardiff University) using Spartan 10 v. 1.1.0 run on MacBook Air. Conformer distribution at the AM1 semi-empirical level of theory.

In order to assess this theory, reaction of **227** with other nucleophiles was attempted. No reaction was observed after refluxing **227** for 12 hours in THF containing the bulky nucleophile sodium thiophenolate. To determine whether the lack of reactivity towards the iodide was limited to sterically encumbered nucleophiles, the reactivity towards cyanide was examined. A solution containing **227** and an excess of potassium cyanide in DMF was heated to 80 °C for 24 hours. The TLC of the reaction indicated that no reaction had taken place.

2.5 Synthesis of AH-2-P via Strecker reaction

Scheme 2.13 shows the proposed synthesis of Pbf protected AH-2-P (**189b**) proceeding via a Strecker synthesis. Silyl ether cleavage is followed by oxidation of the alcohol to the aldehyde. Formation of a Schiff base and addition of cyanide is expected to produce amino nitrile **229**. This can then undergo conversion to the amino acid via reduction and hydrolysis, followed by hydrogenolysis.



i. I₂, MeOH, 65 °C (**89** %); ii. C₂O₂Cl₂, DMSO, TEA, CH₂Cl₂, -78 – 25 °C; iii. Ph₂CHNH₂, KCN; iv. a) DIBALH, THF, -78 °C, b) HCl (0.1 M); v. H₂, Pd(OH)₂, MeOH, 1 atm.

Scheme 2.13 – Attempted synthesis of Pbf protected AH-2-P (**192b**) via a Strecker reaction.

2.5.1 TBS Removal

2.5.1.1 TBAF mediated removal

Employing the same conditions used for silyl removal of **209** resulted in complete conversion to the bicyclic guanidino alcohol **229** as indicated by TLC. The purification of the product again proved problematic. Purification by recrystallization was only possible following an aqueous work up and consequently gave a poor yield of 52 %. It seemed that a high percentage of **229** remained in the aqueous phase following the work up procedure.

Purification through a small plug of silica allowed removal of the silyl fluoride, formed during the reaction. However, due to the high polarity of the mobile phase (7:3 EtOAc:MeOH 1 % TEA) that was necessary to elute the product from the column, the tetrabutyl ammonium cation was also present in high concentration.

The use of an acidic extraction followed by neutralisation with NH₄HCO₃ resulted in partial cleavage of the Pbf moiety, even when only 0.1 M HCl was used. Flash chromatography of the lyophilised product resulted in isolation of **229**, although again in an uninspiring yield (53 %).

2.5.1.2 CsF mediated removal

Cesium fluoride (CsF) has seen some success as a reagent for the removal of silyl protecting groups from a variety of primary, secondary and tertiary alcohols.¹⁸⁶ Using this approach, which involved stirring the silyl ether (**215**) and 10 equivalents of CsF in wet acetonitrile at room temperature,

failed to produce the unprotected alcohol. TLC showed that no reaction was taking place, even after 36 hours. Refluxing the reaction resulted in some silyl cleavage but also resulted in removal of PbF.

2.5.1.3 TBS cleavage using Iodine

Removal of the TBS group was finally achieved using a similar method to Vaino.¹⁸⁷ TLC showed that refluxing **209** in 1 % I₂ in MeOH (w/v) for 12 hours resulted in complete consumption of the silyl ether. As already discussed above, **229** has a high solubility in water and so the use of an aqueous work up was impractical. Purification through a small plug of silica was possible, but required a high polarity mobile phase (7:3 EtOAc:MeOH containing 1 % TEA) and ultimately resulted in a mixture of **229** and triethylamine hydroiodide, the latter of which, could not be removed. It was found that quenching the reaction with Na₂S₂O₃ followed by stirring with NaHCO₃ was necessary to remove excess I₂ and any HI produced during the reaction. Pure **229** was isolated as the HI salt by trituration from EtOAc (89 %).

2.5.2 Oxidation

Consideration of the choice of oxidising agent was important for the oxidation of bicyclic guanidino alcohol **229**. Care would need to be taken to avoid over oxidation to the acid. Pyridinium chlorochromate (PCC) is a useful reagent for the oxidation of alcohols to aldehydes. However, it was predicted that removal of the Cr(IV) salts from the reaction would prove to be very challenging. It was therefore decided that Swern oxidation would be a useful method for the oxidation of **229** to its corresponding aldehyde (**230**).

The Swern oxidation was attempted by addition of a solution of DMSO in anhydrous DCM to a solution of anhydrous DCM containing oxalyl chloride at -78 °C under an inert atmosphere. After 10 minutes a solution of **229** in DCM was added and the resulting mixture was stirred for 15 minutes. An excess of TEA was added and stirring continued at -78 °C for a further 30 minutes. TLC after this time indicated that no reaction had taken place. Altering the number of equivalents of the reagents used during the reaction also failed to produce a reaction.

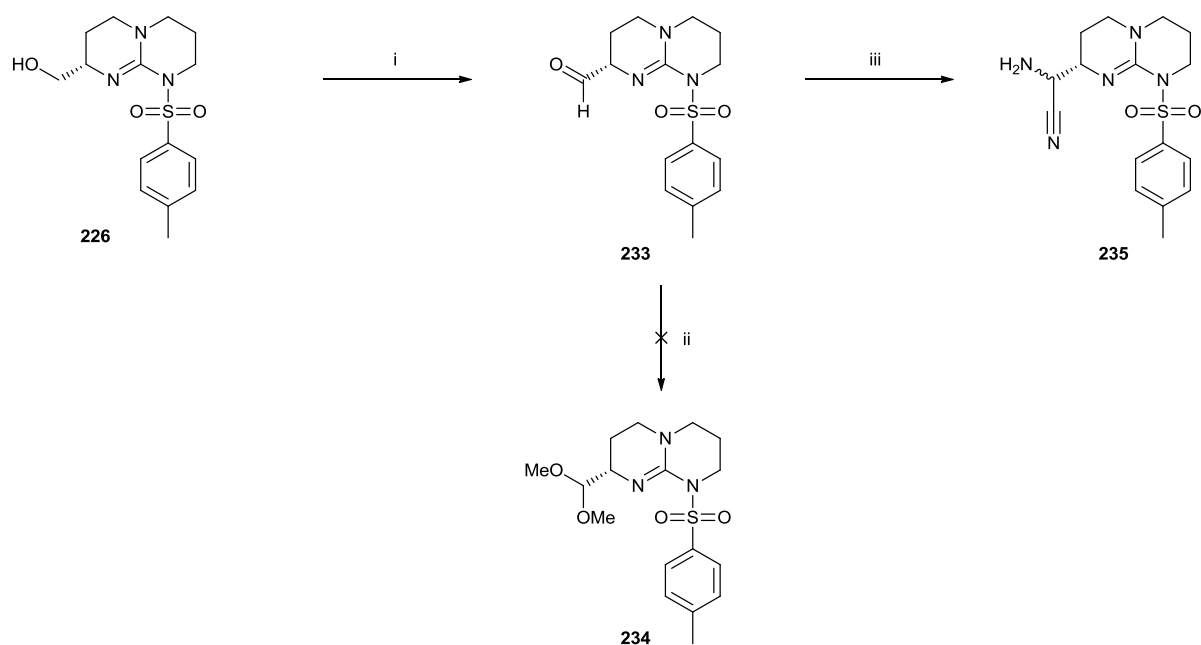
Oxidation using Dess-Martin periodinane (DMP) was attempted due to the failure of the Swern oxidation. DMP was added in one portion to a solution of **229** in anhydrous DCM, the reaction was monitored by TLC but after 12 hours, no reaction could be observed by TLC (staining with DNP indicated no aldehyde had been produced). Meyer *et al.* noticed that addition of 1.1 equivalents of water to the DMP oxidation results in an increase in reaction rate and in many cases increases

reaction yield.¹⁸⁸ Addition of 1.1 equivalents of water (in DCM) to the reaction again showed no indication of a reaction taking place.

When considering the structure of **229** it was perceived that the alcohol could adopt the required geometry to form a six membered intramolecular H-bond with the guanidinium moiety. This could result in the inhibition of the oxidation of the alcohol. In an effort to assess this theory, it was expected that the lower homologue of **229** (although containing a different protecting group), bicyclic guanidino alcohol **226**, would not possess the required geometry to form this intramolecular H-bond and thus should undergo oxidation.



Swern oxidation of **226** was attempted in the same manner as previously discussed. TLC of the reaction 10 minutes after addition of TEA indicated that a reaction had taken place (developed using DNP). A strong smell of DMS gave further indication that oxidation had occurred. However, attempts to isolate the aldehyde were unsuccessful. It was likely that the aldehyde hydrate was formed during the aqueous work up and that this remained in the aqueous phase after extraction. Flash chromatography was not favoured due to the indistinguishable R_f values of alcohol **226** and aldehyde **233**. Conversion of aldehyde **233** to its corresponding dimethyl acetal was attempted by refluxing the crude reaction mixture, which had previously been dried under reduced pressure, in anhydrous methanol containing a catalytic amount of *p*-toluenesulfonic acid (*p*-TsOH) and 3 Å molecular sieves. However, this failed to produce acetal **234** as indicated by TLC, this was possibly due to the presence of TEA, which could have remained from the Swern oxidation. Addition of further *p*-TsOH (up to one equivalent) was unable to encourage reaction.



i. Oxalyl Chloride, DMSO, TEA, CH₂Cl₂, -78 °C; ii. MeOH, *p*-TsOH, 3 Å MS, 70 °C; iii. KCN, NH₄OH, H₂O, 40 °C.

Scheme 2.14 – Oxidation and Strecker synthesis of **235**.

Performing the Strecker synthesis with the crude aldehyde was expected to produce the amino nitrile and thus provide evidence that the aldehyde had been formed. The crude aldehyde was concentrated to a white residue and dissolved in methanol, this was added to a solution of potassium cyanide in aqueous ammonium hydroxide. The reaction vessel was sealed and the reaction was heated to 40 °C. After 12 hours the TLC indicated that no aldehyde remained so the reaction mixture was extracted with DCM. Isolation of the product again proved challenging. **235** was retained strongly by silica, while flash chromatography with neutral alumina employed as the sorbent failed to separate the components of the crude mixture.

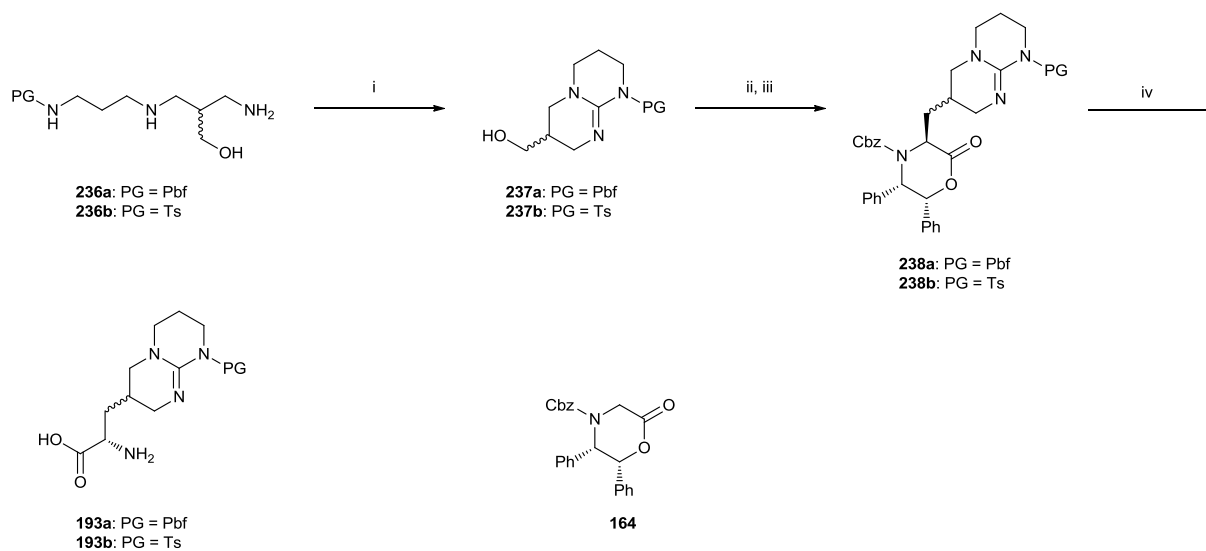
Reverse-phase HPLC of the crude reaction mixture displayed the presence of several peaks. Mass spectra of these peaks were obtained, and two of the five main peaks had a molecular mass consistent with the formation of amino nitrile **235**, which suggested the presence of both diastereoisomers. However, purification was not possible, as recrystallisations and precipitations from various solvents and solvent mixtures were attempted but subsequently failed to purify the crude mixture.

Further experiments would need to be carried out to conclusively confirm that amino nitrile **235** had been successfully synthesised. Performing the Strecker synthesis using benzhydramine as the amino source could permit purification using silica gel.

3. Results and discussions. Synthesis of AH-3-P

3.1 Introduction

Like with the synthesis of AH-2-P (chapter 2), the synthesis of AH-3-P can be divided into two parts. Firstly, the synthesis of the hydroxymethyl substituted triamine (**236**) and secondly, its cyclization and conversion to the amino acid. It was decided that the latter could be achieved in a similar manner to that of AH-2-P, as depicted in scheme 3.1. Following construction of triamine **236** its cyclization to bicyclic guanidine amino acid **237** would precede its conversion to the iodide. In an analogous approach to that attempted in section 2.4.3, Williams' template would displace the iodide to give the amino acid precursor **238**, which could be converted by hydrogenolysis to amino acid **192**.



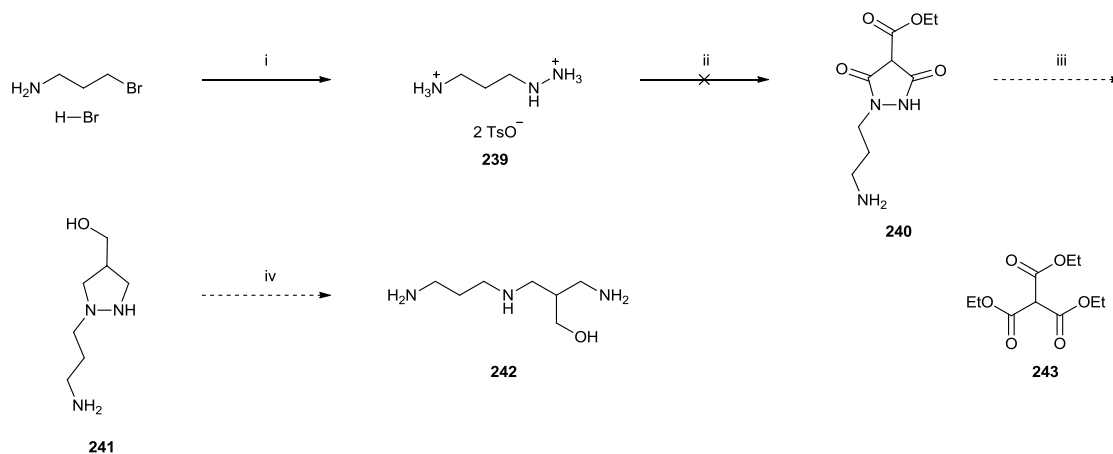
i. a) CSCl_2 , NaHCO_3 , CH_2Cl_2 , b) MeOTf , DIEA , CH_2Cl_2 ; ii. I_2 , PPh_3 , imidazole, CH_2Cl_2 , -20 - 25 °C; iii. Li or Na HMDS, **164**, THF , -78 °C; iv. H_2 , $\text{Pd}(\text{OH})_2$, MeOH .

Scheme 3.1 – Proposed synthesis of AH-3-P from triamine **236**.

3.2 Hydroxymethyl-triamine (**236**) synthesis via pyrazolidinedione

It was first necessary to develop a synthetic route to the synthesis of hydroxymethyl substituted triamine **236**. The original approach (scheme 3.2) focused on formation of

pyrazolidinedione **240**, which was expected to be achieved through coupling of 3-hydrazinylpropan-1-amine (**239**) and triester **243**. Reduction followed by N-N bond cleavage using Raney® Nickel was expected to give the hydroxymethyl triamine **242**, subsequent N-protection would give the desired hydroxymethyl triamine **236**.



i. (a) $\text{N}_2\text{H}_4 \cdot \text{H}_2\text{O}$, H_2O , 80 – 100 °C; (b) TsOH, EtOH (**40 % 2 steps**); ii. **243**, DIEA, imidazole, MeOH, 70 °C; iii. LiAlH_4 , THF; iv. H_2 , Raney Ni.

Scheme 3.2 – Synthetic pathway to triamine **242** via formation of pyrazolidinedione **240**.

3.2.1 Hydrazinyl propylamine (239)

The synthesis of 3-hydrazino-1-propylamine was achieved using the approach described by Cvetovich *et al.*¹⁸⁹ The product was obtained by refluxing 1-bromopropylamine hydrobromide with hydrazine hydrate in water. Following ion-exchange chromatography (Amberlite® IRA-400, HO^- form), **239** was isolated as its bis-tosic acid salt (60 %).

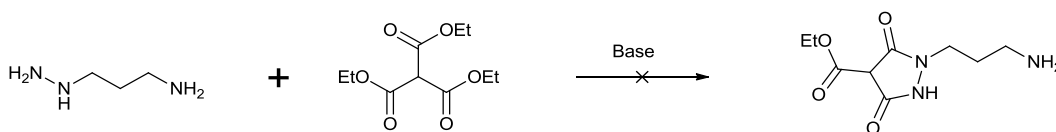
3.2.2 Coupling to the triester

The coupling of **239** to **243** was expected to proceed cleanly, liberating ethanol to give the pyrazolidinedione (**240**). However, introduction of 3-hydrazino-1-propylamine to triester **243** resulted in no reaction under a range of conditions.

Addition of one equivalent of base to the reaction of **239** and **243** was expected to deprotonate only the hydrazinyl moiety ($\text{p}K_{\text{a}} \sim 8\text{-}9$) while the amino moiety ($\text{p}K_{\text{a}} \sim 10$)

would remain protonated and thus unable to react with triester **243**. The hydrazinyl moiety was expected to react with triester **243** via nucleophilic attack at two of the carboxyl groups and thus liberate two molecules of ethanol to give pyrazolidinedione **240**. However, addition of one equivalent of DIEA to **239** and **243** in methanol, followed by refluxing for 12 hours, resulted in no reaction. Altering the base to DBU and using EtOH as the reaction medium while heating to 80 °C also produced no reaction, even after extended reaction times (up to 48 h).

An excess of base was used in an attempt to force a reaction to take place, but even after addition of up to five equivalents of DIEA, only starting material was observed on the TLC. Performing the reaction at further elevated temperatures was achieved by using toluene as the solvent while using the free amino from of **239** as opposed to the bis-tosylate, again this resulted in no reaction, as did using the deprotonated species in pyridine.



Entry	Salt	Solvent	Base ^a	Conditions
1	Bis-tosic acid	MeOH	DIEA (1)	50 °C 4 h, reflux 12 h
2	Bis-tosic acid	MeOH	DIEA (2)	50 °C 4 h, reflux 12 h
3	Bis-tosic acid	MeOH	DIEA (3)	65 °C 15 h
4	Free amine	Toluene	-	110 °C 10 h
5	Bis tosic acid	EtOH	DBU (1)	80 °C 5.5 h
6	Bis tosic acid	EtOH	DBU (1)	80 °C 48 h
7	Free amine	EtOH	Pyridine (2)	80 °C 20 h

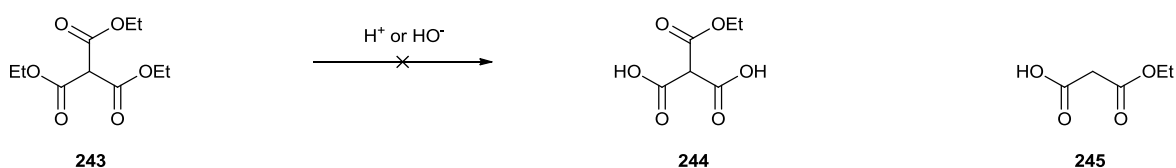
^a Number of equivalents in parenthesis.

Table 3.1 – Addition of 3-hydrazino-1-propylamine to triester **243**.

The lack of reactivity observed during this reaction was expected to be due to the reluctance of ethoxide to act as a leaving group. It was predicted that conversion of one or

two of the ester groups to the acid chloride, would allow rapid reaction at those sites and thus yield the desired pyrazolidinedione (**240**).

It was first necessary to hydrolyse **243** to the di or mono ester. It was predicted that care would need to be taken at this stage because it would be possible to over hydrolyse **243** to the tri-acid. Therefore, regular monitoring of the hydrolysis using TLC was important. The hydrolysis however, proved to be very difficult. A variety of conditions were attempted, as summarised in table 3.2.



Entry	Base	Molarity	Solvent	Duration	Temp (°C)	Product
1	NaOH	0.25 M	THF/ H ₂ O	2 h	0	243
2	NaOH	0.25 M	THF/ H ₂ O	24 h	25	243
3	LiOH·H ₂ O	0.25	THF/ H ₂ O	12 h	25	243
4	LiOH·H ₂ O	0.50	THF/ H ₂ O	12 h	25	243
5	KOH	0.55	EtOH	12 h	25	243
6	LiOH·H ₂ O	0.25	THF/ H ₂ O	4 h	40	243 & 245
7	LiOH·H ₂ O	0.25	THF/ H ₂ O	12 h	55	245
8	LiOH·H ₂ O	0.50	THF/ H ₂ O	12 h	54	245
9	KOH	0.55	EtOH	24 h	75	245
10	KOH	0.30	EtOH	48 h	25	243 & 245
11	HCl	1 M	H ₂ O /EtOH	12 h	25	243
12	HCl	1 M	H ₂ O /EtOH	4 h	53	243 & 245
13	HCl	1 M	H ₂ O/EtOH	12 h	53	245
14	HCl	2	H ₂ O	12	75	245
15	HCl	0.5	H ₂ O /EtOH	24	75	245

Table 3.2 – Hydrolysis of triester **243**.

Initially base hydrolysis was attempted using a range of hydroxylic bases. Potassium, sodium and lithium hydroxide were all employed, with molarities between 0.25-0.55. Performing the reactions at or below room temperature proved to be ineffective, with no hydrolysis taking place even after 24 hours (table 3.2, entries 1-5). Elevating the reaction temperature did evoke the hydrolysis of **243** (entries 6-9). However, the spectral data obtained for the product suggested that de-carboxylation was taking place following hydrolysis. The mass spectrum and ¹H NMR spectrum were consistent with that of mono-ethyl malonate (**245**).¹⁹⁰ Using KOH in ethanol and extending the reaction time to 48 hours resulted in a mixture of starting material and the undesired mono-ethyl malonate (entry 10).

The same trend was witnessed when using HCl to hydrolyse **243**. At ambient temperature, no reaction took place (entry 11), while at elevated temperatures, the de-carboxylated product (**245**) was exclusively formed (entries 12-15).

3.3 Hydroxymethyl triamine (**236**) synthesis via acrylic acid derivative

A different synthetic pathway to **236** was devised due to the problems with the reactivity of triester **243** and 3-hydrazino-1-propylamine (**239**). Beginning the synthesis from substituted acrylic acid derivatives was thought to be advantageous because amino functionality could be added to the molecule in three possible places as displayed in figure 3.1. It was proposed that the versatility of the molecule could allow amino introduction at any or all of these sites.

Introduction of amino functionality could take place at site-a, simply by displacement of bromide in the cases of **246-248**, or by activation of the hydroxyl of **250** followed by its displacement with an amine. Introduction of amino functionality could also be achieved through aza-Michael addition at site-b. Moreover, the possibility of coupling an amine to site-c using a peptide coupling protocol would present further means of amino introduction.

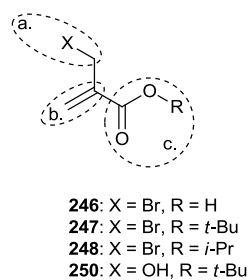
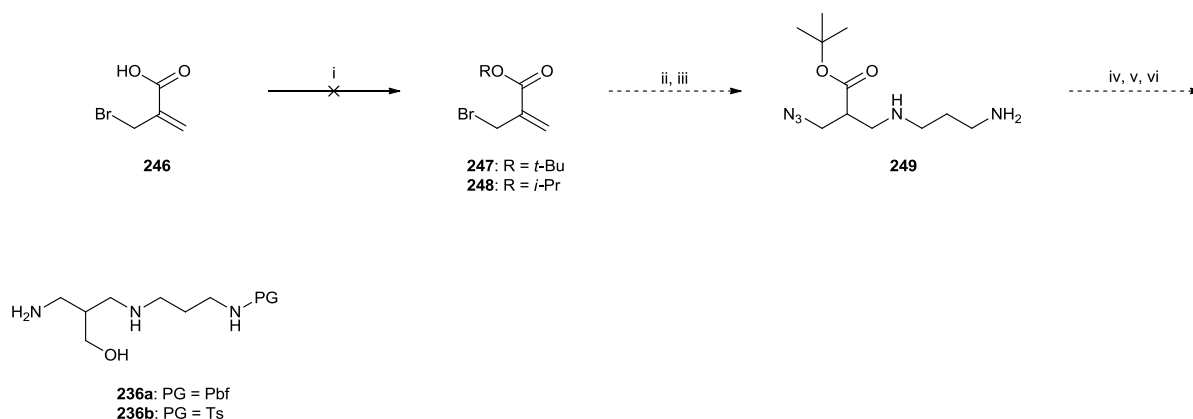


Figure 3.1 – Acrylic acid derivatives highlighting possible sites for amino introduction.

The proposed synthetic pathway was a modification of the work by Grillot and Hart¹⁹¹ and involved *t*-butyl protection of the acidic moiety of **246** followed by nucleophilic substitution of azide. 1,3-Diaminopropane, deprotonated by *n*-butyl lithium, could then undergo an aza-Michael addition to give **249**. *N*-Pbf protection followed by hydrogenation and reduction would then give the Pbf-*N*-triamine **236**.



i. H₂SO₄, *t*-BuOH, 25 °C; ii. NaN₃, H₂O, 100 °C; iii. CH₂(CH₂NH₂)₂, MeOH; iv. H₂, Pd/C, MeOH; v. PG-Cl, CH₂Cl₂, reflux; vi. LiAlH₄, Et₂O.

Scheme 3.3 – Synthetic route to protected triamine **236** from 2-(bromomethyl)acrylic acid (**246**).

3.3.1 Protection of acrylic acid

Due to the formation of a disfavoured di-anionic intermediate during the reaction, the acrylic acid **246** was a poor Michael acceptor. Therefore, it was of course necessary to convert the acid to a more appropriate Michael acceptor. Conversion to an ester would be a

useful place to start. However, it was predicted that conversion to the methyl or ethyl esters could possibly promote 1,2 addition as well as 1,4 addition during the Michael reaction, an issue which had been encountered by Grillot and Hart.¹⁹¹ Formation of the bulky *t*-butyl ester would alleviate this potential problem, allowing the aza-Michael addition to take place.

The conversion of the acrylic acid to *t*-butyl acrylate **247** proved very difficult. Table 1.2 summarises the range of methods employed to convert the acid into its *t*-butyl ester. First attempts involved bubbling isobutylene through a solution of acrylic acid **246** in the presence of concentrated H₂SO₄ in DCM (table 3.3, entries 1-2). However, this failed to produce *t*-butyl acrylate **247**.

Attempts using *t*-butyl alcohol (*t*-BuOH) as the tertiary butyl source also proved to be unsuccessful. Altering the molar equivalents of *t*-BuOH in DCM and using a drying reagent and H₂SO₄ only yielded starting material (entries 3 and 4). Refluxing in an excess of thionyl chloride (SOCl₂) in DCM overnight was expected to produce the acid chloride. Stirring this in *t*-BuOH once again failed to produce acrylate **247**. Attempting to activate the acidic moiety using the coupling reagent EDC, prior to displacement with *t*-butanol also proved to be ineffective (entry 5).

Activating the acid, through formation of an anhydride was attempted by reacting **246** with di-*tert*-butyl dicarbonate (Boc anhydride or Boc₂O) in the presence of base and catalytic amounts of 4-dimethylaminopyridine (4-DMAP) in *t*-butanol (entries 6-8). The TLC showed **246** remained but also suggested that a reaction was taking place. However, *t*-butyl acrylate **247** was never recovered. It was suspected that the reaction taking place was due to the displacement of the bromide by 4-DMAP. Repeating this reaction in the absence of catalyst resulted in no reaction even after extending the reaction duration to 2 days. This confirmed that the reaction taking place was due to the presence of 4-DMAP.



Entry	<i>t</i> -butyl source ^a	Reagents ^b	Solvent	Temperature (°C)	Duration (h)
1	isobutylene	H ₂ SO ₄ (3)	CH ₂ Cl ₂	-20 – 25 ^c	12
2	isobutylene	H ₂ SO ₄ (3.1)	CH ₂ Cl ₂	25	17 ^d
3	<i>t</i> -BuOH (5)	H ₂ SO ₄ (1), MgSO ₄ (4)	CH ₂ Cl ₂	25	16
4	<i>t</i> -BuOH (5)	H ₂ SO ₄ (2), MgSO ₄ (4)	CH ₂ Cl ₂	25	20
5	<i>t</i> -BuOH (2.5)	EDC (1.1), DIEA (3)	CH ₂ Cl ₂	0 – 25 ^e	24
6	Boc ₂ O (2)	4-DMAP (0.3)	<i>t</i> -BuOH	30	3
7	Boc ₂ O (1.5)	TEA (3), 4-DMAP (0.11)	CH ₂ Cl ₂	25	2
8	Boc ₂ O (1.5)	DIEA (2)	CH ₂ Cl ₂	25	48
9	<i>t</i> -BuOH (excess)	SOCl ₂ (excess), DIEA (2)	CH ₂ Cl ₂ / <i>t</i> -BuOH	-5 – 25 °C ^f (overnight)	24 ^g
10	<i>i</i> -PrOH (excess)	SOCl ₂ (excess), DIEA (2)	CH ₂ Cl ₂ / <i>t</i> -BuOH	25 – 60 °C ^h	24 ^g
11	<i>i</i> -PrOH (5)	H ₂ SO ₄ (2.2), MgSO ₄ (4)	CH ₂ Cl ₂	25	24

^a Number of equivalents in parenthesis; ^b Number of equivalents in parenthesis; ^c Reagents added at -20 °C and temperature maintained for 20 minutes, then allowed to warm to 25 °C; ^d Isobutylene was bubbled through reaction for 5 h, then reaction was sealed and stirred for a further 12 h; ^e Reagents were added at 0 °C and temperature maintained for 1.5 h, then allowed to reach 25 °C; ^f Reaction was performed at -5 °C then allowed to warm to room temperature after addition of SOCl₂; ^g Reaction was stirred for 10 hours with SOCl₂, concentrated to dryness and stirred for further 14 hours after addition of alcohol; Reaction was heated to 60 °C after addition of alcohol.

Table 3.3 – Protection of 2-(bromomethyl)acrylic acid

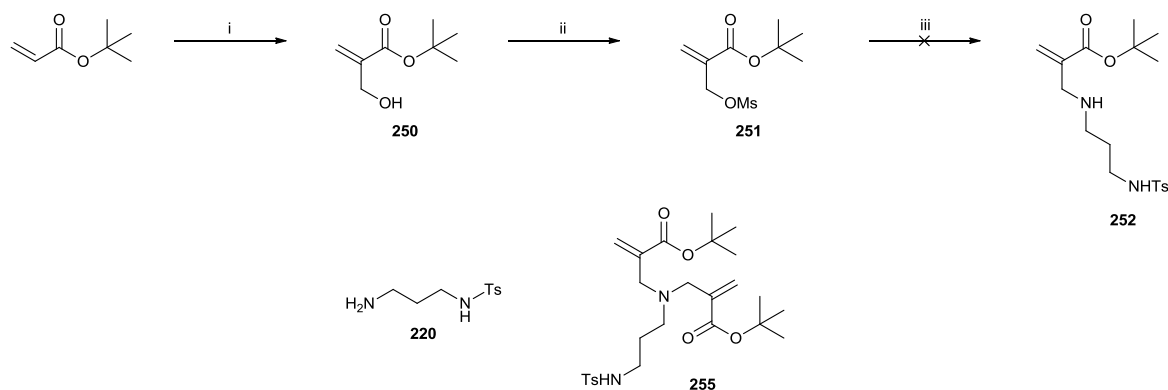
Conversion of **246** to its highly reactive acid chloride was expected to encourage reaction with *t*-butanol. Conversion of the acid to the acid chloride was attempted by refluxing **246** in DCM containing an excess of thionyl chloride. However, it was difficult to determine whether the acid chloride was actually formed due to its probable hydrolysis when

carrying out the TLC. Following concentration under reduced pressure, anhydrous *t*-butanol was added and the mixture stirred for 12 hours. This method failed to produce *t*-butyl ester **247** (entry 9), although it could not be confirmed if this failure was due to the lack of reactivity displayed by *t*-butanol, whether the acid chloride was actually formed or if the acid chloride hydrolysed prior to reaction with *t*-butanol.

Although desirable for the protection of the acidic moiety, it was predicted that the bulkiness of *t*-Butyl group was in fact inhibiting the attempts at protection. It was anticipated that conversion to the less hindered isopropyl acrylate (**248**) should be possible and still prevent 1,2 addition at the carboxyl. However, conversion to the acid chloride (in the same manner as above) followed by stirring in anhydrous isopropanol failed to produce acrylate **248**. Furthermore, attempts to liberate water by addition of H₂SO₄ in isopropanol again ended in failure.

3.4 Synthesis of triamine via hydroxyl activation

Due to the difficulties encountered when trying to protect 2-bromomethyl acrylic acid (**246**) as well as its high cost, led to the consideration of a different approach (scheme 3.4). This method focused on forming *t*-butyl-2-hydroxymethyl acrylate (**250**) from *t*-butyl acrylate using a Baylis Hillman reaction. The hydroxyl group could then be activated by conversion to mesylate **251**. Introduction of Ts-*N*-1,3-diaminopropane (**220**) at this juncture would be advantageous as this would supply one half of triamine **236** required for cyclization.



i. H_2CO , DABCO, TEA, THF, H_2O , 25 °C (45 %); ii. MsCl, DIEA, CH_2Cl_2 , 0 – 25 °C (30 %); iii. **220**, THF, 25 °C..

Scheme 3.4 –Attempted conversion of **250** to **252** via mesylate **251**.

3.4.1 Baylis Hillman

Huang *et al.* described a method to the synthesis of *t*-butyl 2-hydroxymethyl acrylate (**250**) from *t*-butyl acrylate via a Baylis Hillman reaction.¹⁹² Using their reaction conditions, which involved reaction of *t*-butyl acrylate with formalin, DABCO and TEA in THF, **250** was produced in 45 % yield following fractional distillation. Despite the low yield obtained from this reaction, it was a useful method to produce **250** due to the low costing starting materials and the ease at which the reaction can be performed on a relatively large scale (78 mmol).

3.4.2 Activation of hydroxyl group

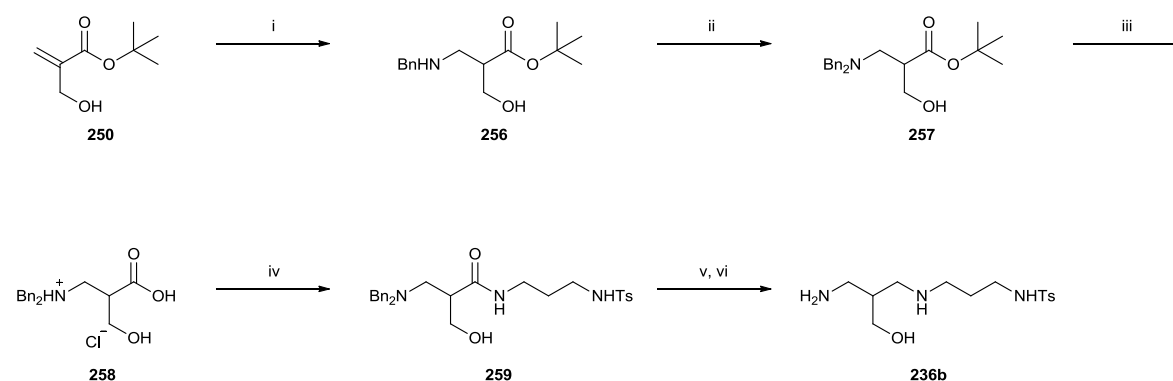
Activation of the hydroxyl group of the Baylis Hillman adduct **250** would enable the introduction of amino functionality by displacement of the activated oxygen atom. Activation of the hydroxyl moiety was attempted by conversion to the mesylate. However, the reaction never proceeded to completion according to TLC regardless of the conditions employed. Even the use an equimolar amount of NaH failed to drive the reaction to proceed to completion. The most successful attempt involved the addition of mesyl chloride to a solution of **250** and DIEA in anhydrous DCM at 0 °C. However, following flash chromatography only a 30 % yield of mesylate **251** was recovered.

3.4.3 Coupling to diamine

The coupling of **220** and **251** takes place through the nucleophilic attack from the amino group of **220** expelling the mesylate. The order of addition of the compounds was expected to be important for this reaction due to the prospect that the alkylated amine would be a stronger nucleophile than **220**. It was anticipated that this could result in dialkylation of **220**. Therefore the reaction was performed using the dropwise addition of a solution of mesylate **251** in THF to a solution of diamine **220** in THF over 5 hours, this was to ensure an excess of **251** was never present. However, the dialkylated product (**255**) was still produced from the reaction. Repeating the reaction at sub-zero temperatures and increasing the addition time (up to 10 hours) produced the same result, as did performing the reaction at weaker concentrations.

3.5 Triamine synthesis through amide bond formation

Due to the dialkylation products mentioned previously an alternative approach was studied. Using the previously synthesised Baylis-Hillman adduct (**250**) as a Michael acceptor in the aza-Michael addition would introduce amino functionality. Following deprotection of the *t*-butyl ester, it was predicted that the corresponding acid (**258**) could be coupled to the diamine **220** using peptide coupling protocol. Removal of protecting groups and reduction would thus give triamine **236b**.



i. BnNH_2 , MeOH , 30°C (**77 %**); ii. BnBr , K_2CO_3 , MeCN , 25°C (**86 %**); iii. (a) 80 % TFA - DCM , 25°C , (b) 0.5 M HCl - H_2O , sonication (**52 %**, 2 steps); iv. **220**, HBTU, DIEA, DMF; v. LiAlH_4 , THF; vi. H_2 , Pd/C, MeOH.

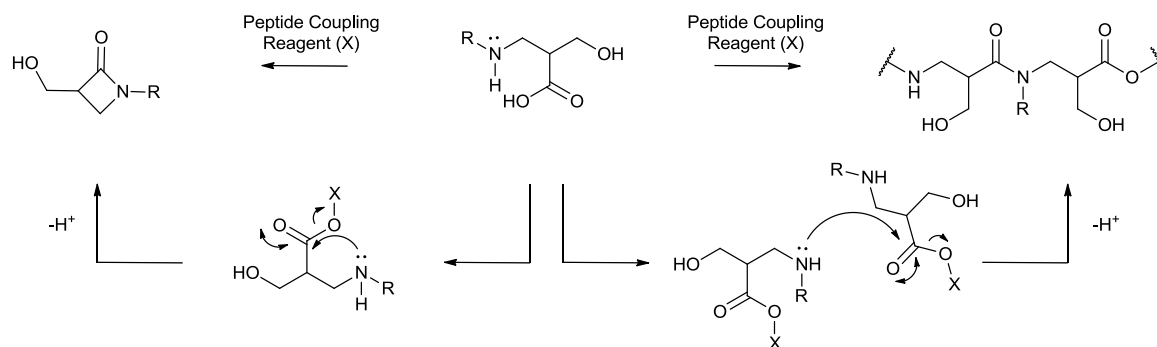
Scheme 3.5 – Synthesis of triamine **236b** via peptide coupling of protected diamine **220**.

3.5.1 Aza-Michael addition

Introduction of Ts-*N*-diaminopropane (**220**) would have made significant progress towards the desired hydroxymethyl triamine **236b**. However, despite using a variety of reaction conditions the product was never produced, and instead, only starting material was recovered. It transpired that altering the choice of solvent, ranging from strongly polar to highly non-polar failed to produce a reaction. Increasing the reaction temperature produced the same results, as did prolonging the reaction duration up to 5 days. Deprotonating the protected diamine **220** using a strong base was not favourable as the deprotonation was expected to take place at the sulfonamide instead of at the free amine, and consequently, the Michael adduct would be protected at the incorrect amino moiety.

The difficulties encountered when introducing **220** at site-a and site-b (figure 3.1) switched the focus to manipulation of site-c for its introduction. It was predicted that this could be achieved using peptide coupling protocol of the deprotected carboxyl, which will be discussed later (section 3.5.4). It was however, still necessary to add further amino functionality to the molecule. The aza-Michael addition would be an ideal way to achieve this and so several compounds were tested (summarised in table 3.3).

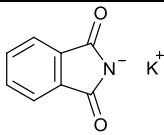
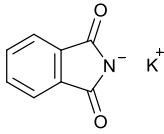
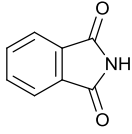
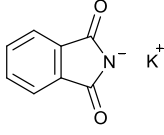
Considerations of possible intra or intermolecular reactions led to the conclusion that it would be necessary to use secondary amines which could be easily converted to the free amine. This would alleviate the potential for lactam formation or possible polymerisation (scheme 3.6) when performing amide bond formation at a later stage.



Scheme 3.6 – Possible lactamisation and polymerisation

Phthalimide was thought to be a useful compound for the 1,4 addition as this would inhibit the potential amino side reactions mentioned above. Furthermore, it can be readily removed using hydrazine. The use of phthalimide however, failed to produce the Michael adduct when performed in a range of solvents (table 3.4, entries 1-5). Even when employing the more nucleophilic potassium salt of phthalimide, no reaction took place despite extended reaction times (up to seven days). A literature procedure by Duan *et al.* suggested the use of ceric ammonium nitrate (CAN) as a catalyst as this has been used with many acrylate derivatives.¹⁹³ However, this too failed to produce the Michael adduct.

Dibenzylamine was predicted to be another useful Michael donor as it is commercially available, inexpensive and can be removed using palladium-catalysed hydrogenolysis to give the free amine. This also displayed a complete lack of reactivity. Again altering the solvent and using longer reaction times failed to produce the Michael adduct. Employing CAN as a catalyst once more proved unsuccessful.

Entry	Amine	Solvent	Catalyst	Temperature (°C)	Duration	Yield
1		EtOH	-	80	5 days	-
2		PhMe	18-C-6	115	4 days	-
3		THF	CAN	75	5 days	-
4		-	-	100	5 days	-

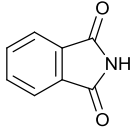
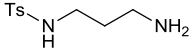
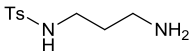
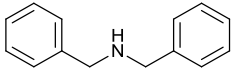
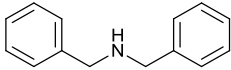
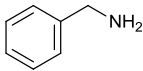
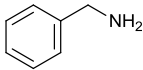
5		THF	CAN	25 (sonication)	30 h	-
6		THF	CAN	75	5 days	-
7		EtOH	-	25 °C – 80	6 days	-
8		H ₂ O	CAN	25 °C – 100	3 days	-
9		PhMe	-	115	3 days	-
10		MeOH	-	25 °C	12 h	32
11		MeOH	-	30	6 h	77

Table 3.4 – Aza-Michael addition to *t*-butyl 2-(hydroxymethyl)acrylate (**250**).

The lack of reactivity displayed by phthalimide and dibenzylamine towards **250** meant other alternatives needed to be explored. Smith *et al.*¹⁹⁴ described the aza-Michael addition of benzylamine to methyl acrylate. Employing benzylamine as the amino source for aza-Michael addition to **250** was attempted and produced a yield of 32 % after stirring in MeOH for 12 hours at 20 °C. Increasing the reaction temperature to 30 °C gave a 77 % yield of **256** after just 6 hours. Additionally, increasing the temperature and extending reaction times beyond this failed to elevate yields further.

3.5.2 Benzyl protection

It was necessary to further protect the amino moiety as the possible intra or intermolecular reactions mentioned previously (scheme 3.6) could take place when performing the amide bond formation later. This protection proved to be simple. Addition of benzyl bromide to a suspension of **256**, potassium carbonate (K_2CO_3) and 18-crown-6 in toluene produced the dibenzyl protected species in a meagre 22 % yield following column chromatography. Yields were increased slightly by heating (48 %), while performing the reaction in the absence of 18-crown-6 in MeCN at room temperature significantly increased the yield of **257** to 86 %.

3.5.3 *t*-Butyl cleavage

Various attempts were made towards the hydrolysis of **257** (as summarised in table 3.5). Hydrolysis using sulfuric acid in DCM (entries 4-6) or varying molarities of HCl (entries 1-3) produced no reaction. Graf *et al.* used an approach which involved refluxing in toluene in the presence of a slight excess of tosic acid.¹⁹⁵ However, when performed using *t*-butyl ester **257** again no reaction was observed. It transpired that hydrolysis required high concentrations of TFA in DCM. Although lower ratios of TFA:DCM produced a degree of hydrolysis (entries 8-14), complete hydrolysis required 80 % TFA-DCM mixtures and was complete in 12 hours.

As mentioned in the next section (section 3.5.4), the presence of the TFA salt was predicted to cause some problems with the coupling reactions, therefore it would be fruitful to convert this to its corresponding HCl salt. This was achieved by sonication of the crude hydrolysis product in 0.5 M HCl. This produced **258** as the HCl salt in 78 % yield (from two steps) following recrystallisation from EtOH.

Entry	Acid	Duration	Temp	Yield (%)
1	2 M HCl in H ₂ O	12	25	-
2	2 M HCl in H ₂ O	24	100	-
3	6 M HCl in H ₂ O	12	100	-
4	0.5 eq (conc.) H ₂ SO ₄ in DCM	48	25	-
5	1 eq (conc.) H ₂ SO ₄ in DCM	48	25	-
6	2 eq (conc.) H ₂ SO ₄ in DCM	48	40	-
7	1.1 eq TsOH in PhMe	12	110	-
8	5 % TFA in DCM	12	25	-
9	20 % TFA in DCM	1	25	4
10	20 % TFA in DCM	5	25	11
11	50 % TFA in DCM	2	25	9
12	50 % TFA in DCM	4	25	26
13	80 % TFA in DCM	12	25	Quant.
14	80 % TFA in DCM (converted to HCl salt)	14 ^a	25	78 ^b

^a Reaction was stirred for 12 hours with 80 % TFA in DCM and for a further 2 hours with 0.5 M HCl; ^b Isolated yield after recrystallisation from EtOH

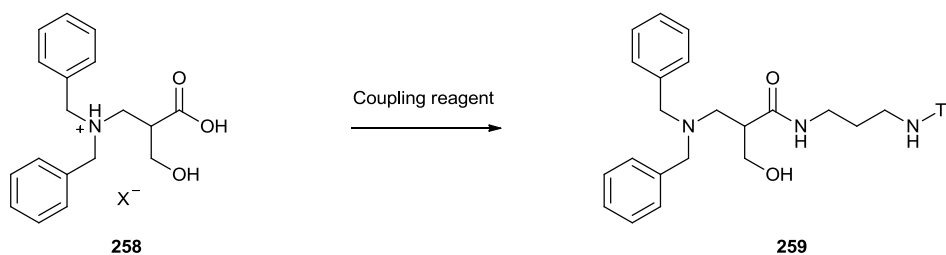
Table 3.5 – Hydrolysis of *t*-butyl ester **257**.

3.5.4 Coupling reactions

3.5.4.1 Peptide coupling

There is a vast array of peptide coupling reagents commercially available and they vary quite significantly in structure. The basic mechanism, by which they work however, is essentially the same (for examples see section 4.2). Activation of an oxygen atom of the acidic moiety is induced on reaction with the coupling reagent. An amino group then performs a nucleophilic attack on the carbonyl expelling the activated oxygen atom thus producing the amide bond.

A variety of coupling reagents were tested for the formation of the amide bond of **259**. Optimisation of peptide bond formation began using benzotriazol-1-yl-oxytripyrrolidinophosphonium hexafluorophosphate (PyBOP) as the coupling reagent. It transpired that regardless of solvent and the number of equivalents of the reagents used, no amide formation was observed (table 1.5, entries 1-5).



Entry	X =	Coupling Reagent ^a	Base ^b	Solvent	Duration (h)
1	TFA	PyBOP (1.1)	TEA (2)	DCM	48
2	TFA	PyBOP (1.5)	TEA (3)	DCM	12
3	TFA	PyBOP (4)	DIEA (4)	DCM	48 ^c
4	Cl	PyBOP (4)	DIEA (4)	DCM	48
5	TFA	PyBOP (3), HOBT (2)	DIEA (4)	DCM	12
6	TFA	DCC (1)	TEA (3)	DCM	8
7	TFA	EDC (1.1)	DIEA (3)	DCM	12
8	TFA	SOCl ₂	DIEA (5)	THF	12
9	TFA	SOCl ₂	DIEA (10)	THF	12
10	TFA	HBTU (1)	DIEA (3)	DMF	12
11	TFA	HBTU (4)	TEA (3)	DMF	15
12	TFA	HBTU (1)	DIEA (4)	DMSO	12
13	Cl	HBTU (2)	DIEA (2)	DMF	24
14	TFA	HBTU (1)	DIEA (4)	NMP	12
15	Cl	HBTU (2) ^d	-	H ₂ N(CH ₂) ₃ NH ₂	12

^a number of equivalents in parentheses. ^b number of equivalents in parentheses, ^c at reflux. ^d diaminopropane was used in place of Ts-protected diamine.

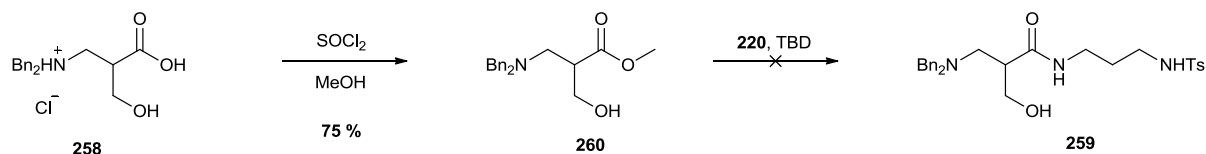
Table 3.6 – Coupling reactions between diamine **220** and acid **258**.

Utilizing *O*-Benzotriazole-*N,N,N',N'*-tetramethyl-uronium-hexafluoro-phosphate (HBTU) as the coupling reagent again resulted in failure to yield the amide **259** (entries 10-14). Although unlikely, it was possible that the TFA salt was causing problems with the coupling. The TFA salt of **258** was successfully converted to its corresponding hydrochloride (*vide supra*) in an attempt to avoid the potential amide bond formation between diamine **220** and the trifluoroacetate itself. However, peptide bond formation still failed, thus suggesting that the counter ion was irrelevant. An attempt to couple the unprotected diamine (1,3-diaminopropane) included the use of an excess of HBTU while employing 1,3-diaminopropane as the reaction solvent. This again failed to produce any reaction (entry 15).

The use of carbodiimides was also explored. However, both dicyclohexylcarbodiimide (DCC) and 1-ethyl-3-(3-dimethylaminopropyl)carbodiimide (EDC) ultimately failed to yield **259** (entries 6 and 7, respectively). Moreover, attempts to convert the acid to its corresponding acid chloride prior to addition of **220** again proved to be unsuccessful (entries 8-9).

3.5.4.2 Aminolysis of ester

The failure to couple Ts-diamine **220** to amino acid **258** using the peptide coupling protocol (*vide supra*) meant alternative methods to the coupling needed to be considered. Sabot *et al.* described a method for the aminolysis of esters using triazabicyclodecene (TBD) as a catalyst.⁵⁸ Their study demonstrated the formation of the amide under solvent free conditions using a range of esters, including lactones and a variety of amines. It was decided that this would be a useful method to couple Ts-*N*-diaminopropane (**220**) with amino acid **258**.



Scheme 3.7 – Aminolysis of methyl ester **260**.

The synthesis of the methyl ester of **260** proceeded smoothly through reaction with an excess of thionyl chloride in anhydrous methanol. This successfully converted the acid to its corresponding methyl ester (**260**) in 75 % yield and required no chromatographic separation.

Performing the aminolysis under the same conditions described by Sabot *et al.* failed to produce any reaction. This is likely to be due to the physical properties of the reagents. In each case described by Sabot *et al.* both the amine and the ester used were liquids at room temperature. Whereas, at room temperature **260** is a viscous oil and **220** is a white solid which does not melt under the conditions used for reaction. The reaction was repeated using the minimal amount of solvent to dissolve all reagents. THF, toluene and acetonitrile were all assessed as solvents for the reaction. However, this again proved to be unsuccessful as did attempts to alter the catalyst choice, with both 4-DMAP, DABCO and DBU also resulting in failure.

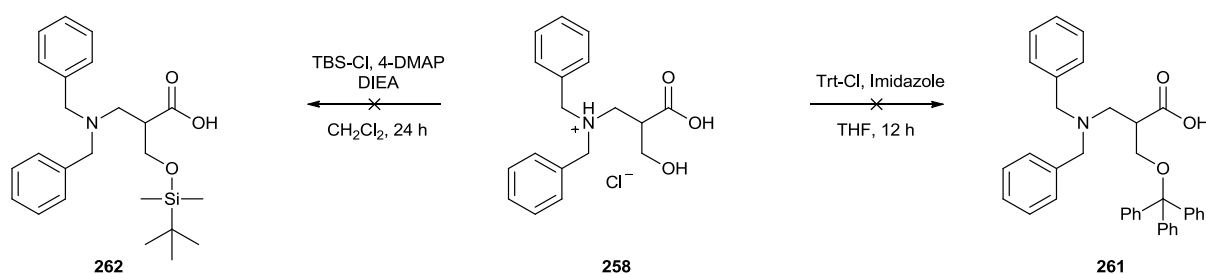
3.6 Hydroxyl protection

The lack of reactivity observed with the aforementioned coupling reactions could possibly be due to inter and intramolecular interactions taking place between the hydroxyl group and the carboxyl group. The potential for the formation of stable 6 membered ring H-bonding systems could inhibit the coupling reactions. Therefore it was decided that the addition of a protecting group would disturb these possible interactions and thus promote the amide bond formation.

When deliberating the choice of protecting group it was important to consider the presence of the acidic moiety, as this was expected to cause difficulties when protecting the hydroxyl. When selecting an appropriate protecting group, chemoselectivity needed to be considered. If protection at both the hydroxyl and the acidic groups was possible, it would be necessary that its removal from the acid could take place using sufficiently mild enough conditions that its removal from the hydroxyl moiety would not take place. Alternatively, protection of the acidic moiety prior to hydroxyl protection could be taken advantage of, providing removal of acid protection could take place while hydroxyl protection remained intact.

3.6.1 Hydroxyl protection of dibenzylamino propanoic acid **258**

Initially triphenylmethyl (trityl) protection of the hydroxyl moiety of the HCl salt of **258** was attempted by reaction with trityl chloride and imidazole in anhydrous THF for 12 hours. TLC indicated the presence of starting material, but also indicated a reaction had taken place. The compound isolated by flash chromatography showed that protection had taken place at both the hydroxyl group and the carboxylate group. Similarly, TBS protection of the hydroxyl group of **258** also yielded only the di-protected product and starting material.



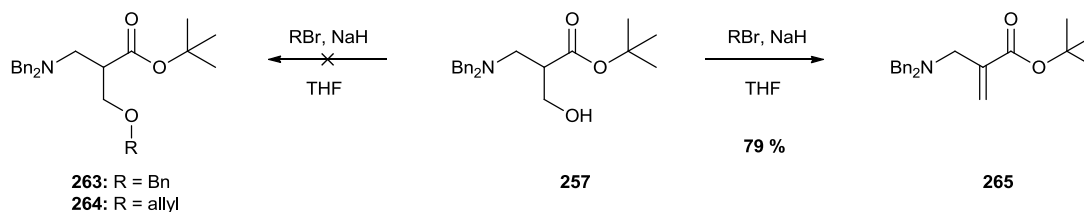
Scheme 3.8 – TBS and Trt protection of 3-(dibenzylamino)2-(hydroxymethyl) propanoic acid hydrochloride **258**.

3.6.2 Hydroxyl protection of esters **257** and **260**

The inherent problems associated with hydroxyl protection of **258** meant a new approach was necessary. Disabling the reactivity of the acidic moiety would prevent unwanted side reactions during the protection of the hydroxyl. This could be achieved by its conversion to an ester. It was crucial that following protection of the hydroxyl, the ester could be easily converted back to the acid, while leaving the hydroxyl protecting group intact.

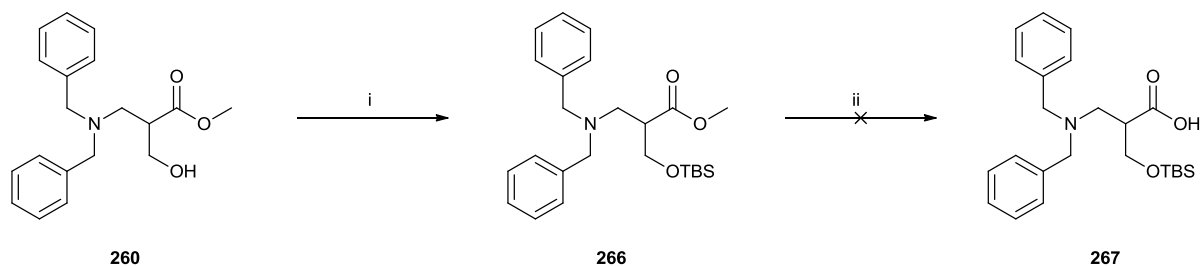
The use of *t*-butyl protection was favoured as it was already present in **257**. However, as described previously its removal requires high percentages of TFA and so many hydroxyl protecting groups would also be removed when hydrolysing back to the acid. The benzyl and allyl protecting groups were predicted to be possible forms of protection that could have been robust enough to withstand the *t*-butyl removal and so, protection of the hydroxyl group of **257** was attempted with these protecting groups.

The initial procedure involved addition of benzyl bromide (BnBr) to the reaction containing **257** and K_2CO_3 in THF at room temperature for 24 hours but resulted in no reaction. Increasing the number of equivalents of BnBr as well as the temperature similarly failed to yield **263**. Exchanging the inorganic base to TEA or DIEA again produced no reaction, while using toluene as the reaction medium also gave no improvement. Furthermore, increasing the reaction duration up to five days and heating to reflux produced no reaction. The same result was obtained when using allyl bromide to allyl protect the hydroxyl moiety. It was deemed necessary to add a strong base, typically, sodium hydride in order to force the reaction to proceed. However, this ultimately produced the elimination product **265** (79 %) (scheme 3.9), as identified by 1H NMR and MS.



Scheme 3.9 – Benzyl and allyl protection of *t*-butyl ester **257**.

The inability to benzyl or allyl protect **257** required a change in strategy. It was unlikely that other hydroxyl protecting groups would survive the harsh conditions required to hydrolyse the *t*-butyl ester to its corresponding acid. The use of the methyl ester (**260**) was expected to be more appropriate as its hydrolysis could take place under much milder conditions than that of its *t*-butyl derivative (**257**). Initial thoughts were to use trityl protection as that should resist mild basic hydrolysis. Trityl protection was attempted by stirring a solution trityl chloride, imidazole and **260** in anhydrous DCM. However, TLC after 12 hours showed only starting materials were present so the reaction was refluxed for a further 12 hours, again though this failed to produce a reaction.

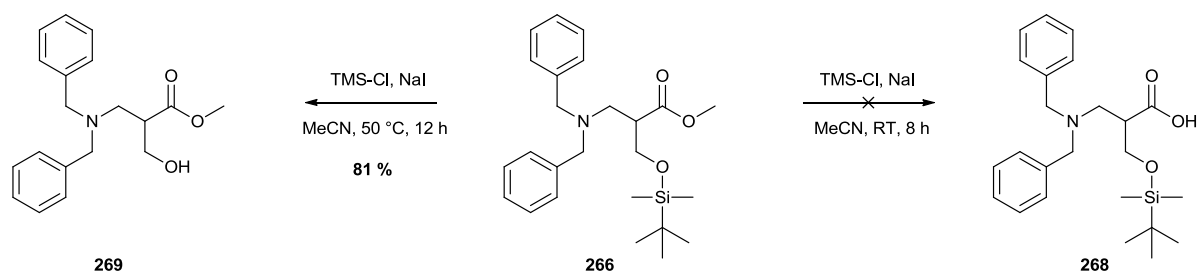


i. TBS-Cl, 4-DMAP, TEA, DMF, 12 h, 25 °C (**78 %**); ii. LiOH·H₂O, H₂O, 24 h, rt.

Scheme 3.10 – TBS protection and hydrolysis of methyl ester **260**.

It was predicted that the silylation of the hydroxyl moiety of **260** would be robust enough to withstand the mild hydrolysis of the methyl ester. Silylation was achieved in 78 % yield after reaction with TBS-Cl, 4-DMAP and TEA in DMF. The hydrolysis of **266** using LiOH·H₂O at 25 °C was attempted and resulted in no reaction after 24 hours. Heating to 50 °C resulted in silyl cleavage while the methyl ester remained intact. The use of more equivalents of base resulted in a similar trend.

In 1977, Jung *et al.* described a method to convert esters to their corresponding acids using trimethylsilyliodide (TMS-I) in chloroform or carbon tetrachloride.¹⁹⁶ This method was adapted by Olah *et al.* to allow the *in situ* generation of TMS-I from TMS-Cl and NaI in anhydrous acetonitrile, addition of the methyl ester followed by heating to 50 °C resulted in the clean conversion to the acid.¹⁹⁷ It was predicted that the method described by Olah *et al.* could be utilised in an attempt to convert methyl ester **266** to its corresponding acid (scheme 3.11). Initially the reaction was performed at room temperature. This failed to produce a reaction after 12 hours so the temperature was elevated to 50 °C for a further 12 hours. TLC indicated the complete consumption of starting material. However, the recovered product was again the desilylated methyl ester (**269**, 81 %).



Scheme 3.11 – Attempted TMS-I conversion of TBS methyl ester **266** to acid **268**.

4. Results and discussions. Peptide synthesis and binding studies

4.1 Introduction

As stated in section 1.3 the overall aim of this thesis was to incorporate the synthesised arginine analogues into peptides. These peptides could then undergo binding studies in order to determine the apparent association constants of the peptides towards several oligonucleotide targets. Comparisons of the binding affinities of these peptides could then be made against peptides comprising the same sequence but containing arginine in place of the non-natural amino acids.

Identification of compounds that interact with the oligonucleotide targets was fundamental and so the preliminary work focussed on the synthesis of a library of peptides. These peptides, which would contain at least one arginine residue per peptide, could then be screened against the nucleic acid targets. The peptide library could be constructed using a split and pool approach on macrobead resin (500-560 μm) (section 4.2.2), producing one compound per bead. This would ultimately produce a library of crude peptides in nanomole quantities.

It was of interest to assess the binding of the peptides towards several targets. Assessment of the binding towards duplex DNA, single stranded DNA and an RNA would allow comparisons between the binding of the peptides towards these different targets. It was decided that a GC rich stem loop of mRNA of the protein TGF- β -1 (38mer) would be used along with GC rich sequences of single and double stranded DNA (23mer). These oligonucleotides all contained a biotin linker at the 5' end of their sequence. This was used to facilitate their immobilisation to the wells of the streptavidin coated microtitre plate.

It was decided that an enzyme-linked immunosorbent assay (ELISA) could be used for detection of peptide bound to the oligonucleotides. It was predicted that screening the peptide library against the oligonucleotides using an ELISA would display peptides that exhibit binding towards the target oligonucleotides.

Library candidates that presented high degrees of binding could then be re-synthesised on a larger scale and purified before undergoing ELISA titrations in order to obtain association constants. The non-natural amino acids AH-2-P and AH-3-P could then be incorporated in place of the arginine residues in peptides consisting of the same sequences. This would enable comparisons between the binding capabilities of the amino acids towards the three target oligonucleotides.

In sections 4.1.1 and 4.1.2 an overview of the techniques used during the synthesis and analysis of the peptides are provided. Later in this chapter (section 4.2) the obtained results are discussed.

4.1.1 Enzyme linked immunosorbent assay (ELISA)

ELISA was developed in the early 1970's by Engvall and Perlmann.¹⁹⁸ The basic premise involved adsorbing an antibody to the surface of a polystyrene tube, which was subsequently incubated with an antigen. Washing with buffer removed all unbound antigen, this was followed by addition of a second antibody, which had been previously conjugated to an alkaline phosphatase. The antibody was retained in the tube after washing, due to its specific interactions with the antigen. A colour change was observed on addition of the substrate *p*-nitrophenylphosphate (*p*NPP) and the absorbance was measured spectrophotometrically.¹⁹⁸

This method was adapted to quantitate the amount of antibodies in antiserum. The procedure used was similar, except in this case it was the antigen that was immobilised on the surface of the tube. Incubation with an antiserum allowed non-covalent binding between the antigen and its antibody. Addition of a second antibody, which was linked to an alkaline phosphatase, specifically interacted with the antibody-antigen complex and was thus retained in the tube after washing.¹⁹⁹

Nowadays, ELISAs are generally performed in wells of microtitre plates. The principle though remains the same, with the antibody/antigen immobilised on the surface of the well. The original ELISA method (as described by Engvall and Perlmann) was later termed an 'indirect-ELISA' due to the necessity to use two antibodies, which in turn, have been

termed the capture antibody and the detector antibody. 'Direct ELISA' on the other hand requires only one antibody. In this method the antibody-enzyme conjugate is added to the adsorbed antigen. Following washing, the substrate is added and the absorbance is measured.

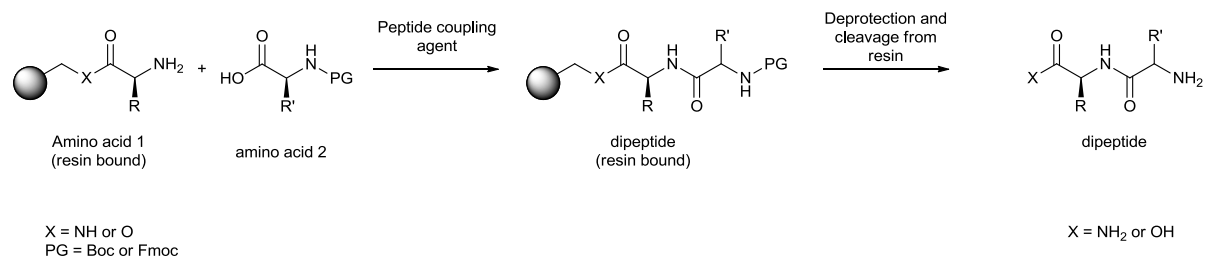
Although the development of the ELISA relied on the attraction of an antigen towards its antibody, the method is not restricted to these types of molecules. In 1994, Poisson *et al.*²⁰⁰ used ELISA to determine the binding affinity of peptides for certain nucleic acid targets. They accomplished this by immobilising peptides to the surface of a microtitre plate and then incubated them with digoxigenin labelled RNA. After washing, the RNA bound peptides were incubated with an anti-digoxigenin-peroxidase conjugate enzyme. A colour change was observed on addition of the substrate (mixture of *o*-phenylenediamine and H₂O₂), this was quenched with H₂SO₄ and the absorbance measured.

Redman *et al.*¹³ used ELISA to identify small-molecule G-quadruplex ligands from a library of unnatural polyamides. The method exploits the high binding affinity of biotin for streptavidin (K_d = 10⁻¹⁴ – 10⁻¹⁵ M) which binds much tighter than an anti-biotin antibody. The method involved incubation of biotinylated-DNA in streptavidin-coated 96 well microtitre plates. Following blocking of sites that could bind the biotin component of the peptide linker and washing, biotinylated peptides were added to the wells. The peptides interacted with the oligonucleotides and were retained following washing cycles. A streptavidin-HRP conjugate was added and specifically bound to the biotin labelled peptide. Addition of 3,3',5,5'-tetramethylbenzidine (TMB) elicited a colour change which was quenched by H₂SO₄. The absorbance was then measured and binding constants determined.

4.1.2 Solid phase peptide synthesis (SPPS)

Since its introduction in 1963,²⁰¹ solid phase peptide synthesis (SPPS) has become the prominent method for peptide production. The process begins with the covalent attachment of an amino acid to the functional sites present on the surface and within a solid support. Deprotection and coupling cycles facilitate the construction of the growing

peptide chain which takes place from the C to N terminus. Once the full sequence has been synthesised the peptide is then cleaved from the resin (Scheme 4.1).



Scheme 4.1 – General method of peptide synthesis.

4.1.2.1 Solid supports

The ability for the solid support to swell when in the presence of solvent is of paramount importance in SPPS. The degree of swelling opens up the resin and thus allows reagents to penetrate its structure, which enables binding of the growing peptide chain at all possible active functional groups within the resin.

A typical solid support used in SPPS is made up of an insoluble polymeric material containing functional sites at which the growing polypeptide chain can be covalently attached. The pioneer in SPPS was Merrifield,²⁰¹ he used a chloromethylated co-polymer of styrene and divinylbenzene as the solid support. This support, often referred to as Merrifield resin (**270**), possessed a porous gel structure which when swollen permitted the penetration of reagents. Following nucleophilic substitution at the chloromethylated sites within and on the surface of the solid support, the peptide chain was assembled. The peptide chain was then released from the resin by saponification.

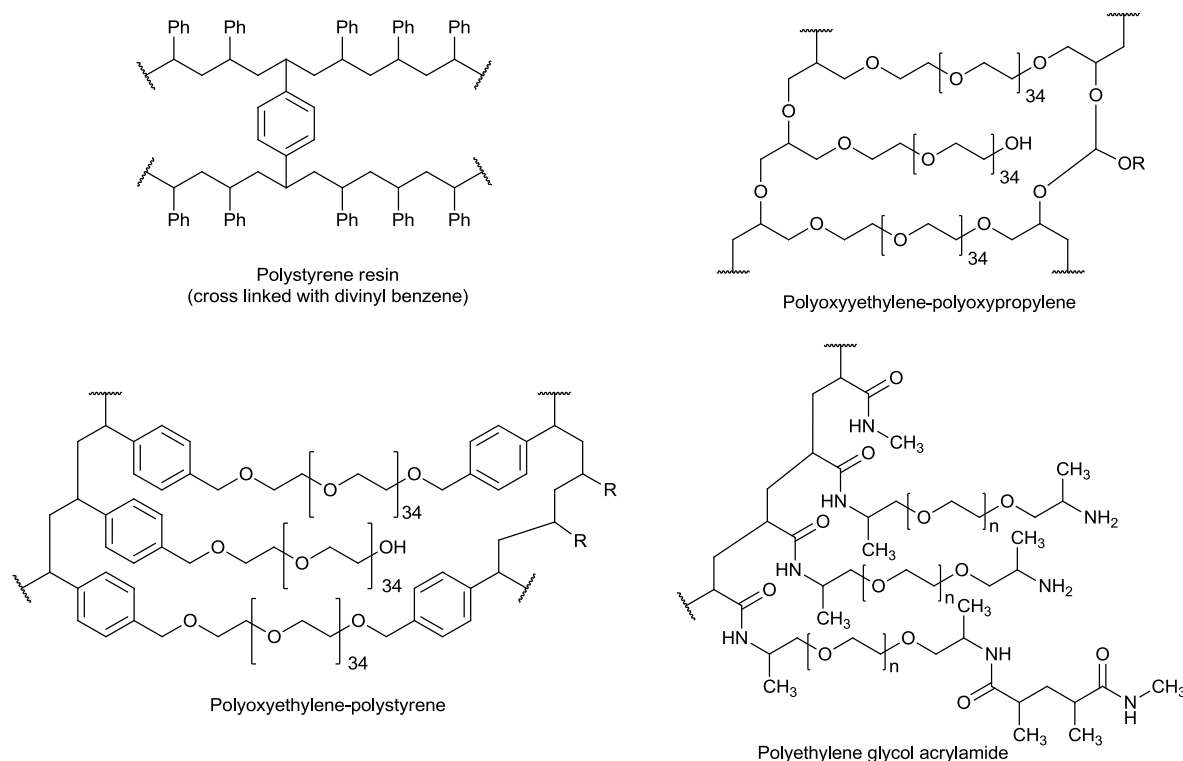


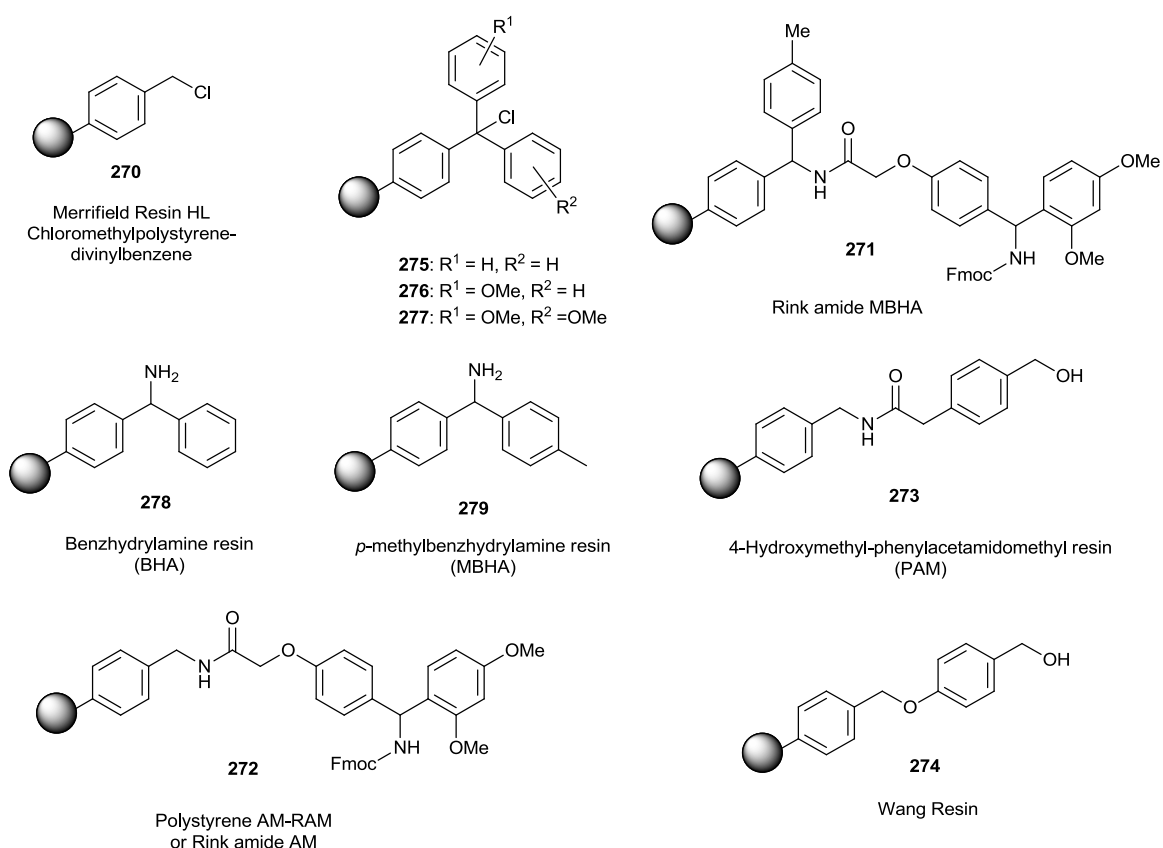
Figure 4.1 – Polymers used as solid supports in SPPS.

Nowadays, a range of solid support materials currently exist (figure 4.1). In addition to the aforementioned polystyrene-based resins, other polymeric materials have been employed as solid supports for SPPS. These include polyacrylamide resins²⁰² and PEG based resins²⁰³ as well as PEG-polystyrene hybrids.²⁰⁴ These resins are commercially available and can be supplied with an array of functionalised linkers.

The choice of linker enables manipulation of the carboxyl terminus of the peptide. Examples of this are the Rink amide MBHA (**271**) and Rink amide AM (**272**) resins which yield the carboxamides following cleavage from the resin. Conversely, the PAM (**273**) and Wang (**274**) resin can be utilised to give the carboxylic acid at the C-terminus of the peptide chain.

The robustness of a resin for certain acidic or basic conditions can be advantageous when performing the synthesis of polypeptides containing sensitive amino acid residues/protecting groups. Formic acid has been shown to cleave peptides bound to

polystyrene-trityl resin (**275**).²⁰⁵ Trityl derived resins, such as methoxytrityl (MMT, **276**) and dimethoxytrityl (DMT, **277**) have undergone peptide cleavage using as little as 1 % TFA in DCM containing triethylsilane (TES).²⁰⁶ Benzhydrylamine (BHA, **278**) and *p*-methylbenzhydrylamine (MBHA, **279**) resins have been used for syntheses that require tolerance of acidic conditions throughout the synthesis, such as those used with Boc protected amino acids (see section 4.1.2.2.2).^{207, 208} The peptide chains can be cleaved from these resins using anhydrous HF or trifluoromethanesulfonic acid.



4.1.2.2 Methodology

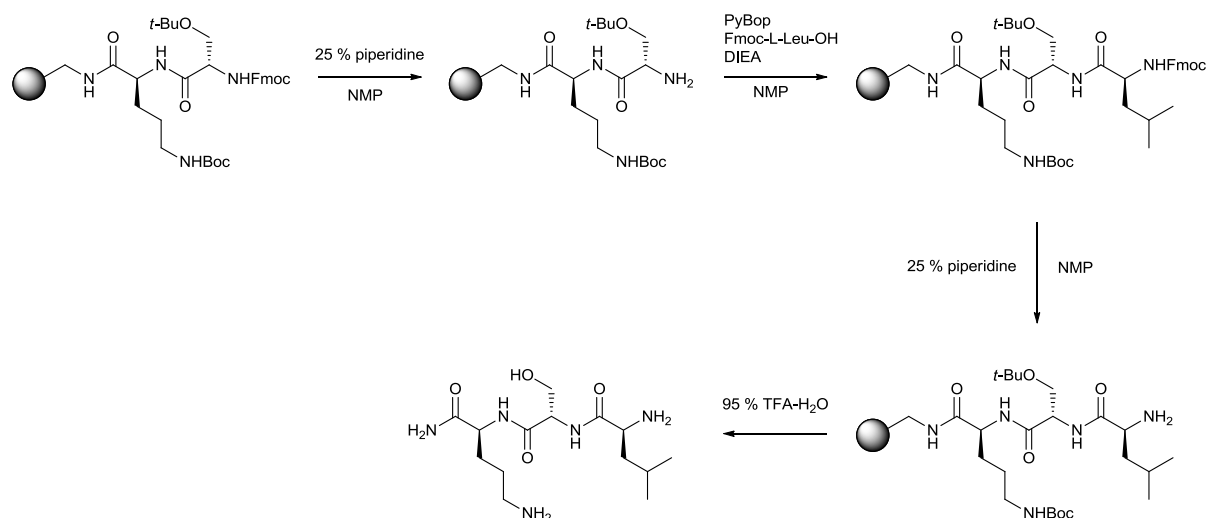
Although automated peptide synthesisers are commonplace, they tend to use large quantities of reagents and thus can prove to be expensive. For this reason the manual method of SPPS is still frequently used today. This method requires the use of a vessel

containing a porous frit. The reaction vessel is fitted with a tap and housed on a vacuum block. The reactions take place within this vessel and at the end of each coupling and deprotection cycle, all the excess reagents are evacuated by suction filtration, while the solid support, on which, the growing peptide chain is bound remains in the vessel.

Solid phase peptide synthesis can be performed using one of two methodologies. The first makes use of Fmoc protected amino acids, and is thus termed the Fmoc method, while the other method involves the use of Boc protected amino acids and is referred to as the Boc method. Although the basic premise for each method is essentially the same, different conditions are used throughout the two methods. It is important during the SPPS that the amino acids used are also protected at their side chains, as this will inhibit side reactions taking place. It is crucial that the side chain protecting groups are robust against the conditions used during the peptide synthesis (e.g. when performing the deprotection cycle).

4.1.2.2.1 Fmoc methodology

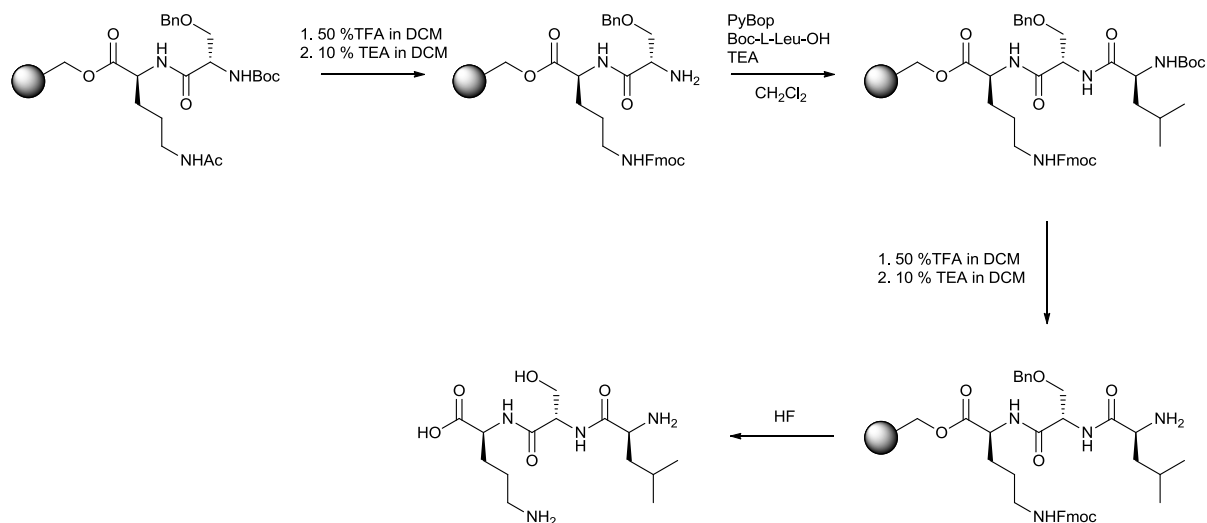
A general Fmoc method (scheme 4.2) involves the coupling of an Fmoc protected amino acid to the solid support, which is facilitated by an excess of coupling reagent and base. Following a washing cycle, the peptide chain undergoes deprotection. This is achieved using a solution of piperidine in the reaction solvent. The next amino acid in the sequence, along with the coupling reagent and base are dissolved in solvent and then added to the vessel. The process is repeated until all amino acids have been coupled to the resin. The peptide is then cleaved from the resin, which is typically achieved using 95 % TFA in the presence of scavengers such as triisopropylsilane (TIPS), *m*-cresol, 1,3-ethanedithiol and thioanisol.



Scheme 4.2 – Standard Fmoc synthesis of tripeptide LSK-CONH₂ on Rink amide resin.

4.1.2.2.2 Boc methodology

The Boc method (scheme 4.3) follows the same route as that for the Fmoc procedure. However, deprotection of Boc amino acids relies on the use of TFA, this produces the trifluoroacetate salt and so deprotection is followed by neutralization of the peptides. Due to the use of TFA, acid labile protecting groups cannot be used during the synthesis. Furthermore, it is necessary that the resin and linker are chemically stable to TFA. Therefore, Boc SPPS often uses Merrifield, BHA or MBHA linker-solid supports which remain intact when treated with TFA, and instead the peptides are cleaved from the solid support using HF or trifluoromethanesulfonic acid.



Scheme 4.3 – Standard Boc synthesis of tripeptide LSK-COOH on Merrifield resin.

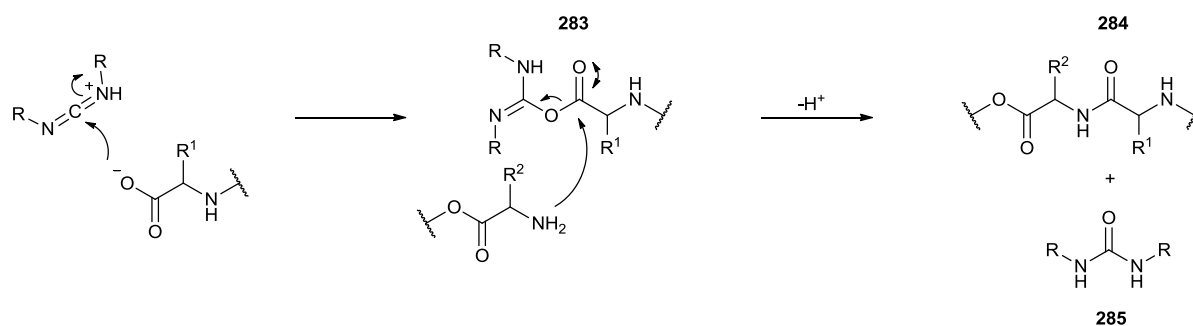
4.1.2.3 Coupling reagents

Peptide coupling reagents are imperative for the amide bond formation between two amino acids in SPPS. They are used to activate the acidic moiety of an amino acid in order to facilitate its nucleophilic substitution with the amino moiety of the next amino acid in the peptide sequence.

There currently exists a wealth of differing peptide coupling agents available for use under various reaction conditions. This repertoire is constantly expanding due to the continual development of new derivatives. Each reagent has its advantages and disadvantages over another reagent. The coupling agents can be divided into several classifications based on their structure.

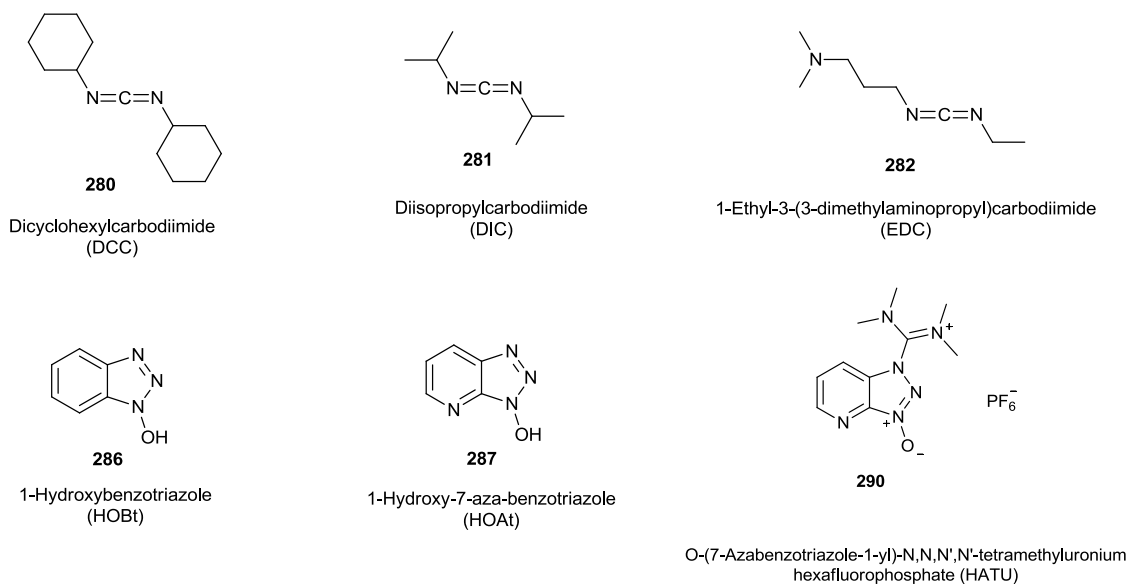
4.1.2.3.1 Carbodiimides

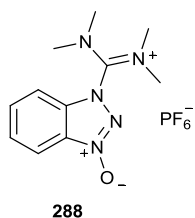
There are several carbodiimides that have been used for peptide synthesis, the most commonly used is dicyclohexylcarbodiimide (DCC, **280**). As depicted in scheme 4.4, the acid is activated by formation of *O*-acylurea **283**. Nucleophilic substitution by the amino moiety of the amino acid liberates the corresponding urea **285** thus producing the amide bond of **284**.



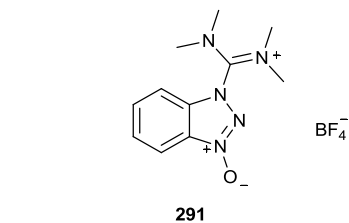
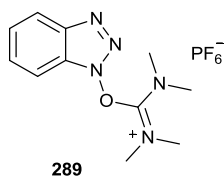
Scheme 4.4 – Amide bond formation activated by carbodiimide.

Several side products are often encountered when using carbodiimides as coupling agents. *N*-acylation of the coupling agent is possible along with formation of the anhydride although both these problems are less frequent when an excess of reagents are used. Another frequently encountered issue involves the racemisation of the amino acid to be coupled. Addition of the additive 1-hydroxybenzotriazole (HOBT, **286**) has been shown to reduce the amount of racemisation,²⁰⁹ while the addition of 1-hydroxy-7-azabenzotriazole (HOAt, **287**) as an additive has suppressed racemisation even further.²¹⁰ Addition of these additives also causes an increase in reaction rate.²¹¹

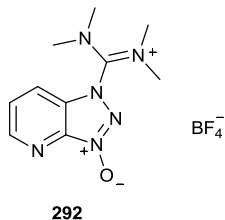




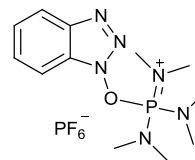
O-Benzotriazole-N,N,N',N'-tetramethyluronium hexafluorophosphate (HBTU)



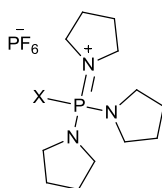
O-(Benzotriazol-1-yl)-N,N,N',N'-tetramethyluronium tetrafluoroborate (TBTU)



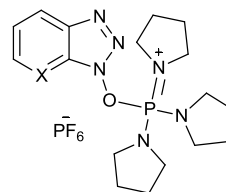
O-(7-Azabenzotriazole-1-yl)-N,N,N',N'-tetramethyluronium tetrafluoroborate (TATU)



293
BOP



294: X = Cl PyClop
295: X = Br PyBrop



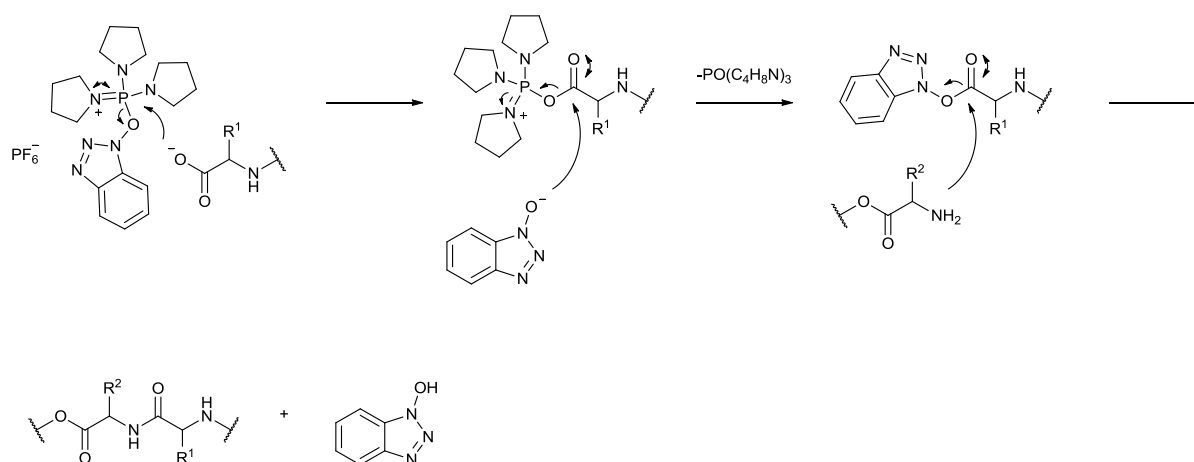
296: X = CH PyBOP
297: X = N PyAOP

4.1.2.3.2 Uronium/guanidinium reagents

A series of HOXt derivatives have been developed as coupling reagents. HBTU was introduced in 1978 as a useful reagent for coupling amino acids to produce a series of tripeptides.²¹² Its structure has been the subject of conjecture. However, it is now accepted that the reagent is the guanidinium (**288**) and not the uronium species (**289**).²¹³ The 7-azabenzotriazole derivative (HATU, **290**) is also a commonly used coupling agent. These reagents are also often used as the tetrafluoroborate anion (TBTU, **291** and TATU **292**, respectively).

4.1.2.3.3 Phosphonium coupling reagents

The coupling agent BOP (**293**) was introduced in the mid-1970s and was demonstrated as a useful compound for the synthesis of dipeptides.²¹⁴ A side product of the BOP coupling reagent was the undesirable and potential carcinogen HMPA. Later work focussed on the synthesis of analogous reagents which avoid the generation of HMPA as a by-product and so PyCloP (**294**), PyBroP (**295**), PyBOP (**296**) and PyAOP (**297**) were developed. The mechanism of peptide coupling is analogous to that of the carbodiimide/HOBt mediated coupling and is illustrated by the PyBOP mediated coupling reaction shown in scheme 4.5.



Scheme 4.5 – PyBOP mediated amide bond formation.

4.2 Results and discussions

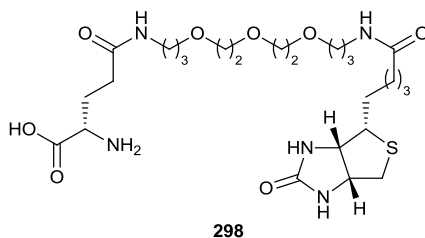
4.2.1 Assessment of applicability of assay

To assess the appropriateness of ELISA as an assay for the affinity of the peptides towards the oligonucleotide targets it was necessary to synthesise controls for the experiment. It was predicted that a peptide containing a lot of basic residues would bind strongly to the nucleic acid due to non-specific electrostatic attractions, while a peptide containing mainly acidic residues should show little or no binding. It was important to assay each control against the three oligonucleotides that were to be used in the ELISA with the peptide library, as this would give a clear understanding of whether the assay would be

appropriate. The response of the ELISA was expected to increase as the amount of bound peptide increased.

4.2.1.1 Synthesis of controls

It was decided that the direct ELISA approach described by Redman *et al.*¹³ would be a practical protocol for the detection of peptides binding oligonucleotides. It was therefore important that the synthesised peptides contained a biotin linker within their sequence. For this (biotin-PEG)-glutamic acid **298** was employed as the first residue in the sequence. It was important that this biotin linker did not interfere with the binding of the peptide to its target. It was therefore decided that this would be separated from the binding site of the peptide by a three glycine linker.



It was expected that the peptide RKRKR-GGG(PEG-biotin)E containing mainly basic residues would bind strongly to the oligonucleotides (positive control), while the acidic peptide EESEE-GGG(PEG-biotin)E would only interact very weakly if at all (negative control). Performing the ELISA with these peptides would give an insight as to whether this assay was appropriate.

The resin used for the synthesis of both the positive and negative controls was Rink amide MBHA, which was swollen in *N*-methylpyrrolidone (NMP) for 2 hours prior to reaction. Standard Fmoc methodology was used for the synthesis. Fmoc deprotection was achieved by two 10 minute cycles in which the resin was agitated with a 50 % solution of piperidine in NMP. This was performed prior to every coupling reaction and again following the addition of the final amino acid. A fourfold excess of PyBOP, DIEA and amino acid were used for each coupling, this was expected to help maximise the yield for the peptide

synthesis and minimise the degree of racemisation. However, due to its high cost, only a twofold excess of **298** was used for its coupling.

Following the final deprotection cycle, the resin was dried and the peptides were cleaved using a 95 % solution of TFA containing thioanisole, 1,2-ethanedithol and *m*-cresol as scavengers. The negative control was agitated with this solution for 3 hours, while the positive control required agitation for 6 hours (2 hours per Pbf protected arginine residue). The peptides were concentrated under a stream of N₂ and precipitated from diethyl ether.

The peptides were purified by reverse phase HPLC and their mass was confirmed by matrix assisted laser desorption ionisation mass spectrometry (MALDI-MS), which indicated that both peptides had been successfully synthesised.

4.2.1.2 Quantitation of peptides

Due to the lack of aromatic residues within the sequences of both the positive and negative controls, as well as the small amount of peptide recovered, the quantification of the peptides proved to be difficult. Kuipers *et al.*²¹⁵ described a method for the prediction of molar extinction coefficients of peptides at 214 nm in 20 % MeCN in H₂O containing 0.1 % formic acid. The prediction of the molar extinction coefficient of the peptide and its UV absorbance would allow the quantitation of the positive and negative controls using the Beer-Lambert law. The method described by Kuipers *et al.* relied on the following equation:

$$\epsilon_{\text{peptide}}(\text{M}^{-1} \text{cm}^{-1}) = \epsilon_{\text{peptidebond}} \times \eta_{\text{peptidebonds}} + \sum_{i=1}^{20} \epsilon_{\text{aminoacid}(i)} \times \eta_{\text{aminoacid}(i)}$$

The $\epsilon_{\text{peptidebond}} = 923 \text{ M}^{-1} \text{cm}^{-1}$ and the extinction coefficients of the amino acids are given in table 4.2. To assess the accuracy of the data, the UV absorbance of a random selection of amino acids was measured and molar extinction coefficients determined. The calculated molar extinction coefficients were in agreement with the published data. It was also necessary to calculate ϵ_{biotin} at 214 nm using the Beer-Lambert law. This gave a molar extinction coefficient of $191 \text{ M}^{-1} \text{cm}^{-1}$ as shown in table 4.1. Using this equation the molar extinction coefficients of the positive and negative controls were calculated to be 9027 M^{-1}

cm⁻¹ and 8985 M⁻¹ cm⁻¹ respectively. UV spectrometry was then used to quantify the peptides.

Building block	ϵ (M ⁻¹ cm ⁻¹)	Building block	ϵ (M ⁻¹ cm ⁻¹)
Proline (P) (not at the N terminus)	2675	Tyrosine (Y)	5375
Histidine (H)	5125	Tryptophan (W)	29050
Phenylalanine (F)	5200		
Peptide bond	923	Methionine (M)	980
Arginine (R)	102	Glutamine (Q)	142
Asparagine (N)	136	Cysteine (C)	225
		Biotin ^a	191
Glycine (G)	21	Valine (V)	43
Proline (P) (at the N terminus)	30	Isoleucine (I)	45
Alanine (A)	32	Leucine (L)	45
Serine (S)	34	Aspartic acid (D)	58
Lysine (K)	41	Glutamic acid (E)	78
Threonine (T)	41		

^a determined by experimental measurement using $A = \epsilon cb$, not part of the original data published by Kuipers et al.²¹⁵

Table 4.1 – Extinction coefficients of amino acids determined at 214 nm (in 20 % MeCN-H₂O 0.1 % HCOOH).

4.2.1.3 ELISA of controls

ELISA titrations were carried out with concentrations ranging from 100 μM to 10 nM of the positive and negative controls. The peptide solutions were added to wells of a microtitre plate which had previously been incubated with the target oligonucleotides and blocked using biotin to inhibit any unspecific binding. A 60,000:1 dilution of streptavidin-HRP conjugate was used to specifically bind the retained peptides. 3,3',5,5'-

tetramethylbenzidine (TMB) substrate was added to each well and the reaction was quenched after 3 minutes and the absorbance was measured at 450 nm.

Peptides binding the mRNA were expected to produce the strongest signal due to the structural complexity of RNA in comparison with dsDNA. The RNA structure is more diverse than that of dsDNA and so there were expected to be more sites at which the binding can take place. The ssDNA should also interact with the peptides at more sites than its duplex counterpart. However, the sequence is 10 base pairs shorter than the mRNA and so the mRNA was expected to possess more binding sites than the ssDNA. The ELISA signal was therefore expected to be strongest for the mRNA, then ssDNA with the weakest signal expected for the dsDNA.

Two wells of the microtitre plate which had been incubated with buffer instead of oligonucleotide were used to obtain a background signal, which was subtracted from the dataset. The ELISA titrations were in line with the initial hypothesis. The negative control displayed no apparent binding, while the positive control displayed binding towards all three oligonucleotide targets. As expected the peptides binding the mRNA stem loop provided the strongest signal while those interacting with the dsDNA produced the weakest signal.

The signal strength (absorbance) of the positive control towards the three oligonucleotides at varying concentrations is summarised in figure 4.3. Although a weak signal was observed with the positive control-dsDNA titrations, a trend was observed in which the absorbance increased with the concentration of peptide. The absorbance of the experiments containing the RNA stem loop displayed similar absorptions across the increasing concentration of peptide. The same trend was observed for the ELISA titrations of the positive control for the ssDNA, albeit with a weaker signal. These data sets suggested that the binding sites for both ssDNA and RNA were being saturated even at concentrations as low as 10 nM, which displays the expected high binding affinity of the positive control for both ssDNA and RNA stem loop.

Positive Control Against Oligonucleotides

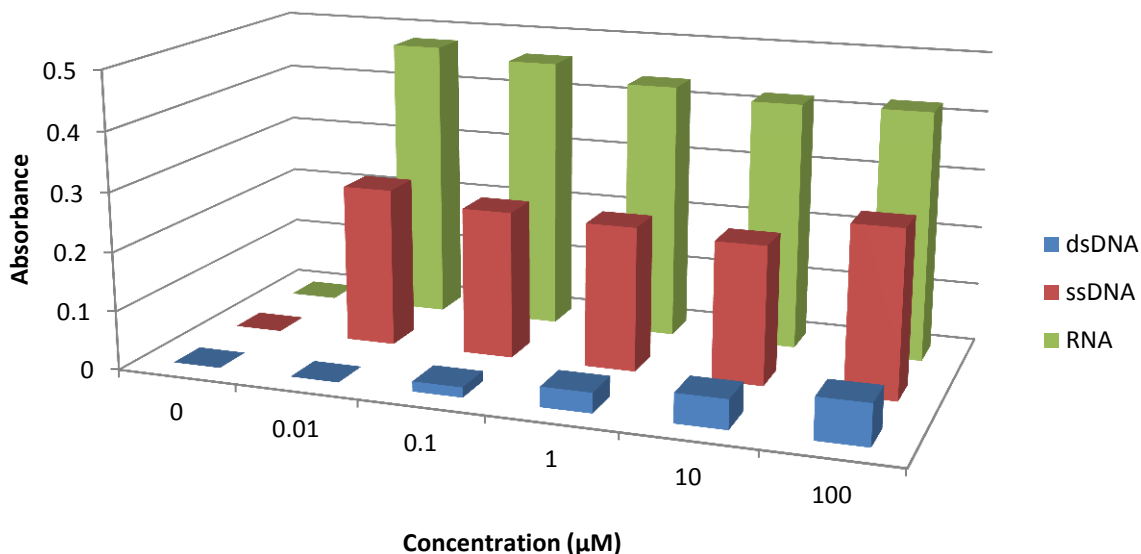


Figure 4.3 – Chart displaying the absorbance signals of the positive control against dsDNA, ssDNA and RNA stem loop at varying concentrations.

The ELISA titrations demonstrated that this method for the detection of oligonucleotide binding peptides was suitable and would therefore be appropriate for the screening of the peptide library and subsequent ELISA titrations.

4.2.2 Peptide library

4.2.2.1 Peptide library design

The split and pool approach was considered to be a useful method for the development of the peptide library. The use of macrobead resin would enable separation and isolation of each bead into individual wells of a microtitre plate (one bead per well) after the completion of the synthesis. Following cleavage from the resin, each well would contain only one compound.

It was necessary to begin the design of the peptide library with the Glu(biotin-PEG) amino acid as this was crucial for the ELISA. It was decided that the sequence of the peptide library would be varied in four positions. These are denoted as X_n in figure 4.4. Varying between four different amino acids at position X_i and X_{iv} as well as varying between two different amino acids at positions X_{ii} and X_{iii} would give rise to a library of up to 64 members.

In an attempt to introduce some secondary structure to the peptide, L-Cys and D-Cys residues were incorporated at positions 5 and 8 respectively. It was predicted that oxidation of the two thiols would give rise to the formation of a disulfide bond, which would thus produce a single turn of an α -helix.

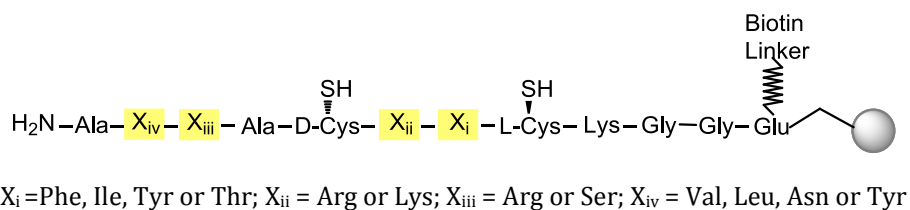


Figure 4.4 – Peptide library sequence.

It was essential to consider the method by which the sequence of the library members could be determined following their synthesis. It was predicted that this could be achieved using MALDI-MS to obtain the molecular weight of the peptides and providing that the identity of the penultimate amino acid was known there would be no ambiguity. This could be achieved by avoiding the recombination of the resin after the coupling of the penultimate amino acid (X_{iv}).

4.2.2.2 Library synthesis

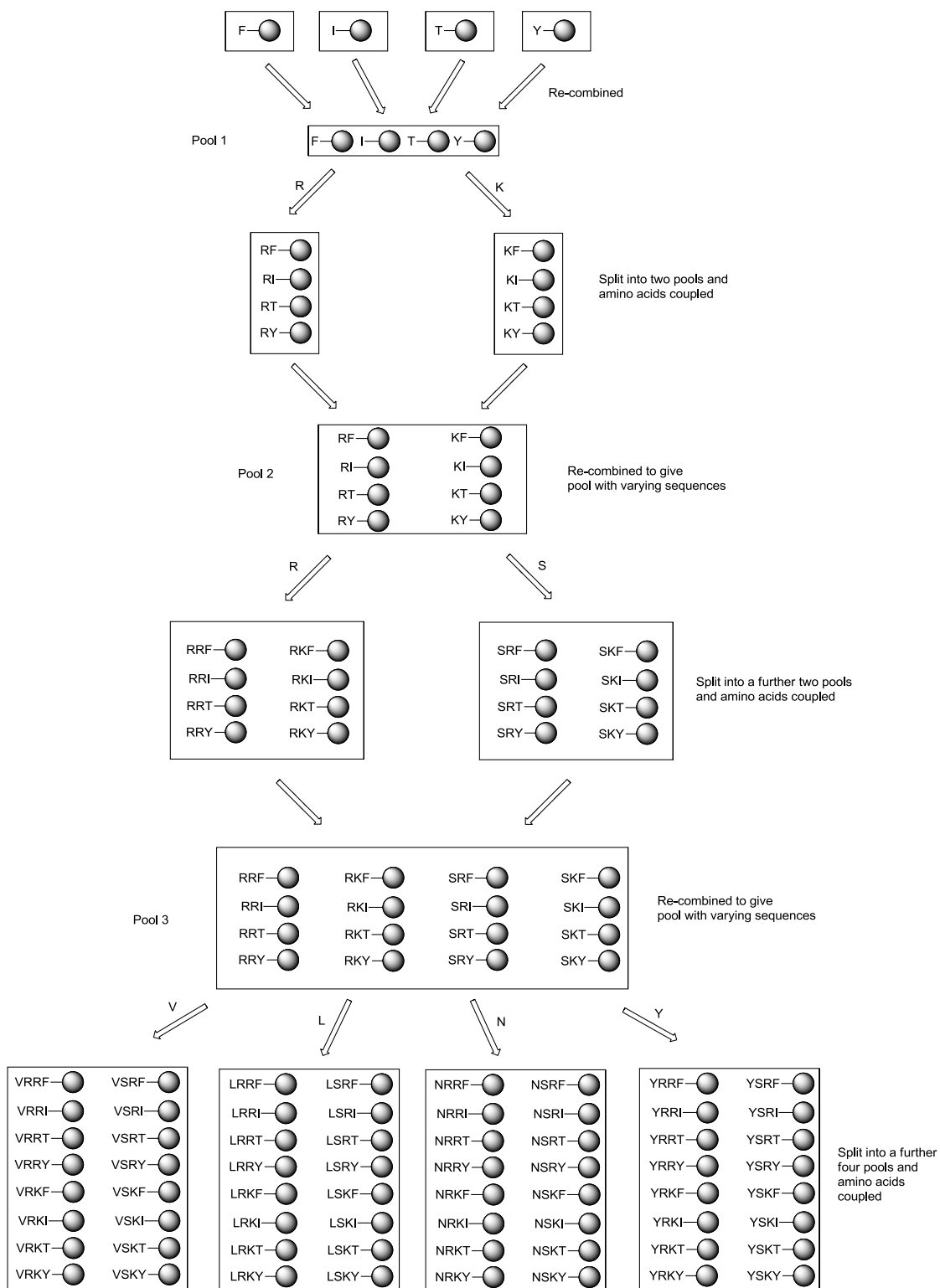
As previously stated, a split and pool approach (figure 4.5) was used for the synthesis of the peptide library, therefore polystyrene AM RAM macrobead resin was used as the solid support. Prior to every coupling two 10 minute deprotection cycles (1:1 piperidine:NMP) were employed, followed by four washing cycles.

The first five amino acids were coupled to the resin using standard Fmoc protocol. After the coupling and deprotection of L-cysteine, the macrobeads were split into four pools. Each pool was deprotected and then a peptide coupling cycle was performed, with each pool coupled to a different amino acid. The pools were then re-combined to give a mixture of peptides differing by only a single amino acid residue, Phe, Ile, Thr or Tyr. The resin was split into a further two pools and the amino acids Arg or Lys were added respectively. This afforded a mixture of 8 possible peptides when re-combined. After coupling of both D-Cys and L-Ala the macrobeads were again split into two pools which were coupled to either Arg or Ser. Following the re-combination of the pools, they were split for the last time, this time into four pools. Addition of Val, Leu, Asn or Tyr to these pools afforded up to 64 possible members of the library (as illustrated in figure 4.4). The final amino acid (Ala) was coupled to each of the four pools to give the final peptide library.

A single macrobead from each of the four final pools was dried and then agitated with the cleaving solution (TFA/TIPS/H₂O, 96:2:2) for 4 hours. The TFA was removed under a stream of N₂ and the peptides were dissolved in H₂O. MALDI-MS of each peptide confirmed that the peptides had been successfully synthesised. The remaining macrobeads were dried and separated into wells of a 96 well microtitre plate, one bead per well and the peptides were then cleaved from the resin.

4.2.2.3 Oxidation of peptides – formation of disulfide bond

It was predicted that oxidation of the two cysteine residues could be achieved by subjecting the peptides to an oxygen rich atmosphere. For oxidation to take place it was crucial for the peptide solution to be basic. This was achieved by addition of an ammonium bicarbonate solution to each of the peptides (10 µl), which had previously been dissolved in water (100 µl). The peptides were incubated in an oxygen atmosphere for 8 hours and then MALDI-MS was performed. The MALDI spectra showed that the molecular weight of the peptides had been reduced by 2 mass units, thus indicating the formation of the disulfide bond (see appendix 2).



The squares represent each vessel, with the letters representing the varying amino acids. The method gives rise to a library of 64 candidates.

Figure 4.5 – Split and recombine method displaying the 64 possible library members.

4.2.2.4 ELISA of peptide library

Streptavidin coated microtitre plates were incubated for 10 hours with the 50 nM solutions of the three oligonucleotides (dsDNA, ssDNA and RNA). A solution of biotin (1 mM) was used as a blocking agent during the screening so as to block sites that bind the biotin linker component of the peptides. A random selection of the crude peptides, with a nominal concentration of 50 μ M based on bead loading, was added to the wells, with each peptide screened against all three oligonucleotides. After an incubation period of one hour the plate was washed and then incubated with the streptavidin-HRP conjugate. Addition of the TMB substrate elicited a colour change which was quenched with H₂SO₄. The absorbance was read immediately at 450 nm.

The ELISA response was expected to increase with affinity of the peptides for the nucleic acids. Therefore a high signal would suggest that the peptide has a high affinity for that oligonucleotide. Peptide-oligonucleotide interactions that produced an absorbance value above that of two standard deviations of the background signal were considered to display an affinity towards the oligonucleotide.

ELISA is a useful tool for identifying potential candidates for re-synthesis from the peptide library. However, the assay is performed using only a single concentration of peptide, which could vary slightly from one peptide sequence to another depending on the efficiency of the synthesis. Furthermore, crude peptide mixtures are used for the ELISA screening. Therefore peptide sequences containing deletions or protected side chains could also be present within the crude peptide solutions. Irrespective of the limitations of the method, the ELISA was still expected to expose peptides that displayed affinity towards the nucleic acid targets. It is important to note that the absorbance value obtained from the ELISA screen is assumed as an approximate indication of affinity.

The results from the ELISA screen indicated that of the three oligonucleotides assessed the highest absorbance readings were, as expected, in the wells incubated with RNA. The peptide duplex-DNA ELISA showed the weakest binding, although again this was expected due to its double helical structure as well as the low absorbance values obtained for the positive control relative to the other oligonucleotides (section 4.2.1.3).

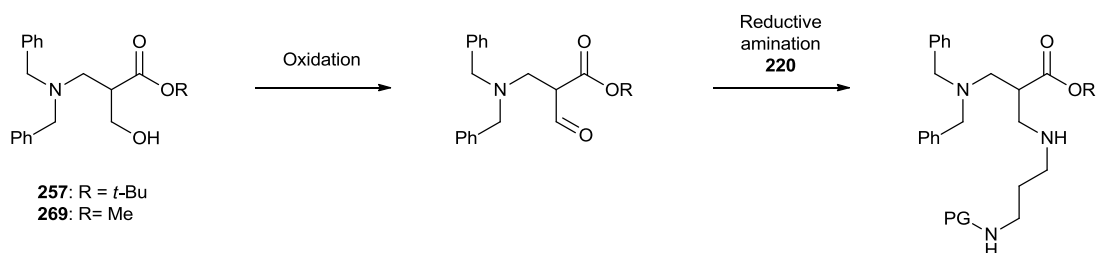
The results also displayed that the three peptides showing the greatest affinity towards dsDNA all contained the amino acid residues K, R and N at positions X_{ii}, X_{iii} and X_{iv} respectively. Interestingly these peptides all showed weak binding towards RNA. The peptides eliciting the highest response towards the ssDNA did not seem to follow any specific pattern in amino acid occurrence other than each of the four sequences possessed two arginine residues. However, three other sequences possessed this trend whilst producing much weaker signals. The highest affinity binding peptides towards RNA all contained arginine and asparagine residues at positions X_{iii} and X_{iv} respectively. However, other examples, although slightly less numerous (four as opposed to six), were seen in peptides with weaker bindings. Full sequences of peptides that display strong binding towards the oligonucleotides are shown in appendix 2.

Overall the results obtained from the ELISA screen give an indication of peptides which display high binding affinity towards the oligonucleotides. However, re-synthesis on a larger scale, preceded by their purification would be necessary to validate these results. ELISA titrations could then be used to determine the apparent association constants of the peptides.

5. Conclusion and recommendations

Two possible routes towards the synthesis of AH-2-P have been discussed. Although the synthesis via both routes has encountered varying issues, there is scope for future work. Further investigation into the synthesis of the amino nitrile analogues using benzylamine or benzydrylamine could allow the purification and thus characterisation of these compounds. The final step (conversion of the amino nitrile to the amino acid is expected to be difficult for Pbf protected compounds. It is likely Pbf would be removed by aqueous acid or base hydrolysis. The aforementioned benzydrylamino/benzylamino amino nitriles could be used as model substrates for their conversion to the amino acids. A possible method requires reduction of the nitrile moiety to the imine using DIBALH (at $-78\text{ }^{\circ}\text{C}$) followed by the mild hydrolysis of the imine with dilute acid. Further studies involving the oxidation could also be undertaken, possibly using Corey-Kim oxidation conditions.

Several approaches to the synthesis of AH-3-P have been attempted. The synthesis proceeding through formation of pyrazolidinedione failed at an early stage. Conversely, the synthetic pathway beginning with *t*-butyl-2-hydroxymethyl acrylate allowed manipulation at three possible sites. However, the coupling reactions proved to be very challenging although there are still many avenues possible to explore. These could include the oxidation of *t*-butyl-3-(dibenzylamino)-2-(hydroxymethyl) propanoate **257** or its methyl ester equivalent (**269**) to their corresponding aldehydes. Reductive amination using diamine **220** could potentially yield the desired triamine **236** (scheme 6.1). Further work could utilise the methoxymethyl protection group (MOM) for the protection of **269**, hydrolysis of the methyl ester should proceed smoothly by base hydrolysis while leaving the methyloxymethyl ether intact.



Scheme 6.1 – Possible oxidation and reductive amination of **257** and **269**.

Positive and negative controls were successfully synthesised using SPPS. These peptides both contained a biotin linker which enabled their detection using an ELISA. The controls proved that the ELISA is a useful method for detection of binding affinity between peptides and the three oligonucleotides.

A peptide library containing up to 64 members was synthesised using SPPS. α -helical structure was incorporated into the peptide library through the formation of a disulfide bond between two cysteine residues. The library members were screened using the previously determined ELISA protocol. The results from the library showed that the peptides generally showed a higher binding affinity towards the RNA stem loop than to the other oligonucleotides. Peptides showing the greatest affinity towards dsDNA all contained the amino acid residues K, R and N at positions X_{ii}, X_{iii} and X_{iv} respectively and were also found to bind much weaker to RNA.

The re-synthesis and purification of the library members which displayed high binding affinity is an area where further work is recommended. Furthermore, the association constants of these peptides can be obtained by performing ELISA titrations over a range of concentrations.

6. Experimental

Chemicals

Tosyl chloride was recrystallised from petroleum ether/toluene (1:1). 18-crown-6 was recrystallised from acetonitrile. Ethyl chloroformate and triethylamine were distilled from CaH₂ at atmospheric pressure. Anhydrous DMF, DMPU and DME were purchased from commercial suppliers. Anhydrous THF, MeCN, DCM and toluene were collected from a solvent purification system. Methanol and ethanol were stored over 3 Å molecular sieves for 24 hours prior to their usage. Similarly, DMSO was stored over 4 Å molecular sieves and HMPA over 10 Å molecular sieves for at least 24 hours before use. Pyridine was distilled from CaH₂. All other reagents were used as supplied, without any further purification. In cases where expulsion of moisture was crucial anhydrous THF that had been distilled from potassium was used. Reactions requiring anhydrous conditions were performed in flame dried glassware under an argon atmosphere.

Diazomethane was distilled as its ethereal by the dropwise addition of a solution of *N*-methyl-*N*-nitroso-*p*-toluenesulfonamide (Diazald™) in diethyl ether to an ethanolic solution of potassium hydroxide at 55 °C. Due to the explosive nature of diazomethane it was necessary to perform the distillation in specialised glassware with clear-seal® glass joints. The distillation was continued until the condensation of the yellow ethereal vapour ceased, this was then used directly in the reaction.

Chemicals were purchased from Acros, Aldrich, Fluka, Molekula, Alfa Aesar and Novabiochem and were used without further purification.

Analytical Methods

Thin Layer Chromatography/ Column Chromatography

Thin Layer Chromatography (TLC) analysis was performed on Merck aluminium sheets with silica (60 Å pore size) and fluorescence marker (F₂₅₄). Detection was carried out by UV (wavelength 254 nm and 366 nm) and by staining solutions (potassium permanganate, cerium/molybdenum, ninhydrin, DNP, I₂ vapour).²¹⁶

Melting Points

Melting points were determined on a Gallenkamp melting point apparatus fitted with a mercury thermometer and are uncorrected.

NMR Spectroscopy

¹H and ¹³C spectra were recorded on a Bruker DPX 400 or on a Bruker 500. As deuterated solvents CDCl₃, D₂O, CD₃OD, (CD₃)₂CO and DMSO-d₆ were used. Chemical shifts are given in parts per million using the residual solvent peak as a reference.

Mass Spectrometry

Mass spectrometry was performed by EPSRC Mass Service Centre, Swansea University or by Dr. R. Jenkins, R. Hicks or D. Walker at Cardiff University.

MALDI-ToF measurements were recorded in positive ion, reflectron mode on a MALDI micro MXTM using α-cyano-4-hydroxycinnamic acid as the matrix, calibration was performed using poly ethylene glycol (PEG) prior to analysis.

IR Spectroscopy

Infrared spectra were recorded on a FT/ IR – 660 plus spectrometer operating from 4000 – 500 cm⁻¹ as thin film or as KBr disk.

X-ray Crystallography

Crystals were grown using the Vapour Diffusion Method and measured by Dr. B. Kariuki

at Cardiff University. Data were collected at 150 K on a Nonius Kappa CCD diffractometer using graphite monochromated Mo K α radiation ($\lambda(\text{Mo-K}\alpha) = 0.71073 \text{ \AA}$) equipped with an Oxford Cryosystems cooling apparatus. The structures were solved using direct methods and refined with SHELX-97 (G. M. Sheldrick, *Acta Cryst. A*, 2008, A64, 112). All non-hydrogen atoms were refined anisotropically, while the hydrogen atoms were inserted in idealised positions with Uiso set at 1.2 or 1.5 times the Ueq of the parent atom.

HPLC

HPLC analyses were performed on a Merck-Hitachi LaChrom D-7000 series instrument with a reverse phase C18 E column ($4.6 \times 100 \text{ mm}$), (flow rate = $1 \text{ cm}^3 \text{ min}^{-1}$ maintained at $30 \text{ }^\circ\text{C}$), using H₂O (A) and MeCN (B) buffered with 0.1 % TFA as elution solvents. Gradient elution was as follows: 100 % to 50 % A over 15 min, followed by 50 % to 5 % A between 15-16 min. Finally, 5 % to 95 % A over 17-19 min.

UV/Vis

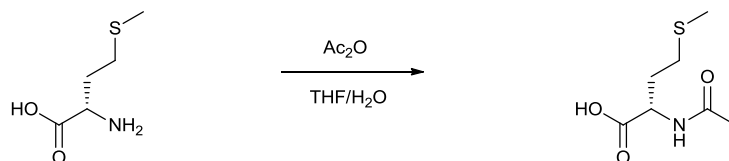
UV/Vis was recorded on a Shimadzu UV-2401PC UV/Vis recording spectrophotometer. 96 well plate measurements were taken with a BMG labtech, Fluostar Omega microplate reader at 450 nm.

Polarimetry

Optical rotations were measured on a Schmidt & Haensch UniPol L polarimeter using a one decimeter cell path length with concentrations expressed in grams per 100 ml.

Procedures

(S)-2-Acetamido-4-(methylthio)butanoic acid (**193**).



To a suspension of L-methionine (3.0 g, 20.10 mmol) in 200 ml THF/H₂O (70:30) was added acetic anhydride (10.4 ml, 0.11 mol) dropwise whilst sonicating. Sonication was continued for 1.5 hours. Solvent was removed under reduced pressure and remaining solid was recrystallised from dichloromethane, yielding **193** as white crystals (3.58 g, 93 %).

TLC (silica gel, CHCl₃:MeOH 10:1, 0.1 % AcOH), $R_f = 0.18$ (CAM)

¹H NMR (400 MHz, MeOD) δ 4.57-4.51 (m, 1H, COOHCH), 2.62-2.48 (m, 2H, CH₃SCH₂), 2.17-2.11 (m, 1H, CH₃SCH₂CHH), 2.09 (s, 3H, NHCOCH₃), 1.99 (s, 3H, SCH₃), 1.97-1.90 (m, 1H, SCH₂CHH).

¹³C NMR (125 MHz, MeOD) δ 175.2 (C=O), 173.5 (C=O), 52.7 (CH), 32.1 (CH₂), 31.2 (CH₂), 22.4 (CH₃), 15.2 (CH₃).

Both ¹H and ¹³C NMR spectra are consistent with literature spectra.²¹⁷

EI+ MS (m/z) 191 [M+H]⁺

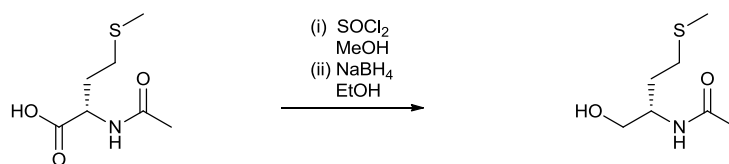
HRMS-EI+ (m/z): calcd for C₇H₁₄NO₃S [M+H]⁺: 191.0616, found 191.0611.

FT-IR (KBr, cm⁻¹) 3334 (s, NH), 2910 (w, aliphatic CH), 1706 (s, C=O), 1621 (s, C=O), 1556 (s, NH), 1260 (m), 1188 (m).

Melting Point 99.5-100.5 °C (literature: 104 °C)²¹⁸

Optical rotation $[\alpha]_D^{20} = -20.1^\circ$ (c 5.9, H₂O), literature: $[\alpha]_D = -20.1^\circ$ ²¹⁸

(S)-N-(1-hydroxy-4-(methylthio)butan-2-yl)acetamide (194).



Thionyl chloride (9.50 ml, 13.10 mmol) was added to a stirring solution of **193** (0.5 g, 2.62 mmol) in anhydrous methanol (10 ml) at 0 °C under an argon atmosphere. The resulting yellow/green solution was stirred at 0 °C for 1 hour and at room temperature for 2 hours. The solvent was removed under reduced pressure yielding a pale yellow oil, which was dissolved in CHCl₃ (15 ml) and extracted with sat. aq. NaHCO₃ (20 ml). The aqueous phase was re-extracted with CHCl₃ (2 × 15 ml). Combined organics were dried over MgSO₄, filtered and concentrated *in vacuo*. The resulting yellow oil was treated with absolute ethanol (10 ml) and cooled to 0 °C. Sodium borohydride (297 mg, 7.85 mmol) was added portion wise, the resulting emulsion was stirred at 0 °C for 1 hour and at room temperature overnight. Hydrochloric acid (0.1 M, 10 ml) was added and stirred for 10 minutes to quench the reaction. After filtration the solvent was removed under reduced pressure and filtered through a plug of silica (eluent 10:1 CHCl₃:MeOH) to give **194** as a colourless oil (407 mg, 88%).

TLC (silica gel, CHCl₃:MeOH 10:1), *R_f* = 0.35 (CAM)

¹H NMR (400 MHz, D₂O) δ 3.88 (m, 1H, NHCH), 3.60 (dd, 1H, ³*J*_{HH} = 4.7 Hz, ²*J*_{HH} = 11.6 Hz, HOCHH), 3.50 (dd, 1H, ³*J*_{HH} = 6.4 Hz, ²*J*_{HH} = 11.6 Hz, HOCHH), 2.61-2.45 (m, 2H, CH₃SCH₂), 2.08 (s, 3H, SCH₃), 2.00 (s, 3H, NHC(=O)CH₃), 1.89-1.78 (m, 1H, SCH₂CHH), 1.74-1.62 (m, 1H, SCH₂CHH).

¹³C NMR (125 MHz, D₂O) δ 174.2 (C=O), 63.4 (CH), 50.5 (CH₂), 29.8 (CH₃), 29.8 (CH₃), 22.1 (CH₂), 14.3 (CH₂).

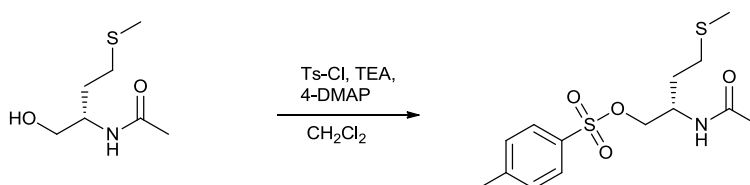
ESI+ MS (*m/z*) 178 [M+H]⁺

HRMS-ESI+ (*m/z*): calcd for C₇H₁₆NO₂S [M+H]⁺: 178.0902, found: 178.0903

FT-IR (neat, cm⁻¹) 3288 (br s, OH), 3090 (br m, aliphatic CH), 1652 (s, C=O), 1553 (s, NH), 1437 (m), 1375 (m), 1303 (m), 1063 (m).

Optical rotation $[\alpha]_D^{20} = -17.3^\circ$ (c = 2.8, MeOH)

(S)-4-(Methylthio)-1-(tosyloxy)butan-2-ylcarbamic acid (195)



Triethylamine (0.36 ml, 2.57 mmol) was added dropwise to a solution of **194** (228 mg, 1.29 mmol) and tosyl chloride (294 mg, 1.95 mmol) in anhydrous DCM (5 ml) under argon. The resulting solution was stirred at room temperature for 14 hours. The solvent was removed under reduced pressure and the white residue was purified by flash chromatography (50 % hexane-EtOAc) to afford **195** (64 mg, 15 %) as a golden oil.

TLC (silica gel, 50 % hexane-EtOAc 1:1), $R_f = 0.56$ (UV)

¹H NMR (500 MHz, CDCl₃) δ 7.75 (d, 2H, $^3J_{HH} = 8.0$ Hz, ArCH), 7.28 (d, 2H, $^3J_{HH} = 8.0$ Hz, ArCH), 5.37 (d, 1H, $^3J_{HH} = 8.1$ Hz, NH), 3.98 (dd, 1H, $^3J_{HH} = 5.1$ Hz, $^2J_{HH} = 11.4$ Hz, OCHH), 3.88 (dd, 1H, $^3J_{HH} = 4.5$ Hz, $^2J_{HH} = 11.4$ Hz, OCHH), 3.67-3.56 (m, 1H, NHCH), 2.53-2.29 (m, 2H, SCH₂), 2.39 (s, 3H, ArCH₃), 1.97 (s, 3H, SCH₃), 1.91 (s, 3H, NHCOCH₃), 1.68 (m, 2H, SCH₂CH₂).

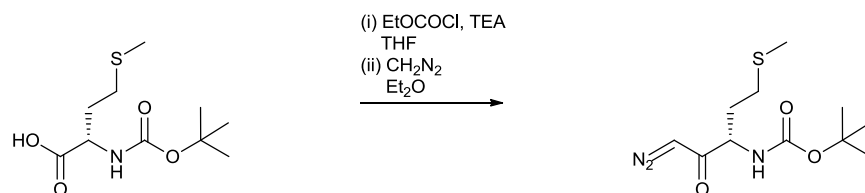
¹³C NMR (125 MHz, CDCl₃) δ 170.8 (C=O), 143.5 (ArC), 138.0 (ArC), 130.0 (ArCH), 127.0 (ArCH), 65.6 (OCH₂), 51.9 (CH), 31.5 (CH₂), 30.1 (CH₂), 21.5 (CH₃), 20.6 (CH₃), 15.2 (CH₃).

ESI+ MS (m/z) 332 [M+H]⁺, 354 [M+Na]⁺.

HRMS-ESI+ (m/z): calcd for C₁₄H₂₂NO₄S₂ [M+H]⁺: 332.0991, found: 332.1120

FT-IR (CHCl₃ film, cm⁻¹) 3684 (m), 3014 (br s, aromatic CH), 2923 (m, aliphatic CH), 2400 (s), 1741 (s, C=O), 1521 (s), 1426 (s), 1200 (br s), 1161 (s)

(S)-tert-butyl (1-diazo-5-(methylthio)-2-oxopentan-3-yl)carbamate (202)



The *N*-Boc-methionine (3.00 g, 12.0 mmol) was dissolved in anhydrous THF (90 ml) under an argon atmosphere. The solution was cooled to $-20\text{ }^{\circ}\text{C}$ and Et₃N (1.85 mL, 13.2 mmol) and ClC(O)OEt (0.93 mL, 12.0 mmol) were added. After 15 minutes the suspension was allowed to warm to $0\text{ }^{\circ}\text{C}$ and an ethereal solution of CH₂N₂ was added (70 mL, ca. 24 mmol), the solution was allowed to warm to room temperature and stirred for 3 h. The yellow suspension was quenched with a few drops of AcOH. The mixture was diluted with H₂O (70 ml) and the THF was removed under reduced pressure. After addition of Et₂O (50 ml) the mixture was washed with saturated aqueous NaHCO₃ (50 ml), NH₄Cl (50 ml) and NaCl (50 ml) solutions. The organics were dried over MgSO₄ and concentrated *in vacuo*. Purification was achieved by column chromatography (50 % hexane-EtOAc), which yielded **202** as yellow needles (1.99 g, 61 %).

TLC (silica gel, 50 % hexane-EtOAc), $R_f = 0.36$ (UV, ninhydrin)

¹H NMR (400 MHz, CDCl₃) δ 5.50 (s, 1H, N₂CH) 5.22 (d, 1H, ³J_{HH} = 8 Hz, NH), 4.32 (m, 1H, NHCH), 2.55-2.52 (m, 2H, SCH₂), 2.10 (s, 3H, SCH₃), 2.08-2.03 (m, 1H, SCH₂CHH), 1.88-1.79 (m, 1H, SCH₂CHH), 1.43 (s, 9H, *t*-Bu).

¹³C NMR (125 MHz, CDCl₃) δ 193.3 (NHCO), 155.3 (C=O), 80.2 (C(CH₃)₃), 54.4 (CH), 32.0 (CH₂), 30.1 (CH₂), 28.3 (*t*-Bu), 15.5 (CH₃).

NSI+ MS (*m/z*) 296 [M+Na]⁺, 569.23 [2M+Na]⁺.

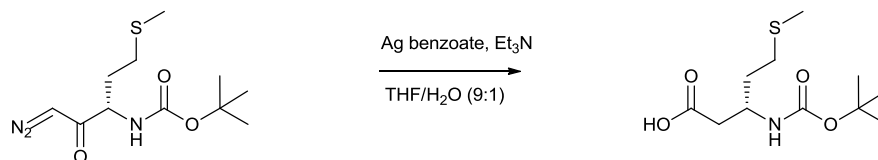
HRMS-NSI+ (*m/z*): calcd for C₁₁H₂₀N₃O₃SNa [M+Na]⁺: 296.1039, found: 296.1043.

FT-IR (KBr, cm⁻¹) 3317 (br m), 2918 (m, aliphatic CH), 2113 (s, CN₂), 1701 (s, C=O), 1609 (s, C=O), 1522 (s, NH), 1366 (s), 1166 (m).

Melting Point 58-58.5 °C

Optical rotation $[\alpha]_D^{20} = -8.6^\circ$ ($c = 0.5$, CHCl_3)

(R)-3-(tert-Butoxycarbonylamino)-5-(methylthio)pentanoic acid (203)



Diazoketone **202** (1.99g, 7.28 mmol) was dissolved in THF/ H_2O (0.25 M, 9/1), cooled to -25°C and protected from light. To this was added a solution of silver benzoate (333 mg, 1.46 mmol) in Et_3N (2.33 ml, 16.74 mmol) and the solution was allowed to warm to room temperature and stirred for 3 hours. The THF was evaporated, the resulting residue was treated with Et_2O (75 ml) and extracted with sat. aq. NaHCO_3 (75 ml). The aqueous layer was cooled to 0°C , carefully acidified to pH 2-3 using 6 M HCl (ca. 30 ml) and extracted with Et_2O (3×50 ml). The combined organics were dried over MgSO_4 and concentrated *in vacuo*. The product was purified by recrystallisation from hexane/ EtOAc to give **203** as a white solid (1.73 g, 90 %).

TLC (silica gel, 10:1 CHCl_3 :MeOH), $R_f = 0.45$ (ninhydrin)

^1H NMR (400 MHz, CDCl_3) δ 6.11, 5.12 (rotamer, 1H, NH), 3.99 (m, 1H, NHCH), 2.62-2.45 (m, 4H, COOHCH_2 , SCH_2), 2.07 (s, 3H, SCH_3), 1.89-1.72 (m, 2H, SCH_2CH_2), 1.40 (s, 9H, *t*-Bu).

^{13}C NMR (125 MHz, CDCl_3) δ 176.2 (COOH), 155.6 (NHCO), 84.5 ($\text{C}(\text{CH}_3)_3$), 46.8 (CH), 38.9 (CH_2), 33.9 (CH_2), 30.7 (CH_2), 28.3 (*t*-Bu), 15.5 (CH_3).

EI+ MS (m/z): 263 [$\text{M}+\text{H}$] $^+$.

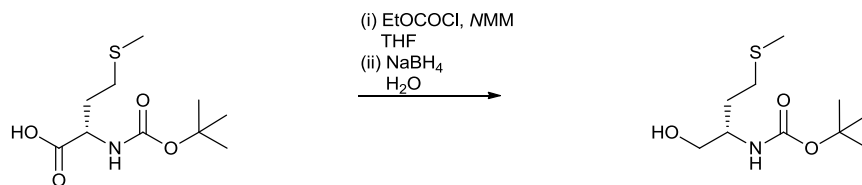
HRMS-EI+ (m/z): calcd for $\text{C}_{11}\text{H}_{22}\text{NO}_4\text{S}$ [$\text{M}+\text{H}$] $^+$: 263.1191, found: 263.1195.

FT-IR (KBr, cm^{-1}) 3366 (m, NH), 2968 (w, aliphatic CH), 1699 (s, C=O), 1685 (s, (C=O)), 1523 (m, NH), 1172 (m, C-O).

Melting Point 76.5-77 °C.

Optical rotation $[\alpha]_D^{20} = -16.2^\circ$ ($c = 0.37$, CHCl_3)

(S)-tert-Butyl 1-hydroxy-4-(methylthio)butan-2-ylcarbamate (204)



Boc-*N*-methionine (4 g, 16 mmol) was dissolved in anhydrous THF (40 ml) and cooled to 0 °C under argon. NMM (1.77 ml, 16 mmol) was added followed by the dropwise addition of ethyl chloroformate (1.5 ml, 19.2 mmol). The heterogeneous mixture was stirred at this temperature for 1 hour. The mixture was filtered, washed with THF and added dropwise over 20 minutes to an ice cold solution of NaBH₄ (1.82 g, 48 mmol) in water (20 ml). The reaction was stirred at 0 °C for 1 hour, then the ice bath was removed and stirring continued overnight. The reaction was quenched by addition of HCl (1 M) until pH 4 (ca. 20 ml). Sat. aq NaHCO₃ (100 ml) was added and then extracted with ether (3 × 70 ml). Combined organics were washed with brine, dried over MgSO₄ and concentrated *in vacuo* giving alcohol **204** as an off white solid (2.91 g, 77 %) which required no further purification.

TLC (silica gel, 10:1 CHCl₃:MeOH), $R_f = 0.60$ (ninhydrin)

¹H NMR (400 MHz, CDCl₃) δ 4.82 (br d, 1H, $^3J_{HH} = 7.5$ Hz, NH), 3.74-3.70 (m, 1H, NHCH), 3.86-3.65 (dd, 1H, $^2J_{HH} = 11.0$ Hz, $^3J_{HH} = 3.7$ Hz, HOCHH), 3.60-3.57 (dd, 1H, = 11.0 Hz, $^2J_{HH} = 5.0$ Hz, HOCHH), 2.60-2.49 (m, 2H, SCH₂), 2.10 (s, 3H, SCH₃), 1.87-1.80 (m, 1H, SCH₂CHH), 1.78-1.70 (m, 1H, SCH₂CHH), 1.43 (s, 9H, *t*-Bu).

¹³C NMR (125 MHz, CDCl₃) δ 156.3 (C=O), 79.7 (C(CH₃)₃), 65.3 (CH₂OH), 51.9 (CH), 31.0 (CH₂), 30.7 (CH₂), 28.3 (*t*-bu), 15.5 (SCH₃).

ESI- MS (m/z): 270 [M+Cl]⁻

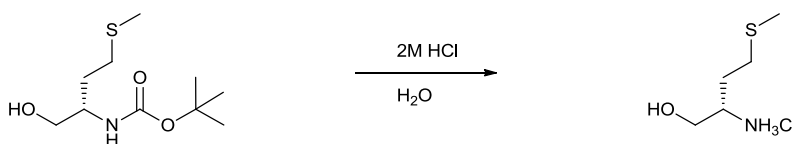
HRMS-ESI- (m/z): calcd for C₁₀H₂₁NO₃SCl [M+Cl]⁻: 270.0931, found: 270.0925

FT-IR (KBr, cm^{-1}) 3358 (br s, NH), 2974 (m, aliphatic CH), 1682 (s, C=O), 1519 (s, NH), 1366 (m) 1243 (m), 1170 (s).

Melting Point 44.5-45.5 °C

Optical rotation $[\alpha]_D^{20} = -11.2^\circ$ ($c = 1.1$, CHCl_3)

(S)-2-Amino-4-(methylthio)butan-1-ol hydrochloride (205)



HCl (2 M, 20 ml) was added to a stirring solution of Boc-*N*-methioninol (2.54 g, 10.8 mmol) in THF (5 ml). The reaction was stirred vigorously for 3 hours with the heterogeneous mixture gradually becoming homogeneous. The solvent was removed under reduced pressure, the clear oil was co-evaporated with EtOH to give **205** as a pale yellow waxy solid in quantitative yield (1.85 g).

TLC (silica gel, 10% AcOH-EtOH), $R_f = 0.47$ (ninhydrin)

^1H NMR (400 MHz, D_2O) δ 3.85-3.81 (dd, 1H, $^2J_{\text{HH}} = 12.4$ Hz, $^3J_{\text{HH}} = 3.5$ Hz, HOCHH), 3.67-3.62 (dd, 1H, $^2J_{\text{HH}} = 12.4$ Hz, $^3J_{\text{HH}} = 6.6$ Hz, HOCHH), 3.50-3.44 (m, 1H, NH_2CH), 2.63 (m, 2H, SCH_2), 2.10 (s, 3H, SCH_3), 2.01-1.86 (m, 2H, SCH_2CH_2).

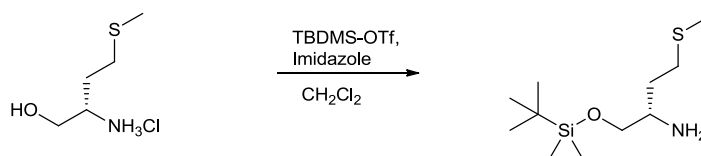
^{13}C NMR (125 MHz, D_2O) δ 60.9 (CH_2OH), 52.3 (CH), 29.2 (CH_2), 28.1 (CH_2), 14.3 (CH_3).

ESI+ MS (m/z): 135 [$\text{M}+\text{H}$] $^+$

HRMS-ESI+ (m/z): calcd for $\text{C}_5\text{H}_{14}\text{NOS}$ [$\text{M}+\text{H}$] $^+$: 135.0723, found: 135.0716

FT-IR (film, cm^{-1}) 3375 (br s, NH_2), 2919 (br s, aliphatic CH), 1602 (s, NH), 1499 (s), 1053 (s, C-O).

(S)-1-(tert-butyldimethylsilyloxy)-4-(methylthio)butan-2-amine (206)



tert-Butyldimethylsilyl triflate (2.97 ml, 12.9 mmol) was added dropwise to a suspension of methioninol hydrochloride (1.85 g, 10.8 mmol) and imidazole (1.47 g, 21.6 mmol) in anhydrous CH₂Cl₂ at 0 °C under an argon atmosphere. The reaction was stirred at this temperature for 2 hours, with the reaction mixture becoming homogenous, and at room temperature overnight. The reaction was concentrated to an orange residue under reduced pressure. The residue was portioned between NaOH (1 M, 50 ml) and hexane (50 ml). The aqueous phase was further extracted with hexane (2 × 50 ml). Combined organics were extracted with H₂O/MeCN/CH₃COOH (60/40/2, 3 × 35 ml). The combined aqueous phases were washed with hexane (4 × 40 ml) and concentrated to half of its volume. NaHCO₃ (solid) was added carefully while cooling until pH 12 was achieved, this was then extracted with ether (3 × 50 ml). Combined organics were dried over MgSO₄ and concentrated *in vacuo* to give **206** as a colourless oil (2.03g, 76 %).

TLC (silica gel, 10:1 CHCl₃:MeOH), *R_f* = 0.50 (ninhydrin)

¹H NMR (400 MHz, CDCl₃) δ 3.54-3.5 (dd, 1H, ²*J*_{HH} = 9.8Hz, ³*J*_{HH} = 4.2Hz, HOCHH), 3.36-3.32 (dd, 1H, ²*J*_{HH} = 9.8Hz, ³*J*_{HH} = 6.8Hz, HOCHH), 2.91-2.86 (m, 1H, NH₂CH), 2.63-2.49 (m, 2H, SCH₂), 2.07 (s, 3H, SCH₃), 1.72-1.63 (m, 1H, SCH₂CHH), 1.53-1.44 (m, 1H, SCH₂CHH), 0.86 (s, 9H, *t*-Bu), 0.02 (s, 6H, Si(CH₃)₂).

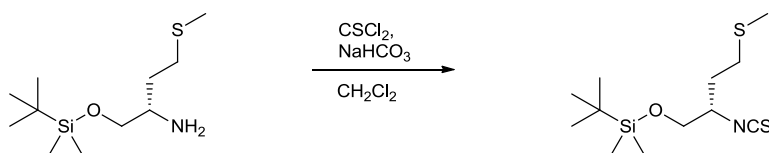
¹³C NMR (125 MHz, CDCl₃) δ 68.5 (CH₂OH), 52.5 (CH), 33.4 (CH₂), 31.5 (CH₂), 26.3 (*t*-bu), 18.7 (C(CH₃)₃), 15.9 (CH₃), -5.2 (Si(CH₃)₂).

ESI+ MS (*m/z*): 250 [M+H]⁺

HRMS-ESI+ (*m/z*): calcd for C₁₁H₂₈NOSiS [M+H]⁺: 250.1661, found: 250.1668

FT-IR (CHCl₃ film, cm⁻¹) 2928 (s, aliphatic CH), 1472 (m, NH), 1257 (s, C-O), 1103 (s).

(S)-tert-Butyl(2-isothiocyanato-4-(methylthio)butoxy)dimethylsilane (207)



Thiophosgene (0.75ml, 9.8mmol) was added dropwise to a suspension of **206** (2.03 g, 8.2 mmol) and NaHCO₃ (3.42 g, 40 mmol) in CH₂Cl₂ (100 ml). The resulting orange suspension was stirred at room temperature overnight. Any toxic gas produced was allowed to escape the reaction vessel through a tube, with the outlet submerged in 2 N NaOH. The reaction was terminated by addition of water (100 ml), the two layers were separated and the aqueous phase was extracted further with CH₂Cl₂ (50 ml). Combined organics were dried over MgSO₄ and concentrated *in vacuo*, yielding **207** as a brown oil (2.35 g, 99 %).

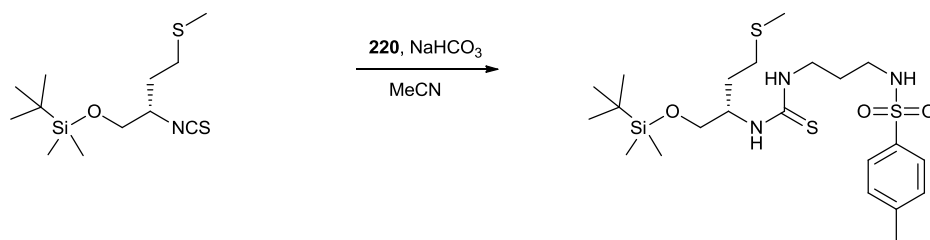
TLC (silica gel, 40:1 hexane:EtOAc), $R_f = 0.48$ (UV, CAM)

¹H NMR (400 MHz, CDCl₃) δ 3.93-3.87 (m, 1H, SCNCH), 3.74-3.69 (m, 2H, OCH₂), 2.72-2.65 (m, 1H, SCHH), 2.61-2.54 (m, 1H, SCHH), 2.11 (s, 3H, SCH₃), 1.93-1.86 (m, 2H, SCH₂CH₂), 0.91 (s, 9H, *t*-Bu), 0.01 (s, 6H, Si(CH₃)₂).

¹³C NMR (125 MHz, CDCl₃) δ 65.4 (CH₂OH), 59.0 (CH), 31.6 (CH₂), 30.7 (CH₂), 25.9 (*t*-Bu), 18.4 (C(CH₃)₃), 15.7 (CH₃), -5.3 (Si(CH₃)₂).

FT-IR (CHCl₃ film, cm⁻¹) 2954 (s, aliphatic CH), 2082 (br s, NCS), 1125 (s, C-O), 838 (s).

(S)-4-Methyl-N-(2,2,3,3-tetramethyl-6-(2-(methylthio)ethyl)-8-thioxo-4-oxa-7,9-diaza-3-siladodecan-12-yl)benzenesulfonamide (208)



A solution of **207** (111 mg, 0.38 mmol) in anhydrous MeCN (6 ml) was added to **220** (87 mg, 0.38 mmol) and NaHCO₃ (64 mg, 0.76 mmol). The heterogeneous mixture was stirred at room temperature under an argon atmosphere overnight, then refluxed for 4.5 hours (until consumption of starting materials, TLC). The reaction was filtered, washed with MeCN and concentrated under reduced pressure. The yellow oil was purified by silica gel column chromatography to give **208** as a golden oil (158 mg, 80 %).

TLC (silica gel, 2:1 hexane:EtOAc), $R_f = 0.29$ (UV, ninhydrin)

¹H NMR (400 MHz, CDCl₃) δ 7.76-7.74 (d, 2H, $^3J_{HH} = 8.3\text{Hz}$, ArCH), 7.30-7.28 (d, 2H, $^3J_{HH} = 8.3\text{Hz}$, ArCH), 3.71-3.66 (m, 2H, OCH₂), 3.64-3.55 (m, 2H, SCNHCH₂), 3.00-2.93 (m, 2H, SO₂NHCH₂), 2.58-2.49 (m, 2H, SCH₂), 2.41 (s, 3H, ArCH₃), 2.07 (s, 3H, SCH₃) 1.85-1.71 (m, 5H, NHCH, SCH₂CH₂, NHCH₂CH₂), 0.87 (s, 9H, *t*-Bu), 0.05 (s, 6H, Si(CH₃)₂).

¹³C NMR (125 MHz, CDCl₃) δ 183.4 (C=S), 143.4 (ArC), 129.8 (ArCH), 127.2 (ArCH), 65.5 (CH₂OH), 54.6 (CH), 40.1 (CH₂), 30.8 (CH₂), 30.7 (CH₂), 29.7 (CH₂), 25.0 (*t*-Bu), 21.6 (ArCH₃), 18.4 (C(CH₃)₃), 15.5 (SCH₃), -5.3 (Si(CH₃)₂).

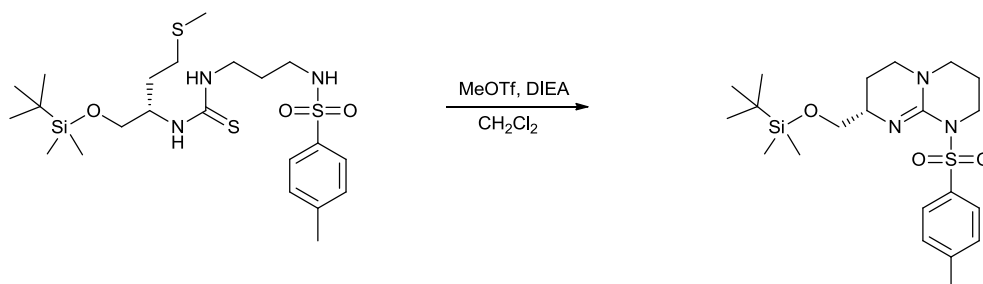
ESI+ MS (m/z): 520 [M+H]⁺, 542 [M+Na]⁺

HRMS-ESI+ (m/z): calcd for C₂₂H₄₂N₃O₃Si₃ [M+H]⁺: 520.2158, found: 520.2154

FT-IR (CHCl₃ film, cm⁻¹) 3350 (br m, NH), 2953 (s, aliphatic CH), 1548 (s), 1158 (s, C-O), 1093 (m).

Optical rotation $[\alpha]_D^{20} = -29.3^\circ$ ($c = 5.5$, CHCl₃)

(S)-8-((tert-Butyldimethylsilyloxy)methyl)-1-tosyl-2,3,4,6,7,8-hexahydro-1H-pyrimido[1,2-a]pyrimidine (209)



208 (1.72 g, 3.32 mmol) was dissolved in anhydrous CH₂Cl₂ (40 ml) and cooled to 0 °C under argon. DIEA (230 μ l, 1.33 mmol) was added, followed by the dropwise addition of MeOTf (1.50 ml, 13.30 mmol). The resulting suspension was stirred in the ice bath for 2.5 hours. DIEA (5.77 ml, 33.20 mmol) was added and the mixture was refluxed overnight. The reaction was concentrated under reduced pressure and the orange residue was partitioned between ether (50 ml) and cold NaOH (1 M, 50 ml), the aqueous phase was re-extracted with ether (2 x 50 ml). Combined organics were washed with brine, dried over MgSO₄ and concentrated *in vacuo*. Purification was achieved by silica gel column chromatography (eluent 0.2-0.4% TEA-EtOAc) to give bicyclic guanidine **209** as a yellow oil (1.12 g, 77 %).

TLC (silica gel, 1 % TEA-EtOAc), R_f = 0.15 (UV,CAM)

¹H NMR (400 MHz, CDCl₃) δ 7.81-7.79 (d, 2H, $^3J_{HH}$ = 8 Hz, ArCH), 7.23-7.21 (d, 2H, $^3J_{HH}$ = 8 Hz, ArCH), 3.92-3.79 (m, 2H, SO₂NCH₂), 3.64-3.60 (m, 1H, OCHH), 3.34-3.27 (m, 1H, NCH), 3.14-2.99 (m, 4H, NCHCH₂CH₂, SO₂NCH₂CH₂CH₂), 2.85-2.80 (m, 1H, OCHH), 2.40 (s, 3H, ArCH₃), 2.07-1.93 (m, 3H, SO₂NCH₂CH₂ and NCHCHH), 1.37-1.25 (m, 1H, NCHCHH), 0.86 (s, 9H, *t*-Bu), 0.01 (s, 6H, Si(CH₃)₂).

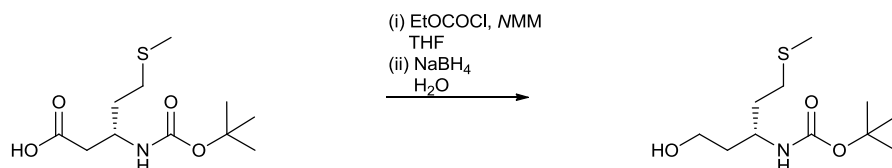
¹³C NMR (125 MHz, CDCl₃) δ 144.4 (ArC), 143.0 (ArC), 128.6 (ArCH), 128.6 (ArCH), 67.5 (CH₂), 54.3 (CH), 48.1 (CH₂), 47.0 (CH₂), 43.5 (CH₂), 26.0 (*t*-Bu), 25.0 (CH₂), 23.6 (CH₂), 21.6 (CH₃), 18.4 (C(CH₃)₃).

ESI+ MS (m/z): 438 [M+H]⁺

HRMS-ES+ (m/z): calcd for C₂₁H₃₆N₃O₂SiS [M+H]⁺: 438.2247, found: 438.2257

FT-IR (CHCl₃ film, cm⁻¹) 3023 (w, aromatic CH), 2955 (s, aliphatic CH), 1642 (s), 1495 (m), 1304 (m), 1162 (s), 1090 (s).

(R)-tert-Butyl 1-hydroxy-5-(methylthio)pentan-3-ylcarbamate (210)



A solution of **203** (1.2 g, 4.56 mmol) and *N*-methyilmorpholine (502 μ l, 4.56 mmol) in anhydrous THF (30 ml) was cooled to 0 °C. Ethyl chloroformate (423 μ l, 5.48 mmol) was added dropwise, the resulting suspension was stirred at room temperature under argon for 1 hour. The reaction mixture was filtered and washed with THF. The filtrate was added dropwise (via dropping funnel) to a solution of NaBH₄ (518 mg, 13.69 mmol) in water (20 ml) at 0 °C. The reaction was allowed to reach room temperature overnight. Reaction was quenched by addition of 1 M HCl until pH 4 was achieved and the solution was stirred for a further 10 minutes. The mixture was extracted with Et₂O (3 \times 20 ml). Combined organics were washed with NaHCO₃ and brine, dried over MgSO₄ and concentrated *in vacuo* to give **210** as a white powder (855 mg, 75 %) which required no further purification.

TLC (silica gel, 20:1 CHCl₃:MeOH), *R_f* = 0.54 (ninhydrin)

¹H NMR (400 MHz, CDCl₃) δ 4.52 (d, 1H, ³*J*_{HH} = 9.1 Hz, NH), 3.96-3.77 (m, 1H,), 3.70-3.56 (m, 2H, HOCHH), 2.65-2.46 (m, 2H, SCH₂), 2.10 (s, 3H, SCH₃), 1.90-1.59 (m, 4H, SCH₂CH₂, HOCH₂CH₂), 1.44 (s, 9H, *t*-Bu).

¹³C NMR (125 MHz, CDCl₃) δ 157.3 (C=O), 80.0(C(CH₃)₃), 58.7 (CH₂OH), 46.9 (CH), 38.9 (CH₂), 35.3 (CH₂), 30.9 (CH₂), 28.3 (*t*-Bu), 15.7 (CH₃).

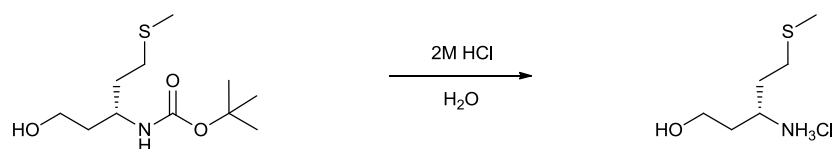
ESI+ MS (*m/z*): 250 [M+H]⁺

HRMS-ESI+ (*m/z*): calcd for C₁₁H₂₄NO₃S [M+H]⁺: 250.1469, found: 250.1460

FT-IR (KBr, cm^{-1}) 3429 (br m, NH_2), 3276 (br m, OH), 3061 (m, aliphatic CH), 1684 (s, $\text{C}=\text{O}$), 1671, (s, $\text{C}=\text{O}$), 1549 (m), 1184 (m).

Melting Point 37.5-38 °C

(R)-3-Amino-5-(methylthio)pentan-1-ol hydrochloride (211)



tert-butyl 1-hydroxy-5-(methylthio)pentan-3-ylcarbamate (**210**) (560 mg, 2.2 mmol) was dissolved in THF (4 ml) and a 2 M solution of HCl in water (20 ml) was added. The reaction was stirred at room temperature for 3 hours. The product was concentrated to a golden oil by co-evaporations with EtOH *in vacuo* (quantitative yield).

TLC (silica gel, 1% sat. MeOH- NH_3 , 9% MeOH- CH_2Cl_2), R_f = 0.35 (ninhydrin)

^1H NMR (400 MHz, D_2O) δ 3.76-3.64 (m, 2H, HOCH_2), 3.53-3.45 (m, 1H, NH_2CH), 2.59-2.55 (m, 2H, SCH_2), 2.04 (s, 3H, SCH_3), 1.99-1.74 (m, 4H, HOCH_2CH_2 , SCH_2CH_2).

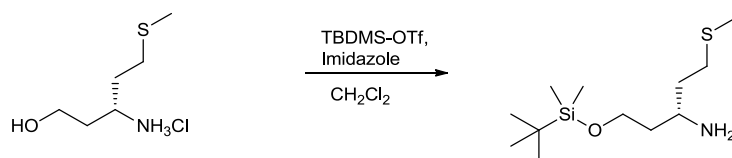
^{13}C NMR (100 MHz, D_2O) δ 58.3 (CH_2OH), 49.5 (CH), 33.4 (CH_2), 31.2 (CH_2), 28.7 (CH_2), 14.0(CH_3).

ESI+ MS (m/z): 150 [$\text{M}+\text{H}$] $^+$.

HRMS-ESI+ (m/z): calcd for $\text{C}_6\text{H}_{16}\text{NOS}$ [$\text{M}+\text{H}$] $^+$: 150.0953, found: 150.0949.

FT-IR (film, cm^{-1}) 3367 (br s, NH_2), 2917 (br s, aliphatic CH), 1613 (m), 1516 (m), 1389 (medium), 1059 (m).

(R)-1-(tert-Butyldimethylsilyloxy)-5-(methylthio)pentan-3-amine (212)



tert-Butyldimethylsilyl triflate (810 μ l, 3.53 mmol) was added dropwise to a suspension of **211** (546 mg, 2.94 mmol) and imidazole (401 mg, 5.89 mmol) in anhydrous CH₂Cl₂ (40 ml) at 0 °C under an argon atmosphere. The resulting mixture was stirred for 1 hour at this temperature and then at room temperature overnight. The solvent was removed under reduced pressure and the resulting residue was partitioned between 1 N NaOH (40 ml) and hexane (40 ml). The aqueous phase was further extracted with hexane (4 \times 40 ml). Combined organics were washed with water (3 \times 30 ml) and extracted with H₂O/MeCN/CH₃COOH (60/40/2, 3 \times 35 ml). The combined aqueous phases were washed with hexane (4 \times 30 ml) and concentrated to half of its volume. NaHCO₃ (solid) was added carefully while cooling until pH 9 was achieved, this was then extracted with ether (3 \times 40 ml). Combined organics were dried over MgSO₄ and concentrated *in vacuo* to give a colourless oil (568 mg, 74 %).

TLC (silica gel, 10:1 CHCl₃:MeOH), *R_f* = 0.46 (ninhydrin)

¹H NMR (400 MHz, CDCl₃) δ 3.80-3.69 (m, 2H, OCH₂), 3.24-3.17 (m, 1H, NH₂CH), 2.55-2.51 (m, 2H, SCH₂), 2.02 (s, 3H, SCH₃), 1.78-1.56 (m, 4H, OCH₂CH₂, SCH₂CH₂), 0.83 (s, 9H, *t*-Bu), 0.01 (s, 6H, Si(CH₂)₂).

¹³C NMR (100 MHz, CDCl₃) δ 61.0 (CH₂O), 48.5 (CH), 40.0 (CH₂), 37.1 (CH₂), 30.9 (CH₂), 25.9 (*t*-Bu), 18.2 (C(CH₃)₃), 15.5 (CH₃).

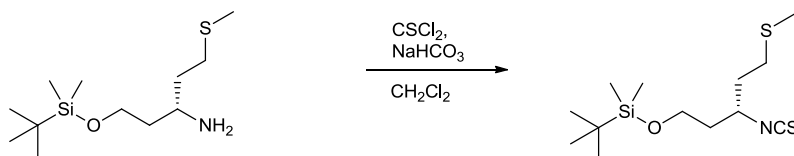
ESI+ MS (*m/z*): 264 [M+H]⁺

HRMS-ESI+ (*m/z*): calcd. for C₁₂H₃₀NOSiS [M+H]⁺: 264.1817, found: 264.1814

FT-IR (CHCl₃ film, cm⁻¹) 2954 (m, aliphatic CH), 1576 (br w), 1256 (m), 1097 (m).

Optical rotation $[\alpha]_D^{20} = -7.8^\circ$ (*c* = 4.2, CHCl₃)

(R)-tert-Butyl(3-isothiocyanato-5-(methylthio)pentyloxy)dimethylsilane (213)



212 (546 mg, 2.16 mmol) was dissolved in CH₂Cl₂ (30 ml) and NaHCO₃ (907 mg, 10.80 mmol) was added in one portion, followed by the dropwise addition of thiophosgene (250 μ l, 3.24 mmol). The resulting heterogeneous mixture was stirred at room temperature overnight. Cold water (20 ml) was added to the reaction and the two layers were separated. The aqueous phase was extracted further with CH₂Cl₂ (20 ml). Combined organics were dried over MgSO₄ and concentrated *in vacuo* to give **213** as a brown oil that needed no further purification (633 mg, 95 %).

TLC (silica gel, 40:1 hexane:EtOAc), $R_f = 0.38$ (UV, CAM)

¹H NMR (400 MHz, CDCl₃) δ 4.13-4.06 (m, 1H, SCNCH), 3.76-3.73 (m, 2H, OCH₂), 2.71-2.65 (m, 1H, SCH₂), 2.62-2.55 (m, 1H, SCH₂), 2.12 (s, 3H, SCH₃), 1.98-1.84 (m, 2H, SCH₂CH₂), 1.82-1.78 (m, 2H, OCH₂CH₂), 0.89 (s, 9H, *t*-Bu), 0.08 (s, 3H, SiCH₃), 0.07 (s, 3H, SiCH₃).

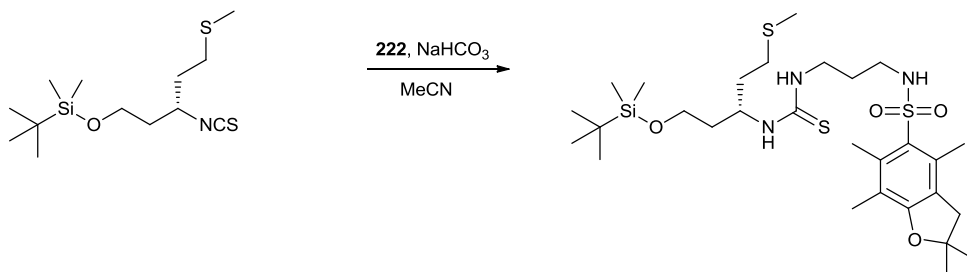
¹³C NMR (100 MHz, CDCl₃) δ 59.2 (CH₂), 54.4 (CH), 38.7 (CH₂), 35.4 (CH₂), 30.8 (CH₂), 26.1 (*t*-Bu), 18.4 (C(CH₃)₃), 15.8 (CH₃), -5.3 (Si(CH₃)₂).

CI+ MS (m/z): 306 [M+H]⁺, 323 [M+NH₄]⁺

HRMS-CI+ (m/z): calcd for C₁₃H₂₈NOSi₂ [M+H]⁺: 306.1376, found: 306.1382.

FT-IR (CHCl₃ film, cm⁻¹) 2954 (m, aliphatic CH), 2086 (br m, NCS), 1257 (m), 1101 (m).

(R)-2,2,4,6,7-Pentamethyl-N-(2,2,3,3-tetramethyl-7-(2-(methylthio)ethyl)-9-thioxo-4-oxa-8,10-diaza-3-silatridecan-13-yl)-2,3-dihydrobenzofuran-5-sulfonamide (214)



A solution of **213** (535 mg, 1.75 mmol) in anhydrous MeCN (15 ml) was added to a solution of **222** (571 mg, 1.75 mmol) and NaHCO₃ (294 mg, 3.51 mmol) in anhydrous MeCN (20 ml). The resulting orange suspension was stirred at reflux overnight. The mixture was filtered and the solvent removed *in vacuo* giving the crude product as white/brown foam. The product was purified by flash chromatography to give thiourea **214** as a white foam (875 mg, 79 %).

TLC (silica gel, 2:1 hexane:EtOAc), $R_f = 0.22$ (UV)

¹H NMR (400 MHz, CDCl₃) δ 3.74-3.65 (m, 4H, OCH₂, SCNHCH₂), 2.99-2.94 (m, 2H, SO₂NHCH₂), 2.97 (s, 2H, furan-CH₂), 2.63-2.52 (m, 2H, SCH₂), 2.56 (s, 3H, ArCH₃), 2.49 (s, 3H, ArCH₃), 2.11 (s, 3H, ArCH₃), 2.07 (s, 3H, SCH₃), 1.81-1.53 (m, 7H, OCH₂CH₂, SCNHCH, SCH₂CH₂, NHCH₂CH₂), 1.47 (s, 6H, (CH₃)₂), 0.89 (s, 9H, *t*-Bu), 0.07 (s, 3H, SiCH₃), 0.06 (s, 3H, SiCH₃).

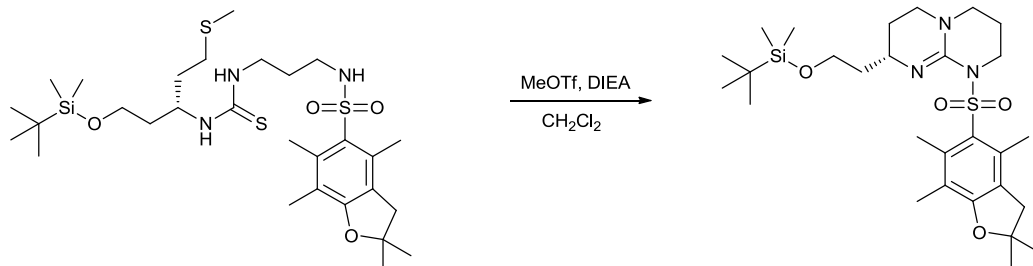
¹³C NMR (400 MHz, CDCl₃) δ 182.5 (C=S), 139.2 (ArC), 135.8 (ArC), 125.2 (ArC), 118.0 (ArC), 86.9 (C(CH₃)₂), 43.1 (CH₂), 39.2 (CH₂), 34.5 (CH₂), 31.0 (CH₂), 28.8 (C(CH₃)₂), 25.0 (*t*-Bu), 19.7 (CH₃), 18.6 (C(CH₃)₃), 18.0 (CH₃), 15.6 (CH₃), 12.7 (CH₃), -5.1 (Si(CH₃)₂).

ESI+ MS (m/z): 632 [M+H]⁺, 654 [M+Na]⁺

HRMS-ESI+ (m/z): calcd for C₂₉H₅₄N₃O₄Si₃ [M+H]⁺: 632.3044, found: 632.3046.

FT-IR (CHCl₃ film, cm⁻¹) 3366 (br s, NH), 2952 (s, aliphatic CH), 1550 (m), 1457 (m), 1304 (s), 1138 (s), 1091 (s).

(S)-8-(2-(*tert*-Butyldimethylsilyloxy)ethyl)-1-(2,2,4,6,7-pentamethyl-2,3-dihydrobenzofuran-5-ylsulfonyl)-2,3,4,6,7,8-hexahydro-1H-pyrimido[1,2-a]pyrimidine (215)



214 (847 mg, 1.34 mmol) was dissolved in anhydrous CH_2Cl_2 (30 ml) and cooled to 0 °C under an argon atmosphere. DIEA (93 μl , 0.54 mmol) was added followed by the dropwise addition of methyl triflate (607 μl , 5.37 mmol). The mixture was stirred at 0 °C for 2.5 hours. DIEA (2.33 ml, 13.42 mmol) was added and the reaction was gently heated to reflux while stirring overnight. The solvent was removed under reduced pressure and the resulting viscous oil was partitioned between 1 N NaOH (15 ml) and Et_2O (20 ml). The aqueous phase was further extracted with Et_2O (2 \times 20 ml). Combined organics were washed with brine, dried over MgSO_4 and concentrated in vacuo. The product was purified by flash chromatography (eluent 0.2-0.4% TEA-EtOAc) to give bicyclic guanidine **215** as a yellow solid (588 mg, 80 %).

TLC (silica gel, 7:3 EtOAc:MeOH 1 % TEA), $R_f = 0.21$ (UV, CAM)

^1H NMR (400 MHz, CDCl_3) δ 3.97-3.86 (m, 2H, SO_2CH_2), 3.42-3.40 (m, 2H, $\text{NCHCH}_2\text{CH}_2$), 3.35-3.29 (m, 1H, NCH), 3.22-3.09 (m, 3H, $\text{SO}_2\text{NCH}_2\text{CH}_2\text{CH}_2$ and OCHH), 3.06-3.02 (m, 1H, OCHH), 3.00 (s, 2H, furan- CH_2), 2.52 (s, 3H, ArCH_3), 2.49 (s, 3H, ArCH_3), 2.14 (s, 3H, ArCH_3), 2.12-2.03 (m, 2H, $\text{SO}_2\text{NCH}_2\text{CH}_2$), 1.84-1.79 (m, 1H, OCH_2CHH), 1.50 (s, 6H, 2 \times ArCH_3), 1.46-1.37 (m, 2H, OCH_2CHH , NCHCHH), 1.21-1.14 (m, 1H, NCHCHH), 0.82 (s, 9H, *t*-Bu), 0.05 (s, 6H, $\text{Si}(\text{CH}_3)_2$).

^{13}C NMR (125 MHz, CDCl_3) δ 159.2 (ArC), 144.2 (ArC), 138.7 (ArC), 134.7 (ArC), 124.5 (ArC), 117.0 (ArC), 86.4 ($\text{C}(\text{CH}_3)_2$), 60.3 (CH_2), 50.3 (CH), 48.3 (CH_2), 47.7 (CH_2), 43.2 (CH_2),

42.1 (CH₂), 40.3 (CH₂), 28.5 (CH₃), 28.5 (CH₃), 27.7 (CH₂), 25.9 (*t*-Bu), 23.3 (CH₂), 19.2 (CH₃), 18.2 (C(CH₃)₃), 17.1 (CH₃), 12.5 (CH₃), -5.3 (Si(CH₃)₂).

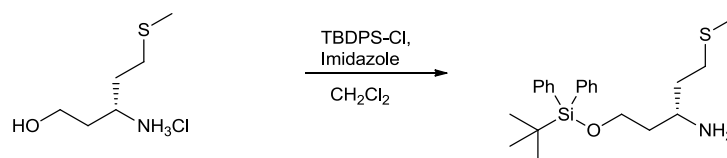
ESI+ MS (*m/z*): 550 [M+H]⁺

HRMS-ESI+ (*m/z*): calcd for C₂₈H₄₈N₃O₄SiS [M+H]⁺: 550.3152, found: 550.3135.

FT-IR (KBr, cm⁻¹) 3448 (br m, NH), 2952 (s, aliphatic CH), 1631 (s), 1428 (m), 1315 (s), 1138 (s), 1091 (s).

Melting Point 80.5-83 °C

(R)-1-(tert-Butyldiphenylsilyloxy)-5-(methylthio)pentan-3-amine (216)



211 (57 mg, 0.38 mmol) and imidazole (57 mg, 0.84 mmol) were dissolved in anhydrous CH₂Cl₂ (5 mL) under an argon atmosphere and cooled to 0 °C. TBDPDS-Cl (0.21 mL, 0.80 mmol) was added and the solution was stirred for 2 hours. The solvent was removed under reduced pressure and the resulting residue was partitioned between 1 N NaOH (4 ml) and hexane (4 ml). The aqueous phase was further extracted with hexane (4 × 4 ml). The combined organics were washed with water (4 × 3 ml) and extracted with H₂O/MeCN/CH₃COOH (60/40/2, 3 × 5 ml). The combined aqueous phases were washed with hexane (4 × 30 ml), made basic by addition of NaHCO₃ (solid) and concentrated to half its volume *in vacuo*. The emulsion was then extracted with ether (3 × 4 ml). Combined organics were dried over MgSO₄ and concentrated *in vacuo* to give **216** as a pale yellow oil (83 mg, 56 %).

TLC (silica gel, CHCl₃:MeOH 10:1), *R_f* = 0.48 (UV, ninhydrin)

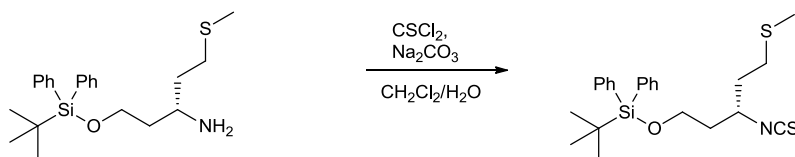
¹H NMR (400 MHz, CDCl₃) δ 7.69-7.66 (m, 4H, ArCH), 7.41-7.36 (m, 6H, ArCH), 3.91-3.77 (m, 2H, OCH₂), 3.28-3.09 (m, 1H, NH₂CH), 3.00-2.74 (br s, 2H, NH₂), 2.66-2.52 (m, 2H, SCH₂), 2.09 (s, 3H, SCH₃), 1.82-1.52 (m, 4H, SCH₂CH₂, OCH₂CH₂) 1.06 (s, 9H, *t*-Bu).

¹³C NMR (100 MHz, CDCl₃) δ 135.6 (ArCH), 135.6 (ArC), 133.6 (ArC), 133.5 (ArCH), 129.7 (ArCH), 127.7 (ArCH), 61.6 (CH₂OSi), 48.4 (CH), 39.5 (CH₂), 36.5 (CH₂), 30.9 (CH₂), 26.9 (*t*-bu), 19.2 (C(CH₃)₃), 15.5 (CH₃).

ESI+ MS (*m/z*): 388 [M+H]⁺

FT-IR (CHCl₃ film, cm⁻¹) 3370 (br m, NH₂), 3070 (m, aromatic CH), 2929 (s, aliphatic CH), 1680 (C=C), 1427 (s), 1111 (s).

(R)-tert-Butyl(3-isothiocyanato-5-(methylthio)pentyloxy)diphenylsilane (217)



216 (105 mg, 0.27 mmol) was dissolved in CH₂Cl₂ (2 mL). Under vigorous stirring a solution Na₂CO₃ (43 mg, 0.4 mmol) in water (2 mL) followed by thiophosgene (23 μ L, 0.3 mmol) in CH₂Cl₂ (2 mL) were added. The biphasic reaction was stirred at room temperature for 4 hours. Toxic fumes were quenched with 1 M NaOH. The two layers were separated and the organic layer was washed with water (4 \times 5 mL) and brine, dried over Mg₂SO₄ and concentrated in vacuo to yield **217** as a yellow oil (102 mg, 88%).

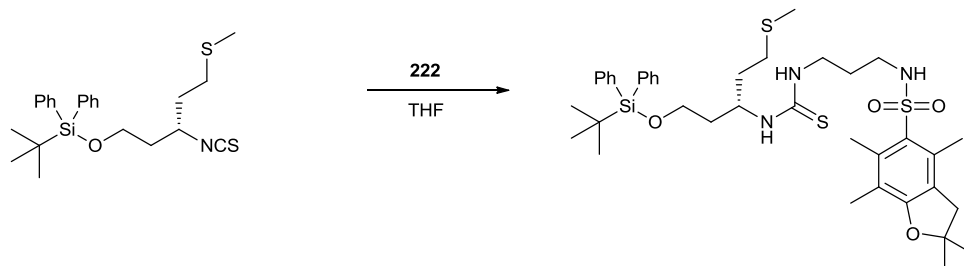
TLC (silica gel, 50:1 hexane:EtOAc), R_f = 0.50 (UV)

¹H NMR (250 MHz, CDCl₃) δ 7.70-7.66 (m, 4H, ArCH), 7.45-7.41 (m, 6H, ArCH), 4.23-4.18 (m, 1H, SCNCH), 3.89-3.73 (m, 2H, OCH₂), 2.73-2.54 (m, 2H, SCH₂), 2.14 (s, 3H, SCH₃), 1.97-1.79 (m, 4H, OCH₂CH₂, SCH₂CH₂), 1.07 (m, 9H, *t*-Bu).

¹³C NMR (100 MHz, CDCl₃) δ 135.7 (ArCH), 135.6 (ArCH), 133.4 (ArC), 133.2 (ArC), 129.91 (ArCH), 127.9 (ArCH), 127.9 (ArCH), 60.0 (CH₂OSi), 54.3 (CH), 38.4 (CH₂), 35.4 (CH₂), 30.74 (CH₂), 26.9 (*t*-bu), 19.3 (C(CH₃)₃), 15.8 (CH₃).

FT-IR (CHCl₃ film, cm⁻¹) 3070 (m, aromatic CH), 2929 (s, aliphatic CH), 2085 (s, NCS), 1427 (s), 1112 (s)..

(R)-N-(2,2-Dimethyl-7-(2-(methylthio)ethyl)-3,3-diphenyl-9-thioxo-4-oxa-8,10-diaza-3-silatridecan-13-yl)-2,2,4,6,7-pentamethyl-2,3-dihydrobenzofuran-5-sulfonamide (218).



A solution of Pbf-diamine **222** (31 mg, 0.1 mmol) in THF was added to a stirring solution of isothiocyanate **217** (41 mg, 0.1 mmol) in THF. The mixture was refluxed at 70 °C overnight. After dilution with water the solution was extracted with (3 × 10 mL) CH₂Cl₂. The combined organics were washed with brine, dried over MgSO₄ and concentrated *in vacuo*. Purification was achieved by flash chromatography (2:1 hexane:EtOAc) to yield **218** as a yellow oil (51 mg, 71 %).

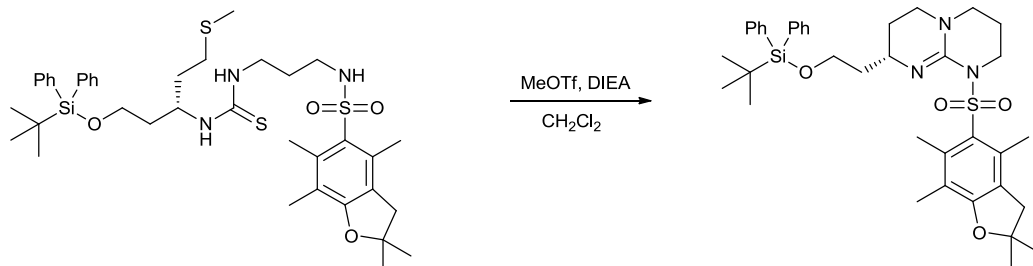
TLC (silica gel, 2:1 hexane:EtOAc), *R_f* = 0.33 (UV)

¹H NMR (400 MHz, CDCl₃) δ 7.63-7.59 (m, 4H, ArCH) 7.43-7.35 (m, 6H, ArCH), 6.18 (d, 1H, *J* = 9 Hz, NH), 5.77 (br s, 1H), 3.84-3.72 (m, 3H, SCNHCH₂, OCHH), 3.53-3.50 (m, 1H, OCHH), 2.97 (s, 2H, furan-CH₂), 2.89-2.86 (m, 2H, SO₂NHCH₂), 2.62-2.48 (m, 2H, SCH₂), 2.54 (s, 3H, ArCH₃), 2.48 (s, 3H, ArCH₃), 2.10 (s, 3H, ArCH₃), 2.07 (s, 3H, SCH₃), 1.79-1.58 (m, 7H, OCH₂CH₂, SCNHCH, SCH₂CH₂ and NHCH₂CH₂), 1.47 (s, 6H, Si(CH₃)₂), 1.06 (s, 9H, *t*-Bu).

¹³C NMR (125 MHz, CDCl₃) δ 182.6 (C=S), 159.6 (ArC), 139.1 (ArC), 135.5 (ArCH), 135.4 (ArCH), 133.8 (ArC), 133.3 (ArC), 130.0 (ArCH), 123.0 (ArCH), 127.9 (ArCH), 125.5 (ArC), 125.1 (ArCH), 117.9 (ArC), 86.7 (C(CH₃)₂), 68.1 (CH₂), 65.9 (CH₂), 60.5 (CH₂), 43.2 (CH₂), 39.6 (CH₂), 34.2 (CH₂), 34.2 (CH₂), 30.8 (CH₂), 30.3 (CH₃), 28.6 (C(CH₃)₂), 27.0 (*t*-bu), 19.6 (CH₃), 19.2 (C(CH₃)₃), 17.8 (CH₃), 15.4 (CH₃), 12.6 (CH₃).

ESI+ MS (*m/z*): 756 [M+H]⁺, 778 [M+Na]⁺, 794 [M+K]⁺.

(S)-8-(2-(*tert*-Butyldiphenylsilyloxy)ethyl)-1-(2,2,4,6,7-pentamethyl-2,3-dihydrobenzofuran-5-ylsulfonyl)-2,3,4,6,7,8-hexahydro-1H-pyrimido[1,2-a]pyrimidine (219**)**



Thiourea **218** (48 mg, 0.064 mmol) was dissolved in CH₂Cl₂ (2 ml) and cooled to -5 °C. DIEA (4.4 μl, 0.025 mmol) and methyl triflate (28 μl, 0.25 mmol) were added. The reaction was monitored by TLC, after completion (ca. 2 hours) diisopropylethylamine (110 μl, 0.64 mmol) was added and the reaction was refluxed gently overnight. The solvent was removed under reduced pressure and the yellow oil was dissolved in ether (5 ml) and extracted with 1 M NaOH. The aqueous layer was washed with Et₂O (2 × 5 ml), combined organics were washed with brine, dried over MgSO₄ and concentrated *in vacuo*. The crude was purified by silica gel chromatography (EtOAc with 0.1% Et₃N) to give the **219** as a brown foam (30 mg, 70%).

TLC (silica gel, 0.1% TEA-EtOAc), *R_f* = 0.16 (UV)

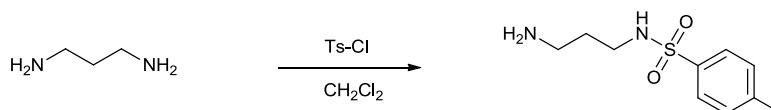
¹H NMR (500 MHz, CDCl₃) δ 7.63-7.59 (m, 4H, ArCH), 7.41-7.35 (m, 6H, ArCH), 3.94-3.89 (m, 1H, SO₂NCHH), 3.84-3.78 (m, 1H, SO₂NCHH), 3.55-3.45 (m, 2H, OCH₂), 3.43-3.33 (br s, 1H, NCH), 3.19-2.92 (br m, 4H, NCHCH₂CH₂, SO₂NCH₂CH₂CH₂), 2.91-2.82 (dd, 2H, ²*J*_{HH} = 15.3, 15.3 Hz, H-12), 2.47 (s, 3H, ArCH₃), 2.44 (s, 3H, ArCH₃), 2.06 (s, 3H, ArCH₃), 2.12-1.97 (m, 2H, SO₂NCH₂CH₂), 1.78-1.68 (br m, 1H, NCH₂CHH), 1.51-1.43 (m, 1H, OCH₂CHH), 1.40 (s, 3H, ArCH₃), 1.35 (s, 3H, ArCH₃), 1.28-1.24 (m, 1H, NCH₂CHH), 1.07-1.04 (m, 1H, OCH₂CHH), 1.01 (s, 9H, *t*-Bu).

¹³C NMR (125 MHz, CDCl₃) δ 159.5 (ArC), 135.6 (ArCH), 135.5 (ArCH), 135.1 (ArC), 134.0 (ArC), 129.5 (ArCH), 127.6 (ArCH), 124.6 (ArC), 117.4 (ArC), 87.0 (C(CH₃)₂), 61.3 (CH₂),

50.4 (CH), 48.3 (CH₂), 47.6 (CH₂), 43.1 (CH₂), 42.0 (CH₂), 40.0 (CH₂), 28.4 (CH₃), 27.0 (CH₂), 26.9 (*t*-Bu), 23.1 (CH₂), 19.3 (CH₃), 19.2 (C(CH₃)₃), 17.2 (CH₃), 12.5 (CH₃).

ESI+ MS (*m/z*): 674 [M+H]⁺.

N-(3-aminopropyl)-4-methylbenzenesulfonamide (220)



A solution of toluenesulfonyl chloride (500 mg, 2.6 mmol) in CH₂Cl₂ (10 ml) was added dropwise to a solution of 1,3-diamino propane (1.1 ml, 13.2 mmol) in CH₂Cl₂ (15 ml). The resulting suspension was heated at reflux for 2 hours. The suspension was filtered, filter cake washed with CH₂Cl₂ and concentrated *in vacuo*. The product was purified by recrystallisation from hot toluene to furnish **220** in as off white crystals (81 % yield, 488 mg).

TLC (silica gel, 10% AcOH-EtOH), *R_f* = 0.41 (UV, ninhydrin)

¹H NMR (400 MHz, MeOD) δ 7.70 (d, 2H, ³*J*_{HH} = 8.0 Hz, ArCH), 7.34 (d, 2H, ³*J*_{HH} = 8.0 Hz, ArCH), 2.85 (t, 2H, ³*J*_{HH} = 6.1 Hz, NHCH₂), 2.62 (t, 2H, ³*J*_{HH} = 6.1 Hz, NH₂CH₂), 2.39 (s, 3H, ArCH₃), 1.60-1.54 (quin, 2H, ³*J*_{HH} = 6 Hz, NH₂CH₂CH₂).

¹³C NMR (125 MHz, MeOD) δ 144.6 (ArC), 138.9 (ArC), 130.8 (ArCH), 128.0 (ArCH), 41.7 (CH₂), 39.7 (CH₂), 33.5 (CH₂), 21.5 (CH₃).

Both ¹H and ¹³C NMR consistent with literature.²¹⁹

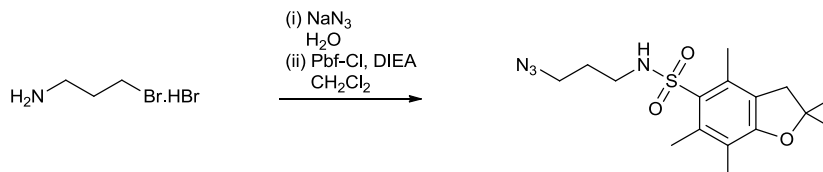
ESI+ MS (*m/z*): 229 [M+H]⁺

HRMS-ESI+ (*m/z*): calcd for C₁₀H₁₆N₂O₂S [M+H]⁺: 229.1011, found: 229.1011

FT-IR (KBr, cm⁻¹) 3359 (s, NH), 3037 (br m, aromatic CH), 2871 (m, aliphatic CH), 1597 (m, NH), 1493 (m), 1321 (s), 1156 (s), 1093 (m).

Melting point 112-113 °C (literature: 112-114 °C)²¹⁹

***N*-(3-azidopropyl)-2,2,4,6,7-pentamethyl-2,3-dihydrobenzofuran-5-sulfonamide
(221)**



A solution of 1-bromopropylamine hydrobromide (600 mg, 2.74 mmol) and sodium azide (452 mg, 8.22 mmol) in water (8 ml) was heated at 80 °C for 20 hours. The reaction was cooled in an ice bath, CH₂Cl₂ (10 ml) and KOH (800 mg) were added and stirring was continued until all the KOH had dissolved. The layers were separated and the aqueous layer was extracted with CH₂Cl₂ (2 × 10 ml), combined organics were dried over MgSO₄ and added to a round bottomed flask containing Pbf-Cl (500 mg, 1.73 mmol) and 4 Å molecular sieves. DIPEA (450 µl, 2.60 mmol) was added and the reaction was refluxed at 45 °C for 4 hours. The mixture was extracted with sat. aq. NH₄Cl, organic layer washed twice further with sat. aq. NH₄Cl, dried over MgSO₄ and concentrated *in vacuo*. The orange residue was purified by silica gel chromatography (3:1 hexane:EtOAc) to give **221** (482 mg, 80 %).

TLC (silica gel, 3:1 hexane:EtOAc), *R_f* = 0.39 (UV, ninhydrin)

¹H NMR (400 MHz, CDCl₃) δ 4.76-4.73 (t, 1H, ³*J*_{HH} = 6.4 Hz, NH), 3.37-3.34 (t, 2H, ³*J*_{HH} = 6.4 Hz, N₃CH₂), 3.01-2.96 (m, 4H, NHCH₂, furan-CH₂), 2.54 (s, 3H, ArCH₃), 2.49 (s, 3H, ArCH₃), 2.17 (s, 3H, ArCH₃), 1.77-1.70 (quin, 2H, ³*J*_{HH} = 6.4 Hz, N₃CH₂CH₂), 1.48 (s, 6H, C(CH₃)₂).

¹³C NMR (125 MHz, CDCl₃) δ 159.8 (ArC), 141.7 (ArC), 134.1 (ArC), 127.7 (ArC), 125.3 (ArC), 118.1 (ArC), 86.9 (C(CH₃)₂), 49.0 (CH₂), 43.2 (CH₂), 40.1 (CH₂), 28.8 (CH₂), 28.6 (C(CH₃)₂), 19.4 (CH₃), 17.7 (CH₃), 12.6 (CH₃).

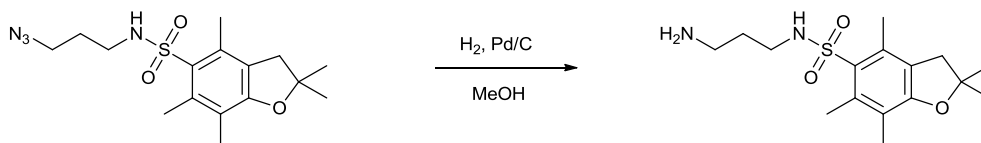
APCI+ MS (*m/z*): 353 [M+H]⁺, 416 [M+MeCNa]⁺.

HRMS-APCI+ (*m/z*): calcd for C₁₆H₂₅N₄O₃S [M+H]⁺: 353.1647, found: 353.1647.

FT-IR (KBr, cm^{-1}) 3308 (br s, NH), 2971 (s, aliphatic CH), 2098 (s, CN_3), 1574 (s), 1460 (s), 1411 (s), 1318 (s), 1257 (s), 1140 (s), 1090 (s), 996 (s).

Melting point 97.5-98 °C.

***N*-(3-aminopropyl)-2,2,4,6,7-pentamethyl-2,3-dihydrobenzofuran-5-sulfonamide (222)**



A suspension of **221** (50 mg, 0.14 mmol) and 10% Pd/C (10 mg) in MeOH was stirred at room temperature for 5 hours under a hydrogen atmosphere. The reaction was filtered and washed through Celite® and concentrated under reduced pressure yielding *N*-(3-aminopropyl)-2,2,4,6,7-pentamethyl-2,3-dihydrobenzofuran-5-sulfonamide (**222**) as an off white foam without need for further purification (46 mg, 99%).

TLC (silica gel, 1 % sat MeOH- NH_3 , 9% MeOH- CH_2Cl_2), R_f = 0.40 (UV, ninhydrin)

^1H NMR (400 MHz, CDCl_3) δ 3.00 (m, 4H, NHCH_2 , furan- CH_2), 2.82-2.77 (t, 2H, $^3J_{\text{HH}} = 6.2$ Hz, NH_2CH_2), 2.52 (s, 3H, ArCH_3), 2.47 (s, 3H, ArCH_3), 2.09 (s, 3H, ArCH_3), 1.66-1.56 (quin, 2H, $^3J_{\text{HH}} = 6.2$ Hz, $\text{NH}_2\text{CH}_2\text{CH}_2$), 1.46 (s, 6H, $\text{C}(\text{CH}_3)_2$).

^{13}C NMR (100 MHz, CDCl_3) δ 159.6 (ArC), 139.3 (ArC), 134.2 (ArC), 128.6 (ArC), 125.2 (ArC), 118.0 (ArC), 86.8 ($\text{C}(\text{CH}_3)_2$), 43.4 (CH_2), 42.3 (CH_2), 41.0 (CH_2), 31.1 (CH_2), 28.7 ($\text{C}(\text{CH}_3)_2$), 19.5 (CH_3), 17.8 (CH_3), 12.7 (CH_3).

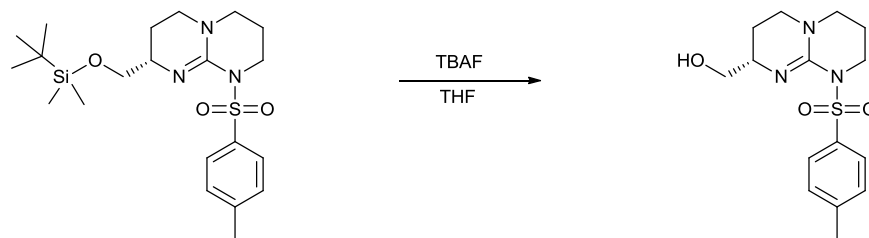
ESI+ MS (m/z): 327 [$\text{M}+\text{H}$]⁺, 368 [$\text{M}+\text{MeCNNH}$]⁺, 390 [$\text{M}+\text{MeCNNa}$]⁺.

HRMS-ESI+ (m/z): calcd for $\text{C}_{16}\text{H}_{27}\text{N}_2\text{O}_3\text{S}$ [$\text{M}+\text{H}$]⁺: 327.1742, found: 327.1756.

FT-IR (KBr, cm^{-1}) 3370 (s, NH), 2934 (s, aliphatic CH), 1575 (s, NH), 1459 (s), 1308 (s), 1142 (s), 1092 (s).

Melting point 92.5-94 °C

**(S)-(1-Tosyl-2,3,4,6,7,8-hexahydro-1H-pyrimido[1,2-a]pyrimidin-8-yl)methanol
(226)**



TBAF (440 μ l, 0.44 mmol) was added dropwise to a solution of **209** (164 mg, 0.37 mmol) in THF (5 ml). The resulting pale orange mixture was stirred at room temperature until all starting material had been consumed (ca. 3 hours, TLC). The solvent was removed under reduced pressure. The brown oil was partitioned between cold NaOH (1M, 10 ml) and ether (3 x 10 ml). Combined organics were dried over Na₂SO₄ and concentrated *in vacuo* to give a white residue which was purified by recrystallisation from hexane/EtOAc to give bicyclic guanidino alcohol **226** as white crystals (64 mg, 53 %).

TLC (neutral alumina, 60:1 CHCl₃:MeOH), R_f = 0.36 (UV,CAM)

¹H NMR (400 MHz, CDCl₃) δ 7.69 (d, 2H, ³J_{HH} = 8 Hz, ArCH), 7.19 (d, 2H, ³J_{HH} = 8 Hz, ArCH), 3.91-3.86 (m, 1H, SO₂NCHH), 3.76-3.72 (m, 1H, SO₂NCHH), 3.53-3.50 (m, 1H, HOCHH), 3.29-3.24 (m, 1H, NCH), 3.15-3.10 (m, 2H, HOCHH, NCHCH₂CH₂), 3.06-3.04 (m, 2H, SO₂NCH₂CH₂CH₂), 2.96-2.92 (m, 1H, NCHCH₂CH₂), 2.40 (br s, 1H, OH), 2.32 (s, 3H, ArCH₃), 2.08-1.91 (m, 2H, SO₂NCH₂CH₂), 1.64-1.51 (m, 2H, NCHCH₂).

¹³C NMR (100 MHz, CDCl₃) δ 145.7 (ArC), 143.4 (ArC), 139.0 (ArC), 129.2 (ArCH), 127.6 (ArCH), 66.1 (CH₂), 54.0 (CH), 48.1 (CH₂), 47.3 (CH₂), 43.9 (CH₂), 23.8 (CH₂), 23.8 (CH₂), 21.7 (CH₃).

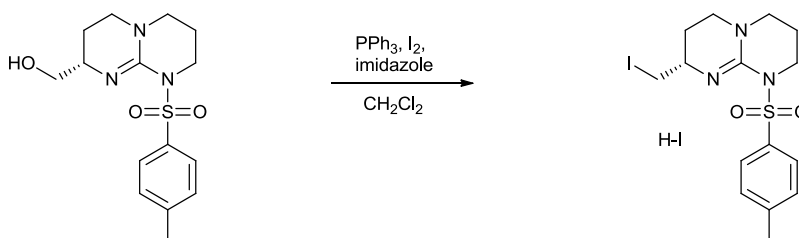
APCI+ MS (m/z): 324 [M+H]⁺, 362 [M+K]⁺, 669 [2M+Na]⁺, 685 [2M+K]⁺

HRMS-APCI+ (m/z): calcd for C₁₅H₂₂N₃O₃S [M+H]⁺: 324.1393, found: 324.1382

FT-IR (KBr, cm⁻¹) 3469 (br m, OH), 2859 (m, aliphatic CH), 1637 (s, NH), 1597, 1497 (m), 1310 (s), 1160 (s), 1092 (m), 1038 (m).

Melting point 127-128 °C

(S)-8-(Iodomethyl)-1-tosyl-2,3,4,6,7,8-hexahydro-1H-pyrimido[1,2-a]pyrimidine hydroiodide (227)



Triphenyl phosphine (970 mg, 3.71 mmol) and imidazole (276 mg, 4.05 mmol) were dissolved in anhydrous CH₂Cl₂ (2 ml), cooled to -20 °C and shielded from light under an argon atmosphere. I₂ (943 mg, 3.71 mmol) was added in one portion and the yellow mixture was stirred at -20 °C for 20 minutes. **226** (400 mg, 1.24 mmol) was added in one portion. After 20 minutes the dry ice acetone bath was removed and stirring continued for 2 hours. The solvent was removed under reduced pressure giving an orange foam which was purified by flash chromatography to furnish **227** as a brown foam (562 mg, 81 %).

TLC (silica gel, 10:1 CHCl₃:MeOH-0.01%TEA), *R_f* = 0.16 (UV,CAM)

¹H NMR (400 MHz, MeOD) δ 7.99 (d, 2H, ³*J*_{HH} = 8.4 Hz, ArCH), 7.56 (d, 2H, ³*J*_{HH} = 8.4 Hz, ArCH), 4.03-3.96 (m, 1H, SO₂NCHH), 3.93-3.85 (m, 2H, SO₂NCHH, NCH), 3.60-3.38 (m, 6H, ICH₂, SO₂NCH₂CH₂CH₂, NCHCH₂CH₂), 2.49 (s, 3H, ArCH₃), 2.24-2.17 (m, 1H, SO₂NCH₂CH₂), 2.11-2.02 (m, 1H, SO₂NCH₂CH₂), 1.92-1.83 (m, 1H, NCHCH₂), 1.81-1.73 (m, 1H, NCHCH₂).

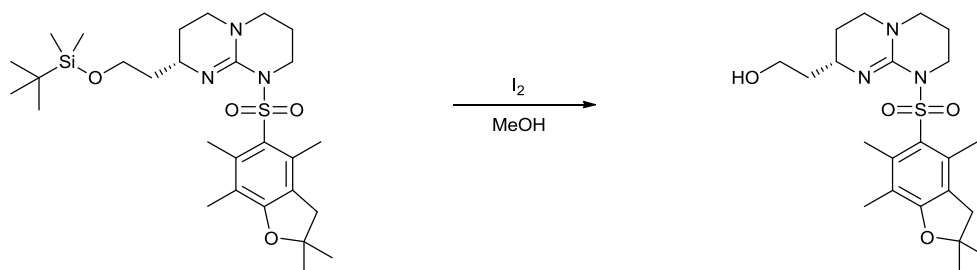
¹³C NMR (125 MHz, MeOD) δ 150.9 (ArC), 148.7 (ArC), 135.0 (ArCH), 129.2 (ArCH), 52.7 (CH), 49.9 (CH₂), 47.9 (CH₂), 45.8 (CH₂), 26.3 (CH₂), 21.8 (CH₂) 21.8 (CH₃), 7.1 (CH₂I).

ESI+ MS (*m/z*): 434 [M+H]⁺

HRMS-ESI+ (*m/z*): calcd for C₁₅H₂₁IN₃O₂S [M+H]⁺: 434.0399, found: 434.0404

FT-IR (KBr, cm⁻¹) 2929 (m, aliphatic CH), 1632 (s), 1517 (m), 1165 (m).

(S)-2-(1-(2,2,4,6,7-Pentamethyl-2,3-dihydrobenzofuran-5-ylsulfonyl)-2,3,4,6,7,8-hexahydro-1H-pyrimido[1,2-a]pyrimidin-8-yl)ethanol (229)



A solution of iodine in methanol (5 ml, 1 % w/v) was added to a flask containing **215** (60 mg, 0.11 mmol), the resulting brown mixture was stirred at 65 °C until consumption of starting material was apparent (TLC, ca. 12 hours). Na₂S₂O₃ (solid) was added until the solution turned colourless and the mixture was filtered and concentrated *in vacuo*. The white residue was treated with CHCl₃ and Na₂HCO₃ (solid) was added. The mixture was stirred at room temperature for five minutes. Following filtration the solvent was removed under reduced pressure yielding a white solid. This was triturated from EtOAc to give **229** as a white amorphous solid (55 mg, 89 %).

TLC (neutral alumina, 60:1 CHCl₃:MeOH), *R_f* = 0.40 (UV,CAM)

¹H NMR (**400 MHz, MeOD**) δ 3.95-3.80 (m, 3H, SO₂NCH₂, HOCHH), 3.78-3.69 (m, 1H, NCH), 3.66-3.59 (m, 2H, HOCHH, NCHCH₂CHH), 3.57-3.52 (m, 3H, NCHCH₂CHH, SO₂NCH₂CH₂CH₂), 3.18 (s, 2H, furan-CH₂), 2.59 (s, 3H, ArCH₃), 2.58 (s, 3H, ArCH₃), 2.28-2.23 (m, 1H, OCH₂CHH), 2.22 (s, 3H, ArCH₃), 2.04-1.89 (m, 5H, NCHCH₂, SO₂NCH₂CH₂, OCH₂CHH), 1.57 (s, 6H, ArCH₃).

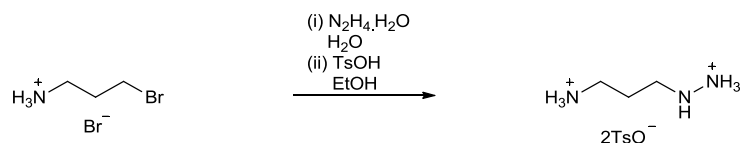
¹³C NMR (**125 MHz, CDCl₃**) δ 161.8 (ArC), 149.3 (ArC), 141.1 (ArC), 136.1 (ArC), 126.8 (ArC), 123.8 (ArC), 119.1 (ArC), 88.1 (C(CH₃)₂), 59.0 (CH₂), 49.9 (CH), 48.0 (CH₂), 47.3 (CH₂), 43.2 (CH₂), 42.3 (CH₂), 36.3 (CH₂), 27.3 (C(CH₃)₂), 25.3 (CH₂), 20.3 (CH₂), 18.2 (CH₃), 16.5 (CH₃), 11.2 (CH₃).

API+ MS (m/z): 436 [M+H]⁺.

HRMS-API+ (m/z): calcd for C₂₂H₃₄N₃O₄S [M+H]⁺: 436.2263, found: 436.2270.

FT-IR (KBr, cm^{-1}) 3466 (br m, NH), 2958 (s, aliphatic CH), 1636 (s), 1428 (m), 1311 (s), 1138 (s), 1091 (s).

2-(3-Ammoniopropyl)hydrazinium 4-methylbenzenesulfonate (**239**)



A solution of 1-bromopropylamine hydrobromide (1.00 g, 4.6 mmol) in water (3 ml) was added to hydrazine monohydrate (1.11 ml, 22.8 mmol) at 80 °C, stirring was continued at this temperature for 30 minutes and then at 100 °C for 5.5 hours. 50% of mixture was removed under reduced pressure and the mixture was concentrated to a white solid by co-evaporating with EtOH. The white solid was dissolved in 40% MeOH and poured onto a column containing Amberlite® IRA-400 ion exchange resin (OH^- form). The resin was washed with several column volumes of water. The combined filtrates were concentrated *in vacuo* and co-evaporated with EtOH to give a clear liquid. The product was dissolved in EtOH and *p*-TsOH (1.7 g) was added. The resulting solution was stirred at room temperature for 1 hour, the crystalline product was filtered, washed with cold EtOH and concentrated *in vacuo* to yield **239** as a white solid (1.18 g, 60 %).

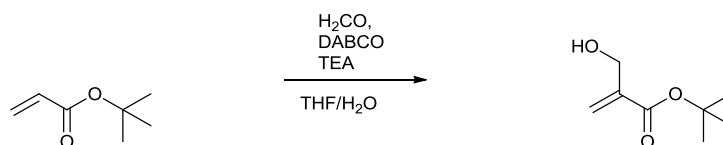
^1H NMR (400 MHz, CDCl_3) δ 7.64 (d, 4H, $^3J_{\text{HH}} = 8.2$ Hz, Ar CH), 7.30 (d, 4H, $^3J_{\text{HH}} = 7.7$ Hz, Ar CH), 3.13 (d, 2H, $^3J_{\text{HH}} = 7.5$ Hz, H-1), 3.04 (d, 2H, $^3J_{\text{HH}} = 7.7$ Hz, H-3), 2.34 (s, 6H, CH_3), (quin, 2H, $^3J_{\text{HH}} = 7.6$ Hz, H-2).

^{13}C NMR (125 MHz, CDCl_3) δ 142.4 (ArC), 139.5 (ArC), 130.0 (ArCH), 126.9 (ArCH), 47.5 (CH_2), 37.6 (CH_2), 27.9 (CH_2), 21.7 (CH_3).

FT-IR (KBr, cm^{-1}) 3378 (s, NH), 3025 (br m, aromatic CH), 2865 (m, aliphatic CH), 1554 (m, NH), 1493 (m), 1321 (s), 1156 (s), 1007 (s)

Melting Point 157-158 °C (decomposes)

tert -butyl 2-(hydroxymethyl)acrylate (250)



A solution containing t-butyl acrylate (11.4 ml, 78.13 mmol), formalin (9.52 ml, 117.19 mmol), DABCO (876 mg, 7.81 mmol), triethylamine (1.09 ml, 7.81 mmol) and water (5 ml) in THF (15 ml) were stirred at room temperature for 3 hours and then at 55 °C for 24 hours. Et₂O (10 ml) was added to the reaction mixture and the phases were separated. The aqueous phase was re-extracted with Et₂O (2 × 20ml). Combined organics were washed with brine, dried over MgSO₄ and concentrated *in vacuo*. Purification by fractional distillation *in vacuo* furnished **250** as a colourless liquid (5.56 g, 45 %).

TLC (silica gel, 10:1 hexane:EtOAc), $R_f = 0.13$ (UV,CAM)

¹H NMR (400 MHz, CDCl₃) δ 6.08 (d, 1H, $^2J_{HH} = 1.5$ Hz, CCHH), 5.70 (d, 1H, $^2J_{HH} = 1.5$ Hz, CCHH), 4.20 (s, 2H, HOCH₂), 3.20 (br s, 1H, OH), 1.42 (s, 9H, *t*-Bu).

¹³C NMR (100 MHz, CDCl₃) δ 165.8 (C=O), 140.8 (C=CH₂), 124.5 (CCH₂), 81.2 (C(CH₃)₃), 62.3 (CH₂), 27.9 (*t*-Bu).

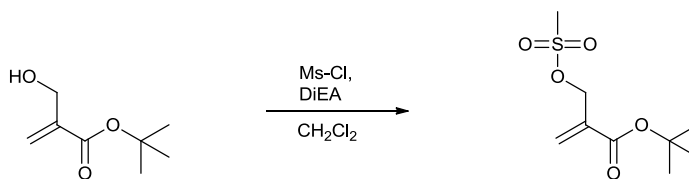
Both ¹H and ¹³C NMR spectra consistent with literature.²²⁰

ESI+ MS (m/z): 339 [2M+Na]⁺

HRMS-ESI+ (m/z): calcd for C₁₆H₂₈O₆Na [2M+Na]⁺: 339.1784, found: 339.1781

FT-IR (neat, cm⁻¹) 3425 (br s, OH), 2979 (s, aliphatic CH), 1709 (s, C=O), 1638 (m), 1369 (s), 1152 (s), 1056 (s).

***tert*-butyl 2-((methylsulfonyloxy)methyl)acrylate (**251**)**



Mesyl chloride (50 μ l, 0.61 mmol) was added dropwise to a solution of **250** (97 mg, 0.61 mmol) and DIEA (160 μ l, 0.92 mmol) in anhydrous CH₂Cl₂ (5 ml) at 0 °C. After stirring for 2 hours the ice bath was removed and stirring was continued for 24 hours. Sat. aq. NaHCO₃ (5 ml) was added and the phases were separated. The aqueous phase was further extracted with CH₂Cl₂ (2 \times 5 ml). Combined organics were dried over MgSO₄ and concentrated *in vacuo* and purified by flash chromatography to give **251** (40 mg, 30 %) as a yellow oil.

TLC (silica gel, 2:1 hexane:EtOAc), R_f = 0.69 (UV)

¹H NMR (400 MHz, MeOD) δ 6.34 (s, 1H, CCHH), 5.91 (s, 1H, CCHH), 4.85 (s, 2H, OCH₂), 3.04 (s, 3H, SCH₃), 1.48 (s, 9H, *t*-Bu).

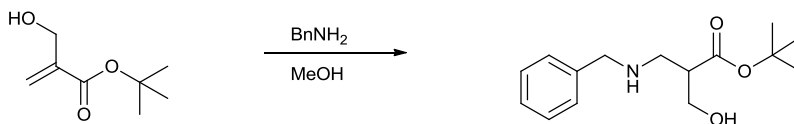
¹³C NMR (125 MHz, CDCl₃) δ 168.0 (C=O), 140.2 (C=CH₂), 126.4 (C=CH₂), 82.7 (C(CH₃)₃), 66.6 (CH₂), 37.2 (CH₃), 29.7 (*t*-Bu).

ESI+ MS (m/z): 237 [M+H]⁺

HRMS-ESI+ (m/z): calcd for C₉H₁₇O₅S [M+H]⁺: 237.0801, found: 237.0792

FT-IR (CHCl₃ film, cm⁻¹) 3425 (br s, OH), 2969 (s, aliphatic CH), 1706 (s, C=O), 1645 (m), 1332 (s), 1152 (s).

***tert*-butyl 3-(benzylamino)-2-(hydroxymethyl)propanoate (256)**



Benzylamine (520 μ l, 4.8 mmol) was added to a solution of **250** (633 mg, 4.0 mmol) in MeOH (8 ml) at 30 °C. The resulting mixture was stirred at this temperature for 6 hours. The solvent was removed under reduced pressure. Purification was achieved through silica gel column chromatography (CHCl₃:MeOH 40:1) which yielded **256** (817 mg, 77 %).

TLC (silica gel, 10:1 CHCl₃:MeOH), R_f = 0.66 (UV, ninhydrin)

¹H NMR (400 MHz, CDCl₃) δ 7.28-7.16 (m, 5H, ArCH), 3.90 (m, 2H, HOCH₂), 3.71 (s, 2H, PhCH₂), 3.01 (dd, 1H, ³J_{HH} = 6.0 Hz, ²J_{HH} = 12.0 Hz, NHCHH), 2.84 (dd, 1H, ³J_{HH} = 4.7 Hz, ²J_{HH} = 12.0 Hz, NHCHH), 2.58-2.53 (m, 1H, OCCH), 1.39 (s, 9H, *t*-Bu).

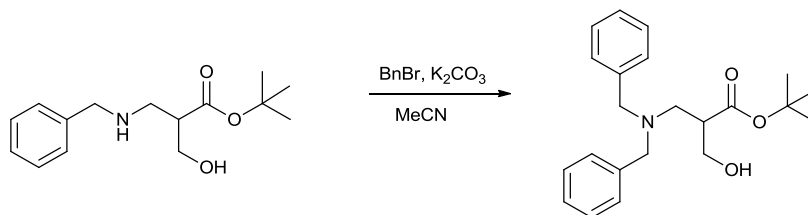
¹³C NMR (125 MHz, CDCl₃) δ 172.4 (C=O), 139.0 (ArC), 128.3 (ArCH), 128.0 (ArCH), 127.0 (ArCH), 80.9 (C(CH₃)₃), 64.5 (CH₂OH), 53.8 (CH₂), 49.6 (CH₂), 46.7 (CH), 27.9 (*t*-Bu).

ESI+ MS (m/z): 266 [M+H]⁺, 531 [2M+H]⁺.

HRMS-ESI+ (m/z): calcd for C₁₅H₂₄NO₃ [M+H]⁺: 266.1756, found: 266.1745

FT-IR (CHCl₃ film, cm⁻¹) 3317 (br m, OH), 3027 (m, aromatic CH), 2977 (m, aliphatic CH), 1723 (s, C=O), 1455 (s), 1367 (s), 1156 (s).

***tert*-Butyl 3-(dibenzylamino)-2-(hydroxymethyl)propanoate (257)**



Potassium carbonate (676 mg, 4.90 mmol) was added in one portion to a solution of **256** (432 mg, 1.63 mmol) in MeCN (40 ml). While stirring vigorously benzyl bromide (370 μ l, 3.10 mmol) was added and the resulting orange mixture was stirred at room temperature overnight. The reaction was terminated by addition of water (20 ml) and extracted with EtOAc (2 \times 25 ml). Combined organics were washed with brine, dried over MgSO₄ and concentrated *in vacuo*. The crude residue was purified by silica gel column chromatography (20 % EtOAc-hexane) to give the title compound as a white solid (500 mg, 86 %).

TLC (silica gel, 20% EtOAc-hexane), R_f = 0.33 (UV)

¹H NMR (400 MHz, MeOD) δ 7.26-7.14 (m, 10H, ArCH), 3.57 (d, 2H, $^3J_{HH}$ = 13.5 Hz, PhCH₂), 3.50 (d, 2H, $^3J_{HH}$ = 6.8 Hz, HOCH₂), 3.37 (d, 2H, $^3J_{HH}$ = 13.5 Hz, PhCH₂), 2.82-2.75 (m, 1H, OCCH), 2.64 (dd, 1H, $^3J_{HH}$ = 8.6 Hz, $^2J_{HH}$ = 12.6 Hz, NCHH), 2.39 (dd, 1H, $^3J_{HH}$ = 6.1 Hz, $^2J_{HH}$ = 12.6 Hz NCHH), 1.39 (s, 9H, *t*-Bu).

¹³C NMR (125 MHz, MeOD) δ 174.9 (C=O), 140.2 (ArC), 130.2 (ArCH), 129.2 (ArCH), 128.1 (ArCH), 81.7 (C(CH₃)₃), 63.5 (CH₂OH), 59.4 (PhCH₂), 54.2 (NCH₂), 46.6 (CH), 28.5 (*t*-Bu).

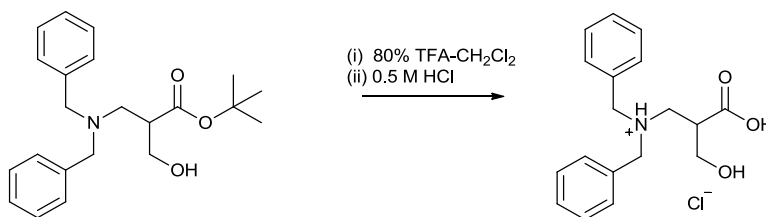
ESI+ MS (m/z): 356 [M+H]⁺

HRMS-ESI+ (m/z): calcd for C₂₂H₃₀NO₃ [M+H]⁺: 356.2226, found: 356.2210

FT-IR (CHCl₃ film, cm⁻¹) 3438 (br, m, OH), 3027 (m, aromatic CH), 2977 (m, aliphatic CH), 1726 (s, C=O), 1453 (m), 1367 (s), 1154 (s).

Melting point: 61.5-62.5 °C

3-(Dibenzylamino)-2-(hydroxymethyl)propanoic acid hydrochloride (**258**)



257 (783 mg, 2.20 mmol) was dissolved in CH₂Cl₂ (2 ml) and added to a stirring solution of trifluoroacetic acid (8 ml). The mixture was stirred at room temperature for 5 hours. The solvent was removed under reduced pressure and the resulting yellow-brown oil was treated with HCl (0.5 M, 10 ml) and sonicated for 3 hours. The product was concentrated *in vacuo* to a white solid, which was recrystallisation from absolute ethanol to give **258** as white crystals. (442 mg, 78 %)

TLC (silica gel, 10:1 CHCl₃:MeOH), *R_f* = 0.17 (UV)

¹H NMR (400 MHz, CH₃OD) δ 7.45-7.40 (m, 10H, ArCH), 4.37 (s, 4H, (PhCH₂)₂), 3.72-3.69 (dd, 1H, ³*J*_{HH} = 3.9 Hz, ²*J*_{HH} = 10.8 Hz, HOCHH), 3.61-3.50 (m, 2H, NCHH and HOCHH), 3.33-3.28 (dd, 1H, ³*J*_{HH} = 5.8 Hz, ²*J*_{HH} = 13.6 Hz, NCHH), 3.22-3.20 (m, 1H, OCCH).

¹³C NMR (125 MHz, CH₃OD) δ 172.6 (C=O), 130.8 (ArCH), 130.0 (ArCH), 129.2 (ArCH), 61.4 (CH₂OH), 58.0 (PhCH₂), 52.3 (NCH₂), 41.8 (CH).

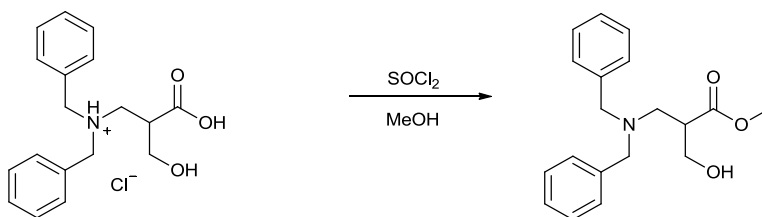
ESI+ MS (*m/z*): 300 [M+H]⁺, 599 [2M+H]⁺.

HRMS-ESI+ (*m/z*): calcd for C₁₈H₂₂NO₃ [M+H]⁺: 300.1600, found: 300.1591

FT-IR (KBr, cm⁻¹) 3246 (br s, OH), 3039 (s, aromatic CH), 2962 (s, aliphatic CH), 1699 (s, C=O), 1464 (s), 1412 (s), 1361 (s), 1205 (s), 1073 (s).

Melting Point 167-168 °C

Methyl 3-(dibenzylamino)-2-(hydroxymethyl)propanoate (**260**)



Thionyl chloride (0.46 ml, 7.10 mmol) was added to a solution of **258** (238 mg, 0.71 mmol) in anhydrous MeOH (10 ml) at 0 °C under argon. The mixture was stirred at this temperature for 1 hour and for a further 3 hours at room temperature. The solvent was removed under reduced pressure. The white residue was dissolved in EtOAc (10 ml) containing a small amount of MeOH (which was necessary to completely dissolve residue, ca. 0.5 ml) and extracted with 1 N NaOH (10 ml). The aqueous phase was re-extracted with EtOAc (2 × 10 ml). Combined organics were washed with brine, dried over MgSO₄ and concentrated *in vacuo* to give **260** as a golden oil (167 mg, 75 %).

TLC (silica gel, 2:1 hexane:EtOAc), $R_f = 0.43$ (UV)

¹H NMR (400 MHz, CHCl₃) δ 7.40-7.28 (m, 10H, ArCH), 3.89-3.3.85 (dd, 1H, $^3J_{HH} = 5.1$ Hz, $^2J_{HH} = 10.9$ Hz HOCHH), 3.82 (d, 2H, $^2J_{HH} = 13.3$ Hz, PhCH₂) 3.74-3.71 (dd, 1H, $^3J_{HH} = 6.8$ Hz, $^2J_{HH} = 10.9$ Hz, HOCHH), 3.69 (s, 3H, OCH₃), 3.42 (d, 2H, $^2J_{HH} = 13.3$ Hz, PhCH₂), 3.04-2.99 (m, 1H, OCCH), 2.92-2.81 (m, 2H, NCH₂).

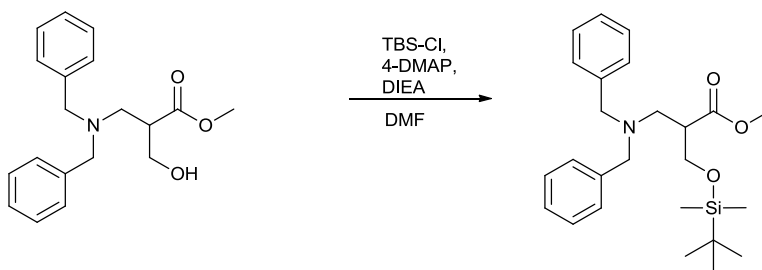
¹³C NMR (125 MHz, CHCl₃) δ 173.2 (C=O), 138.0 (ArC), 129.0 (ArCH), 128.4 (ArCH), 127.3 (ArCH), 63.5 (CH₂OH), 58.7 (PhCH₂), 53.8 (NCH₂), 51.7 (CH₃), 44.9 (CH).

ESI+ MS (m/z): 314 [M+H]⁺

HRMS-ESI+ (m/z): calcd for C₁₉H₂₄NO₃ [M+H]⁺: 314.1756, found: 314.1750

FT-IR (CHCl₃ film, cm⁻¹) 3014 (s, aromatic CH), 2849 (w, aliphatic CH), 2400 (s), 1732 (s, C=O), 1522 (s), 1425 (s), 1208 (br s), 1045 (s).

Methyl 3-(*tert*-butyldimethylsilyloxy)-2-((dibenzylamino)methyl)propanoate (**266**)



TBS-Cl (90 mg, 0.6 mmol) was added to a solution of **260** (125 mg, 0.4 mmol), 4-diemthylaminopyridine (5 mg, 60 μ mol) and diisopropylethylamine (140 μ l, 0.8 mmol) in anhydrous DMF at 0 $^{\circ}$ C under argon. The mixture was stirred at this temperature for 1 hour and allowed to reach room temperature overnight. The solvent was removed under reduced pressure to give a brown residue which was partitioned between 1 N NaOH (15 ml) and Et₂O (10 ml). The aqueous phase was re-extracted with Et₂O (2 \times 10 ml). Combined organics were washed with brine, dried over MgSO₄ and concentrated *in vacuo*. The crude product was purified by flash chromatography to give the title compound as a golden oil (113 mg, 78 %).

TLC (silica gel, 4 % EtOAc-hexane), R_f = 0.34 (UV, KMnO₄)

¹H NMR (500 MHz, CHCl₃) δ 7.31-7.27 (m, 8H, ArCH), 7.23-7.20 (m, 2H, ArCH), 3.71-3.62 (m, 7H, PhCH₂, OCH₂, OCH₃), 3.47 (d, 2H, ² J_{HH} = 13.6 Hz, PhCH₂), 2.95-2.90 (m, 1H, OCCH), 2.75-2.70 (dd, 1H, ³ J_{HH} = 8.4 Hz, ² J_{HH} = 13.0 Hz, NCHH), 2.58-2.55 (dd, 1H, ³ J_{HH} = 6.1 Hz, ² J_{HH} = 13.0 Hz, NCHH), 0.84 (s, 9H, *t*-Bu), 0.0 (s, 3H, SiCH₃), -0.02 (s, 3H, SiCH₃).

¹³C NMR (125 MHz, CHCl₃) δ 174.1 (C=O), 139.2 (ArC), 129.0 (ArCH), 128.2 (ArCH), 127.0 (ArCH), 62.9 (CH₂OSi), 58.5 (PhCH₂), 52.5 (NCH₂), 51.4 (CH₃), 47.9 (CH), 25.8 (*t*-Bu), 18.2 (C(CH₃)₃), -5.5 (Si(CH₃)₂).

ESI+ MS (m/z): 428 [M+H]⁺

HRMS-ESI+ (m/z): calcd for C₂₅H₃₈NO₃Si [M+H]⁺: 428.2621, found: 428.2614

FT-IR (CHCl₃ film, cm⁻¹) 3015 (s, aromatic CH), 2958 (m, aliphatic CH), 2400 (s), 1522 (s), 1424 (s), 1228 (br s).

General procedure for peptide synthesis

Resin preparation:

The resin was added to a fritted plastic vessel. The outlet of the syringe was connected to a membrane pump *via* a collecting tank. NMP was added for resin swelling and left for at least 2 h before the solvent was removed by vacuum filtration.

Fmoc-Deprotecting / Coupling cycle:

For Fmoc removal, a 50 % piperidine/NMP (v/v) solution was added and shaken for 10 min. at room temperature. The solvent was removed by vacuum filtration and this step was repeated. The resin was then washed four times with NMP. A solution of Fmoc protected amino acid (4 eq.; 2 eq. for amino acid with biotinyl tag), HOBT (4 eq.), PyBOP or HBTU (4 eq.) and DIEA (4 eq.) in NMP was added and shaken for 1 hour at room temperature. The solvent was removed by vacuum filtration and the resin was washed four times with NMP.

The deprotecting / coupling cycle was repeated for each of the subsequent amino acid residues.

Removal of the *N*-terminal Fmoc group and drying the peptide resin:

A 50% piperidine/NMP (v/v) solution was added and shaken for 10 min. at room temperature. The solvent was removed by vacuum filtration and this step was repeated. The resin was washed three times with NMP, three times with chloroform, three times with methanol and three times with diethyl ether and finally dried *in vacuo*.

Cleavage of the peptide from resin and deprotection of side chains:

Mixture of thioanisole (5.0%), 1,2-ethanedithiol (2.5%), *m*-cresol (5.0%), water (5.0%) and TFA (82.5%) was added to the peptide resin and left for 6 h at room temperature. The filtrate was collected and the resin washed with TFA. Diethyl ether (10 mL) was added to a tube containing the combined filtrate and washing to precipitate the peptide. The tube was centrifuged (5 min., 4 °C) and the solution decanted. The pellet was then washed with diethyl ether (10 mL), resuspended in Et₂O and centrifuged three more times.

Library Synthesis

Polyamide synthesis was prepared by standard Fmoc methodology (outlined above) on macrobead resin (polystyrene AM RAM, 0.53 mmol g⁻¹, ~114 nmol per bead (based on average bead weight × loading = 2.15×10⁻⁴ g × 0.53 mmol g⁻¹ = 114 nmol)). Side chain protecting groups were: Arg(Pbf), Lys(Boc), Asn/Cys(Trt) and Thr/Tyr/Ser(tBu). Double coupling were employed for each amino acid. Variation was introduced to the *N*-terminal at four positions (GGKC-X₁-X₂-CA-X₃-X₄-A) using the split-and-recombine method where X₁ = Phe, Ile, Thr or Tyr; X₂ = Lys or Arg; X₃ = Arg or Ser; X₄ = Leu, Asn, Val or Tyr. The beads were not recombined after the final splitting stage so the identity of the final variation was known. Library beads were dispensed individually into wells of a 96 well polypropylene plate and 200 µl cleavage reagent (95 % TFA, 2.5 % H₂O and 2.5 % TIPS) was added. The plate was covered and left to stand for 4 hours at room temperature. The reagent was evaporated under a stream of nitrogen, followed by drying *in vacuo*.

Oxidation of thiols to disulfide bond

The dried peptides were diluted with H₂O (100 µl) and an aq. sol. NH₄CO₃ (0.5 M, 1 µl) was added. The compounds were subjected to an oxygen atmosphere for 8 hours. The formation of the disulfide bond was confirmed by MALDI-ToF MS (Appendix 2).

Oligonucleotides

RandZif 5' Biotin-CGG AGT ATC GGG TAT GTG CGG C 3'. TGF-β-1 5' Biotin-CAG GGG GGA CGC CCC GUC CGG GGC ACC CCC CGG CUC UG 3'. Dup 5' Biotin CGG AGT ATC GGG TAT GTG CGG C 3' hybridized to 5' GCC GCA CAT ACC CGA TAC TCC G 3'. Annealing for ELISA was performed using oligonucleotides at a nominal concentration of 40 µM in phosphate buffer (50 mM potassium phosphate, 100 mM KCl, pH 7.4). Annealed stocks were standardised using the absorbance at 260nm.

ELISA Screening

Phosphate buffer was used throughout (50 mM potassium phosphate, 100 mM KCl, pH 7.4). Streptavidin coated plates (96 well Streptawell Highbind, Roche) were incubated and

annealed with dsDNA (Rand zif), ssDNA (Rand zif) and RNA (TGF- β) biotinylated oligonucleotides in adjacent wells (300 μ l, 50 nM DNA/RNA) for 6 hours at room temperature. Plates were washed with buffer (4 \times 300 μ l), incubated for 1 hour after addition of blocking solution (1 mM biotin in buffer, 300 μ l) and again washed with buffer (4 \times 300 μ l).

Stock solutions of the crude oxidised polyamides (1 mM concentration based on bead loading) were prepared. 10 μ l of each stock solution was diluted to a total volume of 200 μ l with buffer and 50 μ l of this was added to the nucleic acid coated wells. Following incubation for 1 hour the plates were washed with buffer (4 \times 300 μ l). Streptavidin-HRP conjugate (Sigma, S 2438) (60000:1 dilution in buffer containing 0.05% Tween 20) was applied to each well, with the exception of wells H11 and H12 as these were used for controls. After incubating for 1 hour the plates were washed with buffer containing 0.05% Tween 20 (4 \times 300 μ l). TMB substrate (100 μ l, prepared as described later) was added to all wells using a multichannel pipettor, followed by quenching after 3 minutes with H₂SO₄ (0.2 mM, 50 μ l). The absorbance was measured immediately at 450 nm. Subtract background.

7.0 References

1. D. Wilczyńska, P. Kosson, M. Kwasiborska, A. Ejchart and A. Olma, *J. Pept. Sci.*, 2009, **15**, 777-782.
2. D. Podwysocka, P. Kosson, A. W. Lipkowski and A. Olma, *J. Pept. Sci.*, 2012, **18**, 556-559.
3. L. Rajender Reddy, K. Prasad and M. Prashad, *J. Org. Chem.*, 2012, **77**, 6296-6301.
4. P. A. Lander and L. S. Hegedus, *J. Am. Chem. Soc.*, 1994, **116**, 8126-8132.
5. L. J. Drummond and A. Sutherland, *Tetrahedron*, 2010, **66**, 5349-5356.
6. K. Harada, *Nature*, 1963, **200**, 1201-1201.
7. M. S. Iyer, K. M. Gigstad, N. D. Namdev and M. Lipton, *J. Am. Chem. Soc.*, 1996, **118**, 4910-4911.
8. M. S. Sigman, P. Vachal and E. N. Jacobsen, *Angew. Chem. Int. Ed.*, 2000, **39**, 1279-1281.
9. Y. Wen, Y. Xiong, L. Chang, J. Huang, X. Liu and X. Feng, *J. Org. Chem.*, 2007, **72**, 7715-7719.
10. E. J. Corey and J. O. Link, *J. Am. Chem. Soc.*, 1992, **114**, 1906-1908.
11. R. M. Williams, P. J. Sinclair, D. Zhai and D. Chen, *J. Am. Chem. Soc.*, 1988, **110**, 1547-1557.
12. T. Koolmeister, M. Södergren and M. Scobie, *Tetrahedron Lett.*, 2002, **43**, 5969-5970.
13. J. E. Redman, S. Ladame, A. P. Reszka, S. Neidle and S. Balasubramanian, *Org. Biomol. Chem.*, 2006, **4**, 4364-4369.
14. J. E. Redman, *Methods*, 2007, **43**, 302-312.
15. N. J. Ede, J. Hill, J. K. Joy, A.-M. Ede and M. L. Koppens, *J. Pept. Sci.*, 2012, **18**, 661-668.
16. H. Wu, M. N. Amin, Y. Niu, Q. Qiao, N. Harfouch, A. Nimer and J. Cai, *Org. Lett.*, 2012, **14**, 3446-3449.
17. R. Wing, H. Drew, T. Takano, C. Broka, S. Tanaka, K. Itakura and R. E. Dickerson, *Nature*, 1980, **287**, 755-758.
18. J. Allers and Y. Shamoo, *J. Mol. Biol.*, 2001, **311**, 75-86.
19. Y. Mandel-Gutfreund, O. Schueler and H. Margalit, *J. Mol. Biol.*, 1995, **253**, 370-382.
20. C. O. Pabo and R. T. Sauer, *Annu. Rev. Biochem.*, 1984, **53**, 293-321.
21. N. C. Seeman, J. M. Rosenberg and A. Rich, *Proc. Natl. Acad. Sci. U.S.A.*, 1976, **73**, 804-808.
22. C. Hélène, *FEBS Lett.*, 1977, **74**, 10-13.
23. B. W. Matthews, *Nature*, 1988, **335**, 294-295.
24. C. O. Pabo and R. T. Sauer, *Annu. Rev. Biochem.*, 1992, **61**, 1053-1095.
25. N. P. Pavletich and C. O. Pabo, *Science*, 1991, **252**, 809-817.
26. M. Suzuki, *Structure*, 1994, **2**, 317-326.
27. N. M. Luscombe, R. A. Laskowski and J. M. Thornton, *Nucleic Acids Res.*, 2001, **29**, 2860-2874.
28. S. Jones, P. van Heyningen, H. M. Berman and J. M. Thornton, *J. Mol. Biol.*, 1999, **287**, 877-896.
29. H. Kono and A. Sarai, *Proteins Struct. Funct. Bioinf.*, 1999, **35**, 114-131.
30. M. M. Gromiha and K. Fukui, *J. Chem. Inf. Model.*, 2011, **51**, 721-729.
31. P. Zhou, F. Tian, Y. Ren and Z. Shang, *J. Chem. Inf. Model.*, 2010, **50**, 1476-1488.
32. M. A. Schumacher, K. Y. Choi, H. Zalkin and R. G. Brennan, *Science*, 1994, **266**, 763-770.
33. M. Y. Tolstorukov, A. V. Colasanti, D. M. McCandlish, W. K. Olson and V. B. Zhurkin, *J. Mol. Biol.*, 2007, **371**, 725-738.
34. J. W. Locasale, A. A. Napoli, S. Chen, H. M. Berman and C. L. Lawson, *J. Mol. Biol.*, 2009, **386**, 1054-1065.
35. T. J. Richmond and C. A. Davey, *Nature*, 2003, **423**, 145-150.
36. R. Rohs, S. M. West, A. Sosinsky, P. Liu, R. S. Mann and B. Honig, *Nature*, 2009, **461**, 1248-1253.
37. J. Mendieta, L. Pérez-Lago, M. Salas and A. Camacho, *Nucleic Acids Res.*, 2007, **35**, 3252-3261.
38. J. D. Puglisi, R. Tan, B. J. Calnan, A. D. Frankel and Williamson, *Science*, 1992, **257**, 76-80.

39. S. Jones, D. T. A. Daley, N. M. Luscombe, H. M. Berman and J. M. Thornton, *Nucleic Acids Res.*, 2001, **29**, 943-954.
40. D. Lejeune, N. Delsaux, B. Charlotiaux, A. Thomas and R. Brasseur, *Proteins Struct. Funct. Bioinf.*, 2005, **61**, 258-271.
41. M. Treger and E. Westhof, *J. Mol. Recognit.*, 2001, **14**, 199-214.
42. J. J. Ellis, M. Broom and S. Jones, *Proteins Struct. Funct. Bioinf.*, 2007, **66**, 903-911.
43. J. Kondo and E. Westhof, *Nucleic Acids Res.*, 2011, **39**, 8628-8637.
44. A. C. Cheng, W. W. Chen, C. N. Fuhrmann and A. D. Frankel, *J. Mol. Biol.*, 2003, **327**, 781-796.
45. B. Burke, S. An and K. Musier-Forsyth, *Biochim. Biophys. Acta, Proteins Proteomics*, 2008, **1784**, 1222-1225.
46. H. Kim, E. Jeong, S.-W. Lee and K. Han, *FEBS Lett.*, 2003, **552**, 231-239.
47. C. H. Li, L. B. Cao, J. G. Su, Y. X. Yang and C. X. Wang, *Proteins Struct. Funct. Bioinf.*, 2012, **80**, 14-24.
48. M. S. Khalaf, S. H. Oakley, M. P. Coles and P. B. Hitchcock, *CrystEngComm*, 2008, **10**, 1653-1661.
49. A. C. Finlay, F. A. Hochstein, B. A. Sobin and F. X. Murphy, *J. Am. Chem. Soc.*, 1951, **73**, 341-343.
50. S. Nomoto, T. Teshima, T. Wakamiya and T. Shiba, *Tetrahedron*, 1978, **34**, 921-927.
51. Y. Kashman, S. Hirsh, O. J. McConnell, I. Ohtani, T. Kusumi and H. Kakisawa, *J. Am. Chem. Soc.*, 1989, **111**, 8925-8926.
52. A. P. Davis and K. J. Dempsey, *Tetrahedron: Asymmetry*, 1995, **6**, 2829-2840.
53. F. P. Schmidtchen, A. Gleich and A. Schummer, *Pure Appl. Chem.*, 1989, **61**, 1535-1546.
54. M. P. Coles, *Chem. Commun.*, 2009, 3659-3676.
55. V. Alcázar, J. R. Morán and J. de Mendoza, *Tetrahedron Lett.*, 1995, **36**, 3941-3944.
56. W. Ye, J. Xu, C.-T. Tan and C.-H. Tan, *Tetrahedron Lett.*, 2005, **46**, 6875-6878.
57. I. Cota, F. Medina, J. E. Sueiras and D. Tichit, *Tetrahedron Lett.*, 2011, **52**, 385-387.
58. C. Sabot, K. A. Kumar, S. Meunier and C. Mioskowski, *Tetrahedron Lett.*, 2007, **48**, 3863-3866.
59. D. Simoni, M. Rossi, R. Rondanin, A. Mazzali, R. Baruchello, C. Malagutti, M. Roberti and F. P. Invidiata, *Org. Lett.*, 2000, **2**, 3765-3768.
60. A. F. McKay and M. E. Kreling, *Can. J. Chem.*, 1962, **40**, 1160-1163.
61. A. F. McKay and J. R. Gilpin, *J. Am. Chem. Soc.*, 1956, **78**, 486-488.
62. A. F. McKay, W. G. Hatton and R. O. Braun, *J. Am. Chem. Soc.*, 1956, **78**, 6144-6147.
63. A. F. McKay, O. R. Braun, G. Y. Paris, *Can. Pat.* US002816896, 17th December, 1957.
64. A. F. McKay and M.-E. Kreling, *Can. J. Chem.*, 1957, **35**, 1438-1445.
65. F. A. Cotton, C. A. Murillo, X. Wang and C. C. Wilkinson, *Dalton Trans.*, 2006, 4623-4631.
66. A. Kosasayama, T. Konno, K. Higashi and F. Ishikawa, *Chem. Pharm. Bull.*, 1979, **27**, 841-847.
67. R. A'Court, *Eur. Pat. Appl.* 0198680, 22nd October, 1986.
68. F. A. Cotton, C. A. Murillo, X. Wang and C. C. Wilkinson, *Inorganic Chemistry*, 2006, **45**, 5493-5500.
69. B. A. Minch, C. R. Hickenboth, R. F. Karabin, S. R. Zawacky, G. J. Miccolum, *United States Pat.* WO2009137728A2, 8th May, 2009.
70. H. Shen, Y. Wang and Z. Xie, *Org. Lett.*, 2011, **13**, 4562-4565.
71. J. L. H. Van Gelder, A. H. M. Raeymaekers, L. F. C. Roevens, W. J. Van Laerhoven, *United States Pat.* 3925383, 2nd December, 1975.
72. A. Kosasayama, T. Konno, K. Higashi and F. Ishikawa, *Chem. Pharm. Bull.*, 1979, **27**, 848-857.
73. F. P. Schmidtchen, *Chem. Ber.*, 1980, **113**, 2175-2182.
74. A. Kosasayama, T. Konno, K. Higashi and F. Ishikawa, *Chem. Pharm. Bull.*, 1979, **27**, 841-847.
75. F. A. Cotton, C. A. Murillo, X. Wang and C. C. Wilkinson, *Dalton Trans.*, 2007, 3943-3951.
76. P. Molina, M. Alajarin and A. Vidal, *J. Chem. Soc., Chem. Commun.*, 1992, 295-296.
77. P. Molina, M. Alajarin and A. Vidal, *J. Org. Chem.*, 1993, **58**, 1687-1695.

78. P. Molina, M. J. Lidón and A. Tárraga, *Tetrahedron*, 1994, **50**, 10029-10036.
79. V. D. Jadhav, E. Herdtweck and F. P. Schmidtchen, *Chem. Eur. J.*, 2008, **14**, 6098-6107.
80. E. J. Corey and M. Ohtani, *Tetrahedron Lett.*, 1989, **30**, 5227-5230.
81. E. J. Corey and M. J. Grogan, *Org. Lett.*, 1999, **1**, 157-160.
82. W. Ye, D. Leow, S. L. M. Goh, C.-T. Tan, C.-H. Chian and C.-H. Tan, *Tetrahedron Lett.*, 2006, **47**, 1007-1010.
83. T. Misaki, G. Takimoto and T. Sugimura, *J. Am. Chem. Soc.*, 2010, **132**, 6286-6287.
84. H. Kurzmeier and F. P. Schmidtchen, *J. Org. Chem.*, 1990, **55**, 3749-3755.
85. F. P. Schmidtchen, *Tetrahedron Lett.*, 1990, **31**, 2269-2272.
86. I. Münster, U. Rolle, A. Madder and P. J. De Clercq, *Tetrahedron: Asymmetry*, 1995, **6**, 2673-2674.
87. E. Antonio, G. Amalia, M. J. de and S. Armando, *Helv. Chim. Acta*, 1988, **71**, 685-693.
88. V. D. Jadhav and F. P. Schmidtchen, *J. Org. Chem.*, 2007, **73**, 1077-1087.
89. P. H. Boyle, A. P. Davis, K. J. Dempsey and G. D. Hosken, *J. Chem. Soc., Chem. Commun.*, 1994, 1875-1876.
90. T. Isobe, K. Fukuda, K. Yamaguchi, H. Seki, T. Tokunaga and T. Ishikawa, *J. Org. Chem.*, 2000, **65**, 7779-7785.
91. Y. Kitani, T. Kumamoto, T. Isobe, K. Fukuda and T. Ishikawa, *Adv. Synth. Catal.*, 2005, **347**, 1653-1658.
92. A. Nefzi, C. Dooley, J. M. Ostresh and R. A. Houghten, *Bioorg. Med. Chem. Lett.*, 1998, **8**, 2273-2278.
93. A. N. Acharya, A. Nefzi, J. M. Ostresh and R. A. Houghten, *J. Comb. Chem.*, 2001, **3**, 189-195.
94. J. M. Ostresh, C. C. Schoner, V. T. Hamashin, A. Nefzi, J.-P. Meyer and R. A. Houghten, *J. Org. Chem.*, 1998, **63**, 8622-8623.
95. J. Ostresh, J. -P. Mayer, C. Dooley, R. Houghten, S. Blondelle, C. Schoner, *United States Pat.* WO9834113, 6th August, 1998.
96. A. Grillot and D. J. Hart, *Tetrahedron*, 1995, **51**, 11377-11392.
97. A. Strecker, *Liebigs Ann. Chem.*, 1850, **75**, 27-45.
98. H.-S. Wang, L.-F. Zhao and Z.-M. Du, *Chin. J. Chem.*, 2006, **24**, 135-137.
99. B. A. B. Prasad, A. Bisai and V. K. Singh, *Tetrahedron Lett.*, 2004, **45**, 9565-9567.
100. K. Matsumoto, J. C. Kim, H. Iida, H. Hamana, K. Kumamoto, H. Kotsuki, G. Jenner, *Helv. Chim. Acta*, 2005, **88**, 1734-1753.
101. K. Matsumoto, J. C. Kim, N. Hayashi and G. Jenner, *Tetrahedron Lett.*, 2002, **43**, 9167-9169.
102. K. Niknam, D. Saberi and M. N. Sefat, *Tetrahedron Lett.*, 2010, **51**, 2959-2962.
103. G. Olah, T. Mathew, C. Panja, K. Smith and G. Surya Prakash, *Catal. Lett.*, 2007, **114**, 1-7.
104. M. S. Patel and M. Worsley, *Can. J. Chem.*, 1970, **48**, 1881-1884.
105. K. Harada and T. Okawara, *J. Org. Chem.*, 1973, **38**, 707-710.
106. K. Harada, T. Okawara and K. Matsumoto, *Bull. Chem. Soc. Jpn.*, 1973, **46**, 1865-1868.
107. H. Kunz and W. Sager, *Angew. Chem. Int. Ed.*, 1987, **26**, 557-559.
108. H. Kunz, W. Sager, W. Pfrengle and D. Schanzenbach, *Tetrahedron Lett.*, 1988, **29**, 4397-4400.
109. T. K. Chakraborty, G. V. Reddy and K. Azhar Hussain, *Tetrahedron Lett.*, 1991, **32**, 7597-7600.
110. T. K. Chakraborty, K. Azhar Hussain and G. Venkat Reddy, *Tetrahedron*, 1995, **51**, 9179-9190.
111. F. A. Davis, R. E. Reddy and P. S. Portonovo, *Tetrahedron Lett.*, 1994, **35**, 9351-9354.
112. F. A. Davis, P. S. Portonovo, R. E. Reddy and Y.-h. Chiu, *J. Org. Chem.*, 1996, **61**, 440-441.
113. F. A. Davis and V. Srirajan, *J. Org. Chem.*, 2000, **65**, 3248-3251.
114. F. A. Davis, V. Srirajan, D. L. Fanelli and P. Portonovo, *J. Org. Chem.*, 2000, **65**, 7663-7666.
115. S. Mabic and A. A. Cordi, *Tetrahedron*, 2001, **57**, 8861-8866.
116. J. Huang and E. J. Corey, *Org. Lett.*, 2004, **6**, 5027-5029.

117. S. B. Tsogoeva, M. J. Hateley, D. A. Yalalov, K. Meindl, C. Weckbecker and K. Huthmacher, *Bioorg. Med. Chem.*, 2005, **13**, 5680-5685.
118. S. B. Tsogoeva, D. A. Yalalov, M. J. Hateley, C. Weckbecker and K. Huthmacher, *Eur. J. Org. Chem.*, 2005, **2005**, 4995-5000.
119. M. S. Sigman and E. N. Jacobsen, *J. Am. Chem. Soc.*, 1998, **120**, 4901-4902.
120. P. Vachal and E. N. Jacobsen, *Org. Lett.*, 2000, **2**, 867-870.
121. P. Vachal and E. N. Jacobsen, *J. Am. Chem. Soc.*, 2002, **124**, 10012-10014.
122. D. E. Fuerst and E. N. Jacobsen, *J. Am. Chem. Soc.*, 2005, **127**, 8964-8965.
123. S. J. Zuend, M. P. Coughlin, M. P. Lalonde and E. N. Jacobsen, *Nature*, 2009, **461**, 968-970.
124. G.-W. Zhang, D.-H. Zheng, J. Nie, T. Wang and J.-A. Ma, *Org. Biomol. Chem.*, 2010, **8**, 1399-1405.
125. M. Rueping, E. Sugiono and C. Azap, *Angew. Chem. Int. Ed.*, 2006, **45**, 2617-2619.
126. C. Becker, C. Hoben and H. Kunz, *Adv. Synth. Catal.*, 2007, **349**, 417-424.
127. S. Saravanan, A. Sadhukhan, N.-u. H. Khan, R. I. Kureshy, S. H. R. Abdi and H. C. Bajaj, *J. Org. Chem.*, 2012, **77**, 4375-4384.
128. S. C. Pan and B. List, *Org. Lett.*, 2007, **9**, 1149-1151.
129. M. S. Sigman and E. N. Jacobsen, *J. Am. Chem. Soc.*, 1998, **120**, 5315-5316.
130. Y. Hamashima, D. Sawada, M. Kanai and M. Shibasaki, *J. Am. Chem. Soc.*, 1999, **121**, 2641-2642.
131. H. Nogami, S. Matsunaga, M. Kanai and M. Shibasaki, *Tetrahedron Lett.*, 2001, **42**, 279-283.
132. M. Mori, H. Imma and T. Nakai, *Tetrahedron Lett.*, 1997, **38**, 6229-6232.
133. W. Mansawat, W. Bhanthumnavin and T. Vilaivan, *Tetrahedron Lett.*, 2003, **44**, 3805-3808.
134. C. A. Krueger, K. W. Kuntz, C. D. Dzierba, W. G. Wirschun, J. D. Gleason, M. L. Snapper and A. H. Hoveyda, *J. Am. Chem. Soc.*, 1999, **121**, 4284-4285.
135. H. Ishitani, S. Komiyama, Y. Hasegawa and S. Kobayashi, *J. Am. Chem. Soc.*, 2000, **122**, 762-766.
136. M. Chavarot, J. J. Byrne, P. Y. Chavant and Y. Vallée, *Tetrahedron: Asymmetry*, 2001, **12**, 1147-1150.
137. S. Masumoto, H. Usuda, M. Suzuki, M. Kanai and M. Shibasaki, *J. Am. Chem. Soc.*, 2003, **125**, 5634-5635.
138. E. J. Corey, J. O. Link and R. K. Bakshi, *Tetrahedron Lett.*, 1992, **33**, 7107-7110.
139. E. J. Corey, X.-M. Cheng, K. A. Cimprich and S. Sarshar, *Tetrahedron Lett.*, 1991, **32**, 6835-6838.
140. E. J. Corey, J. O. Link and Y. Shao, *Tetrahedron Lett.*, 1992, **33**, 3435-3438.
141. G. M. Lee and S. M. Weinreb, *J. Org. Chem.*, 1990, **55**, 1281-1285.
142. V. K. Aggarwal and A. Mereu, *J. Org. Chem.*, 2000, **65**, 7211-7212.
143. M. K. Gupta, Z. Li and T. S. Snowden, *J. Org. Chem.*, 2012, **77**, 4854-4860.
144. S. Karady, J. S. Amto and L. M. Weinstock, *Tetrahedron Lett.*, 1984, **25**, 4337-4340.
145. D. Seebach, M. Boes, R. Naef and W. B. Schweizer, *J. Am. Chem. Soc.*, 1983, **105**, 5390-5398.
146. U. Schöllkopf, *Tetrahedron*, 1983, **39**, 2085-2091.
147. R. M. Williams, D. Zhai and P. J. Sinclair, *J. Org. Chem.*, 1986, **51**, 5021-5022.
148. P. J. Sinclair, D. Zhai, J. Reibenspies and R. M. Williams, *J. Am. Chem. Soc.*, 1986, **108**, 1103-1104.
149. R. M. Williams and M. N. Im, *J. Am. Chem. Soc.*, 1991, **113**, 9276-9286.
150. R. M. Williams and J. A. Hendrix, *J. Org. Chem.*, 1990, **55**, 3723-3728.
151. Z. Weixu, *Tetrahedron*, 1988, **44**, 5425-5430.
152. R. M. Williams, P. J. Sinclair and W. Zhai, *J. Am. Chem. Soc.*, 1988, **110**, 482-483.
153. D. Zhai, W. Zhai and R. M. Williams, *J. Am. Chem. Soc.*, 1988, **110**, 2501-2505.
154. R. M. Williams, *Aldrichim. Acta*, 1992, **25**, 11-24.
155. Z. Weixu and R. M. Williams, *Tetrahedron*, 1988, **44**, 5425-5430.
156. R. M. Williams and M.-N. Im, *Tetrahedron Lett.*, 1988, **29**, 6075-6078.
157. Adrianus M. C. H. van den Nieuwendijk, Nicole M. A. J. Kriek, J. Brussee, Jacques H. van Boom and A. van der Gen, *Eur. J. Org. Chem.*, 2000, **2000**, 3683-3691.

158. R. M. Williams, M. N. Im and J. Cao, *J. Am. Chem. Soc.*, 1991, **113**, 6976-6981.
159. Y. Aoyagi and R. M. Williams, *Tetrahedron*, 1998, **54**, 10419-10433.
160. S. Singh and M. W. Pennington, *Tetrahedron Lett.*, 2003, **44**, 2683-2685.
161. J. F. Dellaria and D. S. Bernard, *Tetrahedron Lett.*, 1988, **29**, 6079-6082.
162. J. F. Dellaria and B. D. Santarsiero, *J. Org. Chem.*, 1989, **54**, 3916-3926.
163. T. Gustafsson, M. Schou, F. Almquist and J. Kihlberg, *J. Org. Chem.*, 2004, **69**, 8694-8701.
164. K. Takatori, M. Nishihara and M. Kajiwara, *J. Labelled Compd. Radiopharm.*, 1999, **42**, 701-708.
165. K. Takatori, M. Nishihara, Y. Nishiyama and M. Kajiwara, *Tetrahedron*, 1998, **54**, 15861-15869.
166. C. Song, S. Tapaneyakorn, A. C. Murphy, C. Butts, A. Watts and C. L. Willis, *J. Org. Chem.*, 2009, **74**, 8980-8987.
167. J. R. Casimir, C. Didierjean, A. Aubry, M. Rodriguez, J.-P. Briand and G. Guichard, *Org. Lett.*, 2000, **2**, 895-897.
168. N. A. Petasis and I. A. Zavialov, *J. Am. Chem. Soc.*, 1997, **119**, 445-446.
169. N. A. Petasis, A. Goodman and I. A. Zavialov, *Tetrahedron*, 1997, **53**, 16463-16470.
170. N. A. Petasis, *United States Pat.* WO9800398, 8th January, 1998.
171. H. Jourdan, G. Gouhier, L. Van Hijfte, P. Angibaud and S. R. Piettre, *Tetrahedron Lett.*, 2005, **46**, 8027-8031.
172. T. J. Southwood, M. C. Curry and C. A. Hutton, *Tetrahedron*, 2006, **62**, 236-242.
173. N. A. Petasis and I. A. Zavialov, *J. Am. Chem. Soc.*, 1998, **120**, 11798-11799.
174. S. Lou and S. E. Schaus, *J. Am. Chem. Soc.*, 2008, **130**, 6922-6923.
175. Y. Li and M.-H. Xu, *Org. Lett.*, 2012, **14**, 2062-2065.
176. K. Shindo, H. Suzuki and T. Okuda, *Biosci. Biotechnol. Biochem.*, 2002, **66**, 2444-2448.
177. M. P. Bosch, F. Campos, I. Niubó, G. Rosell, J. L. Díaz, J. Brea, M. I. Loza and A. Guerrero, *J. Med. Chem.*, 2004, **47**, 4041-4053.
178. R. Alexander, A. Balasundaram, M. Batchelor, D. Brookings, K. Crépy, T. Crabbe, M.-F. Deltent, F. Driessens, A. Gill, S. Harris, G. Hutchinson, C. Kulisa, M. Merriman, P. Mistry, T. Parton, J. Turner, I. Whitcombe and S. Wright, *Bioorg. Med. Chem. Lett.*, 2008, **18**, 4316-4320.
179. A. Karim, A. Mortreux, F. Petit, G. Buono, G. Peiffer and C. Siv, *J. Organomet. Chem.*, 1986, **317**, 93-104.
180. H. E. Gottlieb, V. Kotlyar and A. Nudelman, *J. Org. Chem.*, 1997, **62**, 7512-7515.
181. M. J. McKennon, A. I. Meyers, K. Drauz and M. Schwarm, *J. Org. Chem.*, 1993, **58**, 3568-3571.
182. D. Seebach, M. Overhand, F. N. M. Kühnle, B. Martinoni, L. Oberer, U. Hommel and H. Widmer, *Helv. Chim. Acta*, 1996, **79**, 913-941.
183. A. Giannis and K. Sandhoff, *Angew. Chem. Int. Ed.*, 1989, **28**, 218-220.
184. Y. Kaburagi and Y. Kishi, *Org. Lett.*, 2007, **9**, 723-726.
185. T. Mukhopadhyay and D. Seebach, *Helv. Chim. Acta*, 1982, **65**, 385-391.
186. P. F. Cirillo and J. S. Panek, *J. Org. Chem.*, 1990, **55**, 6071-6073.
187. A. R. Vaino and W. A. Szarek, *Chem. Commun.*, 1996, 2351-2352.
188. S. D. Meyer and S. L. Schreiber, *J. Org. Chem.*, 1994, **59**, 7549-7552.
189. R. J. Cvetovich, B. Pipik, F. W. Hartner and E. J. J. Grabowski, *Tetrahedron Lett.*, 2003, **44**, 5867-5870.
190. S. Niwayama and H. Cho, *Chem. Pharm. Bull.*, 2009, **57**, 508-510.
191. A.-L. Grillot and D. J. Hart, *Tetrahedron*, 1995, **51**, 11377-11392.
192. Y. Li, Y. Zhang, D. Yang, C. Feng, S. Zhai, J. Hu, G. Lu and X. Huang, *J. Polym. Sci. Part A: Polym. Chem.*, 2009, **47**, 6032-6043.
193. Z. Duan, X. Xuan, T. Li, C. Yang and Y. Wu, *Tetrahedron Lett.*, 2006, **47**, 5433-5436.
194. D. L. Steer, R. A. Lew, P. Perlmutter, A. I. Smith and M. I. Aguilar, *J. Pept. Sci.*, 2000, **6**, 470-477.
195. C.-D. Graf, C. Malan, K. Harms and P. Knochel, *J. Org. Chem.*, 1999, **64**, 5581-5588.

196. M. F. Jung and M. A. Lyster, *J. Am. Chem. Soc.*, 1977, **99**, 968-969.
197. G. A. Olah, S. C. Narang, B. G. B. Gupta and R. Malhotra, *J. Org. Chem.*, 1979, **44**, 1247-1251.
198. E. Engvall, K. Jonsson and P. Perlmann, *Biochim. Biophys. Acta, Protein Struct.*, 1971, **251**, 427-434.
199. E. Engvall and P. Perlmann, *J. Immunol.*, 1972, **109**, 129-135.
200. F. Poisson, P. Roingeard and A. Goudeau, *J. Virol. Methods*, 1995, **55**, 381-389.
201. R. B. Merrifield, *J. Am. Chem. Soc.*, 1963, **85**, 2149-2154.
202. M. A. Findeis and E. T. Kaiser, *J. Org. Chem.*, 1989, **54**, 3478-3482.
203. M. Meldal, *Tetrahedron Lett.*, 1992, **33**, 3077-3080.
204. S. A. Kates, B. F. McGuinness, C. Blackburn, G. W. Griffin, N. A. Solé, G. Barany and F. Albericio, *Pept. Sci.*, 1998, **47**, 365-380.
205. C. Chen, L. A. A. Randall, R. B. Miller, A. D. Jones and M. J. Kurth, *J. Am. Chem. Soc.*, 1994, **116**, 2661-2662.
206. S. Mourtas, C. Katakalous, A. Nicolettou, C. Tzavara, D. Gatos and K. Barlos, *Tetrahedron Lett.*, 2003, **44**, 179-182.
207. G. R. Matsueda and J. M. Stewart, *Peptides*, 1981, **2**, 45-50.
208. G. Mez'ó, N. Mihala, G. Kóczán and F. Hudecz, *Tetrahedron*, 1998, **54**, 6757-6766.
209. W. König and R. Geiger, *Chem. Ber.*, 1970, **103**, 788-798.
210. L. A. Carpino, *J. Am. Chem. Soc.*, 1993, **115**, 4397-4398.
211. L. A. Carpino, A. El-Faham and F. Albericio, *Tetrahedron Lett.*, 1994, **35**, 2279-2282.
212. V. Dourtoglou, J.-C. Ziegler and B. Gross, *Tetrahedron Lett.*, 1978, **19**, 1269-1272.
213. L. A. Carpino, H. Imazumi, A. El-Faham, F. J. Ferrer, C. Zhang, Y. Lee, B. M. Foxman, P. Henklein, C. Hanay, C. Mügge, H. Wenschuh, J. Klose, M. Beyermann and M. Bienert, *Angew. Chem. Int. Ed.*, 2002, **41**, 441-445.
214. B. Castro, J. R. Dormoy, G. Evin and C. Selve, *Tetrahedron Lett.*, 1975, **16**, 1219-1222.
215. B. J. H. Kuipers and H. Gruppen, *J. Agric. Food Chem.*, 2007, **55**, 5445-5451.
216. M. C. Pirrung, in *The Synthetic Organic Chemist's Companion*, John Wiley & Sons, Inc., Editon edn., 2007, pp. 171-172.
217. A. Erxleben and J. Kottmann, *Inorg. Chim. Acta*, 2006, **359**, 13-24.
218. S. M. Birnbaum, L. Levintow, R. B. Kingsley and J. P. Greenstein, *J. Biol. Chem.*, 1952, **194**, 455-470.
219. G. Antonopoulou, V. Magrioti, D. Stephens, V. Constantinou-Kokotou, E. A. Dennis and G. Kokotos, *J. Pept. Sci.*, 2008, **14**, 1111-1120.
220. J. Holz, B. Schäffner, O. Zayas, A. Spannenberg and A. Börner, *Adv. Synth. Catal.*, 2008, **350**, 2533-2543.

8.0 Appendix

Appendix 1

Selected crystallographic data for structures discussed in the text.

Table A1. Crystal data and structure refinement for **227**.

Identification code	jer1101
Empirical formula	C ₁₅ H ₂₁ I ₂ N ₃ O ₂ S
Formula weight	561.21
Temperature	150(2) K
Wavelength	0.71073 Å
Crystal system	Orthorhombic
Space group	P212121
Unit cell dimensions	a = 6.6117(2) Å α = 90°. b = 10.1482(2) Å β = 90°. c = 28.1444(9) Å γ = 90°.
Volume	1888.40(9) Å ³
Z	4
Density (calculated)	1.974 Mg/m ³
Absorption coefficient	3.453 mm ⁻¹
F(000)	1080
Crystal size	0.40 x 0.20 x 0.20 mm ³
Theta range for data collection	2.96 to 27.44°.
Index ranges	-8 ≤ h ≤ 8, -13 ≤ k ≤ 13, -36 ≤ l ≤ 36
Reflections collected	4080
Independent reflections	4080 [R(int) = 0.0000]
Completeness to theta = 27.44°	98.0 %
Max. and min. transmission	0.5451 and 0.3388
Refinement method	Full-matrix least-squares on F ²
Data / restraints / parameters	4080 / 0 / 210
Goodness-of-fit on F ²	1.035

Final R indices [$I > 2\sigma(I)$]	R1 = 0.0308, wR2 = 0.0693
R indices (all data)	R1 = 0.0345, wR2 = 0.0716
Absolute structure parameter	-0.01(3)
Extinction coefficient	0.0068(3)
Largest diff. peak and hole	0.755 and -0.791 e.Å ⁻³

Table A2. Atomic coordinates ($\times 10^4$) and equivalent isotropic displacement parameters ($\text{Å}^2 \times 10^3$) for jer1101. $U(\text{eq})$ is defined as one third of the trace of the orthogonalized U^{ij} tensor.

	x	y	z	U(eq)
C(1)	-3559(7)	2979(4)	3545(2)	18(1)
C(3)	-5230(7)	1594(5)	4148(2)	23(1)
C(4)	-7178(7)	1880(5)	3890(2)	24(1)
C(5)	-6760(8)	1837(5)	3364(2)	27(1)
C(7)	-4511(9)	2707(5)	2723(2)	26(1)
C(8)	-3484(8)	4008(5)	2620(2)	23(1)
C(9)	-1588(7)	4144(4)	2919(2)	20(1)
C(11)	-851(7)	5559(5)	2918(2)	23(1)
C(16)	-4311(7)	5036(5)	4450(2)	19(1)
C(17)	-6223(7)	4988(5)	4664(2)	20(1)
C(18)	-7392(7)	6127(5)	4662(2)	24(1)
C(19)	-6729(8)	7277(4)	4442(2)	22(1)
C(20)	-8055(10)	8482(5)	4420(2)	35(1)
C(21)	-4799(8)	7297(5)	4230(2)	26(1)
C(22)	-3596(7)	6183(5)	4236(2)	22(1)
I(1)	1835(1)	5837(1)	3336(1)	27(1)
I(2)	1728(1)	4518(1)	1752(1)	27(1)
N(2)	-3745(6)	2639(4)	4025(1)	18(1)
N(6)	-4940(6)	2585(4)	3237(2)	22(1)
N(10)	-1988(6)	3702(4)	3410(1)	21(1)
O(14)	-3200(6)	2891(3)	4889(1)	23(1)
O(15)	-797(5)	3955(4)	4336(1)	23(1)
S(13)	-2831(2)	3609(1)	4460(1)	18(1)

Table A3. Bond lengths [Å] and angles [°] for jer1101 – Symmetry transformations used to generate equivalent atoms

C(1)-N(6)	1.320(6)	N(2)-S(13)	1.685(4)
C(1)-N(10)	1.328(6)	N(10)-H(10)	0.88
C(1)-N(2)	1.400(6)	O(14)-S(13)	1.429(3)
C(3)-N(2)	1.486(6)	O(15)-S(13)	1.433(3)
C(3)-C(4)	1.507(7)		
C(3)-H(3A)	0.99	N(6)-C(1)-N(10)	121.4(4)
C(3)-H(3B)	0.99	N(6)-C(1)-N(2)	119.8(4)
C(4)-C(5)	1.507(7)	N(10)-C(1)-N(2)	118.8(4)
C(4)-H(4A)	0.99	N(2)-C(3)-C(4)	108.4(4)
C(4)-H(4B)	0.99	N(2)-C(3)-H(3A)	110
C(5)-N(6)	1.466(6)	C(4)-C(3)-H(3A)	110
C(5)-H(5A)	0.99	N(2)-C(3)-H(3B)	110
C(5)-H(5B)	0.99	C(4)-C(3)-H(3B)	110
C(7)-N(6)	1.479(6)	H(3A)-C(3)-H(3B)	108.4
C(7)-C(8)	1.513(7)	C(5)-C(4)-C(3)	108.1(4)
C(7)-H(7A)	0.99	C(5)-C(4)-H(4A)	110.1
C(7)-H(7B)	0.99	C(3)-C(4)-H(4A)	110.1
C(8)-C(9)	1.516(7)	C(5)-C(4)-H(4B)	110.1
C(8)-H(8A)	0.99	C(3)-C(4)-H(4B)	110.1
C(8)-H(8B)	0.99	H(4A)-C(4)-H(4B)	108.4
C(9)-N(10)	1.475(5)	N(6)-C(5)-C(4)	112.0(4)
C(9)-C(11)	1.516(7)	N(6)-C(5)-H(5A)	109.2
C(9)-H(9)	1	C(4)-C(5)-H(5A)	109.2
C(11)-I(1)	2.150(5)	N(6)-C(5)-H(5B)	109.2
C(11)-H(11A)	0.99	C(4)-C(5)-H(5B)	109.2
C(11)-H(11B)	0.99	H(5A)-C(5)-H(5B)	107.9
C(16)-C(22)	1.393(7)	N(6)-C(7)-C(8)	110.3(4)
C(16)-C(17)	1.401(6)	N(6)-C(7)-H(7A)	109.6
C(16)-S(13)	1.748(5)	C(8)-C(7)-H(7A)	109.6
C(17)-C(18)	1.390(7)	N(6)-C(7)-H(7B)	109.6
C(17)-H(17)	0.95	C(8)-C(7)-H(7B)	109.6
C(18)-C(19)	1.391(7)	H(7A)-C(7)-H(7B)	108.1
C(18)-H(18)	0.95	C(7)-C(8)-C(9)	110.1(4)
C(19)-C(21)	1.409(8)	C(7)-C(8)-H(8A)	109.6

C(19)-C(20)	1.506(7)	C(9)-C(8)-H(8A)	109.6
C(20)-H(20A)	0.98	C(7)-C(8)-H(8B)	109.6
C(20)-H(20B)	0.98	C(9)-C(8)-H(8B)	109.6
C(20)-H(20C)	0.98	H(8A)-C(8)-H(8B)	108.2
C(21)-C(22)	1.383(7)	N(10)-C(9)-C(11)	110.4(4)
C(21)-H(21)	0.95	N(10)-C(9)-C(8)	110.1(4)
C(22)-H(22)	0.95	C(11)-C(9)-C(8)	110.5(4)
N(10)-C(9)-H(9)	108.6	C(19)-C(20)-H(20C)	109.5
C(11)-C(9)-H(9)	108.6	H(20A)-C(20)-H(20C)	109.5
C(8)-C(9)-H(9)	108.6	H(20B)-C(20)-H(20C)	109.5
C(9)-C(11)-I(1)	112.8(3)	C(22)-C(21)-C(19)	120.3(5)
C(9)-C(11)-H(11A)	109	C(22)-C(21)-H(21)	119.8
I(1)-C(11)-H(11A)	109	C(19)-C(21)-H(21)	119.8
C(9)-C(11)-H(11B)	109	C(21)-C(22)-C(16)	119.5(5)
I(1)-C(11)-H(11B)	109	C(21)-C(22)-H(22)	120.2
H(11A)-C(11)-H(11B)	107.8	C(16)-C(22)-H(22)	120.2
C(22)-C(16)-C(17)	121.4(5)	C(1)-N(2)-C(3)	117.3(4)
C(22)-C(16)-S(13)	120.6(4)	C(1)-N(2)-S(13)	121.8(3)
C(17)-C(16)-S(13)	118.0(4)	C(3)-N(2)-S(13)	119.0(3)
C(18)-C(17)-C(16)	118.1(5)	C(1)-N(6)-C(5)	124.4(4)
C(18)-C(17)-H(17)	121	C(1)-N(6)-C(7)	118.9(4)
C(16)-C(17)-H(17)	121	C(5)-N(6)-C(7)	116.0(4)
C(17)-C(18)-C(19)	121.6(5)	C(1)-N(10)-C(9)	125.2(4)
C(17)-C(18)-H(18)	119.2	C(1)-N(10)-H(10)	117.4
C(19)-C(18)-H(18)	119.2	C(9)-N(10)-H(10)	117.4
C(18)-C(19)-C(21)	119.0(5)	O(14)-S(13)-O(15)	119.4(2)
C(18)-C(19)-C(20)	121.1(5)	O(14)-S(13)-N(2)	104.7(2)
C(21)-C(19)-C(20)	119.9(5)	O(15)-S(13)-N(2)	107.6(2)
C(19)-C(20)-H(20A)	109.5	O(14)-S(13)-C(16)	109.9(2)
C(19)-C(20)-H(20B)	109.5	O(15)-S(13)-C(16)	108.6(2)
H(20A)-C(20)-H(20B)	109.5	N(2)-S(13)-C(16)	105.7(2)

Table A4. Anisotropic displacement parameters ($\text{\AA}^2 \times 10^3$) for jer1101. The anisotropic displacement factor exponent takes the form: $-2^2 [h^2 a^2 U^{11} + \dots + 2 h k a^* b^* U^{12}]$

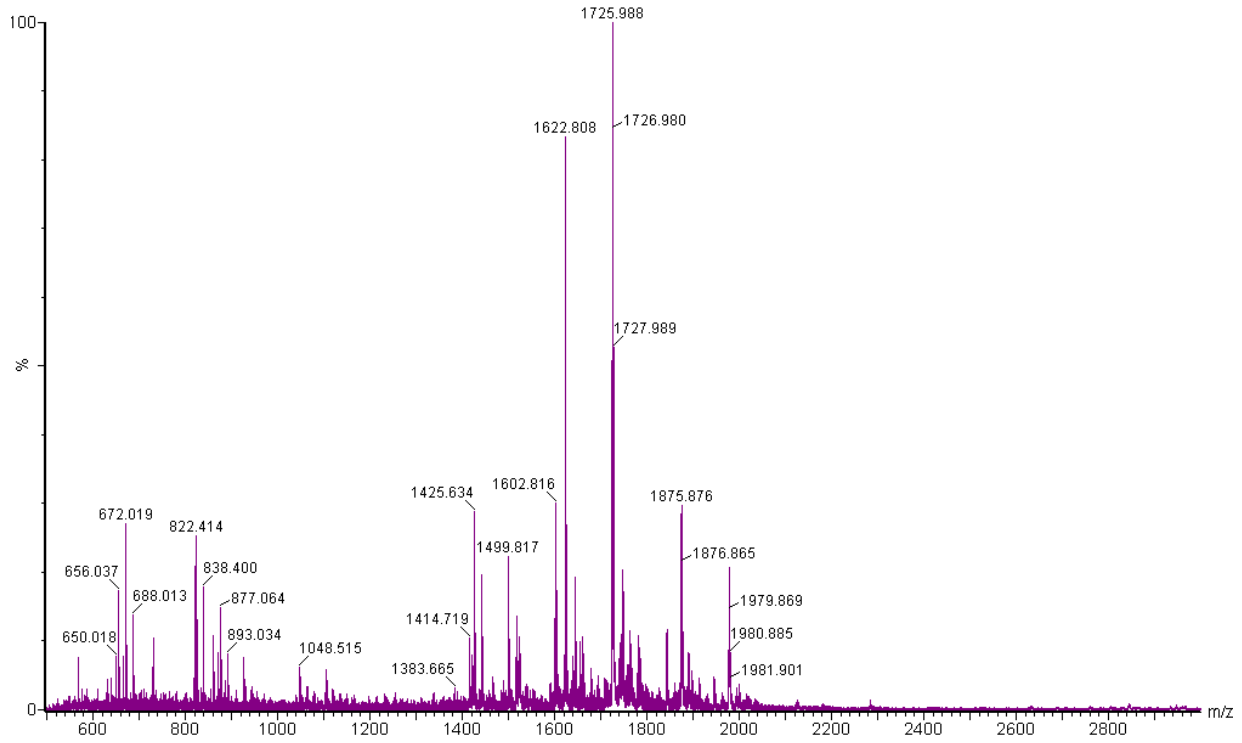
	U ¹¹	U ²²	U ³³	U ²³	U ¹³	U ¹²
C(1)	21(2)	15(2)	17(2)	-2(2)	0(2)	3(2)
C(3)	22(2)	21(3)	26(3)	0(2)	2(2)	-4(2)
C(4)	19(2)	25(3)	29(3)	-2(2)	2(2)	-3(2)
C(5)	24(2)	25(2)	32(3)	-1(2)	-2(3)	-4(2)
C(7)	34(3)	33(3)	12(2)	0(2)	-1(2)	0(2)
C(8)	30(3)	24(2)	14(2)	2(2)	-3(2)	2(2)
C(9)	23(2)	20(2)	17(2)	2(2)	1(2)	-1(2)
C(11)	21(2)	27(3)	20(2)	2(2)	-5(2)	2(2)
C(16)	16(2)	22(2)	18(2)	-3(2)	-2(2)	-2(2)
C(17)	21(2)	18(2)	20(2)	3(2)	0(2)	-3(2)
C(18)	23(2)	23(3)	26(3)	-4(2)	1(2)	-1(2)
C(19)	27(2)	19(2)	20(2)	-1(2)	-1(2)	2(2)
C(20)	45(3)	29(3)	32(3)	-2(2)	1(3)	11(3)
C(21)	31(3)	22(3)	25(3)	1(2)	3(2)	-2(2)
C(22)	25(3)	22(2)	20(2)	-1(2)	0(2)	-8(2)
I(1)	25(1)	32(1)	24(1)	3(1)	1(1)	-4(1)
I(2)	25(1)	30(1)	25(1)	-1(1)	2(1)	-3(1)
N(2)	22(2)	18(2)	13(2)	3(2)	2(1)	-2(2)
N(6)	20(2)	28(2)	17(2)	1(2)	-3(2)	-2(2)
N(10)	19(2)	25(2)	19(2)	1(2)	-1(2)	1(2)
O(14)	29(2)	27(2)	14(2)	5(1)	-1(2)	2(2)
O(15)	15(2)	35(2)	20(2)	-2(2)	1(1)	-1(1)
S(13)	19(1)	21(1)	15(1)	1(1)	-2(1)	1(1)

Table A5. Hydrogen coordinates ($\times 10^4$) and isotropic displacement parameters ($\text{\AA}^2 \times 10^3$) for jer1101.

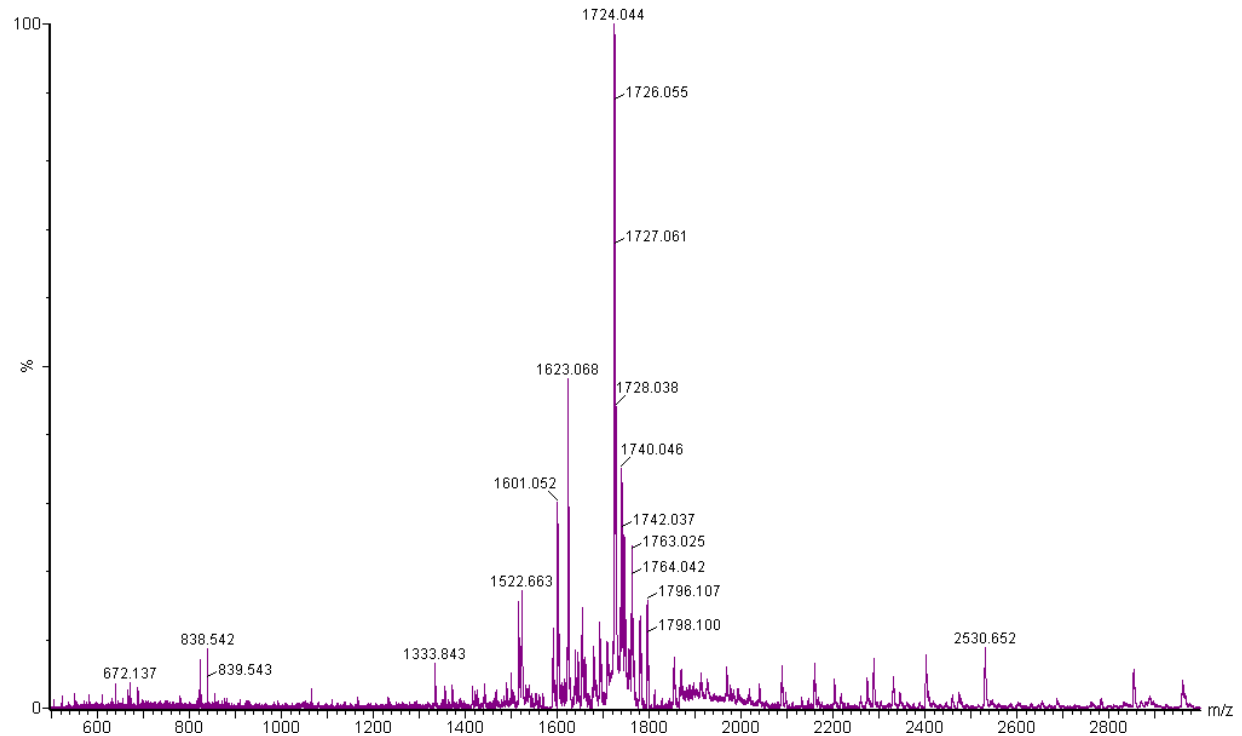
	X	y	z	U(eq)
H(3A)	-5467	1583	4495	28
H(3B)	-4703	721	4051	28
H(4A)	-8213	1215	3974	29
H(4B)	-7693	2761	3981	29
H(5A)	-6589	909	3263	33
H(5B)	-7934	2205	3190	33
H(7A)	-5791	2650	2542	32
H(7B)	-3627	1973	2621	32
H(8A)	-4422	4742	2692	27
H(8B)	-3125	4055	2279	27
H(9)	-509	3572	2780	24
H(11A)	-1935	6135	3042	27
H(11B)	-571	5829	2586	27
H(17)	-6707	4200	4806	23
H(18)	-8675	6120	4814	29
H(20A)	-9303	8321	4599	53
H(20B)	-8388	8677	4088	53
H(20C)	-7337	9234	4560	53
H(21)	-4322	8080	4083	31
H(22)	-2291	6199	4095	27
H(10)	-1115	3937	3630	25

Appendix 2

MALDI-ToF mass spectrum for peptide sequence E(biotin-PEG)GGKCIKCARYA:



MALDI-ToF mass spectrum for oxidised peptide sequence E(biotin-PEG)GGKCIKCARYA:



Appendix 3

Table A6. Peptide sequences:

Strong dsDNA binding:	Strong ssDNA:	Strong RNA binding:
ANKACKTKGG(PEG-biotin)	ALRACRYKGG(PEG-biotin)	ANRACKFKGG(PEG-biotin)
ANRACKIKGG(PEG-biotin)	ANRACRYKGG(PEG-biotin)	ANRACRYKGG(PEG-biotin)
ANRACKYKGG(PEG-biotin)	ANRACRNKGG(PEG-biotin)	ANRACRFKGG(PEG-biotin)
	AVRACRIKGG(PEG-biotin)	ANRACKIKGG(PEG-biotin)
		ANRACKFKGG(PEG-biotin)
		ANRACRFKGG(PEG-biotin)